CORONARY HAEMODYNAMICS AND WAVE INTENSITY ANALYSIS IN AORTIC STENOSIS

Christopher James Broyd

National Heart and Lung Institute

PhD degree of Imperial College London

Declaration of originality

I declare that all this work is my own. Where other material is used or referred to, it is appropriately referenced.

Copyright declaration

Dedication

This manuscript is dedicated to my family. Over three decades of their support is the building block on which this work is based.

Acknowledgements

I wish to express profound gratitude and thanks for the support and friendship from my supervisors: Dr Justin Davies, Dr Ghada Mikhail and Professor Jamil Mayet. I am proud to have developed my clinical and academic skills under their mentorship and I will always be grateful for what they invested in me.

The synergistic brains of Professor Kim Parker and Professor Alun Hughes have made this 'ride' so much smoother. I am grateful for the careful, intelligent and detailed explanations to all my questions along with the expert development of the Pulsecor software. Additionally, Professor Darrel Francis has been a continual source of inspiration and most importantly has demonstrated the value of high quality, robust research.

My skills in non-invasive coronary imaging would be non-existent with Professor Fausto Rigo. His enthusiasm for this field, along with his kind and patient practical teaching sessions were invaluable. Additionally, his hospitality at all stages of this project, both in Venice and elsewhere, was tremendous and I value our friendship and future collaborations.

My thanks also extend to my research colleagues, friends and fellow "cave-dwellers": Dr Sayan Sen, Dr Ricardo Petraco, Dr Sukh Nijjer and Dr Nicolas Foin. I particularly want to acknowledge Dr Nijjer for his help during much of the practical work (especially the invasive data acquisition and exercise physiology work) and for his moral support and continual encouragement.

I also want to acknowledge and thank Jessica Parker – both in terms of help, support and enthusiasm but also in assisting me in trying to rid the Hammersmith Hospital of all its coffee!

A huge expression of gratitude must go to the Cath Lab staff at the Hammersmith Hospital both for their understanding and invaluable assistance. This research was often time consuming and I would not have achieved it without them and their patience.

I would like to thank the British Heart Foundation and the Imperial College Healthcare Charity for their financial support.

Finally, to the patients I have met, helped treat and had the privilege to follow up for long periods of time: it has been a pleasure, and often an inspiration, to know you and see you improve. Patient confidentiality precludes me listing names but my fondest memories go to the WWII soldier who crawled home from a German POW camp, my Irish friend who wanted to go back to his manual-labour-based work carrying his oxygen cylinder, the lady who always came to see me with her sister and the Welshman with whom I talked more about rugby than his health - you brightened my days.

CJB, December 2014

Abstract

Introduction: Coronary Wave Intensity Analysis (WIA) provides an invasive measure of energy transfer within the coronary circulation. I set out to derive a non-invasive measure of the backward expansion wave (BEW) responsible for coronary flow and assess it during exercise and in aortic stenosis (AS).

Methods: 17 patients (mean age 60, 11 male) with normal cardiac function underwent invasive LAD WIA calculation using a pressure- and flow-tipped wire. Non-invasive WIA was calculated immediately after angiography from simultaneous PW Doppler of the LAD and a suprasystolic-cuff derived measure of central pressure. Non-invasive WIA was then assessed in 9 healthy volunteers whilst exercising on an exercise bike, 25 patients with varying degrees of AS (AVmax range: 2.41-5.43m/s) and 29 patients before, after and at 6 and 12 months following aortic valve intervention for severe AS.

Results: Mean peak BEW was -14.7± 8.7x10^4 $Wm^{-2}s^{-2}$ invasively and -14.4± 8.2 $Wm^{-2}s^{-2}$ non-invasively and increased with exercise (at peak: -20.5±6.8$Wm^{-2}s^{-2}$, p=0.02) along with a rise in coronary flow (28.8cm/s to 42.1cm/s, p 0.06).

A significant correlation was noted with the BEW and AS severity, strongest when valvulo-arterial impedence was assessed (r=-0.66, p<0.001). In severe AS, a reduction in coronary flow (0.41 to 0.33m/s, p<0.01) and the BEW (-22.1 vs 10.9x$10^4$$Wm^{-2}s^{-2}$, p<0.01) was seen after intervention. With LVH regression BEW increased (-21.6±12.6x10^4 $Wm^{-2}s^{-2}$ at 6 months) without a significant change in coronary flow.

Conclusion: It is possible to construct a non-invasive measure of coronary WIA thus markedly increasing its applicability. Using this technique, the BEW is seen to increase during progressive levels of exercise accounting for the increase in coronary flow. The

BEW progressively climbs with increasing AS, falls to sub-normal levels after aortic valve intervention but then increases to normal levels with LVH regression.

Contents

LIST OF FIGURES

LIST OF TABLES

LIST OF EQUATIONS

ABBREVIATIONS

AS – Aortic Stenosis

AVR – Aortic Valve Replacement

BEW – Backward-travelling Expansion Wave

BSA – Body Surface Area

CFR – Coronary Flow Reserve

FCW – Forward-travelling Compression Wave

IVSd – IntraVentricular Septal wall thickness in diastole

IVSs – IntraVentricular Septal wall thickness in systole.

LAD – Left Anterior Descending artery

LMS – Left Main Stem

LV – Left Ventricle

LVEDD – Left Ventricular End Diastolic Dimension

LVEDP – Left Ventricular End Diastolic Pressure

LVEDS – Left Ventricular End Systolic Dimension

LVH – Left Ventricular Hypertrophy

LVOT – Left Ventricular Outflow Tract

MG – Mean Pressure Gradient

MRI – Magnetic Resonance Imagining

PRF – Pulse Repetition Frequency

PWd – Posterior Wall thickness in diastole

PWs – Posterior Wall thickness in systole

SAP – Systolic Arterial Pressure

SD – Standard Deviation

SEM – Standard Error of the Mean

SV – Stroke Volume

SVi – Stroke Volume Index

TAVI – Transcatheter Aortic Valve Implantation

TOE – TransOesophageal Echocardiography

TTE – TransThoracic Echocardiography

VTI – Velocity Time Integral

WIA – Wave Intensity Analysis

Zva –Valvulo-Arterial Impedance

1 INTRODUCTION: MYOCARDIAL ISCHAEMIA IN AORTIC STENOSIS AND THE APPLICATION OF WAVE INTENSITY ANALYSIS

1.1 Aortic Stenosis and Symptoms

Calcific aortic stenosis (AS) is the most common reason for aortic valve replacement (AVR) in developed countries and affects 2-3% of individuals by the age of 65(Lindroos et al., 1993). As the disease state progresses, it is associated with left ventricular hypertrophy (LVH), a process characterised by the enlargement of cardiac myocytes, accumulation of sarcomeric proteins and reorganisation of the myofibrillar structures(Yang et al., 2007). This is initially a compensatory mechanism to maintain an appropriate ejection fraction but ultimately results in myocardial ischaemia. This is reflected clinically as the well-recognised symptoms of aortic stenosis: chest pain, shortness of breath or syncope.

The occurrence of symptoms also leads to a rapid decline in prognosis and this is felt therefore to represent the onset of *significant* myocardial ischaemia and, uncorrected, leads to a decline in cardiac function(Ross and Braunwald, 1968) with a 50% mortality over the following 1-3 years(Ross and Braunwald, 1968, Caruthers et al., 2003, Leon et al., 2010). This marker of symptom-onset is therefore used to guide the need for aortic valve intervention(Bonow et al., 2008).

However, this apparent 'binary' nature of ischaemia aortic stenosis is not quite so straight-forward as even in asymptomatic patients there is evidence of myocardial ischaemia through exercise testing(Rafique et al., 2009), BNP levels(Rajani et al., 2010), exercise ejection fraction(Marechaux et al., 2007), peak aortic velocity or valve area(Rosenhek et al., 2010), and strain patterns(Kitai et al., 2011). Moreover, other studies have demonstrated that both mild and moderate aortic stenosis impart a higher risk of cardiovascular events than the background population(Horstkotte and Loogen, 1988, Kennedy et al., 1991, Otto et al., 1997, Rosenhek et al., 2004)

It is therefore perhaps not surprising that more recent studies have promoted the idea that asymptomatic aortic stenosis may not be so benign, particularly when very severe(Rosenhek et al., 2010, Kitai et al., 2011) and the merits of pursuing a more aggressive treatment strategy in these patients has been demonstrated(Kang et al., 2010), although strong evidence for this approach is lacking at present(McCann et al., 2011). Despite this, current guidelines would advocate the onset of symptoms as the most reliable marker of myocardial ischaemia and this is used to guide the need for aortic valve intervention as (Bonow et al., 2008, Vahanian et al., 2007).

1.2 CAUSE OF CALCIFIC AORTIC STENOSIS AND LEFT VENTRICULAR HYPERTROPHY

The concept of calcific aortic valve disease as a degenerative and unmodifiable process induced by long-term mechanical stress has now been revised. Recent studies have suggested that the calcification process in aortic valves is actively regulated(Yetkin and Waltenberger, 2009) with the observance of inflammatory (Akat et al., 2008) and neovascular (Mazzone et al., 2004) changes at a histological level. Aortic valve calcification is most likely initiated in a similar fashion to atherosclerosis as a "response-to-injury"(Rajamannan et al., 2002). For example, a correlation has been noted between aortic valve sclerosis (without valve leaflet restriction) and relative risk of death(Otto et al., 1999), a new coronary event(Aronow et al., 1999) or prognosis in patients who suffer with chest pain(Chandra et al., 2004). This initially promoted the idea that statins may be used in the treatment of aortic stenosis which was supported by retrospective studies (Chua and Kalb, 2006, Chan et al., 2010). Initial prospective work using atorvastatin failed to show a benefit on aortic valve calcification or velocity

(Cowell et al., 2005); however, a later study demonstrated a protective effect of rosuvastatin in terms of aortic valve gradient and area (Moura et al., 2007).

The process of myocardial hypertrophy is also a dynamic one. Left ventricular wall thickness has a constant relationship with its systolic pressure(Gaasch, 1979) and hypertrophy is considered one of the most important mechanisms in adapting to the haemodynamic overload of aortic stenosis allowing cardiac performance to be maintained despite these high outflow pressures(Grossman et al., 1975). Wall-stress can therefore be displayed mathematically as a relationship between pressure and wall thickness as in **Equation 1-1** so that as pressure increases, so does wall thickness(Gould and Carabello, 2003).

$$\text{Wall stress} = \text{Pressure} \times \text{Radius} / \text{Thickness}$$

EQUATION 1-1. WALL STRESS AND ITS RELATIONSHIP TO PRESSURE AND WALL THICKNESS

Myocytes make up 75% of the left ventricle by weight and their hypertrophy is seen in all conditions that produce either pressure or volume overload of the ventricles. Myocyte hypertrophy can be seen in various extreme physiological conditions where individuals undergo high levels of isometric exercises (such as weightlifters) without adverse prognostic implications. However, this hypertrophy is histologically well organised and there is no increase in collagen content, parenchymal cell loss or fibrosis in contrast to LVH secondary to AS or hypertension(Gradman and Alfayoumi, 2003).

The myocardial hypertrophy of LVH is mediated through an increase in sarcomere synthesis which reflects a switch to foetal gene expression and begins almost

immediately after pressure loading(Yetkin and Waltenberger, 2009). There is also evidence of apoptosis in both experimental and clinical cardiac hypertrophy(Yetkin and Waltenberger, 2009) and in those with severe AS and LVH(Galiuto et al., 2006). The presence of LVH increases cardiac morbidity and mortality(Villa et al., 2006) and in aortic stenosis LV mass predicts the presence of systolic dysfunction and heart failure independent of the severity of valvular obstruction(Kupari et al., 2005).

1.3 EVIDENCE FOR CORONARY MICROVASCULAR DYSFUNCTION IN AORTIC STENOSIS

Myocardial ischaemia results when cellular oxygen demand exceeds supply. In patients with severe aortic stenosis and angiographically normal coronary arteries, angina is reported in 30-40%(Julius et al., 1997) and this is one of the crudest demonstrations of the presence of ischaemia in aortic stenosis. Appropriately therefore, it is also a marker of severity and increases the risk of sudden death(Kelly et al., 1988).

Microvascular dysfunction is often expressed investigatively as coronary flow reserve (CFR), a measure of maximal flow capacity of the resistance vessels. It is defined as the maximal increase in myocardial blood flow above its resting level for a given perfusion pressure where the coronary vasculature is maximally dilated(Garcia et al., 2009). In the absence of epicardial (angiographically-demonstrable) disease, CFR reflects microvascular dysfunction(Kaufmann and Camici, 2005). It has been speculated that the microvascular dysfunction in severe aortic stenosis may be a major component in the progression to heart failure and may also allow ventricular arrhythmias to emerge(Levy et al., 1987).

Several investigative tools have been used since the late 1960s to demonstrate microvascular dysfunction in aortic stenosis as summarised below.

1.3.1 LACTIC ACIDOSIS PRODUCTION

Coronary microvascular dysfunction was initially noted in invasive studies of humans(Fallen et al., 1967) and animals(Griggs et al., 1973) with aortic stenosis and no angiographic disease. It was appreciated that these subjects had a relative increase in myocardial lactate production in response to pharmacological stimulation compared to controls.

1.3.2 THALLIUM-201 POSITRON TOMOGRAPHY AND HOLTER MONITORS

Thallium scans of patients with significant aortic stenosis often demonstrate perfusion deficits. However, 43% of the patients scanned in one study had normal coronary arteries at angiography(Kupari et al., 1992). ST segment shift has also been observed on 24-hour holter monitors of patients with LVH and normal angiograms suggesting episodes of ischaemia occurred over this period of time(Scheler et al., 1992).

1.3.3 THERMODILUTION AND INVASIVE DOPPLER TECHNIQUES

CFR, as obtained from the coronary sinus thermodilution technique, has been shown to be significantly reduced in patients with severe AS and anginal-symptoms compared to both asymptomatic patients with severe AS and controls(Julius et al., 1997). This value improved when reassessed 12 months after valve replacement(Eberli et al., 1991). Invasive coronary Doppler has also demonstrated a reduced CFR in AS with LVH measured at the time of aortic valve replacement using a brief occlusion of the Left Anterior Descending Artery (LAD) to generate hyperaemia(Marcus et al., 1982).

1.3.4 ECHOCARDIOGRAPHY

Echocardiography (largely, so far, transoesophageal - TOE) has been used to measure coronary flow in aortic stenosis. Patients with severe aortic stenosis have been

shown to have a higher peak diastolic coronary flow velocity compared with normal subjects (Meimoun et al., 2012) and an inverse relationship between peak systolic velocity and aortic valve gradient. It was also recognised that asymptomatic patients with aortic stenosis had a lower coronary velocity to mass index compared to symptomatic patients (Isaaz et al., 1994).

Additionally, Omran *et al*. demonstrated a liner relationship between aortic valve gradients and peak diastolic velocity with higher velocities in aortic stenosis patients with chest pain or syncope compared to those who were asymptomatic. This group also showed that peak diastolic velocity in patients with severe aortic stenosis and shortness of breath did not differ significantly from controls(Omran et al., 2011).

More recently, quantitative myocardial contrast echocardiography has shown that myocardial blood flow in the subendocardium but not subepicardium is reduced in patients with aortic stenosis(Galiuto et al., 2006). As assessed by this method, subendocardial blood flow improved immediately after aortic valve replacement (at 2 weeks) and was maintained in the long term (at 1 year)(Miyagawa et al., 2009).

The effect of transcatheter aortic valve implantation (TAVI) on coronary flow velocity has also been assessed using TOE and has demonstrated an immediate increase in coronary flow velocity after TAVI(Ben Dor et al., 2009) although this may reflect anaesthetic or iatrogenic-inotropic effects.

Stress echocardiography using adenosine demonstrated a reduced CFR in patients with severe aortic stenosis as well as highlighting an improvement in CFR and LVH six months after valve replacement (Hildick-Smith and Shapiro, 2000). Impairment

of the coronary flow reserve in these patients has been linked with aortic valve area and peak aortic gradient rather than the degree of LVH(Kume et al., 2004).

1.3.5 PET SCANNING

PET scanning is another novel way to assess the myocardial burden from AS. Studies have clearly demonstrated reduced myocardial perfusion and have even been able to confirm this is most severe in the subendocardial layer echoing the results found in experimental animal models of aortic stenosis(Vinten-Johansen and Weiss, 1980).

Using PET, the severity of CFR impairment has been linked to aortic valve area, imposed haemodynamic load and diastolic perfusion time rather than left ventricular mass(Rajappan et al., 2003, Rajappan et al., 2002), similar to those results found with TOE (Isaaz et al., 1994, Omran et al., 2011). PET scanning can also be used to distinguish types of low-flow, low-gradient aortic stenosis where a reduced CFR separates those with severe AS but preserved myocardial reserve from those with heart failure and low-output(Burwash et al., 2008).

1.4 CAUSE OF MYOCARDIAL ISCHAEMIA IN AORTIC STENOSIS

Several potential mechanisms have been suggested in the aetiology of myocardial ischaemia in aortic stenosis(Kingsbury et al., 2000). Some of these proposed concepts are based on studies of LVH induced by obstruction after the origin of the coronary vessels (e.g. though aortic banding or hypertension). Aortic stenosis obviously produces pressure changes before their origin so these results should be interpreted cautiously but the results remain interesting and may still be applicable to AS.

1.4.1 DECREASED DENSITY OF CORONARY RESISTANCE VESSELS IN HYPERTROPHIED MYOCARDIUM

Changes in the vascular bed do not seem to parallel myocyte growth in LVH. In pig(Breisch et al., 1986) and dog(Mueller et al., 1978) models of left ventricular hypertrophy with impaired CFR, anatomical studies showed hypertrophy causes a reduction in endomyocardial capillary density. Interestingly, a separate study has shown this phenomenon is less evident at one year suggesting there may be a lag, rather than absolute deficit, between LVH and new vessel growth(Bishop et al., 1996).

A similar relative reduction in cardiac vessel growth during hypertrophy has also been demonstrated in rats by assessing cardiac cyclic-GMP (cGMP) kinase levels; c-GMP is a protein involved in the regulation of vascular smooth muscle tone(Ecker et al., 1989). In humans, autopsy studies of patients with LVH due to aortic stenosis have shown a decrease in coronary capillary density in comparison to controls(Rakusan et al., 1992).

1.4.2 INCREASED PERIVASCULAR COMPRESSION DUE TO CHANGES IN MYOCARDIAL STRUCTURE AND A GREATER COMPRESSIVE EFFECT OF SYSTOLE

In humans, there is a linear correlation between coronary resistance and left ventricular end diastolic pressure (LVEDP) suggesting the importance of these external compressive forces(Gould and Carabello, 2003); however, the reduction in coronary reserve is proportionally greater than the increase in LVEDP reinforcing the multi-factorial nature of this problem. In the guinea pig model, the effect of perivascular compression, as well as the increase in the compressive effect of systole has been demonstrated to impact negatively on coronary flow reserve with LVH(O'Gorman et al., 1992).

Studies with PET scanning in adults pre- and post-aortic valve replacement for aortic stenosis have shown a strong correlation between CFR and the haemodynamic load on the left ventricle and haemodynamic severity of the valve stenosis. They did not find a relationship with left ventricular mass and go on to suggest microvascular dysfunction results predominantly from extravascular compressive mechanisms as well as changes in diastolic perfusion time (see 6)(Vinten-Johansen and Weiss, 1980, Rajappan et al., 2003).

1.4.3 INCREASED MUSCLE MASS

Obviously, the more muscle mass present, the higher the oxygen demands of the heart will be. On a relatively macroscopic level, the size of the large coronary arteries increases with LVH and after aortic valve replacement the arteries return to normal(Villari et al., 1992). Studies in animals and humans have suggested that the increase in size is not proportional to the increase in cross-sectional muscle mass creating a relative imbalance in oxygen supply and demand(Breisch et al., 1986, Schwartzkopff et al., 1992).

However, it is important to acknowledge that the increased oxygen demand from LVH and relative mismatch in supply play less of a role than once thought. This is illustrated by the fact that after an aortic valve replacement the left ventricle progressively remodels over a period of years(Monrad et al., 1988) but it is well recognised the angina and the risk of sudden death decrease instantly(Gould and Carabello, 2003). Additionally, the degree of LVH does not seem to bear relation to the development of anginal symptoms(Julius et al., 1997).

Furthermore, in animal models an 8% reduction in LV mass produced a significantly larger improvement in coronary flow reserve(Gould and Carabello, 2003).

Similar results have been obtained from PET scans of humans before and after aortic valve replacement(Carpeggiani et al., 2008b). This data may seem to conflict with the above correlation between LV mass and the presence of systolic dysfunction(Kupari et al., 2005); this likely reflects the multi-factorial nature of both CFR and heart failure in AS.

1.4.4 INCREASED DIFFUSION DISTANCE FROM CAPILLARY TO CENTRE OF HYPERTROPHIED MYOCARDIAL CELLS

It has also been suggested that as the myocytes increase in size, there is an increased diffusion distance from the capillary to the centre of the cell(Zhu et al., 1996, Just et al., 1996). Additionally, the pressure within the myocardial cells is increased(Carpeggiani et al., 2008b) and these factors will impair oxygen transfer. However, these findings are not supported in all studies(Anversa et al., 1986).

1.4.5 RELATIVELY LOW AORTIC PRESSURES

Classical teaching states that aortic stenosis is associated with a relatively low aortic pressure and a narrow pulse pressure(Purcell and Kalra, 2011). As the disease progresses and the ejection fraction falls, the pressure within the coronary sinus falls even further, exacerbating the ischaemic effects of AS(Skalidis and Vardas, 2008).

1.4.6 PROLONGATION OF SYSTOLE WITH SHORTENING OF DIASTOLE

PET scans of patients with LVH pre- and post-aortic valve replacement for AS have demonstrated interesting results. These studies have shown that the changes seen in the coronary microcirculation are not directly dependent on the regression of left ventricular mass but suggest an increase in diastolic perfusion time to be one of the

main mechanisms contributing to this(Rajappan et al., 2003, Rajappan et al., 2002). This is likely exacerbated further by abnormal relaxation during diastole(Paulus et al., 1988).

1.4.7 ENDOTHELIAL DYSFUNCTION

Structural changes in coronary vasculature may not fully account for the reduction in coronary reserve and there may in fact be a change at the endothelial level as well. For example, coronary reserve has been shown to be reduced in hypertensive patients(Antony et al., 1993, Brush et al., 1988) and animal models(Rodriguez-Porcel et al., 2006) prior to the development of LVH. Rats with LVH have been shown to have a reduced production of coronary nitric oxide synthase, another reflection of endothelial dysfunction(Crabos et al., 1997). Using explanted coronary arteries from a guinea-pig model of LVH, Mcgoldrick *et al.* confirmed that coronary vessels from hypertrophied hearts have impaired relaxation to endothelial-dependent and independent agents(McGoldrick et al., 2007).

Additionally, LVH also results in a greater propensity to anaerobic metabolism due to an attenuated microvascular response to hyperaemia(Kingsbury et al., 2000, McAinsh et al., 1995). They are therefore more vulnerable to the effects of myocardial ischaemia as they are unable to recover as well from such insults. For example, in dogs with LVH, occlusion of the circumflex artery resulted in a much larger area of infarction than controls(Koyanagi et al., 1982).

1.4.8 INCREASE IN WALL THICKNESS TO LUMEN RATIO

Structural changes in the vascular bed as a result of left ventricular hypertrophy will also affect oxygen handling and transfer. A number of studies have demonstrated an increase in the thickness of the coronary vessel wall in relation to the lumen size in left ventricular hypertrophy in both guinea pigs(Kingsbury et al., 2000, Crabos et al., 1997,

Mihaljevic et al., 2003) and rats(Brilla et al., 1991b, Kalkman et al., 1996, Tomanek et al., 1985). However, this finding has not been reproduced in ventricular biopsies taken from humans with LVH(Opherk et al., 1984) or in pig models(Breisch et al., 1986). More specifically, autopsy specimens from patients with LVH secondary to aortic stenosis do not show intra-myocardial arteriole wall thickening but do in patients with LVH secondary to hypertension.

1.5 Summary: Potential causes of myocardial Ischaemia in aortic stenosis

Myocardial ischaemia is evident in patients with aortic stenosis as demonstrated by a wide variety of investigative tools. This is the cause of angina in aortic stenosis with normal coronary arteries and given the poor prognosis related to this symptom it is almost certainly connected with arrhythmias, heart failure and risk of sudden death.

Aortic stenosis leads to the development of LVH which increases the oxygen requirements of the myocardium out of proportion to that of coronary vessel expansion. However, it has become apparent that this only plays a small part on the aetiology of myocardial ischaemia particularly given the lack of a relationship between LV mass and CFR in some studies.

Possibly the more important factors in the development of myocardial ischaemia have been demonstrated through PET scanning and include the extravascular pressure effects as well as a reduction in diastolic perfusion time. Other factors such as reduced capillary density, increased oxygen diffusion distance and low coronary sinus pressure are all likely to play a role.

Coronary endothelial dysfunction is obvious in hypertension-induced LVH but it is not completely clear if this can be applied to AS-driven LVH given the pressure of hypertension originates after the coronary sinuses. Likewise, there is evidence to show that thickening occurs within the walls of coronary vessels in LVH secondary to hypertension but this has not been reproduced consistently nor has it been demonstrated in aortic stenotic patients and therefore may not be involved in myocardial ischaemia in AS.

1.6 Application of Coronary Wave Intensity Analysis in Aortic Stenosis

Despite these interesting findings there are some limitations with these investigative methods, particularly when measuring coronary flow rate and coronary flow reserve alone in patients with aortic stenosis. Whilst changes in flow patterns can both demonstrate and *quantify* the burden aortic stenosis places on the myocardium, it is unable to *qualify* the origin of this burden. The technique of wave intensity analysis is a solution to this issue. Using simultaneously acquired measures of pressure and flow it is able to ascertain both the magnitude of force acting on coronary flow blood as well as separate and sub-qualify the force's originating location. In disease states where coronary anatomy is not the primary issue and the problem is one at the myocardial level, this obviously has a profound advantage in terms of acknowledging the burden and effect of myocardial disease. The primary focus for this thesis therefore is the application of wave-intensity analysis to patients at varying stages in the management of their aortic stenosis.

1.7 APPROACH

There were several arms to this research and they are divided by chapter accordingly:

1. *CONSTRUCTION OF NON-INVASIVE WAVE-INTENSITY ANALYSIS*

Aortic stenosis is a continually evolving condition. Over time the burden placed on the myocardium increases. After aortic-valve intervention there is a rapid and sudden decline in outflow-tract obstruction. Further changes occur at the myocardial level after valve intervention with a gradual regression of left ventricular hypertrophy. In patients in whom heart failure ensues before aortic valve intervention the force generated by the myocardium declines despite a persistent high outflow tract obstruction.

Given the dynamism of aortic stenosis I felt it would be very useful to construct and validate a measure of wave-intensity that could be obtained non-invasively without the need for invasive coronary pressure and flow-tipped wires. This would allow several measurements to be obtained from the same individual following intervention or the passage of time.

2. *INVASIVE WAVE INTENSITY ANALYSIS IN AORTIC STENOSIS AND WITH TRANSCATHETER VALVE THERAPY*

Transcatheter aortic valve implantation (TAVI) allows peri-operative invasive measures of coronary physiology both before and after valve implantation. It also does not involve dissection through the pericardium or cardiopulmonary bypass and so the natural cardiac physiology is more accurately preserved than with conventional surgery. Therefore it is possible to obtain accurate invasive wave intensity in patients with severe aortic stenosis before and after valve implantation. Additionally, the TAVI procedure requires the presence of a temporary pacing wire and this could be used to

manipulate heart rate and therefore mimic exercise. I therefore set out to perform invasive wave-intensity analysis peri-procedurally in severe aortic stenotic patients undergoing TAVI.

3. *NON-INVASIVE WAVE INTENSITY ANALYSIS IN PATIENTS AFTER VALVE IMPLANTATION*

After valve replacement there is a continual regression of left ventricular hypertrophy with time, most evident in the first 6 months but also at 1 year. Previous work has demonstrated that the wave-intensity profile in patients with myocardial hypertrophy but structurally normal hearts to be unfavourably altered. Therefore I was interested to learn if the profound regression of left ventricular hypertrophy following aortic valve replacement would result in a change in the wave-intensity profile in patients undergoing either TAVI or conventional valve replacement. To this end, using non-invasive wave-intensity assessments I aimed to follow up these patients for one year after valve intervention.

4. *NON-INVASIVE WAVE INTENSITY ANALYSIS IN PATIENTS WITH MILD AND MODERATE AORTIC STENOSIS*

I also wished to use non-invasive wave intensity to measure the effect of lesser outflow tract obstructions on its profile. I therefore recruited a number of patients with milder versions of the disease and preserved left ventricular function in order to make this calculation. I was thus able to calculate the relationship between outflow tract obstruction and the resultant coronary wave-intensity profile.

1.8 OVERALL GOAL

My overall goal was therefore to construct an accurate picture of the progression of aortic stenosis and the effect of treatment on the wave-intensity profile and to ascertain whether this tool could be applied to the clinical population at large.

2 Construction of Non-Invasive Wave Intensity Analysis

2.1 INTRODUCTION

2.1.1 BACKGROUND: WAVE INTENSITY ANALYSIS

A wave is a disturbance propagated through a medium with an exchange between kinetic and potential energy. Inherent to its definition is the fact that it travels at speeds faster than the underlying medium's own velocity(Sun et al., 2000). In the cardiovascular system, the medium in question is blood and energy is exchanged between the kinetic force generating blood flow and the potential energy in the walls of the expanding elastic vessels.

2.1.2 WAVE INTENSITY ANALYSIS IN NON-CORONARY VASCULAR SYSTEMS

Wave intensity analysis is a mathematical approach to quantify and qualify this energy transfer. At its most fundamental level, it is produced from the first derivatives of pressure and flow across the time (as opposed to frequency) domain; it is therefore more readily applicable to the vascular beds of much of the cardiovascular system than Fourier-based models. Accordingly, it has been used to investigate ventricular-vascular physiology in sheep(Penny et al., 2008), coronary(Sun et al., 2000), aortic(Khir and Parker, 2005), pulmonary(Hollander et al., 2001), venous(Smiseth et al., 1999) and intra-cardiac energy transfer(Flewitt et al., 2007) in dogs, and the effects of intra-aortic balloon pump-drive couterpulsations in pigs(Lu et al., 2012). In humans it has been applied invasively to the aorta and carotid arteries in healthy and disease states(Manisty et al., 2009).

Whilst wave-intensity is a therefore useful tool in all vascular circuits, it is particularly useful in the coronary circulation where the force generating blood flow could originate from either end of the arterial tree. Initial work in dogs by Sun *et al.* identified a

backward-travelling compression wave during isovolumetric contraction that increased coronary pressure and decreased coronary flow as well as a forward-travelling compression wave that occurred after aortic valve opening (Sun et al., 2000, Sun et al., 2004). In the human coronary circulation, seminal work by Davies *et al.* further subdivided the cardiac cycle wave-intensity profile into six waves (Davies et al., 2006a). The magnitudanally-dominant waves were the forward-travelling compression wave (FCW) which is generated by the systolic ejection of blood and the corresponding rise in aortic pressure, and the backward-travelling expansion wave (BEW) which is formed from myocardial relaxation and a resultant 'suction' effect being applied to the coronary circulation retrogradely from its distal origin. Of these two, the latter is responsible for generating myocardial blood and accordingly coincides with the acceleration of coronary blood flow in early diastole. Further work also demonstrated differences in the wave-intensity pattern of the right versus left coronary system accounting for the different flow patterns and values of these arteries but again with ascription of coronary flow to the backward-expansion wave (Hadjiloizou et al., 2008).

Invasive coronary wave-intensity analysis has now been applied to various disease states. In patients with left-ventricular hypertrophy but no valvular pathology, the backward-travelling expansion wave is attenuated implying a reduction in the efficiency of energy transfer(Davies et al., 2006a) which may explain why myocardial hypertrophy is associated with reduced coronary vasodilator capacity(Hamasaki et al., 2000). Coronary wave-intensity has also been used to demonstrate the likelihood of functional myocardial recovery following myocardial infarction using late-gadolinium MRI before and after revascularisation(Silva et al., 2012). Additionally, using wave-intensity analysis Sen *et al.* have demonstrated a portion of the cardiac cycle with minimal

coronary resistance that has aided in the construction of an adenosine-free pressure-based assessment of coronary stenosis (Sen et al., 2012).

2.1.3 NON-INVASIVE WAVE INTENSITY ANALYSIS IN NON-CORONARY BEDS

Traditionally, the simultaneously acquired measurements of coronary pressure and flow necessary for wave-intensity analysis have been recorded invasively. However, recent work has demonstrated that it is possible to construct wave-intensity in the peripheral arterial system using non-invasive methods. Although it is often difficult to measure intra-vascular pressure changes non-invasively, the change in area of the vascular wall can be successfully used as a surrogate. For example, in healthy human participants wave-intensity has been measured from the radial, carotid and brachial arteries using applanation tonometry and pulse-wave Doppler (Zambanini et al., 2005).

In the carotid artery non-invasive wave-intensity can be useful in distinguishing non-obstructive hypertrophic cardiomyopathy from hypertension-driven left ventricular changes (Li and Guo, 2013) and in patients with heart failure a delay and reduction in the magnitude of the systolic compression wave, combined with an increase in the reflective wave is seen compared to controls (Wen et al., 2010)

In patients randomised to receive amlodipine rather than atenolol based blood pressure therapy, carotid pressure is lower in the amlodipine treatment arm and wave-intensity demonstrated this reduction to be due to a reduction in wave reflection(Manisty et al., 2009). In the cerebral circulation, non-invasive wave intensity, constructed from carotid artery diameter and velocity has been useful in delineating cerebrovascular tone(Bleasdale et al., 2003).

Other imaging modalities such as MRI have also been used to calculate wave intensity by assessing area and velocity changes in the aorta(Biglino et al., 2012b) and applied to patients with congenital cardiac abnormalities to demonstrate unfavourable wave profiles(Biglino et al., 2012a).

2.1.4 Variables required for non-invasive calculation of Coronary Wave Intensity

The previously described invasive techniques of measuring coronary wave-intensity analysis have relied on simultaneously acquired measures of coronary flow (*variable 1*) and pressure (*variable 2*). First derivatives of these values are used in the single-point equation for the calculation of wavespeed (*variable 3*) as well as the construction of separated wave-intensity. The other variable required in this latter calculation is an estimate of the density of blood which is taken as 1050 kg m^{-3} (*variable 4*). Therefore, in order to replicate this calculation non-invasively on the coronary system, non-invasive measures of coronary pressure and flow are required. An alternative to pressure would be an estimation of coronary artery vessel size changes in a similar fashion to tonometrically-obtained wave-intensity; however, given the relatively small size of the coronary arteries, this was unlikely to be achievable.

I hypothesized therefore that it would be possible to obtain non-invasive coronary wave-intensity using transthoracic echocardiography to assess coronary flow and suprasystolic brachial pressure waveforms to estimate coronary pressure.

2.2 VARIABLE 1: ACCURATELY OBTAINING CORONARY FLOW NON-INVASIVELY

2.2.1 INTRODUCTION - ECHOCARDIOGRAPHIC ASSESSMENTS OF CORONARY FLOW

2.2.1.1 Historic First Assessments

Direct visualisation of the left main stem has been recognised as a feasible technique for over 20 years and initial studies used trans-oesophageal echo (TOE) were able to demonstrate stenoses through simple visual recognition(Taams et al., 1988).

Echocardiography was then applied to assess coronary flow reserve. The earliest work used TOE to assess proximal coronary artery flow before and after dipyridamole injection. In 9 patients with angiographically normal coronary anatomy the CFR increased with dipyridamole whereas in 6 patients with significant coronary disease, this did not occur (Iliceto et al., 1991) .

A further study comparing 16 patients with significant LAD disease to patients with minor (<30%) or no significant LAD disease demonstrated a CFR of <2.3 to be highly sensitive (88%) for the detection of underlying significant disease and in fact was more sensitive than wall motion analysis (75%). A combination of both CFR and wall motion assessment produced sensitivities of detecting underlying coronary disease of 94%(Hutchison et al., 1996).

Similar results were also achieved using adenosine-driven stress. A CFR of >2.1 had an 86% sensitivity and 79% specificity of predicting the absence of LAD disease in 49 patients(Redberg et al., 1995). Using dobutamine and a CFR cut-off of 1.81, a further study suggested that its sensitivity was equal to regional wall motion assessment in predicting LAD disease in 39 patients with no disease compared to 18 patients with

significant disease; it was also more sensitive in detecting minor (0-70% by angiography) disease in a subset of 21 patients(Stoddard et al., 1995).

2.2.1.2 Transthoracic assessment and atherosclerotic application

Early work suggested measuring coronary flow using transthoracic echocardiography was only possible in a minority of patients(Fusejima, 1987). However, its applicability increased following improvements in echocardiography(Ross et al., 1990, Rigo, 2005) particularly the introduction of second harmonic imaging (allowing better definition of smaller structures), high frequency transducers (up to 8 MHz in second harmonic) and contrast(Caiati et al., 1999). It was then possible to measure coronary flow reserve in the distal LAD; a failure of peak and mean coronary velocity to rise during hyperaemia was seen in patients with significant disease of this artery (Hozumi et al., 1998b).

Additionally, CFR as assessed by TTE Doppler normalised in 45 patients following LAD stenting of significant coronary lesions(Pizzuto et al., 2001) and was able to predict the development of LAD-restenosis in 53 PCI patients followed up for a period of 6 months(Ruscazio et al., 2002). Similar to TOE results, a combination of CFR assessment with wall motion analysis allows a higher sensitivity for ischaemia compared to wall motion analysis alone in stress echocardiography using a transthoracic probe(Rigo, 2005). After acute anterior myocardial infarction, a low CFR has been shown to predict poor LV recovery and a higher likelihood of adverse in-hospital events(Meimoun et al., 2009).

More large scale studies have now been published reflecting the rapidly increasing applicability of this technique. In 4313 patients, a CFR ≤ 2 was shown to be a strong independent predictor of mortality and interestingly conferred additional prognostic value over wall motion analysis(Cortigiani et al., 2012).

2.2.1.3 Non-atherosclerotic application

2.2.1.3.1 Non-ischaemic dilated cardiomyopathy

In 129 patients with a dilated cardiomyopathy of unknown aetiology and normal coronary arteries, a poor CFR (<2.0) as assessed by dipyridamole-stress transthoracic echocardiography is seen in up to 64% of patients and is a predictor of adverse events (defined as worsening of heart failure symptoms or death)(Rigo et al., 2006).

2.2.1.3.2 Hypertrophic Cardiomyopathy

Likewise, an abnormal CFR assessed by Doppler echocardiography is also a marker of poor outcome in hypertrophic cardiomyopathy (defined as LA dilatation, development of AF, hospitalization for unstable angina, ICD insertion, PPM insertion) (Rigo et al., 2007).

2.2.1.3.3 Coronary Syndrome X

An abnormal CFR (mean 1.21) from transoesophageal and transthoracic imaging has been demonstrated in patient with coronary syndrome X compared to asymptomatic controls (Zehetgruber et al., 1995, Galiuto et al., 2007, Rigo, 2005).

2.2.1.3.4 Metabolic Syndrome

33 patients with multiple cardiovascular risk factors (hypertension, diabetes, obesity, impaired glucose tolerance) without coronary artery disease were compared to controls and shown to have an abnormally reduced CFR (mean 2.2 vs. 2.5)(Pirat et al., 2008).

2.2.2 ACCURATELY OBTAINING NON-INVASIVE CORONARY FLOW: METHODS

A good comparison between CFR from coronary Doppler and CFR measures from coronary flow wires (25 patients with a mix of LAD disease)(Caiati et al., 1999) and PET

scanning (36 patients)(Daimon et al., 2001) has previously been demonstrated in experienced hands. To train myself to a level where coronary flow can be accurately measured to such a standard I sought to obtain first hand teaching from real-world experts in this skill who perform non-invasive CFR on a regular basis(Rigo, 2005, Rigo et al., 2007, Rigo et al., 2006, Rigo et al., 2008, Rigo et al., 2010, Cortigiani et al., 2012). It is estimated that it takes between 80 and 100 scans before an operator can reliably obtain flow signals from the left anterior descending artery but ultimately with persistence it can be achieved in up to 95-98% of patients(Rigo, 2005). With further experience, imaging of other sections of the LAD or the distal right coronary artery is even possible(Rigo, 2005, Lethen et al., 2003b).

However, one practical difficulty is that the majority of operators perform LAD assessments for the purposes of CFR calculations during stress echocardiography. They are therefore primarily focused on obtaining peak values but are less concerned in obtaining a 'clean' flow signal envelope for the entire cardiac cycle. To focus on obtaining such a clear coronary flow envelope, particularly in the region of early diastole that is required for the calculation of the backward-expansion wave is therefore a skill unpractised worldwide. It therefore required an adaption and modification of the existing technique for imaging the left anterior descending artery.

2.2.2.1 Echocardiographic Machine Choice

Initial measurements were attempted with a Phillips ie33 echocardiography machine. Whilst this machine is capable of producing excellent transthoracic and transoesophageal images it was not designed to obtain coronary flow. Therefore, appropriate modifications were made to its parameters for both visualising and performing pulse-waved analysis of the artery (Table 2-1). Despite these changes, it

often remained challenging to assess the period of coronary acceleration cleanly due to a high level of background noise in some patients.

However, I was able to take the opportunity to use a machine more geared towards coronary flow imaging - the Esaote MyLabTwice. This machine has been developed in collaboration with experts in the field of coronary artery imaging and consequently has inbuilt parameters designed to optimise coronary flow analysis. The images obtained on this machine were of a more interpretable quality for non-invasive wave intensity analysis (Figure 2-1).

Probe delivery frequency	Colour Doppler PRF	Wall filters	Pulse Doppler Filters	Focus
4-8Mhz as 2nd harmonic	15-25cm/s	High	Low	On

TABLE 2-1. Echocardiographic settings to optimise lad interrogation(RIGO ET AL., 2008)

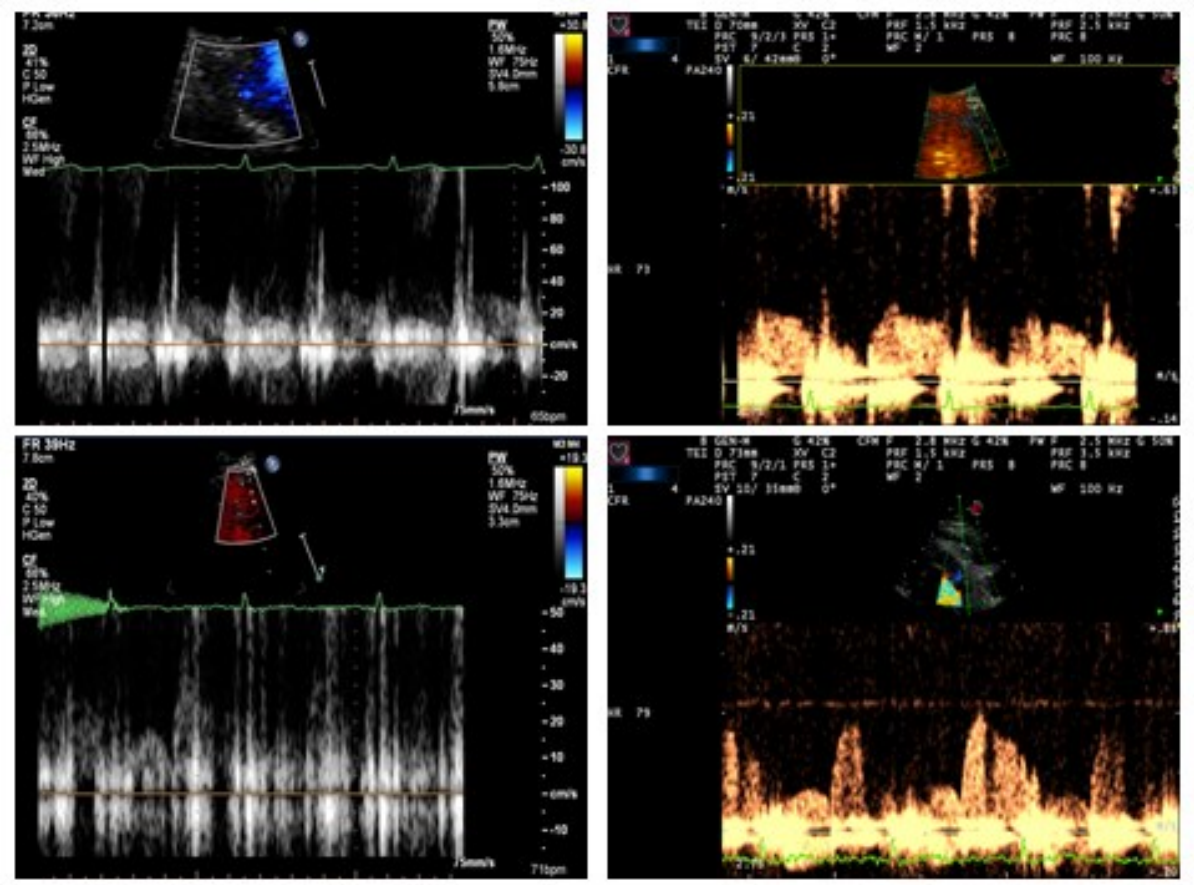

Figure 2-1. Pulse-wave Doppler of the left anterior descending artery in two patients using different machines.

The Phillips ie33 demonstrated in the left hand panels versus the Esaote Mylabtwice on the right. The noise is much less with the esaote machine allowing easier analysis.

2.2.2.2 Views required for coronary flow analysis

Echocardiographic coronary flow assessment is not usually possible in any of the standard echo views. The most appropriate view for visualising the LAD is described as a modified 2- or 3-chamber view. By moving the probe away from the apex and towards the parasternal long axis view and maintaining the position of the interventricular septum in the centre of the screen the mid-LAD is brought into view(Rigo et al., 2008).

Other views that were found occasionally helpful were the three chamber view where the proximal LAD can sometimes be seen above the aortic valve (Figure 2-2) or a modified 4 chamber view to visualise the distal LAD (Figure 2-3). Alternatively, a slightly modified parasternal short axis view may also be helpful at times for imaging the proximal LAD or Left Main Stem (LMS) (Figure 2-4).

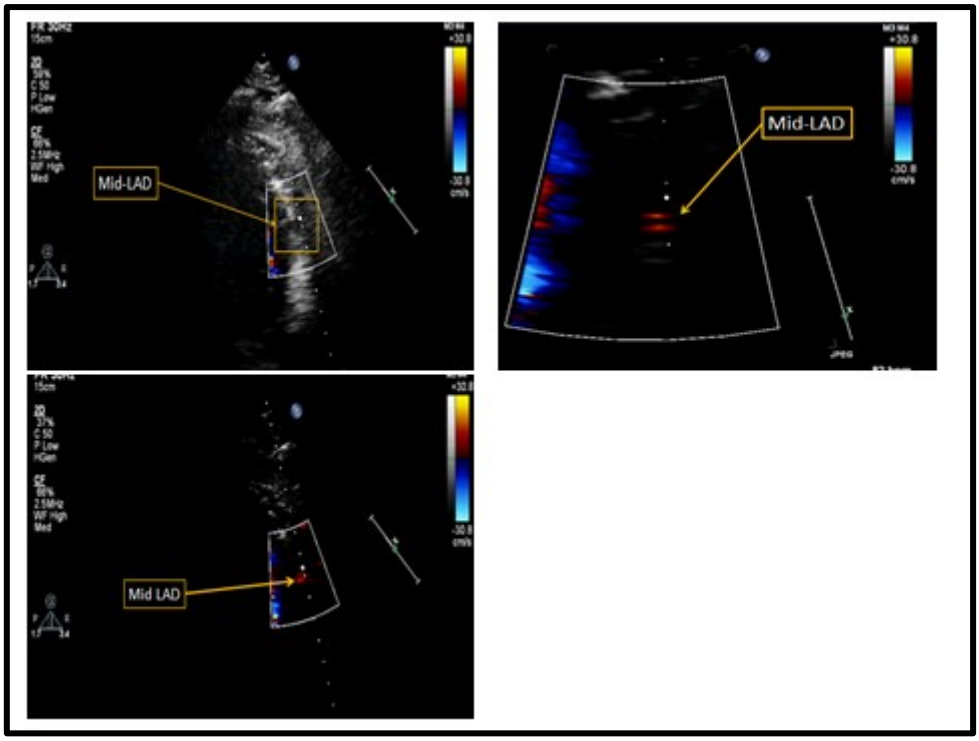

FIGURE 2-2. Mid-LAD visualised using a modified 3 chamber view.

Initial view (upper left panel), view with reduced gain (upper right panel) and zoomed view with reduced gain (lower panel).

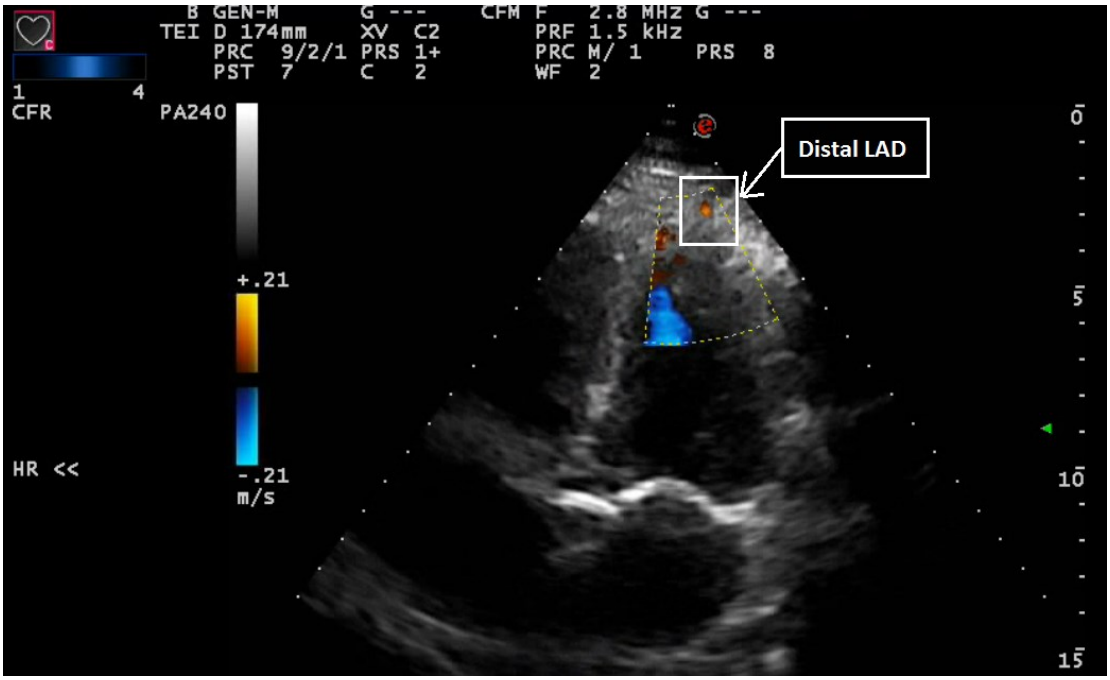

FIGURE 2-3. Distal LAD visualised through a modified 4-chamber view

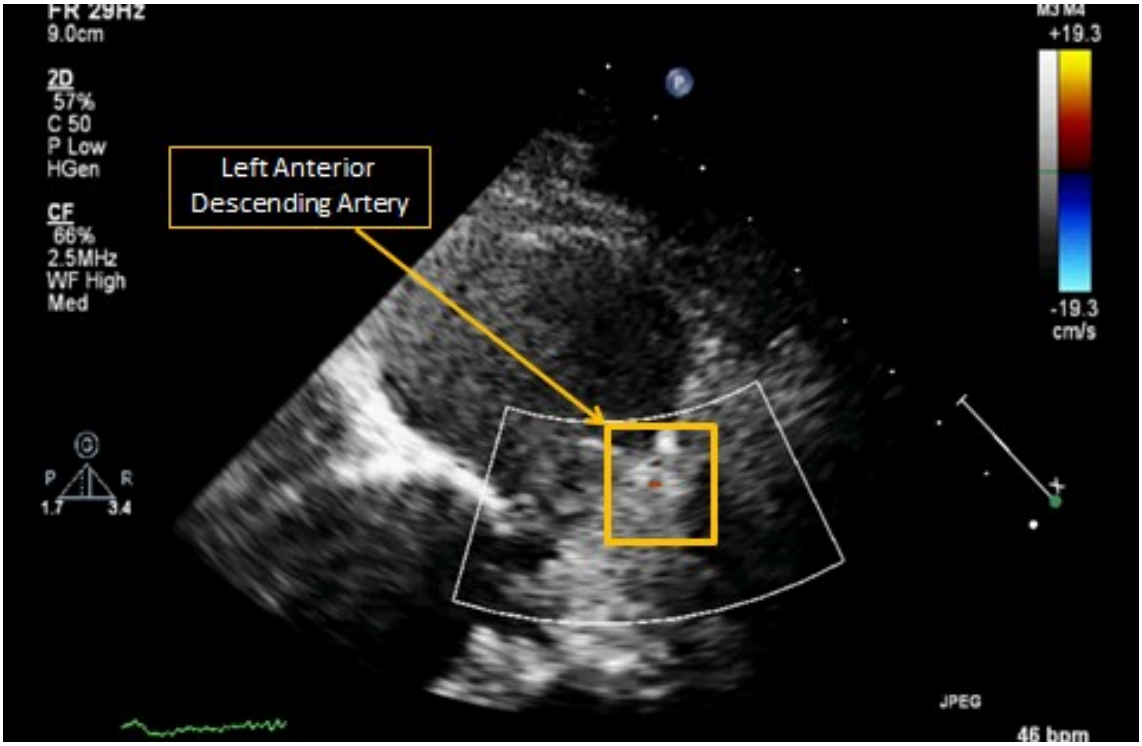

FIGURE 2-4. Proximal LAD visualised through a modified parasternal short axis view

2.2.2.3 Echocardiographic Settings required for Coronary Flow Analysis

2.2.2.3.1 Visualising the Left Anterior Descending Artery

Conventional colour flow will not demonstrate the coronary artery due to the lower velocity at which blood moves through the coronary tree compared to the cardiac chambers. It is important to lower the colour pulse repetition frequency (PRF) to allow this visualisation. Unfortunately, this obviously increases the colour flow generated by myocardial tissue, intercostal vessels and blood moving through the cardiac chambers and it takes considerable practice to recognise coronary flow amongst these other colours.

It is sometimes easy to mistake an intercostal vessel for a coronary artery. However, it is easy to distinguish the two due to the characteristic flow profile from pulsed-wave Doppler of an intercostal artery. Likewise, when the PRF settings are reduced, the myocardium can appear awash with colour, particularly in dynamic healthy ventricles. With experience it becomes possible to visualise the coronary artery amongst this movement; chances of achieving this are increased by reducing the gain settings. Additionally, the majority of coronary flow is seen during diastole compared with the majority of the systolic motion of the myocardium (Figure 2-5). Identification of coronary flow according to the cardiac cycle also a difficult skill to master particularly when the patient's heart rate is raised but with time it is possible. Myocardial velocity is usually higher than coronary therefore the colour patterns are different, again which can be recognised with experience.

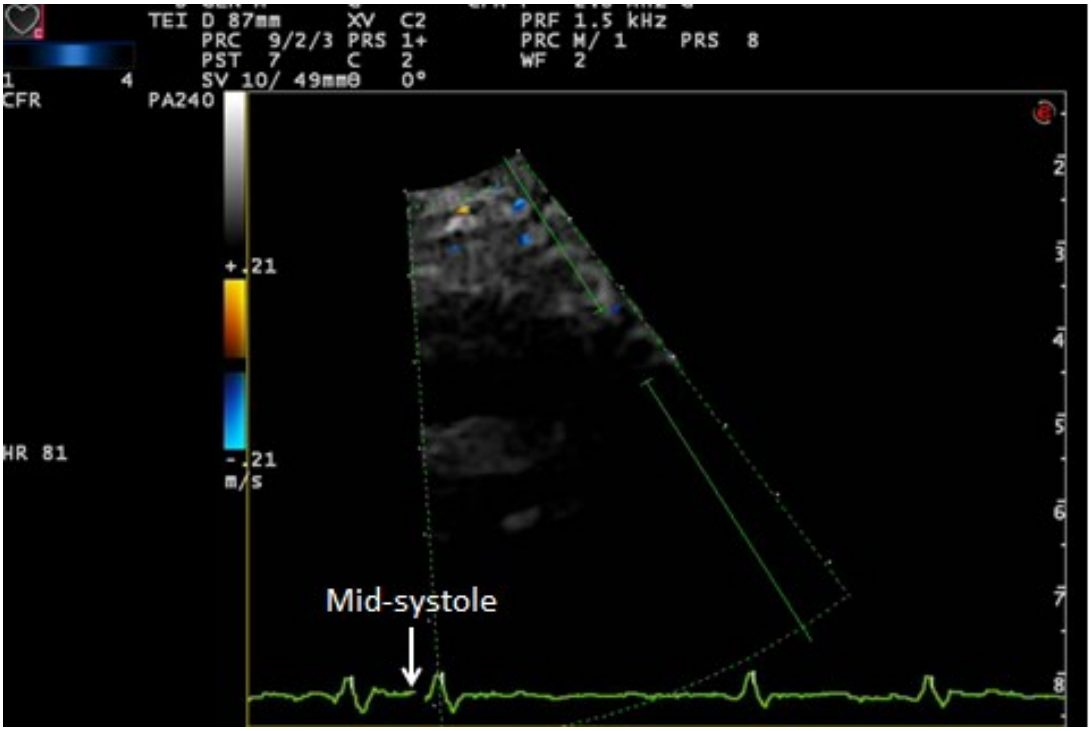

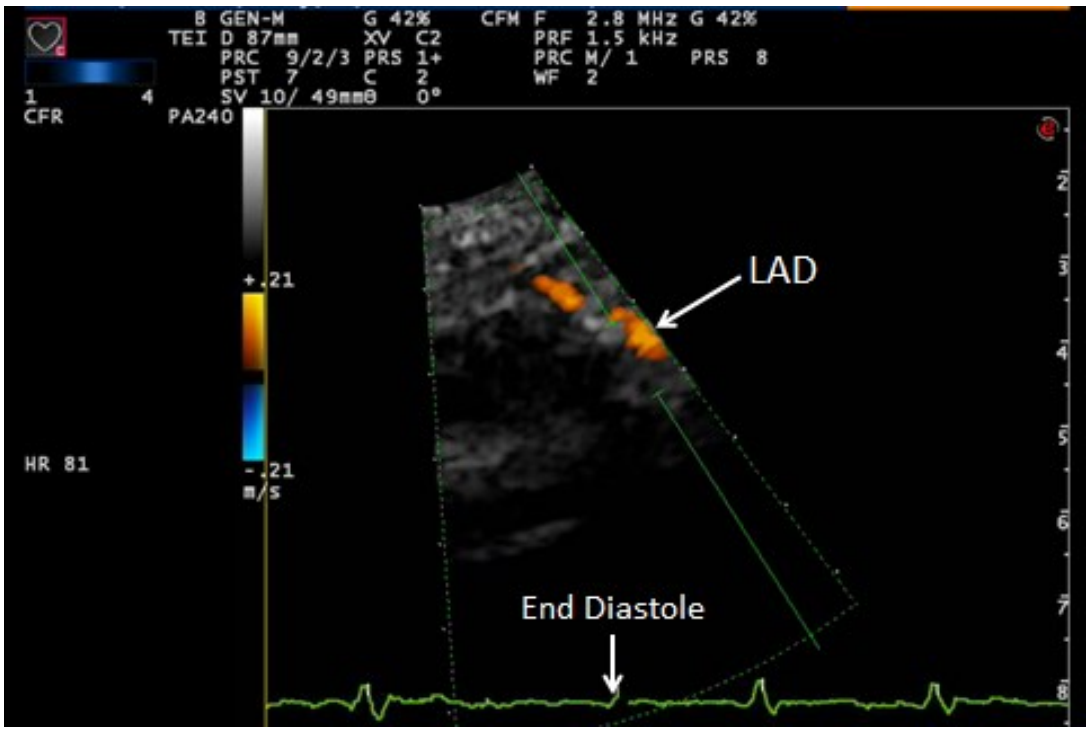

FIGURE 2-5. Coronary flow during the cardiac cycle.

Flow is most prominently seen during diastole (lower panel) as opposed to systole (upper panel), helpful for identification of coronary artery flow.

Finally, when assessing coronary flow in the views described above it is possible to confuse coronary flow with flow within the tip of the right ventricle. Again, a characteristic flow profile is produced to aid in this distinction. The usual solution to this issue is to tilt the probe to point more cranially where the LAD should then appear.

Further problems arise in some patients who have relatively low LAD velocities. It may only be possible to recognise this when one or two pixels are seen in diastole of an appropriate intensity. In these cases, the colour PRF and gain need to be further reduced in conjunction with depth alterations to bring out the shape and direction of the coronary artery. This obviously makes the background myocardial colour-noise even more intense but is often a necessary sacrifice (Figure 2-6).

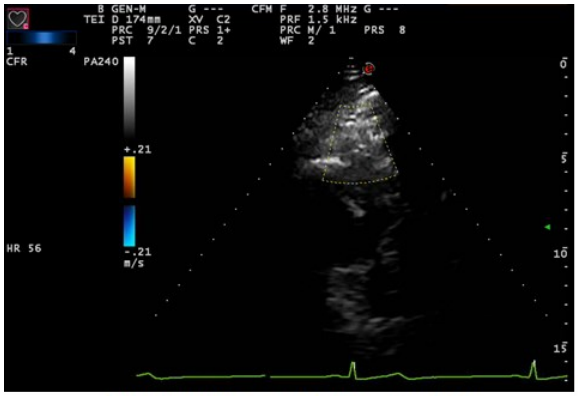

1. Present PRF, preset depth, normal gain

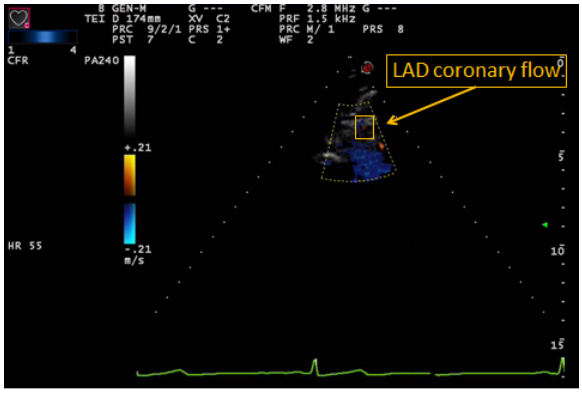

2. Present PRF, preset depth, reduced gain

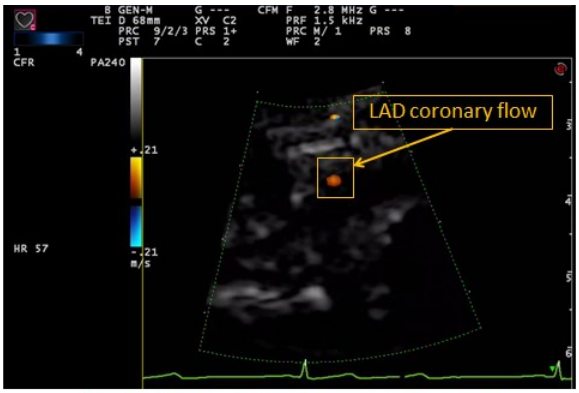

3. Present PRF, increased depth, reduced gain

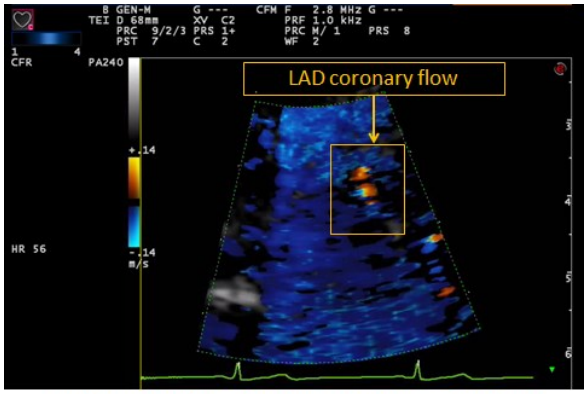

4. Reduced PRF (14m/s), increased depth, reduced gain

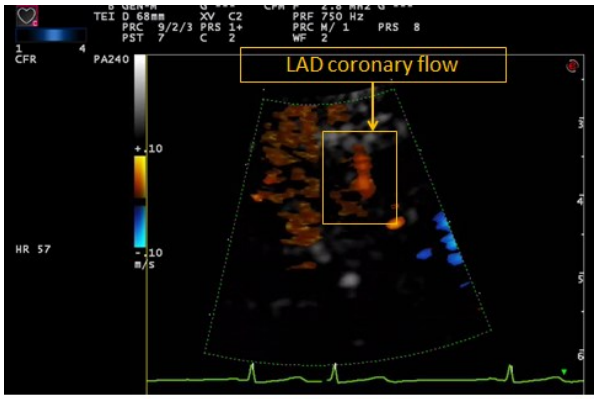

5. Reduced PRF (10m/s), increased depth, reduced gain

FIGURE 2-6. Optimisation of LAD flow demonstrated by manipulation of depth, gain and PRF.

2.2.2.4 Active optimisation of coronary flow profile

Once the LAD is visualised the coronary flow profile can be assessed using pulsed-wave Doppler. The first step in achieving a good flow envelope is to position the probe in as appropriate a plane of scanning as possible. This can usually be achieved by maintaining the coronary artery in the centre of the screen and bring the probe across the chest akin to the rotational technique required to switch from parasternal long- to short-axis whilst maintaining the location of the aortic valve.

One problem inherent to coronary artery analysis, particularly in dynamic young ventricles is the excursional distance the coronary artery travels during one cardiac cycle. In patients with heart failure or aortic stenosis, their ventricles become stiffer and less mobile making assessment their flow profiles more attractive. To combat the problem of the left anterior descending artery moving in and out of the pulse-wave envelope, a large sampling area is required. The pre-set Esaote size is 10mm and this can be reduced (in more static hearts) or (although rarely necessary) increased if required.

If there is a lot of horizontal (rather than lateral movement) of the coronary artery through the pulse-wave envelope, various chronological-sections of the coronary envelope can be visualised individually and amalgamated. Alternatively, to focus on the backward expansion wave, it may be most appropriate to position the sampling area at the point in which the coronary artery is highlighted in the change from systole to diastole (Figure 2-7 and Figure 2-8).

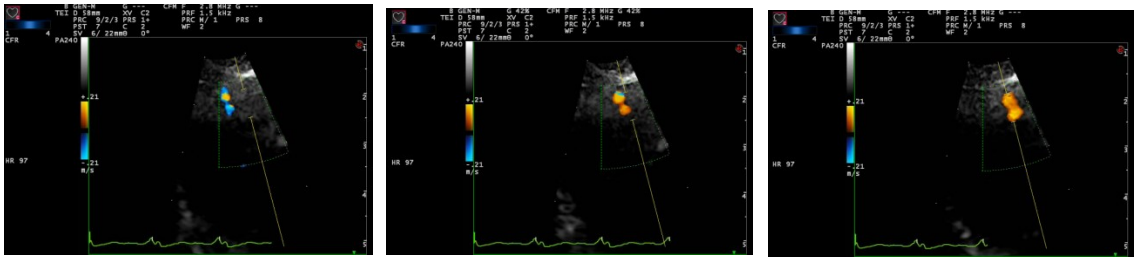

FIGURE 2-7. Example of a coronary artery with a significant amount of lateral excursion.

The pulse wave Doppler is here position to capture the end of diastole / start of systole and moving it to the left would capture early diastole to build a coherent picture.

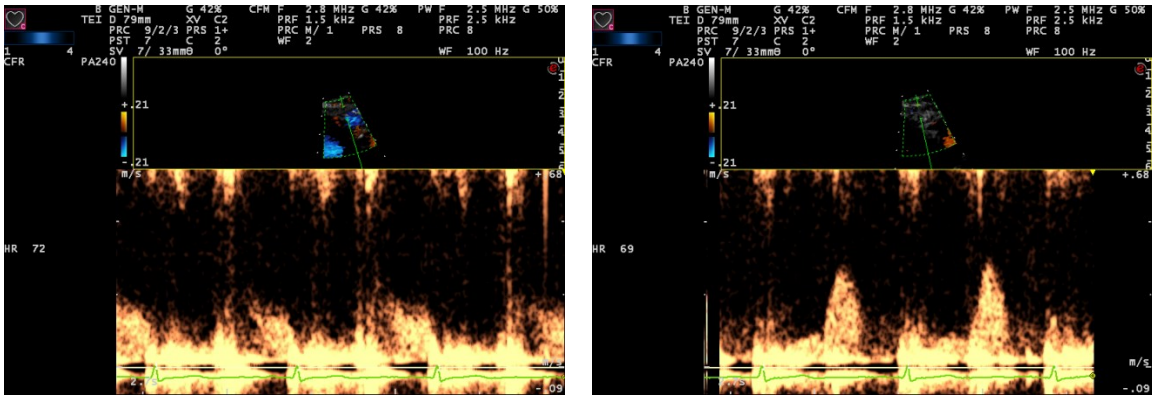

FIGURE 2-8. Example of different parts of coronary cycle imaged through pulse-wave Doppler positioning.

Left hand panel demonstrates end-diastole and early systole, right hand panel late-systole and early diastole. For construction of the backward expansion wave the right-hand panel is essential.

To minimise the noise of the pulse-wave signal recorded, the velocity range needs to be altered. In patients with low velocity profiles this may create a challenge in achieving an acceptably-interpretable trace. However, a balance needs to be struck between background noise and signal (Figure 2-9).

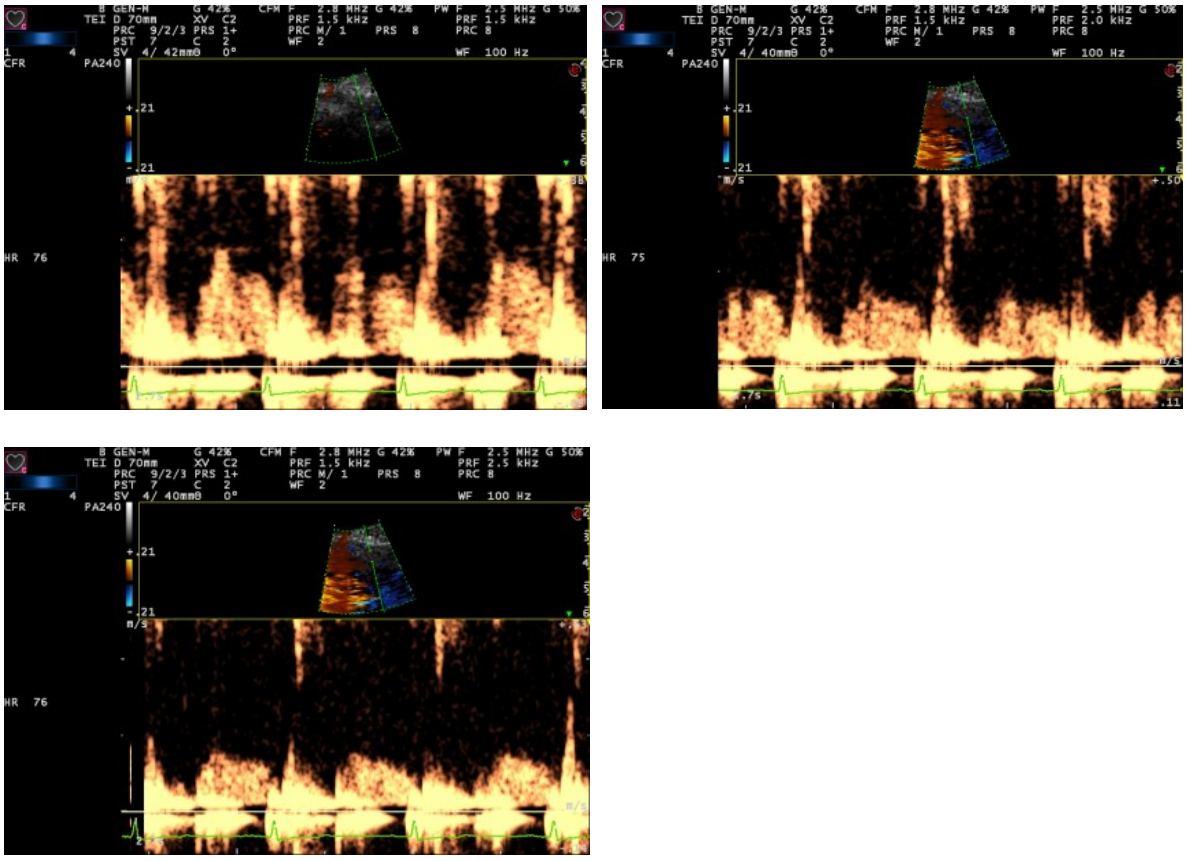

FIGURE 2-9. By decreasing the velocity scale in the same patient, the signal becomes cleaner.

2.2.2.5 Post-Processing: Coronary flow digitalisation

Processing coronary flow required an offline, custom-built Matlab programme which operated through the following steps.

2.2.2.5.1 Manual selection

Images were saved in either jpg or bitmap format. Initially they were processed using a manual selection system. This involved multiple mouse-clicks to delineate the scale, rate of recording and coronary flow signal. Additionally, to gate to the ECG , the Q and T waves had to be manually selected. Example of the imported flow trace is shown in (Figure 2-10).

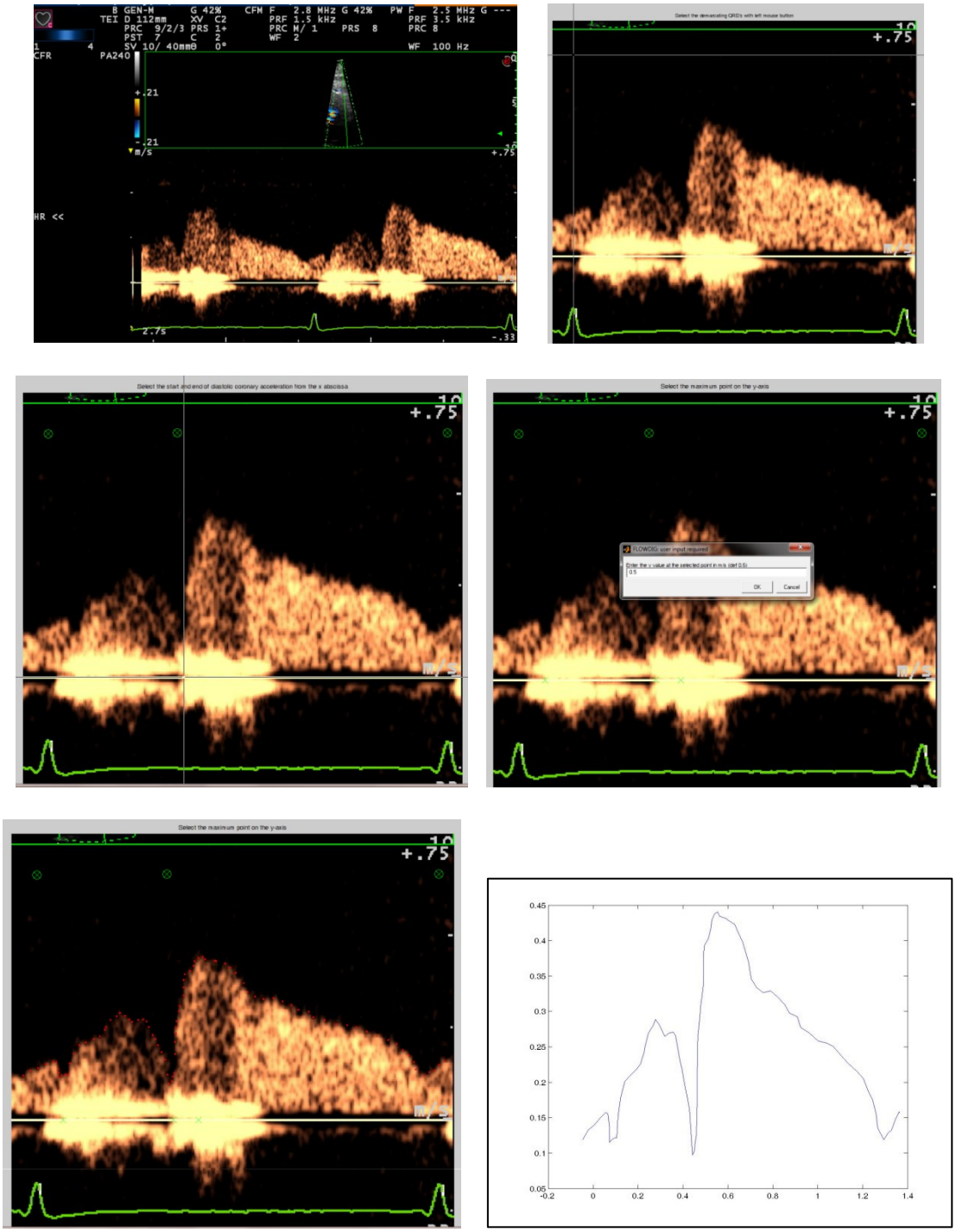

FIGURE 2-10. Post-processing of transthoracic echo-obtained coronary flow.

(from top left to bottom right): a) selection of 1 second, b) zoom and selection of ECG, c) selecting the start of coronary flow and zero on the x axis, d) scaling to the y axis, e) tracing of the flow signal through a series of clicks, f) the digital result.

2.2.2.5.2 Automated selection

Whilst a manual approach to selection was a useful way to begin the analysis, with the high number of patients recruited and interrogated, a more automated system was desirable. With assistance from the some of the software engineers affiliated with our group I was able to semi-automate this process.

The resultant Matlab programme was based around pixel recognition and manipulation. The initial step was to select the jpg or bmp file using the command *uigetfile* and remove the top half of the picture using the code:

```
corflow_image(1:top_of_fig,:,:) = 0;
```

where the variable *top_of_fig* was required as an input so that the top pixel line to be read could be altered according to the position of the flow signal within the image. Following this, 'corflow_image' was then converted to black and white (Figure 2-11):

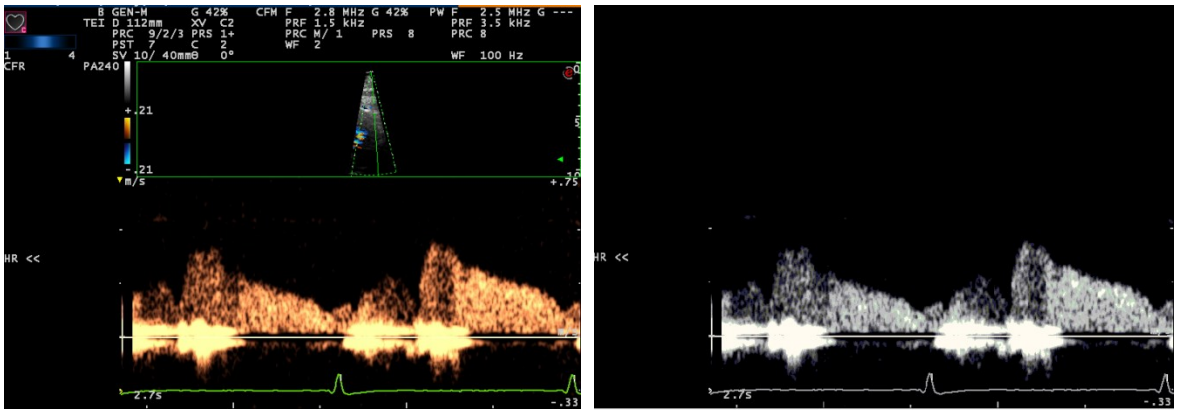

FIGURE 2-11. Removal of top half of figure and conversion to black-and-white.

Two functions were then used to organise these pixels into recognisable and readable areas. Bwmorph 'thicken' was used to add pixels to the exterior of an area. Then, using imfeature to recognise 'area' of greater than 500 grouped pixels. The end result of the code is as follows:

```
tempL = bwmorph(new_im,'thicken');
L = bwlabel(tempL, 8);
all_regions = imfeature(L,'PixelList','Area');
for reg_no = 1:length(all_regions)
        if all_regions(reg_no).Area<500
                pixels = (all_regions(reg_no).PixelList);
                        for each_pix = 1:size(pixels,1)
                        L(pixels(each_pix,2),pixels(each_pix,1))=0;
                end
        end
end
new_im = L>0;
```

To read the top of the coronary envelope, the image was divided up into columns of pixels (now in binary format). Each column was read from top to bottom and the first value of "1" located was stored as the height of the pixel from the base of the image. By allowing an additional step of manual baseline selection, the height from the baseline was then established. Each pixel value thus located was transformed into a vector (Figure 2-12).

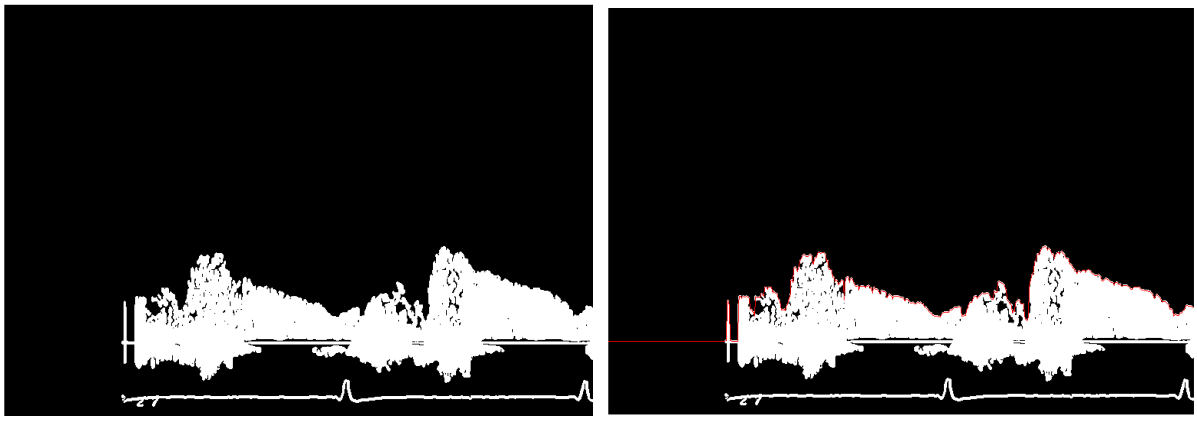

FIGURE 2-12. End result of Matlab pixel manipulation and tracing of envelope.

The image is manipulated as above then 'traced' in the above manner by recognition of the first white (i.e. binary value of 1) value when each column is read from top to bottom. This vector is plotted in red over the pixel-manipulated black-and-white image.

The end result is then displayed to the user (Figure 2-13).

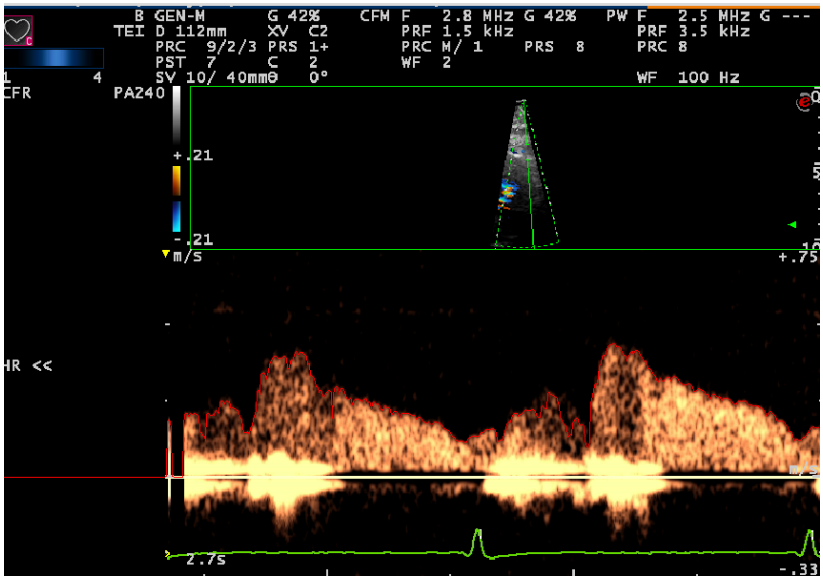

FIGURE 2-13. Coronary flow with automated edge recognition.

2.2.2.5.3 Additional Steps

2.2.2.5.3.1 Threshold:

Additionally, a threshold value for recognising pixels at was added in to allow greater sensitivity in selecting the appropriate pixels (Figure 2-14):

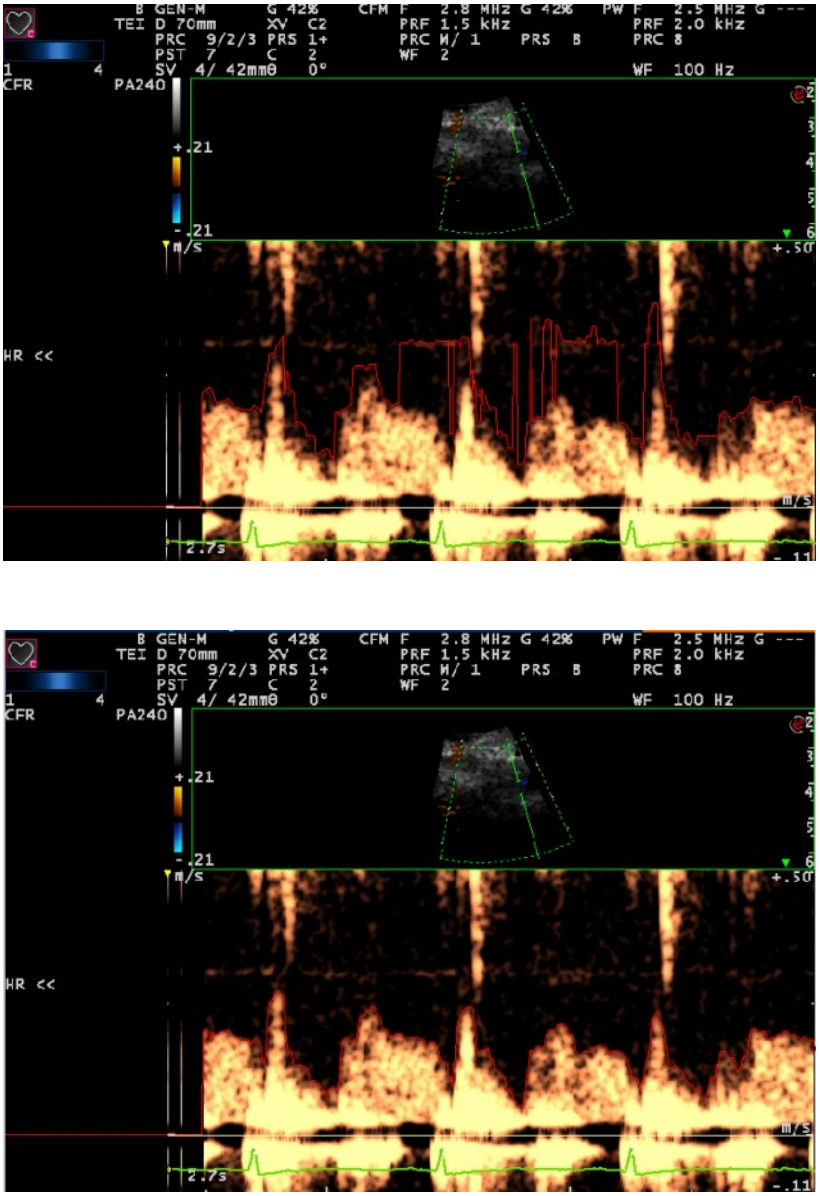

FIGURE 2-14. Threshold manipulation to allow accurate tracking.

A low sensing threshold on the upper panel causing inappropriate tracking of the coronary flow trace. By increasing this threshold, the tracking is more accurate.

2.2.2.5.3.2 Sweep speed

The majority of images were recorded at the same sweep speed which equated to 240 pixels per second. An option to manually enter this number was created in case a different sweep speed or image size was used or a manual selection of one second from the image could be used to calculate the sweep speed in a more bespoke fashion.

2.2.2.5.3.3 Selection of scale

Manual selection of the baseline and velocity scale was required to allow appropriate scaling.

2.2.2.5.3.4 Cut and retrace manually

Finally, by adding in code from the original "click-and-trace" programme, it was possible to manually select areas of the image that had not been traced correctly.

2.2.2.5.4 Final Result

The steps required in the final programme are displayed in the following figure (Figure 2-15).

FIGURE 2-15. Semi-automated coronary flow digitalization.

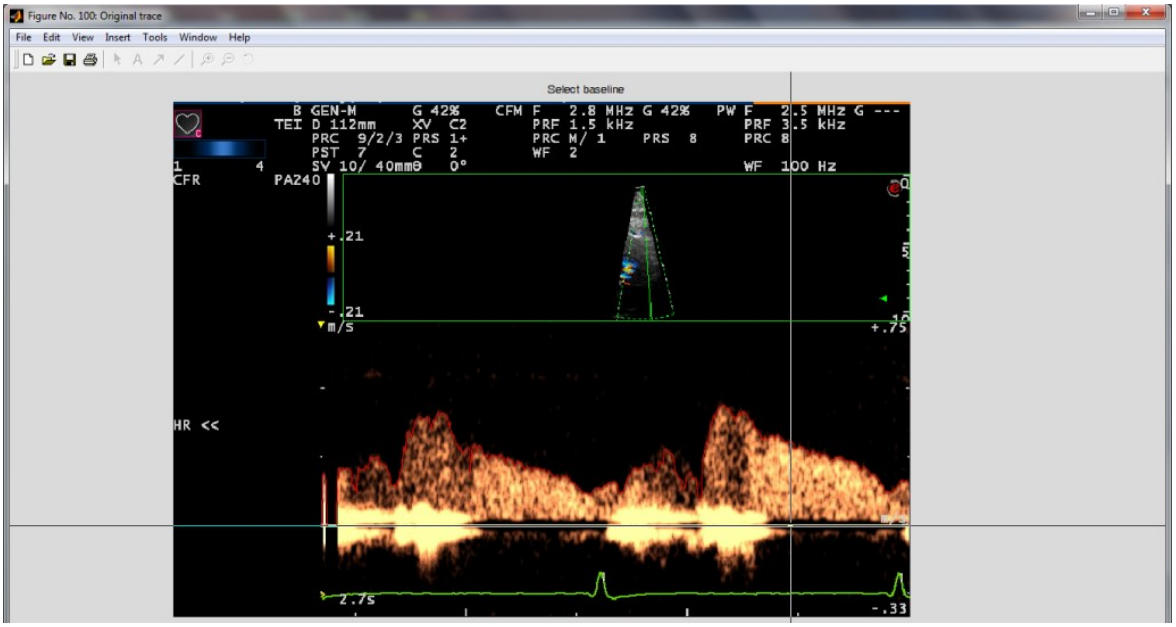

Step 1. Image is called and traced as above. Manual input is then required to select the baseline.

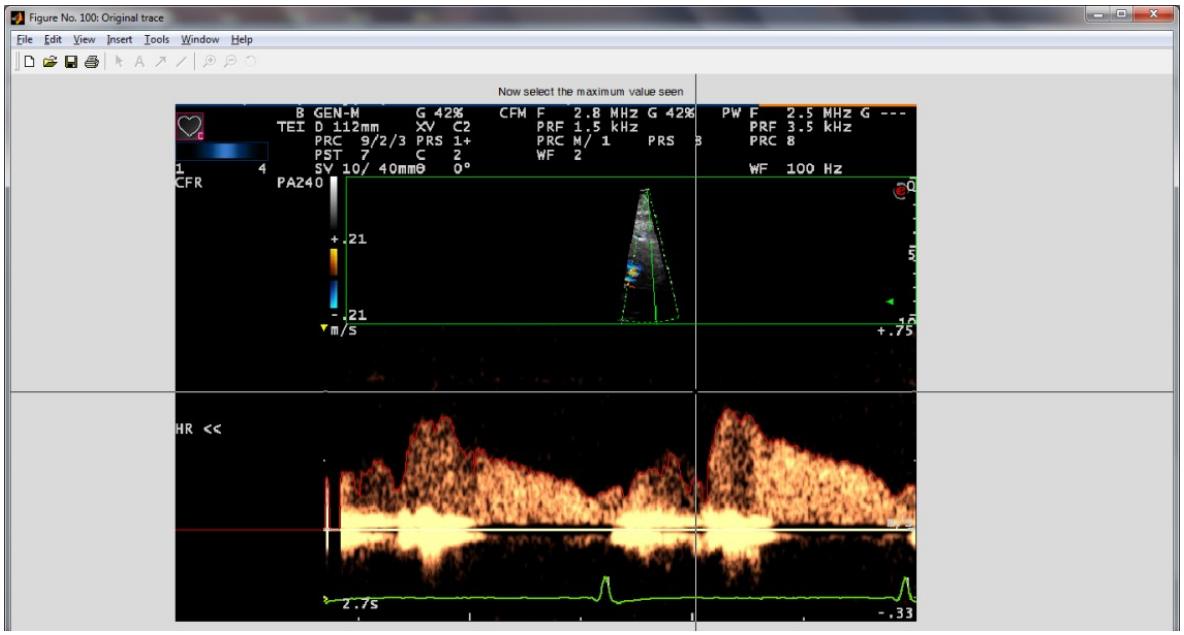

Step 2. The maximum y value seen is then selected.

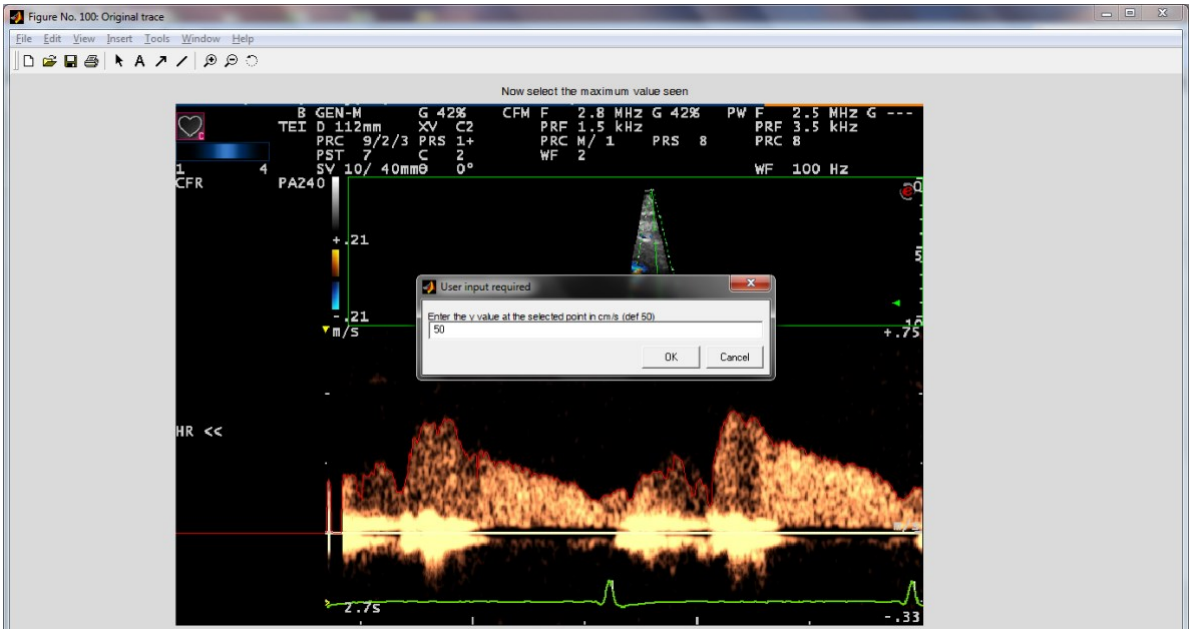

Step 3. That y value is the manually inputted

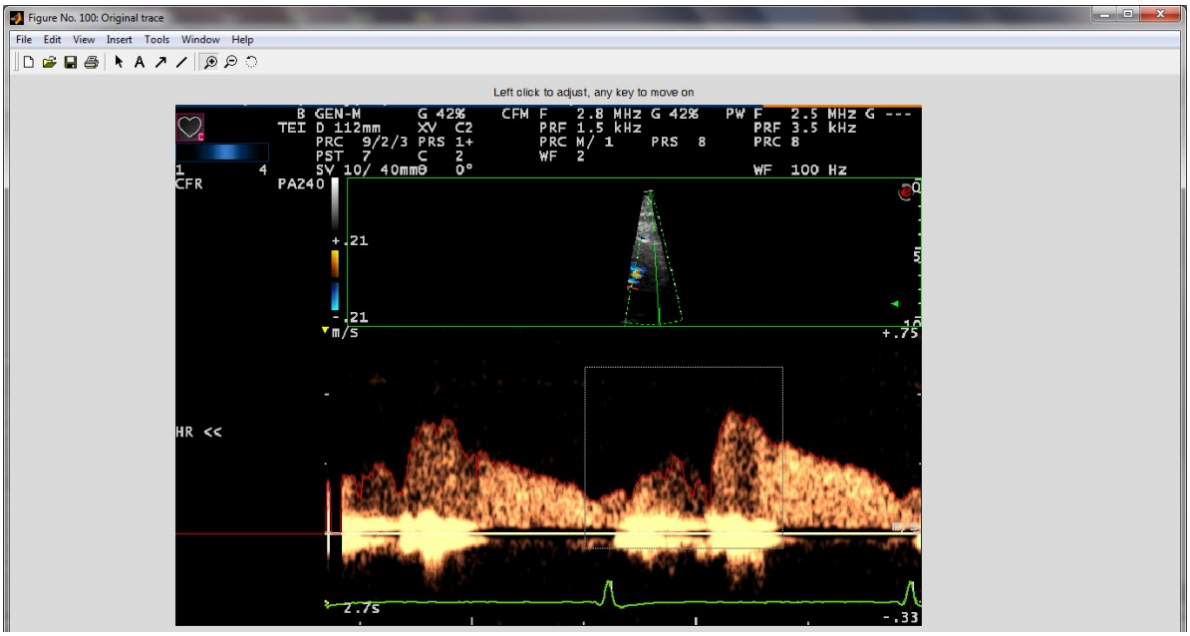

Step 4. If required, a section for the tracing can be selected for manual re-selection

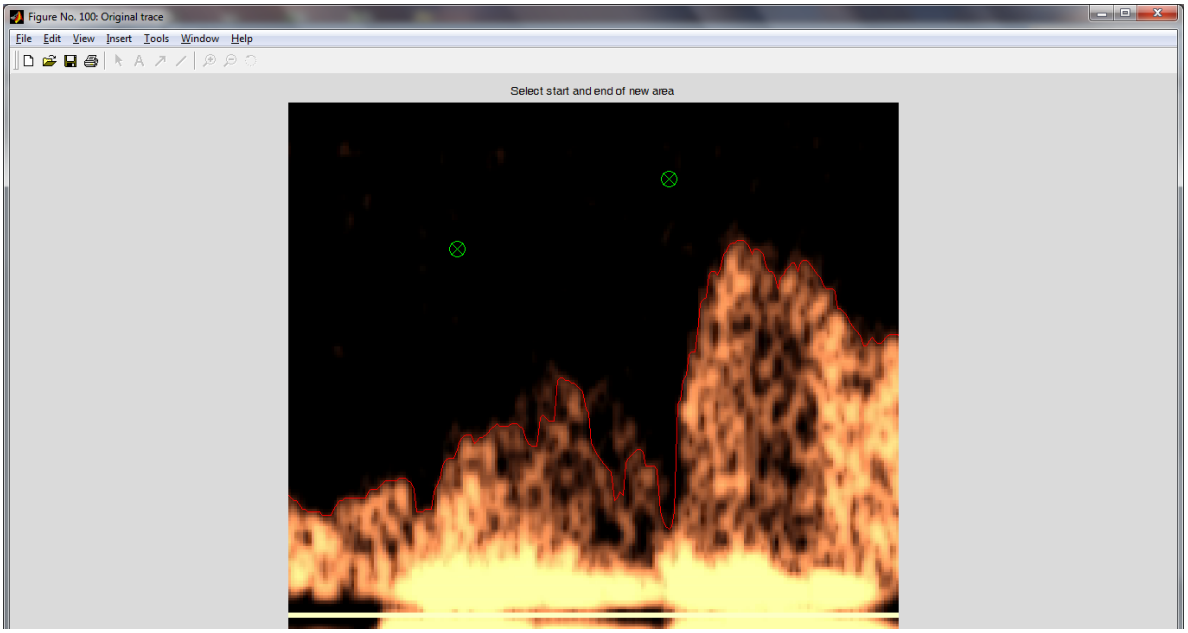

Step 5. The start and end points of the area for reselection are marked.

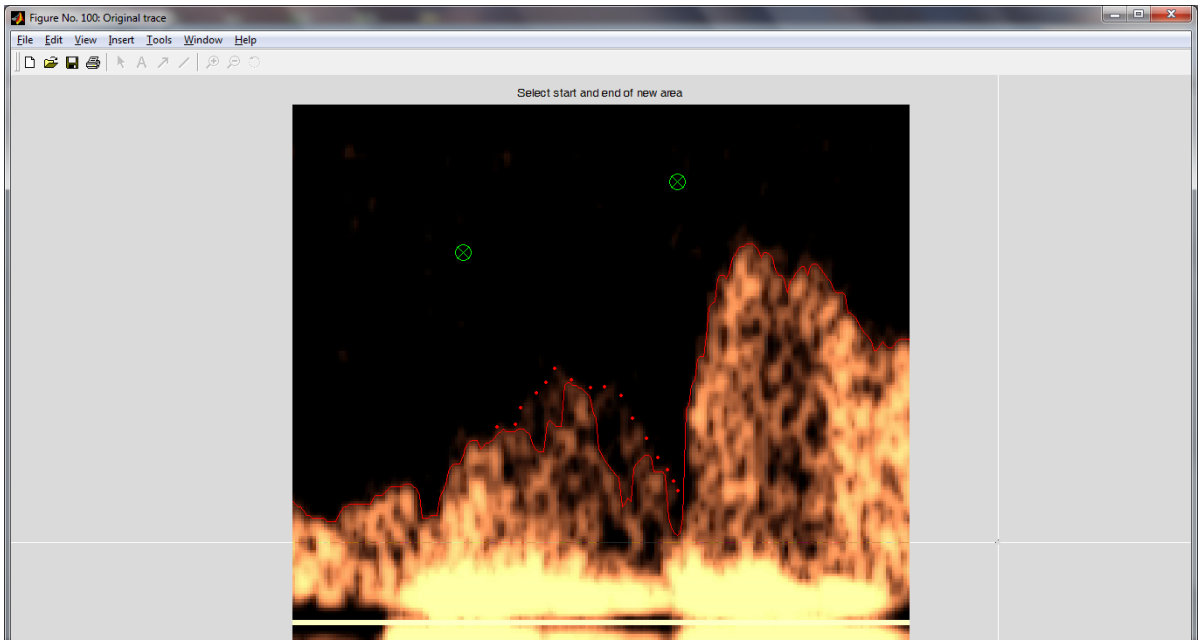

Step 6. Manual click-and-trace is performed to reselect this area. The old vector from this region is discarded.

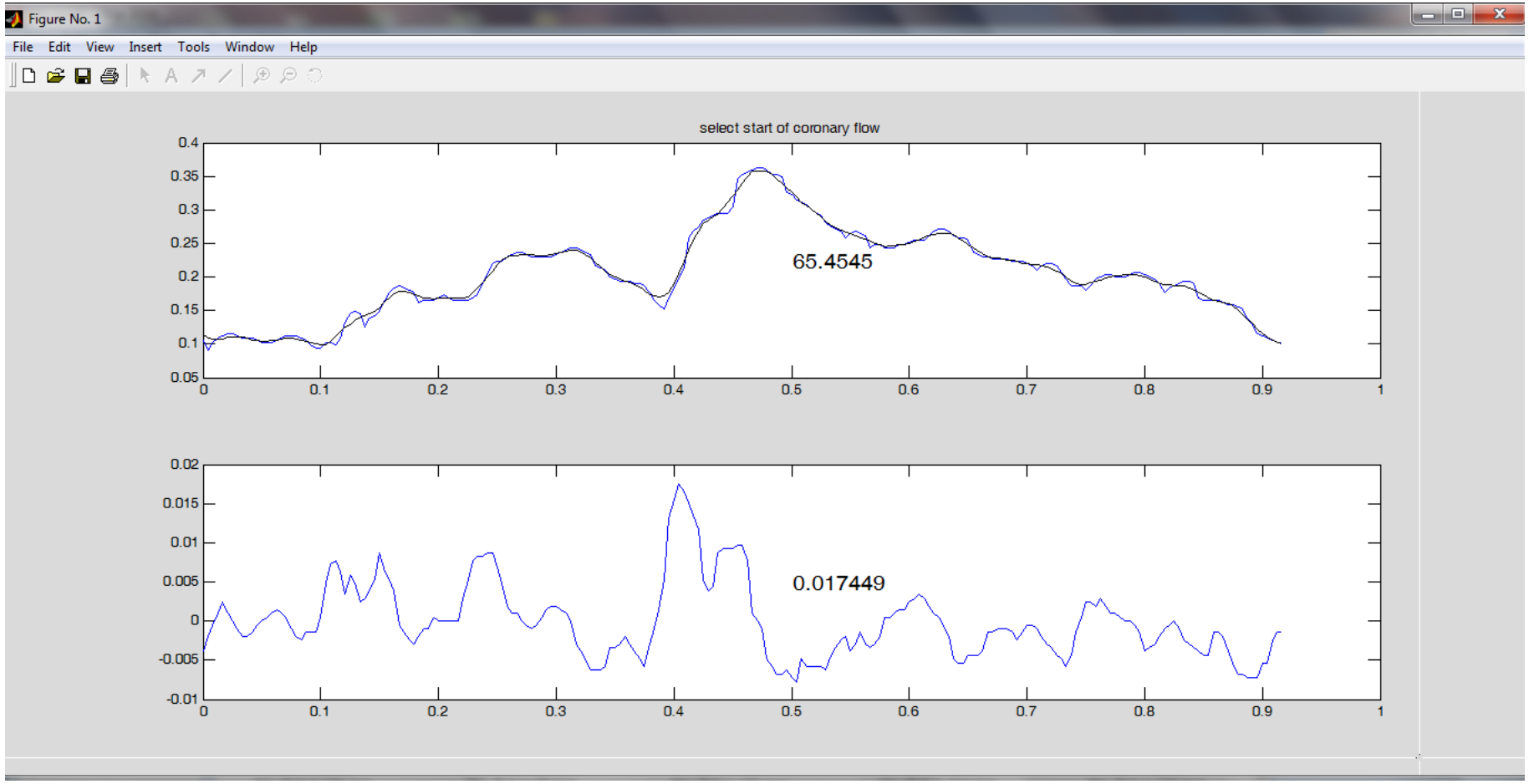

Step 7. Finally, the image and its first derivative can be viewed in vector format.

2.2.2.5.5 Post processing: ECG selection

Again, the R wave could be manually selected. However, for accuracy and speed, I again wrote an automated programme to allow this to occur in an automated fashion. The Matlab software was able to read the unique pixel colour information of the ECG trace and thus export it as a vector from the bmp or jpg. This vector was then converted into its first and second differential and values either above or below a certain value were identified. The default value for this identification was the mean of the vector or it could be inputted manually.

To avoid selection of several values in near proximity to each other it also required an input representing a length to be ignored after the first recognised value. By allowing the programme to then call itself again if required, these values could all be actively manipulated and adopted to allow successful R wave tracking for each cardiac cycle even with heavy interference, small complexes or a wandering trace. An example of this software in use is displayed below (Figure 2-16):

FIGURE 2-16. Automated r wave recognition software.

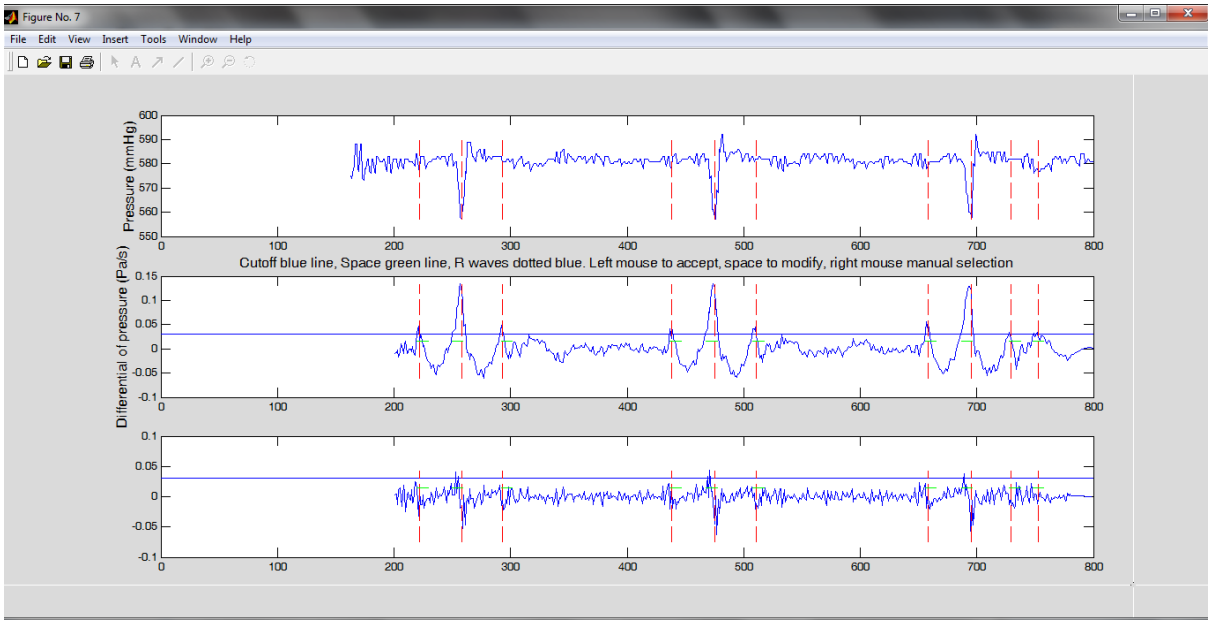

Step 1. The ECG is displayed in the top panel and the first and second differential in the lower panels. For ECG tracking, I found the first differential the most helpful but depending on lead placement there was an option to use the second if required. The vector is smoothed using a Savitzky-Golay filter to avoid amplification of noise. In this case, the cut-off value above which values are recognised, and the length of vector to ignore after this are too low.

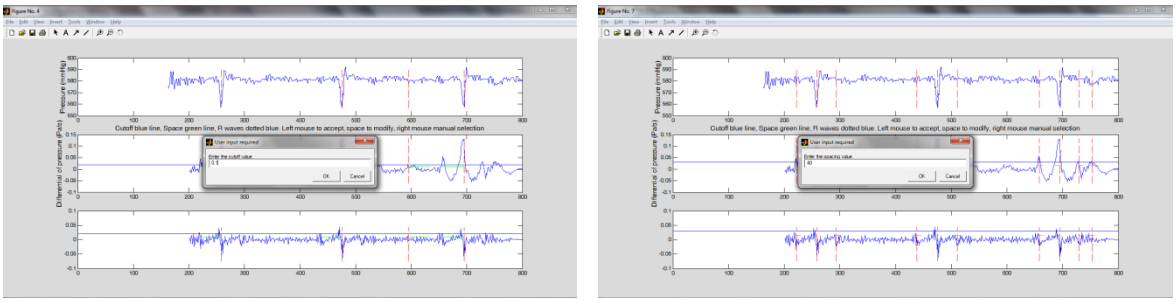

Step 2. Alternation of cut-off value above which values are recognised (left panel) and the space ignored after this value (right value).

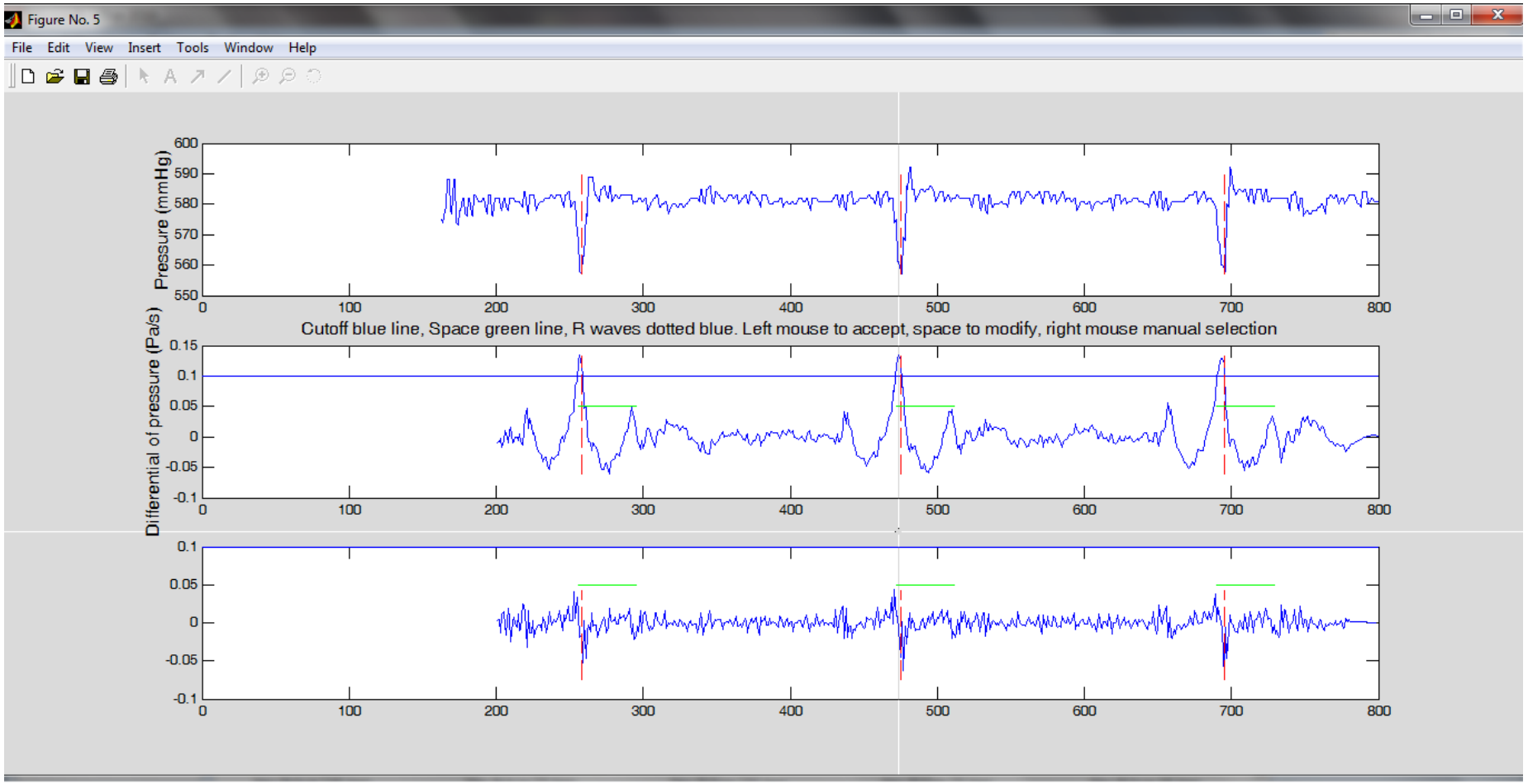

Step 3. End result – the peaks are now selected and the area after them ignored allowing good r wave recognition.

2.2.2.5.6 Post processing: Selection of cardiac cycle

After ECG recognition, the best coronary flow examples can be selected and the poorer traces ignored (Figure 2-17) and the output viewed and saved (Figure 2-18).

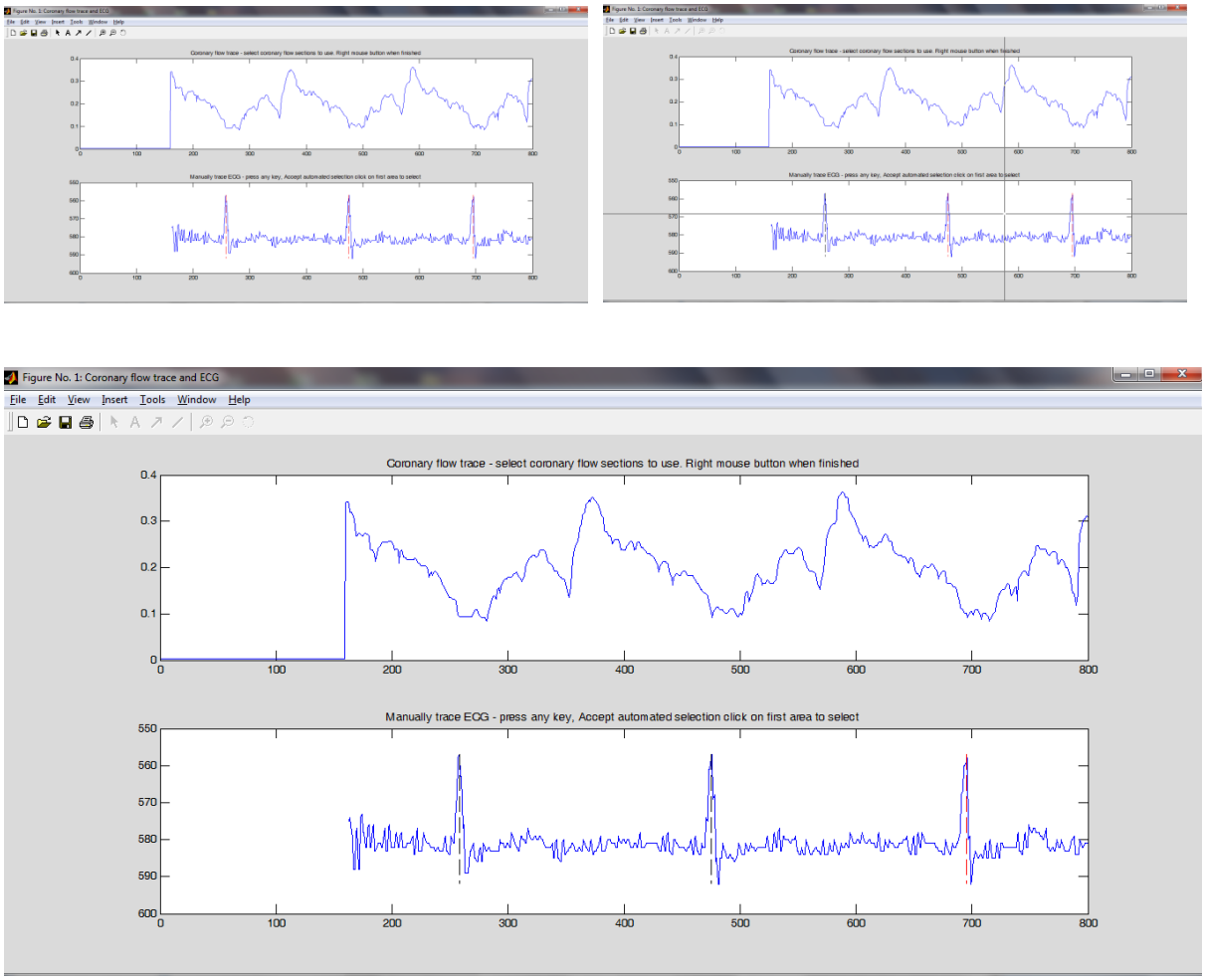

FIGURE 2-17. Manual selection of coronary flow.

By clicking in front of the R wave of the required coronary flow trace, each appropriate flow trace can be selected. Therefore, if there is a flow trace of poor quality this can be ignored and the traces either side selected instead.

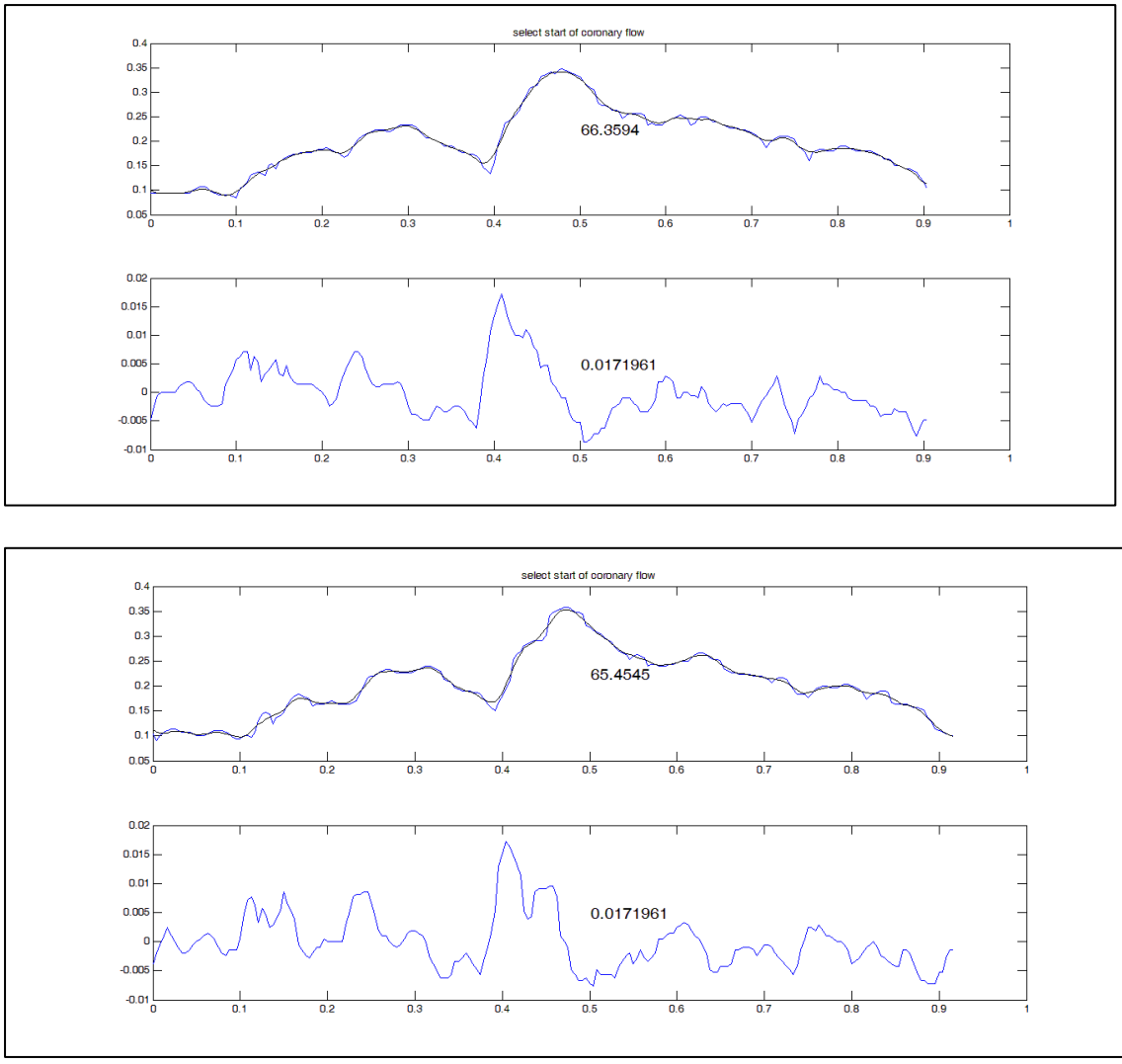

FIGURE 2-18. Coronary flow and its first differential displayed for each selected cardiac cycle.

The heart rate is displayed according the automatically recognised r wave for the upper panel. The peak first differential is shown on the differential panel.

2.2.2.5.7 Post processing: Smoothing

After digitalization of both flow and ECG, an option of smoothing was automated into the programme. Because ensemble-averaging introduces an element of smoothing, a variable Savitzky-Golay filter was used(Savitzky and Golay, 1964) depending on the number of flow traces and if more than 15 traces were ensemble, no filter was employed (Figure 2-19).

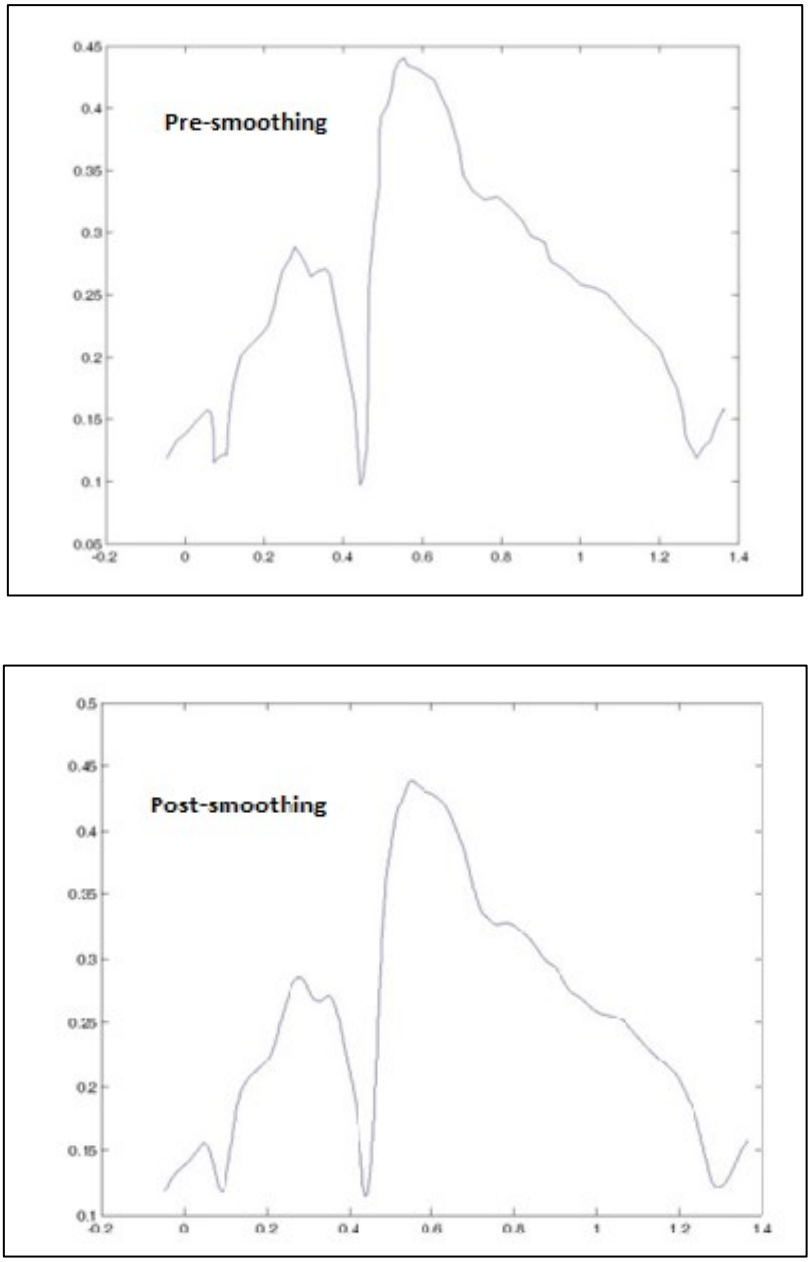

FIGURE 2-19. Smoothing of the digitalized image using a Savitzky-Golay filter.

2.2.2.5.8 Post processing: Ensemble-averaging

After each individual trace was digitalized and processed they were averaged to produce an ensembled coronary flow image. This was performed offline using another custom-built Matlab package. Two methods were proposed for ensemble averaging: alignment from the start of diastolic coronary flow acceleration or alignment according to the R wave from the imported gated ECG. It is possible to perform the former alignment in a semi-automated fashion by recognising the peak of the 2nd differential of coronary flow (Figure 2-20):

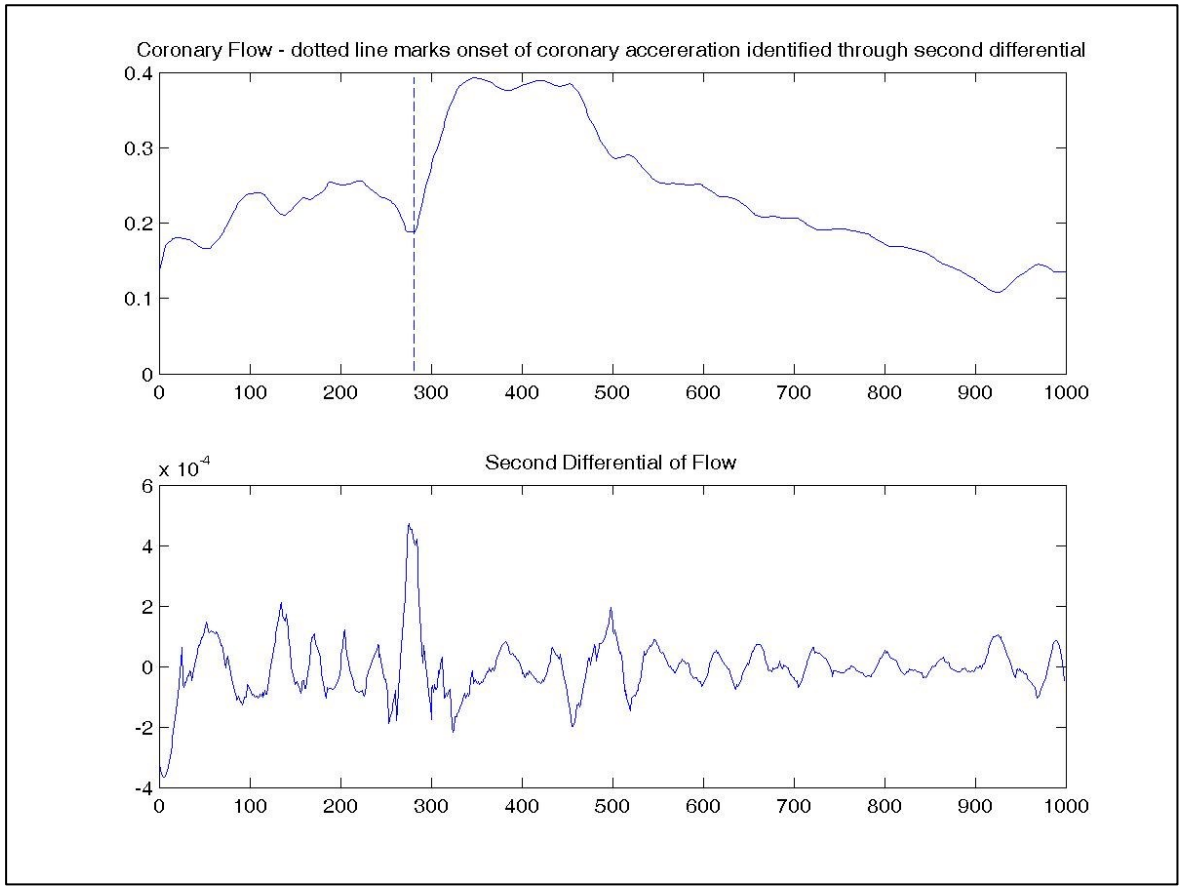

FIGURE 2-20. Coronary flow and the second differential of flow.

The onset of coronary flow is then located automatically by identifying the maximum value of the second differential and in this figure is marked with a dashed line.

2.2.3 STUDY PROTOCOL

2.2.3.1 Assessing coronary flow non-invasively

To assess my ability to accurately obtain non-invasive coronary flow profiles seventeen patients with unobstructed coronary arteries underwent both coronary flow assessment invasively and non-invasively. Demographic, echocardiographic and pharmacological details of these patients are described in chapter 2.5.3.1. Invasive coronary flow was performed at the time of angiography, as described in chapter 2.5.2.2. Coronary flow assessment, processing and analysis was performed after angiography when the patient was recovering on the cardiac day ward, within 60 minutes of the invasive assessment.

2.2.3.2 Coronary flow - choice of machine

Of the two machines available for coronary flow analysis, the Esaote MyLabTwice machine appeared to demonstrate better quality over the Phillips ie33. To objectively quantify this, a correlation was obtained between all patients who had echocardiographic coronary flow assessment as well as invasive coronary flow assessment.

2.2.4 RESULTS

2.2.4.1 Optimisation of Flow Measurements

2.2.4.1.1 ECG alignment and assessment of peak dudt

In order to assess the correct method for ensemble-averaging of the coronary flow trace the two methods of ensembling were applied to each coronary flow trace: alignment at the start of coronary flow or R-wave alignment through ECG-gating. Correlation coefficients were calculated for each trace and Bland-Altman plots produced (Figure 2-21 and Figure 2-22).

Using coronary flow alignment resulted in overall higher mean peak dudt measurements compared with invasive measurements (0.0057 $cm.s^{-2}$ versus 0.0040 $cm.s^{-2}$, p=0.007) whereas ECG-aligned flow resulted in a similar approximation of mean (0.0036 $cm.s^{-2}$ versus 0.0040 $cm.s^{-2}$, p=0.41). There was also a better correlation for coronary flow aligned according to the ECG (r = 0.58, p=0.01 vs r=0.29, p=0.26) and so this method was subsequently employed for coronary flow.

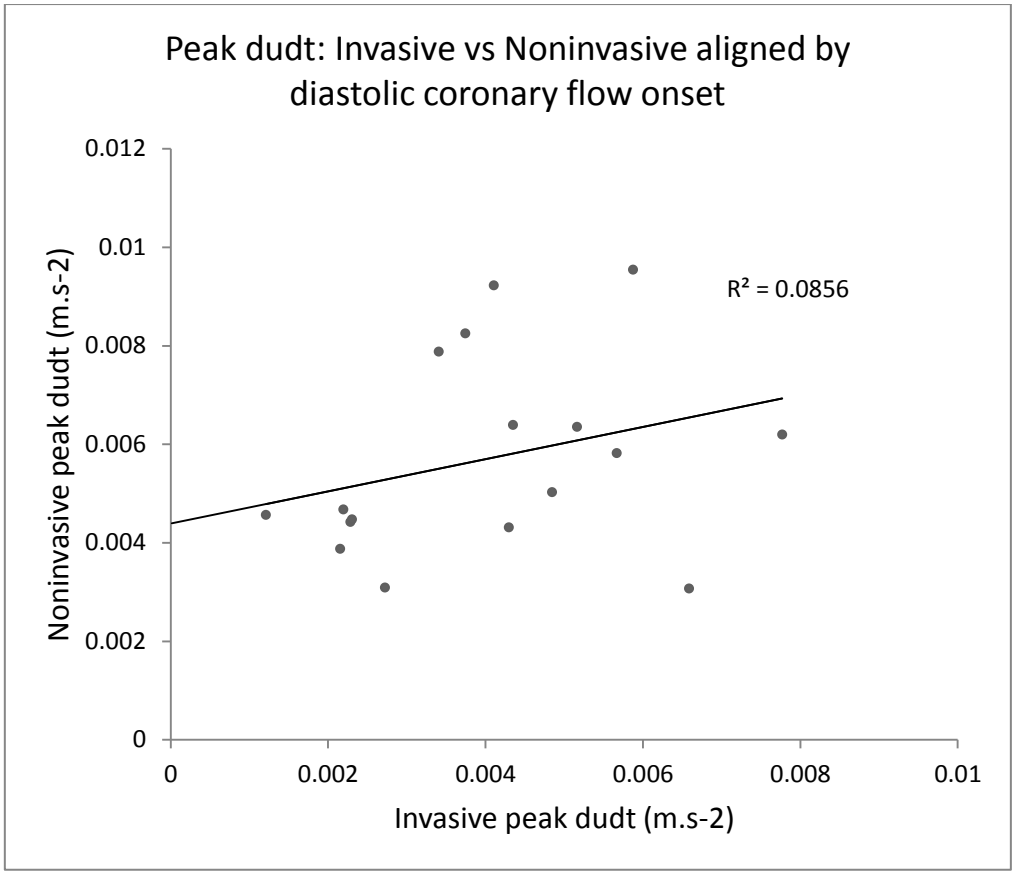

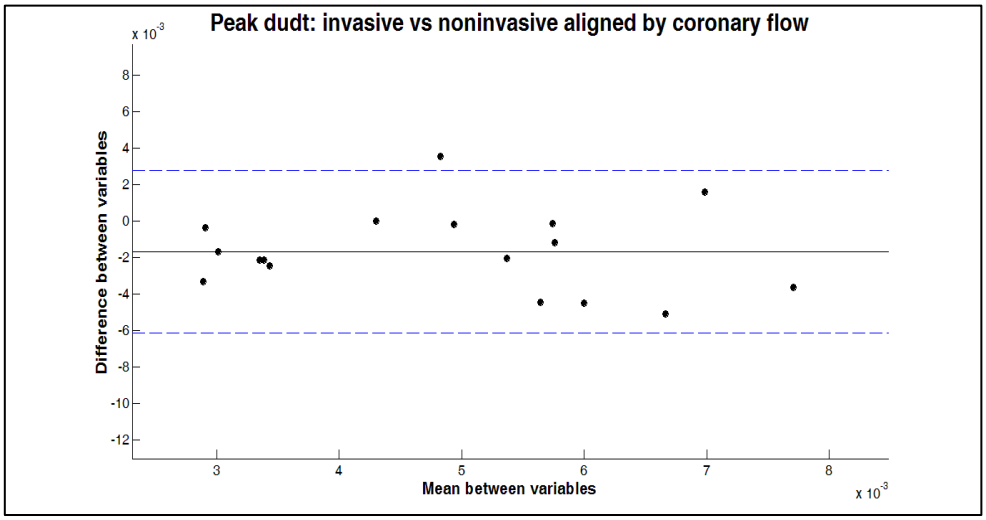

FIGURE 2-21. Scatter and Bland-Altman plot of invasive and non-invasive coronary flow dudt with non-invasive flow aligned by the start of diastolic coronary acceleration.

With this method of alignment there was a significant difference between mean peak dudt and the correlation value was not significant (p=0.26).

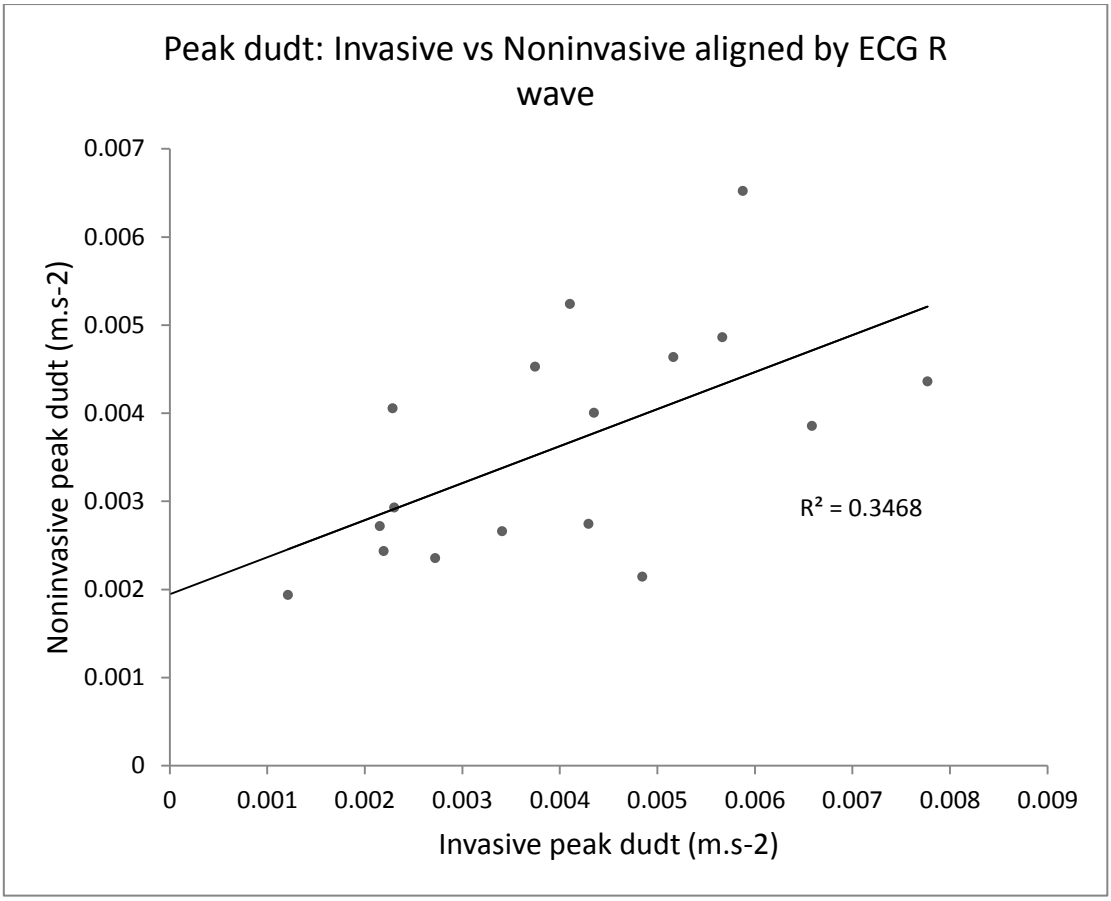

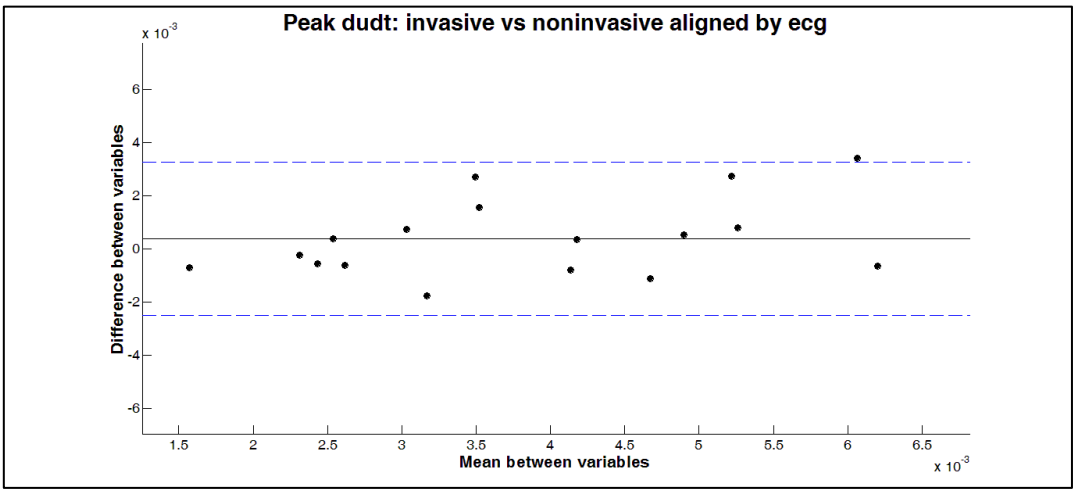

FIGURE 2-22. Scatter and bland-atman plots of invasive and non-invasive coronary flow dudt with non-invasive flow aligned according to ECG R wave.

This produced a much more accurate mean peak dudt value (p=0.41) with a more impressive correlation (r=0.58, p=0.01).

2.2.4.1.2 Estimation of absolute values

2.2.4.1.2.1 Peak coronary flow

Average peak coronary flow velocity was similar in the invasive versus non-invasive groups (0.30 versus 0.28 cm/s, p=0.54) with a good correlation (r=0.65, p=0.004) when aligned by the R wave (Figure 2-23).

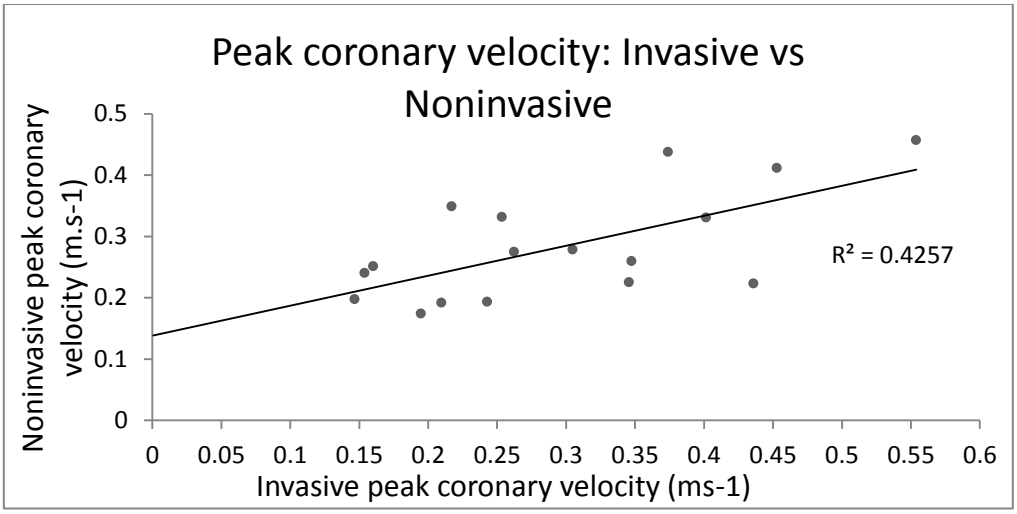

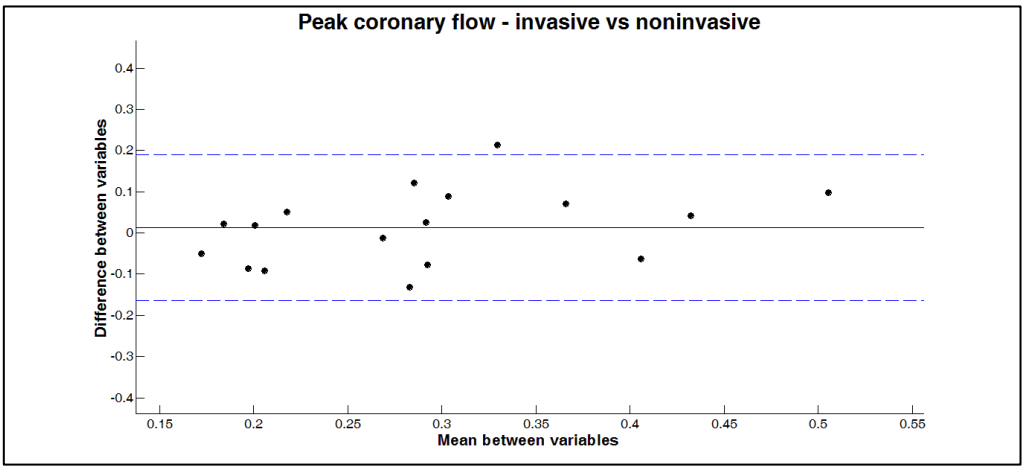

FIGURE 2-23. Scatter plot and Bland-Altman plot of invasive versus non-invasive peak coronary flow.

There was a good estimation of absolute values with a good correlation between invasive and non-invasive measures (r=0.65, p=0.004)

2.2.4.1.2.2 Minimum coronary flow

The average minimum velocity was also similar between the two assessment modalities (0.09 invasive versus 0.11 non-invasive, p=0.10) with a correlation r value of 0.62 (p=0.007) (Figure 2-24).

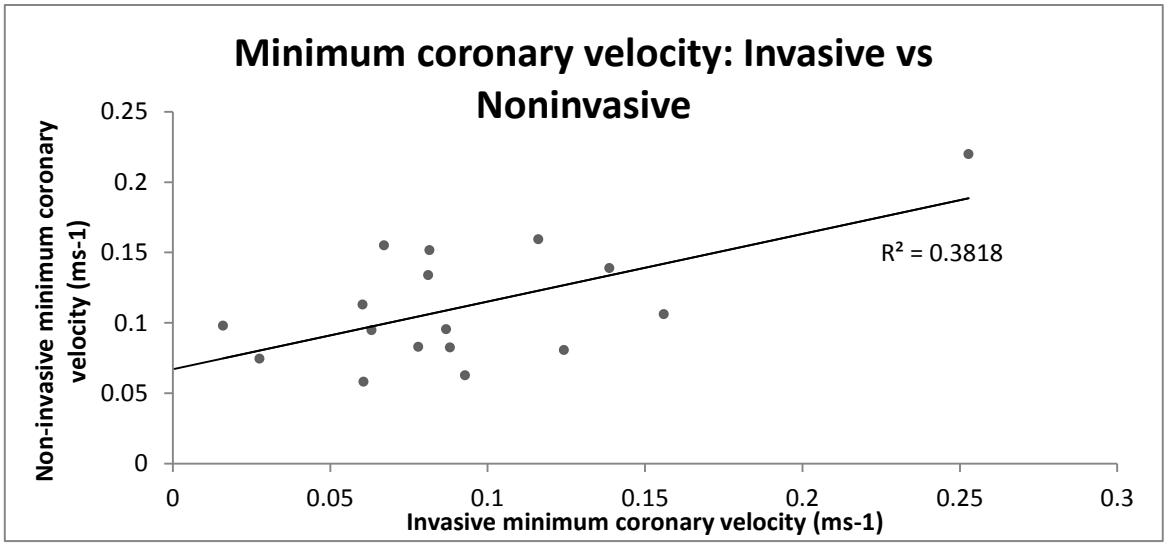

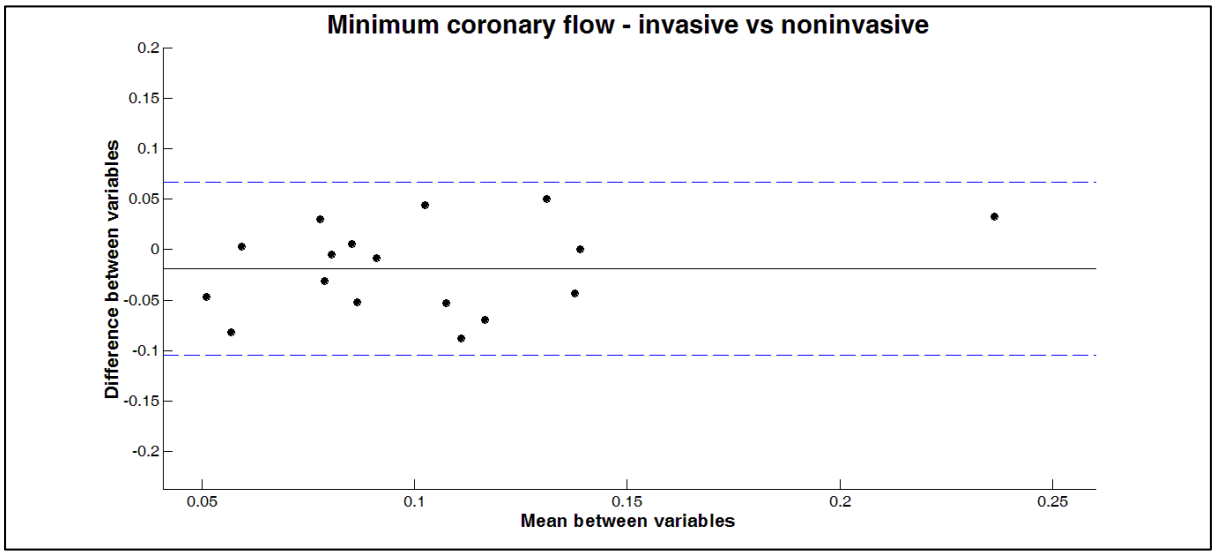

FIGURE 2-24. Scatter plot and Bland-Altman plot of invasive versus non-invasive minimum coronary flow.

There was a good estimation of absolute values with a good correlation between invasive and non-invasive measures (r=0.62, p = 0.007).

2.2.4.2 Demonstration of optimal echocardiographic machine

In total 44 patients with a varying spectrum of aortic valve stenosis but normal coronary arteries underwent combined assessment (31 Phillips, 13 Esaote). Peak dudt, peak velocity and mean velocity were assessed. A stronger correlation was noted in all categories with the Esaote MyLabTwice over the Phillips ie33 (Table 2-2).

		Peak Velocity		Mean Velocity		Peak dudt	
Machine	No of patients	R Value	P Value	R Value	P Value	R Value	P Value
Esaote MyLabTwice	13	0.886	0.00006	0.8207	0.0006	0.5359	0.06
Phillips ie33	31	0.3873	0.03	0.2997	0.1	0.1083	0.56

TABLE 2-2. Comparison of Esaote Mylabtwice and Phillips ie33 with peak and mean velocity and peak dudt.

A better correlation is seen between non-invasive calculations using the Esaote Mylabtwice and invasive Combowire measurements rather than the Phillips ie33.

2.2.5 CONCLUSIONS

Whilst most operators around the world focus on peak values of coronary flow, for the purposes of wave-intensity analysis, a clean coronary flow envelope is required, particularly around the change from systole to diastole when coronary acceleration occurs. Additionally, a smooth complete outline is also essential for an accurate calculation of wavespeed using the single point equation.

I have demonstrated that it is possible to achieve this accurately with values obtained non-invasively by assessing peak and minimum velocity and dudt. I have also shown that the use of a dedicated machine with inbuilt probe and software settings for the assessment of coronary flow is much more useful than standard echocardiographic machines.

In terms of post-processing, ensemble averaging is most accurately obtained through alignment by r wave recognition and this can be done accurately in a semi-automated fashion by recognising the peaks and troughs of the first differential of the ECG trace. Alignment by the onset of coronary flow is possible but results in overestimation of coronary acceleration which translates to a higher dudt.

Therefore, it is apparent that coronary flow can be estimated and processed appropriately for the construction of non-invasive wave intensity analysis and that to provide the most accurate values, the Esaote MyLabTwice machine should be used where possible with alignment by the ECG's r wave.

2.3 VARIABLE 2: ACCURATELY OBTAINING CORONARY PRESSURE NON-INVASIVELY

2.3.1 INTRODUCTION

The most basic definition of wave intensity is as the product of dP and dU (WI = dPdU). As demonstrated above, dU is possible to calculate directly non-invasively using transthoracic echocardiography. However, a direct non-invasive assessment of coronary pressure is impossible. An approximation could be obtained in a fashion similar to tonometry by measuring coronary artery wall expansion using perhaps MRI – however, this value would be so small errors would almost be inevitable.

Pressure curves in normal unobstructed coronary arteries are thought to be identical throughout the epicardial coronary tree and also match that of central aortic pressure and this is the concept on which coronary pressure surrogates of flow-limiting stenoses are based(Pijls et al., 1995, Sen et al., 2012). Therefore, a non-invasive assessment of central aortic pressure could prove useful in estimating coronary dP, if this value is essential for coronary wave intensity analysis.

2.3.1.1 Central aortic pressure measurement through suprasystolic brachial waveform interpretation

Reliable non-invasive measurements of central aortic pressure have been desirable for cardiovascular risk stratification and as such a number of techniques exist. One option involves the application of a generalised transfer function to radial artery waveforms achieved from applanation tonometry. This is produced through averaging the individual functions calibrated to brachial cuff sphygmomanometer-measured BP(Weber et al., 2011, Wassertheurer et al., 2010); the transfer function is necessary to correct for pressure wave amplification in the upper limb. This method is slightly

limited as it assumes the properties of the upper limb arteries are identical among individuals which is not always the case(Payne and Webb, 2008). Other groups have attempted to individualise the transfer function by patient according to characteristics such as age and blood pressure but with limited success(Westerhof et al., 2008).

An alternate option is through use of suprasystolic brachial pressure waveform interpretation (Pulsecor Ltd, Auckland, New Zealand). This system estimates central pressures from brachial cuff pressure fluctuations by inflating to suprasystolic levels (approximately 30mmHg above systolic pressure) and occluding the brachial artery. Intra-arterial pressure waves impinging on the occluded artery transfer part of their energy to the surrounding upper arm tissue and then to the cuff and can be directly related to the intra-arterial pressure oscillations. This also means there are no confounding waves reflected distal to the point of measurement. A time-domain representation of pressure wave reflection within a uniform closed tube has been established and applied to the cuff-sensed pressure to produce central aortic pressure. Measuring central pressure in this method has been demonstrated to be comparable to 'gold-standard' invasive data when systolic and diastolic values were compared (Lin et al., 2012, Lowe et al., 2009).

However, in order to construct wave intensity, again the pressure waveform is required, not just the individual values. Therefore, to assess the Pulsecor machines accuracy in performing this I set out to validate its measures against simultaneously acquired values of invasive central aortic, left main stem and left anterior descending artery pressures. I also wanted to demonstrate the importance of dP in the wave-intensity formula.

2.3.2 METHODS, RESULTS AND FURTHER PROCESSING TO IMPROVE ACCURACY

2.3.2.1 The Importance of Including Pressure in Wave Intensity

Because of the inherent difficulties in directly measuring coronary pressure non-invasively I initially wanted to demonstrate the relative importances of flow and pressure in the construction of wave-intensity to see if an approximation of the backward expansion wave could be constructed from flow alone.

I therefore constructed a 'weighting' algorithm to display the individual effects of pressure and flow on the resultant wave-intensity profile where:

$$WI\ (\text{flow influence}) = \pm\ dudt * 1050 * wavespeed$$

$$WI\ (\text{pressure influence}) = \pm\ dPdt$$

EQUATION 2-1. SEPARATING THE INFLUENCE OF PRESSURE AND FLOW IN WAVE-INTENSITY

This was applied to several data sets and as can be seen from the example in Figure 2-25 the influence of pressure is essential and simply differentiating flow would not be discriminatory.

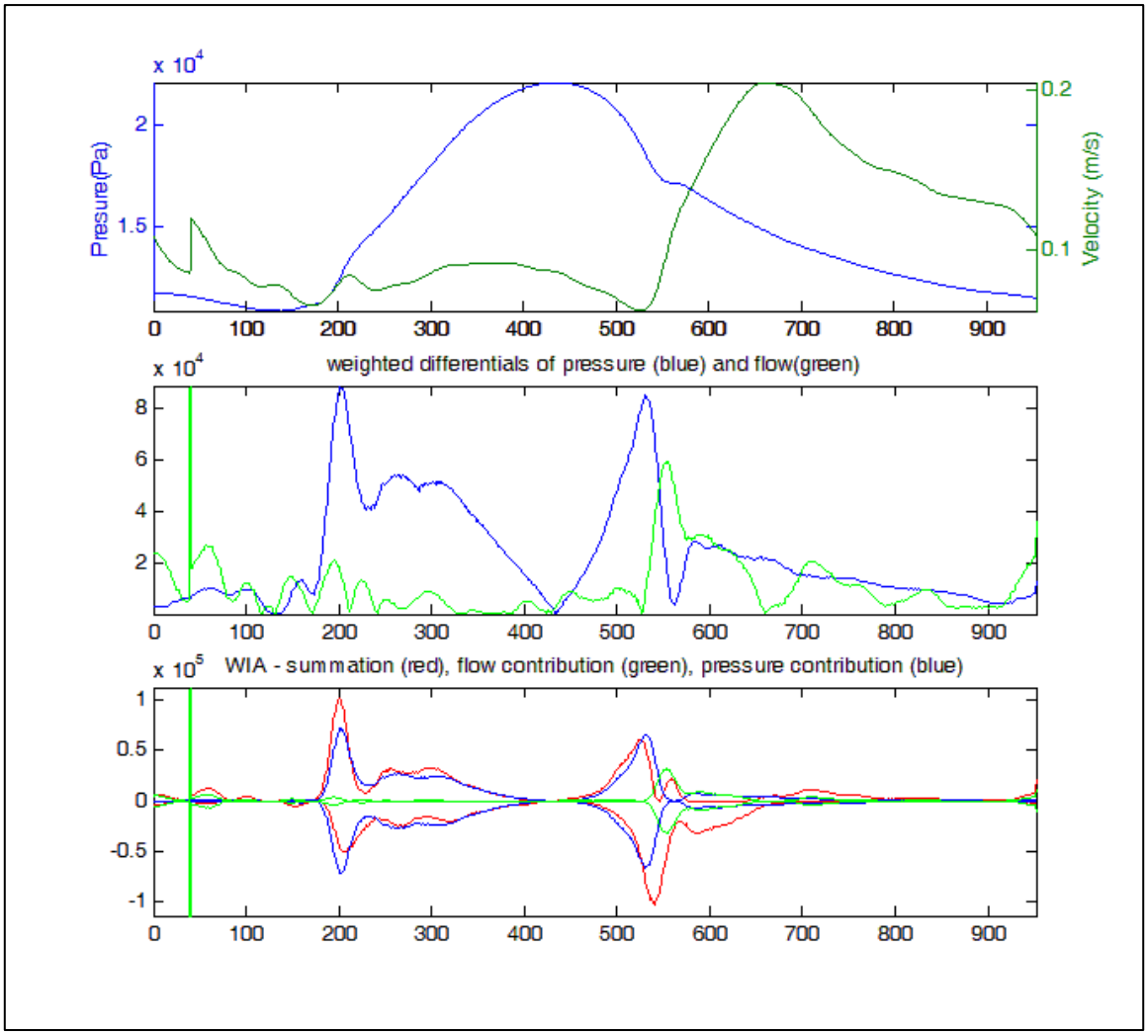

FIGURE 2-25. Separation of wave-intensity components weighted according to wave-intensity principles.

Top panel demonstrates simultaneously acquired pressure and flow. Middle panel demonstrates weighted differentials of flow (dudt * 1050 * wavespeed) and pressure (dpdt). Lower panel demonstrates separated wave-intensity for forward (positive values) and backward (negative values) in red with the respective contributions from pressure (blue) and flow (green).

2.3.3 INVASIVE EXPERIMENTS: USING CENTRAL AORTIC PRESSURE TO ESTIMATE CORONARY PRESSURE

There is no easily applicable technology available to non-invasively estimate coronary pressure directly. Therefore I made the assumption that central aortic pressure is equivalent to left main stem and left anterior descending artery pressure, particularly in terms of differential values and set out to confirm this.

2.3.3.1 Methods

To test this, I divided the first differential of pressure into 3 areas for comparison: peak of the systolic dpdt (1), minimum diastolic dpdt (2) and peak of the diastolic dpdt(3) (Figure 2-26).

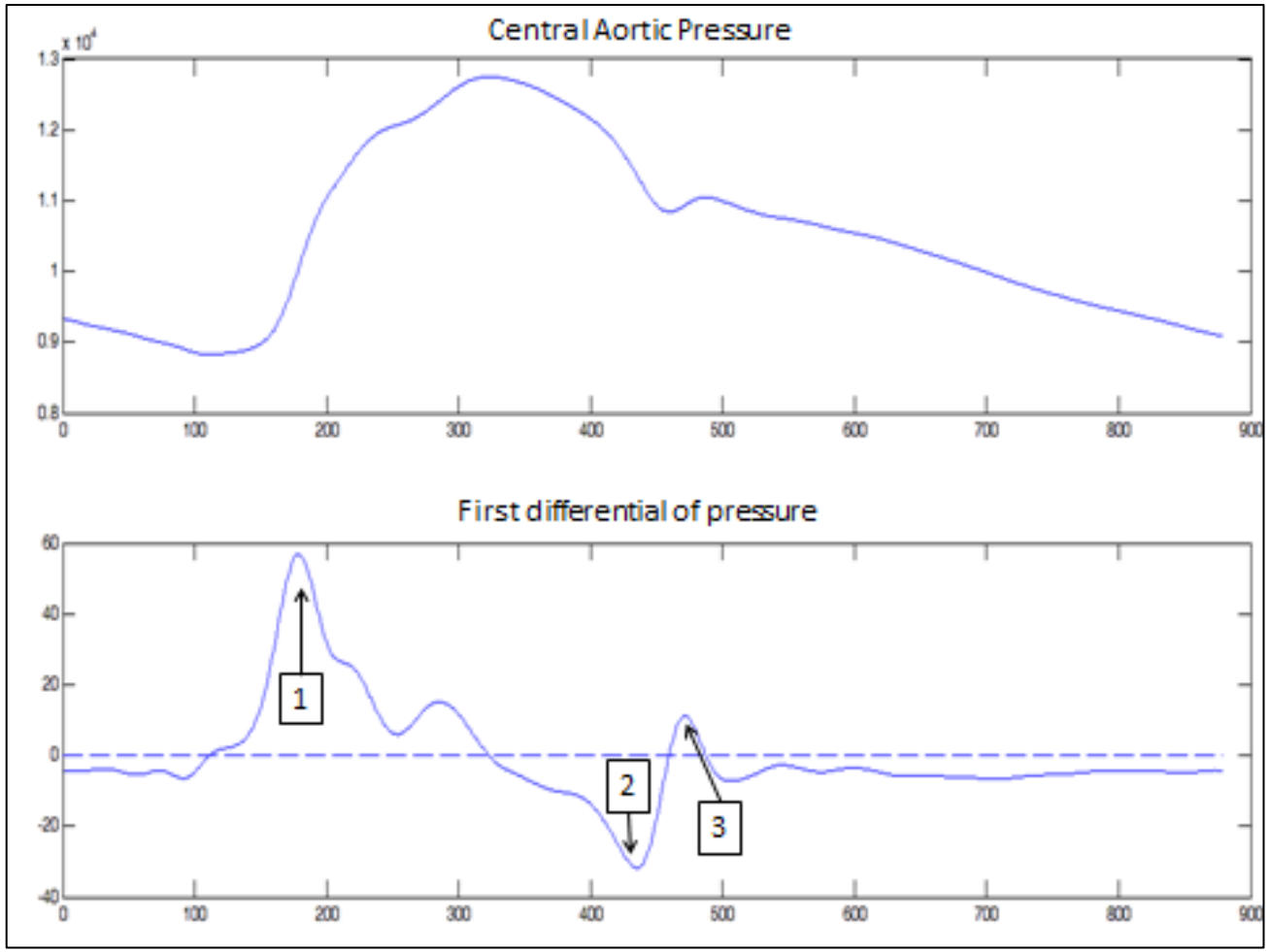

FIGURE 2-26. Central aortic pressure and its first differential.

Peak of systolic dpdt (1), peak of diastolic dpdt (3) and minimum diastolic dpdt (2) are highlighted.

In 27 patients with unobstructed coronary arteries, invasive measurements were made in the left main stem and / or left anterior descending artery using either a Combowire ((Combowire, Volcano Corp – Figure 2-60) or a dedicated pressure-tipped sensing wire (Primewire Prestige, Volcano Corp - Figure 2-27). The left coronary system was intubated from a femoral or radial approach using a Judkins guide catheter and intra-coronary nitrates were used to stabilise the pressure signal. After normalisation with the pressure sensor just outside the catheter tip, the wire was passed into the left main stem or left anterior descending artery. Central aortic pressure data was recorded from the catheter tip.

2.3.3.1.1 Processing

Proximal and distal pressure was recorded live onto a Combomap. The data was then exported as an sdf file and converted to a text file using Study Manager. This was imported into Matlab and processed. Two options for separating the cardiac cycles were employed using either the first differential of the ECG or the second differential of the pressure trace. The latter ultimately gave a more appropriate amalgamation of pressure signals as it was more accurate at recognising the onset of systole (Figure 2-28).

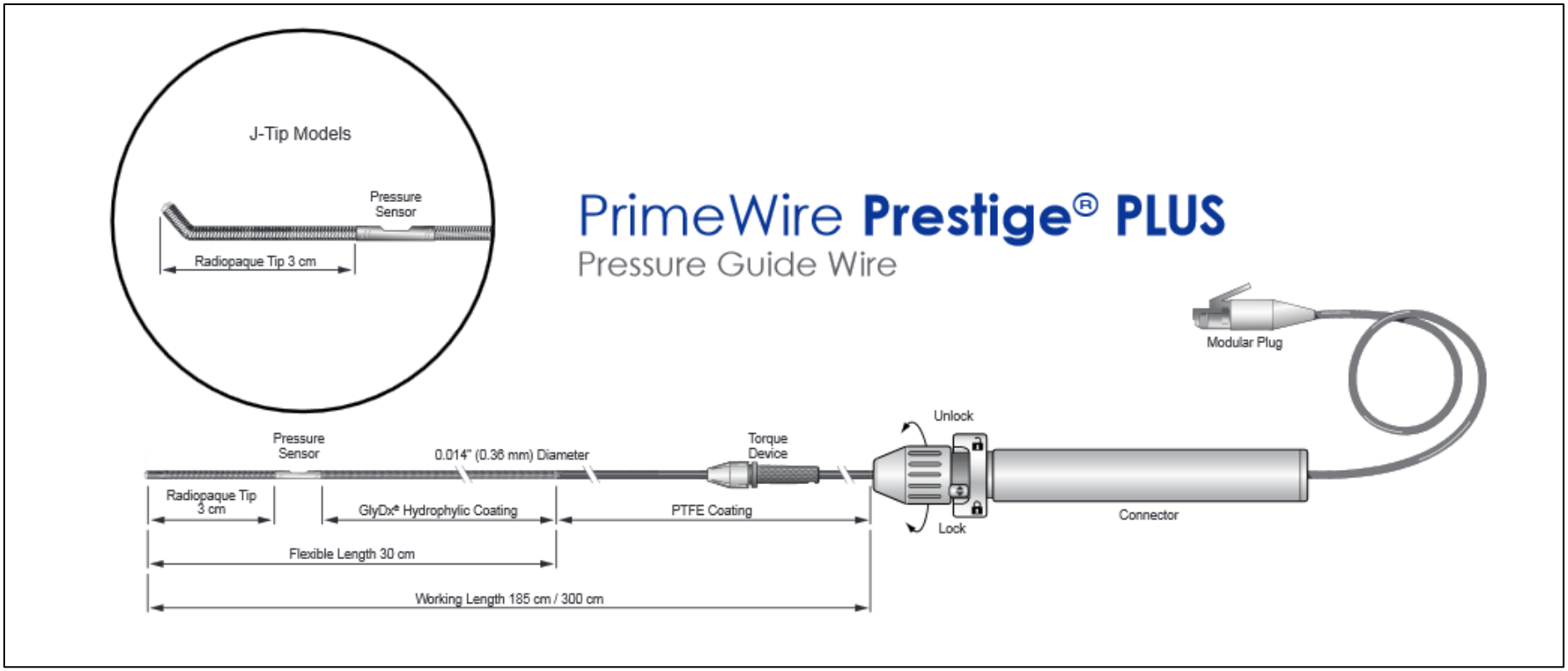

FIGURE 2-27. Schematic depiction of the Volcano Primewire Prestige Plus.

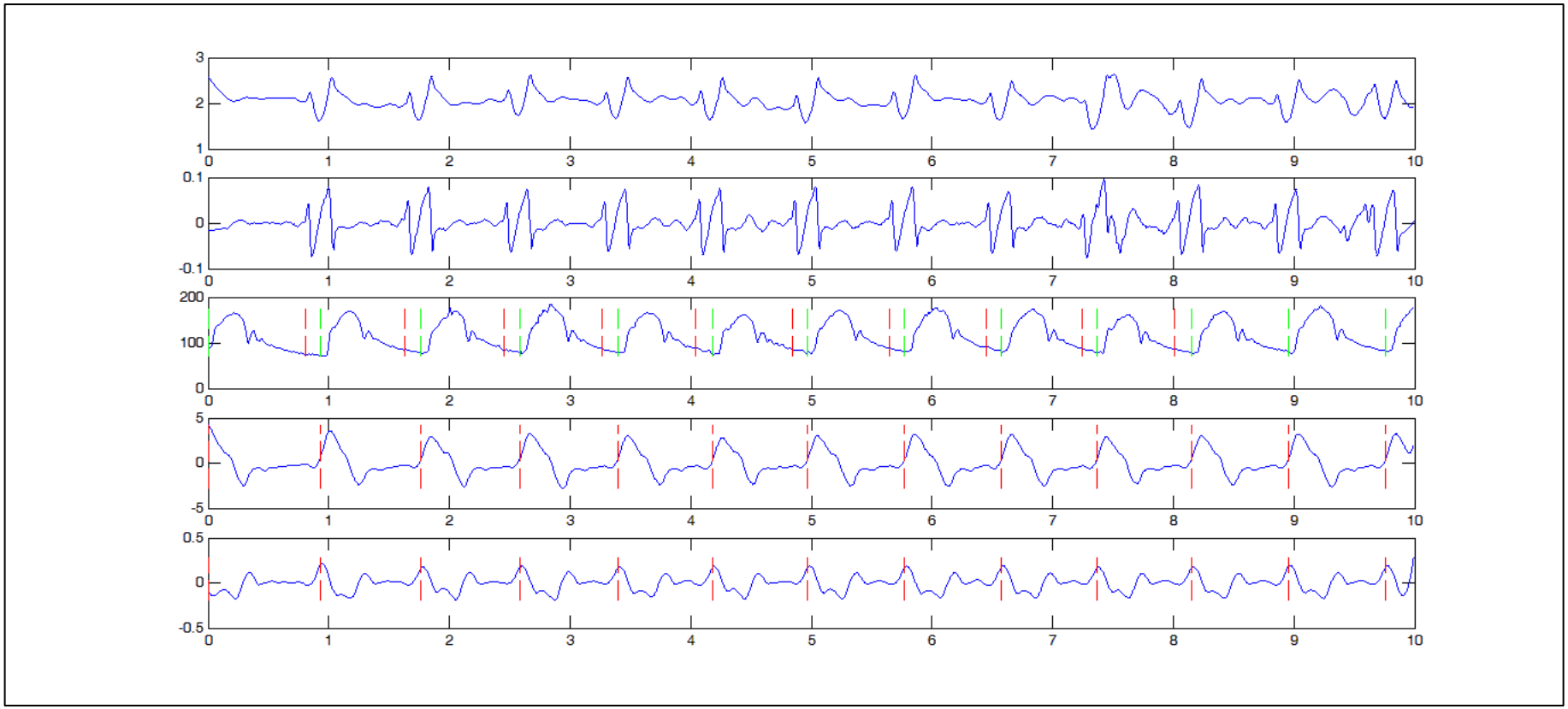

FIGURE 2-28. ECG and its first differential and pressure tracing with is first and second differential.

From top to bottom: ECG, first differential of ECG, pressure trace (red lines – division using first differential of ECG, green lines using second differential of pressure), first differential of pressure, second differential of pressure.

2.3.3.2 Results

In total 55 measurements were made in the left main stem and left anterior descending artery (Figure 2-29). The correlation was good in both systolic dpdt peak (Figure 2-26 #1) (1.8039 vs 1.7268, r=0.966, p<0.001) and diastolic dpdt minimum ((Figure 2-26 # 3) (-1.058 vs -1.073, r=0.9644, p<0.001) values (Figure 2-30 and Figure 2-31). The peak diastolic dpdt ((Figure 2-26 #2) was less strongly correlated but remained statistically significant (0.0455 vs -0.045, r=0.263, p=0.05) (Figure 2-32). Cross correlation was also employed to compare waveforms a strong correlation value of 0.9994 was found.

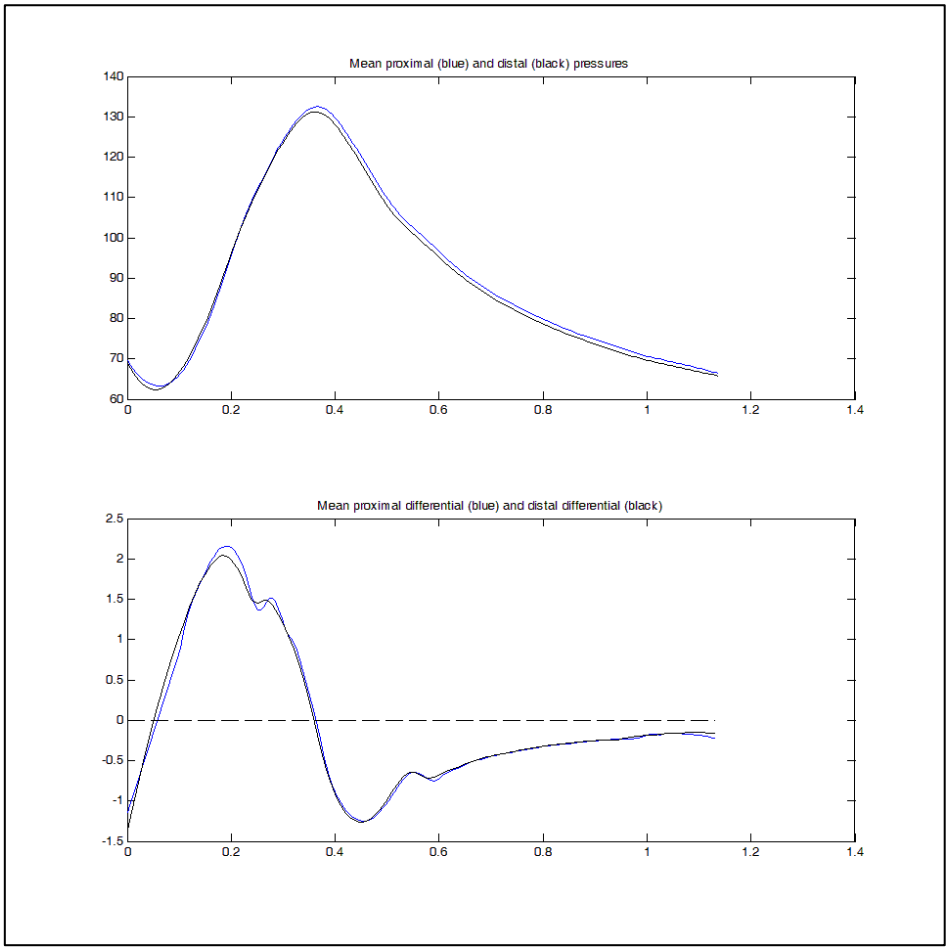

FIGURE 2-29. Example of simultaneously acquired measurement of aortic and mid-lad pressure waveforms with first differential.

Proximal pressure is displayed in blue and distal pressure in black.

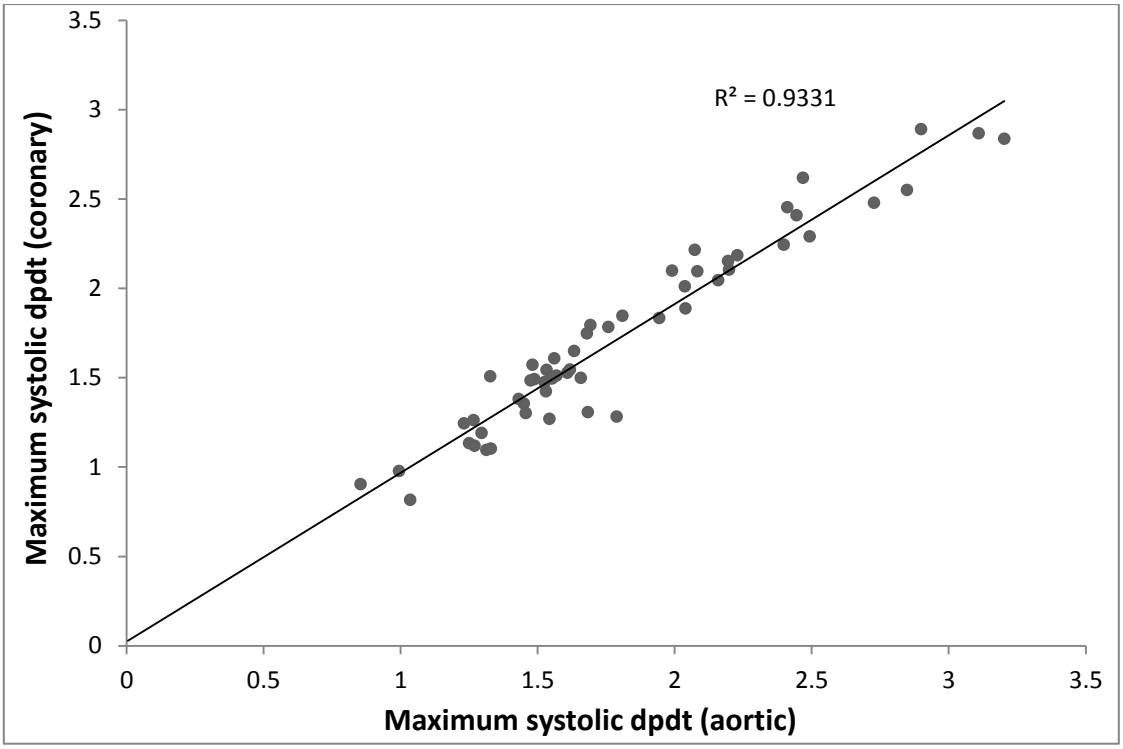

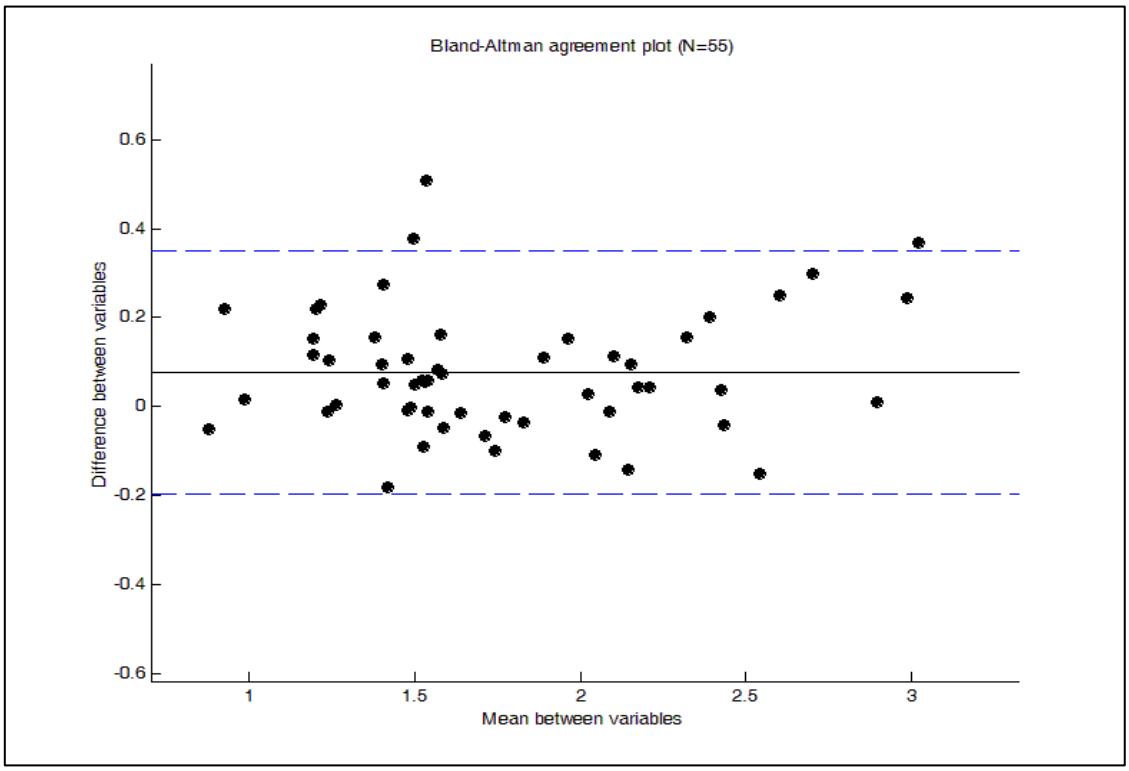

FIGURE 2-30. Scatter and Bland-Altman plot for maximum systolic dpdt measured simultaneously proximally and distally.

A good correlation is seen with the peak dpdt ($r=0.966$, $p<0.001$).

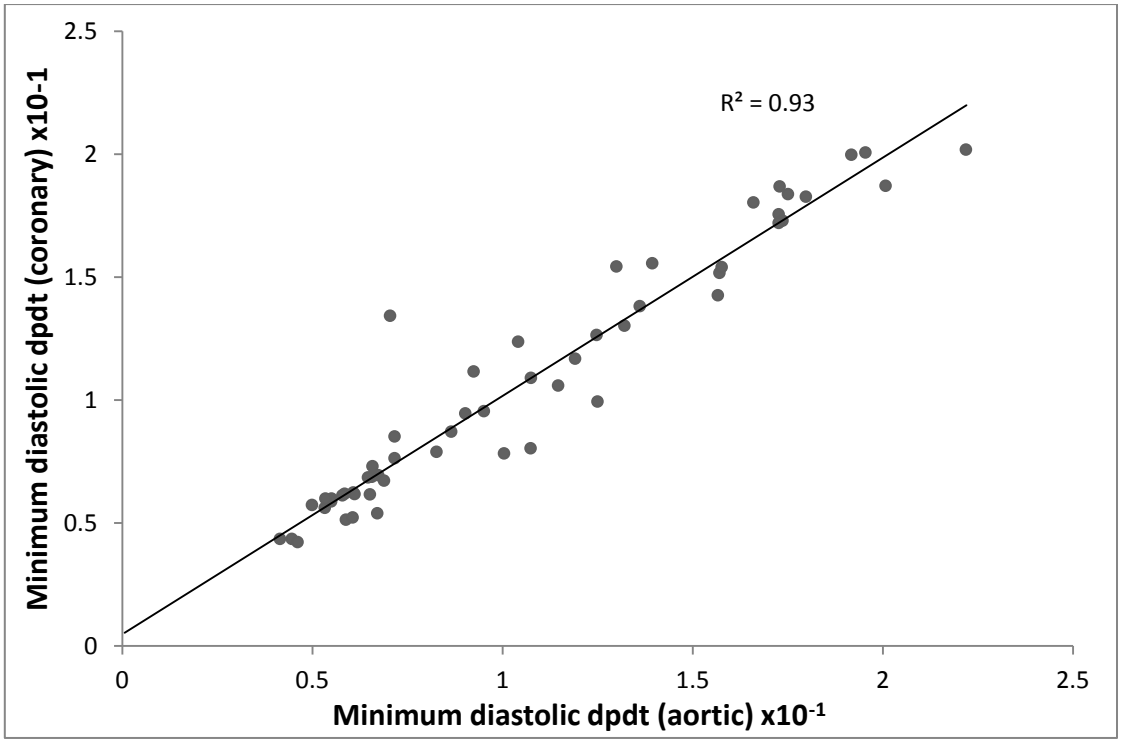

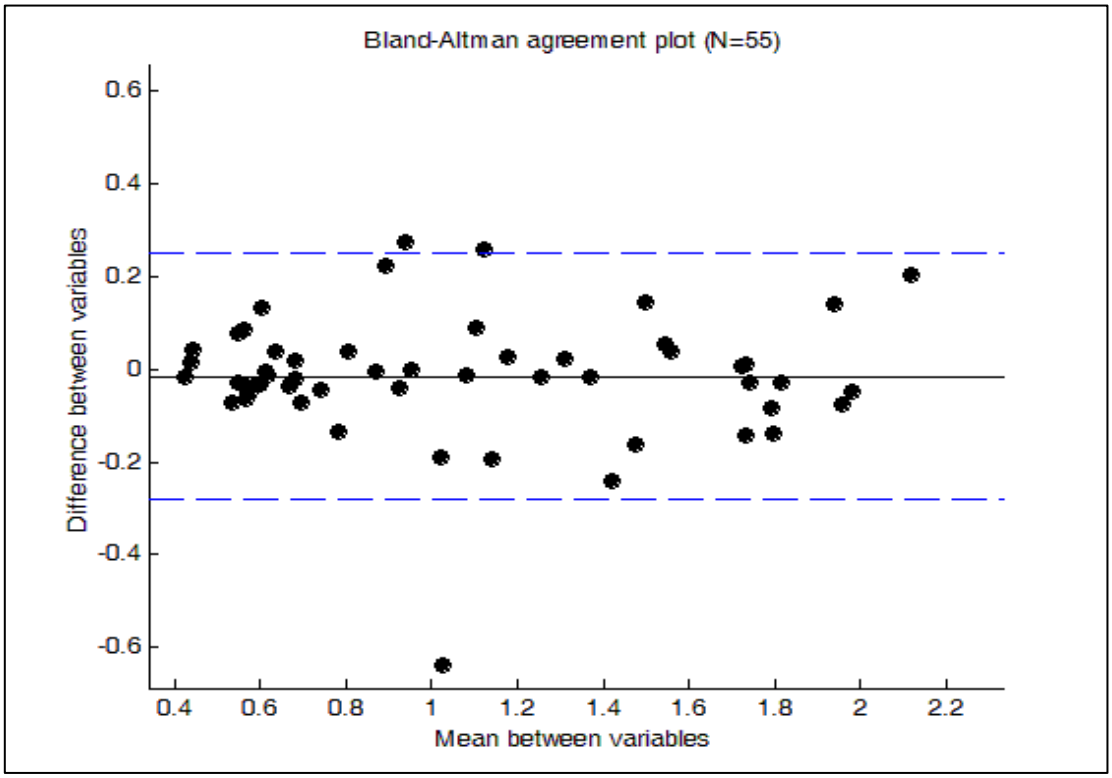

FIGURE 2-31. Scatter and Bland-Altman plot for minimum diastolic dpdt measured simultaneously proximally and distally.

Again, a good correlation is seen in this section of differentiation ($r=0.9644$, $p<0.001$).

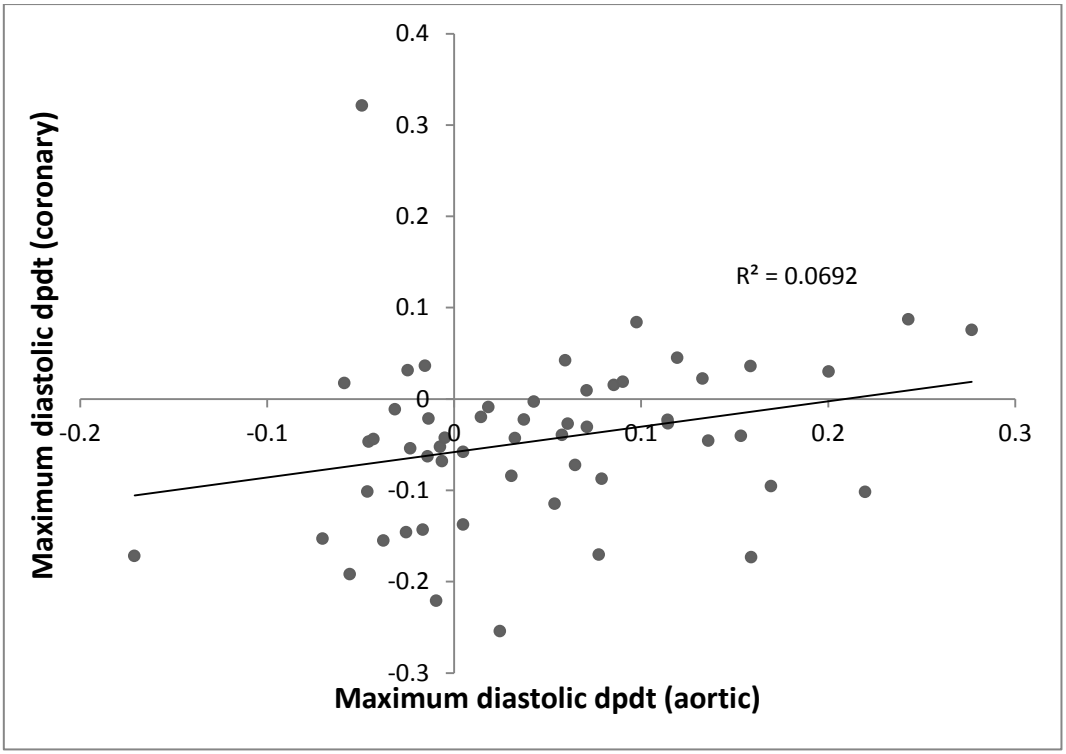

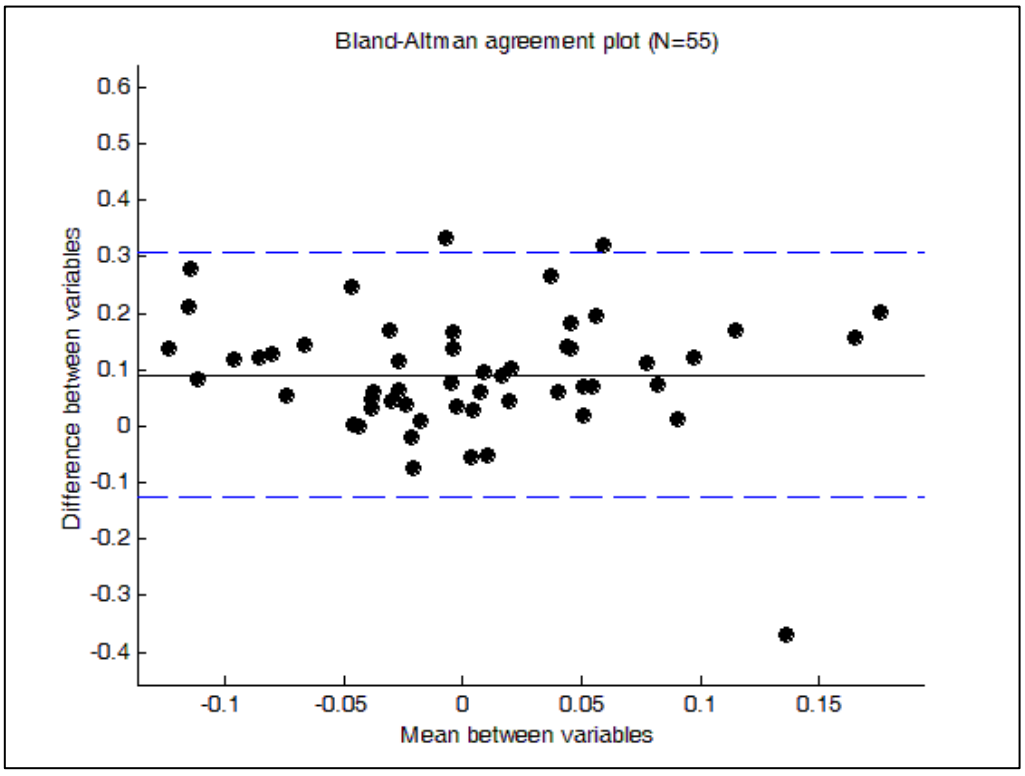

FIGURE 2-32. Scatter and Bland-Altman plot for maximum diastolic dpdt measured simultaneously proximally and distally.

A reasonable correlation is seen (r=0.263, p=0.05).

2.3.3.3 Conclusion

These sets of experiments demonstrate that the central aortic pressure waveform is highly similar to that of the left main stem and left anterior descending arteries in the absence of angiographically demonstrable coronary disease. Therefore, if central aortic pressure can be estimated non-invasively, this is a perfectly acceptable waveform from which to construct non-invasive coronary wave-intensity.

2.3.4 PULSECOR-DERIVED CENTRAL AORTIC PRESSURE – IMPROVING ITS ACCURACY FOR ASSESSING THE BACKWARD EXPANSION WAVE.

2.3.4.1 Introduction

Previous work has demonstrated that the absolute values of central aortic pressure are accurately estimated from suprasystolic blood pressure readings(Lowe et al., 2009, Lin et al., 2012). However, for wave-intensity analysis, it is the waveform that is important. Initial measurements exporting the Pulsecor's inbuilt amalgamated pressure waveform demonstrated that whilst the central aortic pressure was relatively similar to the systolic phase of aortic pressure, the area in diastole appeared to be less well demarcated (Figure 2-33). Given that the backward expansion wave is generated from this section of the pressure waveform, it was important to optimise this areas accuracy.

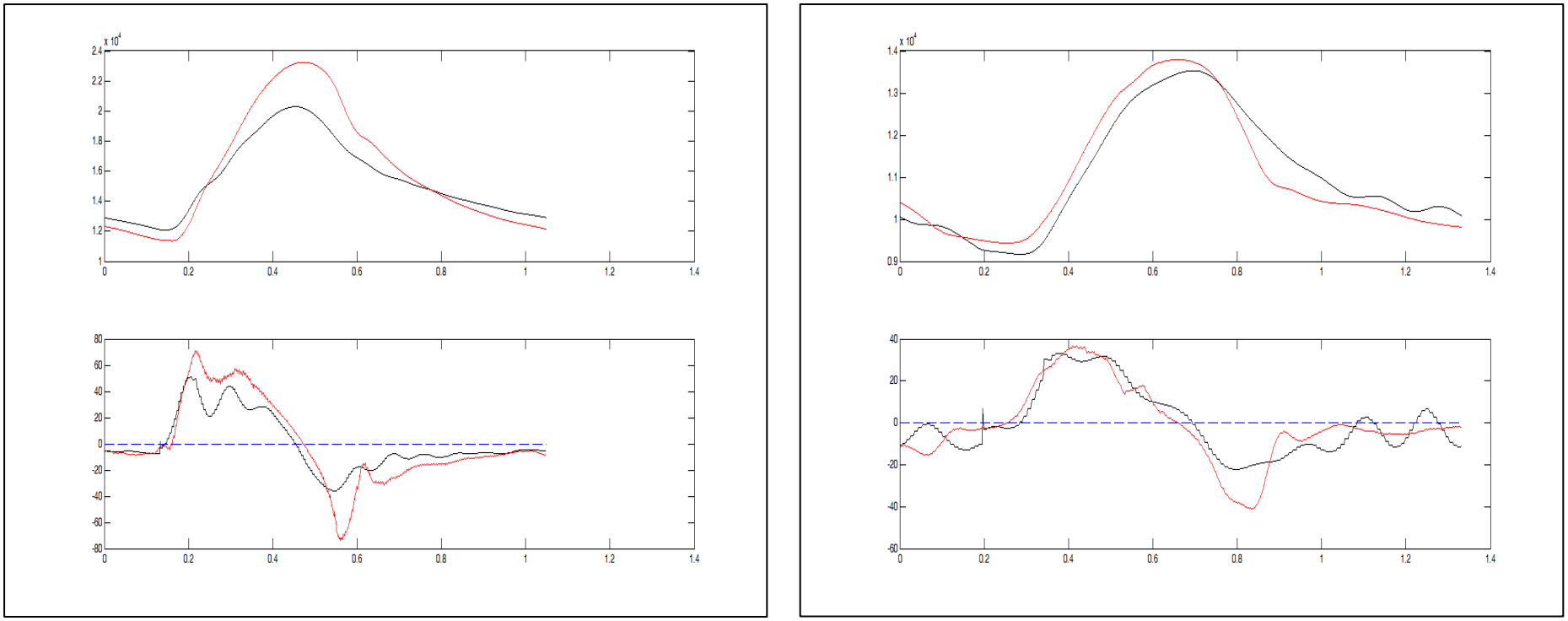

FIGURE 2-33**.** Examples of simultaneously acquired measures of central pressure and first differential from invasive and non-invasive sources.

Invasive data is displayed as red and non-invasive as black. Invasive data was gathered using a Pressure- or combined pressure- and flow-tipped sensor. Non-invasive data was acquired simultaneously using a suprasystolic blood pressure cuff (Pulsecor). The non-invasive pressure tracings appear more 'smoothed' than the invasive data and this is demonstrated by its differentiation.

2.3.4.2 Methods

To further document and elaborate these discrepancies, the differentials of each pressure recordings were broken down into several sections (Figure 2-34).

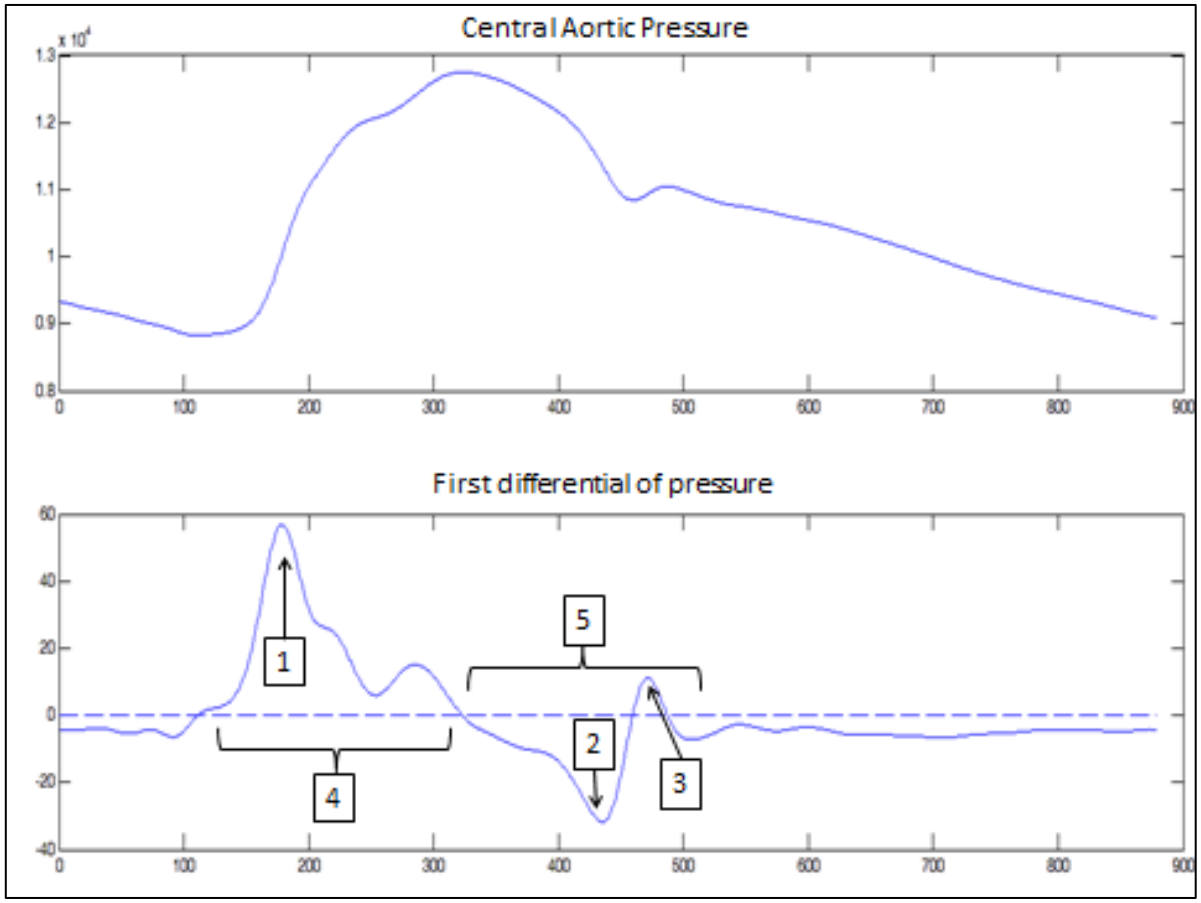

FIGURE 2-34**.** Central aortic pressure obtained invasively and divided into 5 areas for analysis.

1) max systolic dpdt, 2) minimum diastolic dpdt, 3) maximum diastolic dpdt, 4) area under the systolic dpdt pressure curve, 5) area under the diastolic dpdt pressure curve.

Using the principles described in chapters 2.5.2.2 and 2.5.2.3, data was simultaneously obtained in 18 patients undergoing coronary angiography with normal coronary arteries across 38 separate simultaneous recordings from the central aorta, left main stem and left anterior descending arteries.

2.3.4.3 Results

A good correlation was seen between the maximum systolic dpdt (Figure 2-34 - 1) and minimum diastolic dpdt (Figure 2-34 -2) as well as the areas under the systolic (Figure 2-34 -4) and diastolic (Figure 2-34 -5) dpdt curves (Table 2-3). A good correlation was also seen between invasively obtained maximum and minimum BP readings obtained invasively and noninvasively (Table 2-4). The only poor correlation was with the maximum diastolic dpdt readings (Figure 2-34 -3).

In terms of absolute values, the non-invasively obtained pressure recordings were underestimated by 0.53.

Pressure section - Figure 2-34	1	1	2	2	3	3	4	4	5	5
Mean (Pa/ms)	78.0	53.2	72.6	27.4	15.3	0.7	7780	5601	5831	3709
R value	0.4		0.6		-0.1		0.8		0.9	
P value	0.009		<0.001		0.4		<0.001		<0.001	

TABLE 2-3**.** Maximum values of differential according to above figure with r and p values.

	Maximum invasive BP	Maximum non-invasive BP	Minimum invasive BP	Minimum non-invasive BP
Mean (Pa)	18206	16483	10175	10691
R value	0.906317		0.829049	
P value	<0.001		<0.001	

TABLE 2-4. Maximum and minimum invasive and non-invasive BP measurements with r and p values.

2.3.4.4 Conclusions

Whilst the systolic and diastolic values obtained non-invasively using suprasystolic brachial measurements are similar to that obtained invasively, there does appear to be a 'smoothing effect' which is particularly evident when the pressure waveform is differentiated, as is necessary for wave-intensity analysis. This may be because of an insensitivity in the pressure-measuring hardware in the suprasystolic cuff or perhaps because the tracings are amalgamated from the foot of the aortic pressure waveform, thus overly smoothing the diastolic section. Accordingly, further manipulation, either mathematically or through access to the 'raw' (i.e. unamalgamated) Pulsecor data is necessary to improve this accuracy.

2.3.5 IMPROVING THE ACCURACY OF THE DIASTOLIC PORTION OF THE PULSECOR DEVICE

2.3.5.1 Mathematical manipulation of Pulsecor-ensembled waveform

Firstly I endeavoured to improve the diastolic portion of the pressure waveform through mathematical manipulation. One possibility was to multiply the entire vector by a scaling factor of 0.53 (which is the value I had recognised it to be deficient by as above). This would produce a good equivalent peak value but would inappropriately exaggerate the area under the curve. A more appropriate approximation would be achieved by transforming the negative values by a root of 1.2 and positive values by a root of 1.095 (values again obtained from the above experiments) (Figure 2-35).

Using this method of root-scaling, a good correlation was preserved with a better approximation of absolute values (Table 2-5 and Table 2-6).

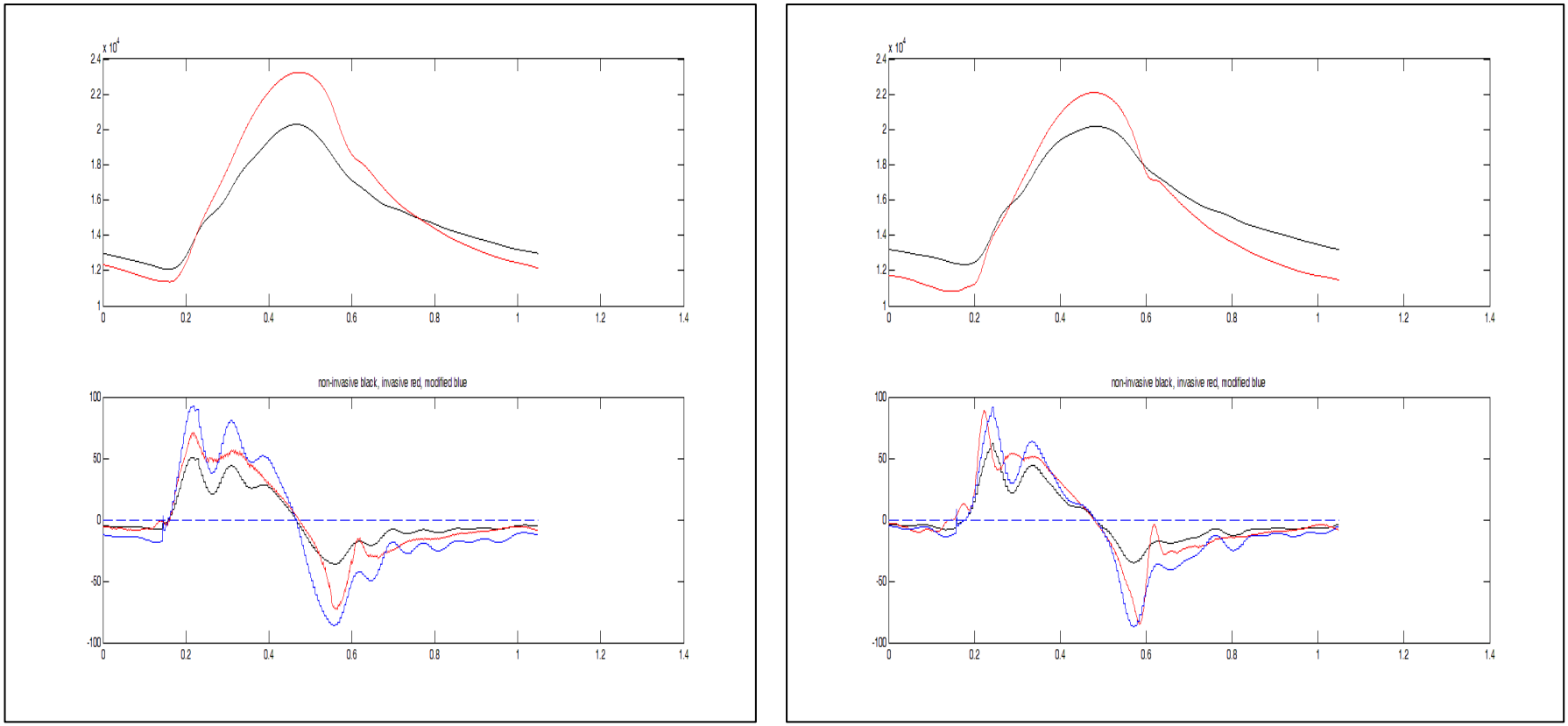

FIGURE 2-35. Pressure manipulation using either vector multiplication or root scaling.

Left panel demonstrating pressure scaling using vector multiplication. Right hand panel demonstrating pressure scaling using a 1.2 root. The data is displayed as black (non-invasive), red (invasive) and blue (manipulated non-invasive). The invasive waveform is more accurately reflected in the root-scaling rather than by multiplication.

Invasive (I) vs Non-invasive(N)	I	N	I	N	I	N	I	N	I	N
Pressure section (Figure 2-34)	1	1	2	2	3	3	4	4	5	5
Mean	77.1	79.7	-72.2	-69.0	19.3	0.48	6872	7184	5355	7539
R value	0.41		0.62		0.23		0.85		0.77	
P value	0.007		<0.001		0.15		<0.001		<0.001	

TABLE 2-5. Invasive (I) and non-invasive (N) maximum values of pressure differential according to FIGURE 2-34 with r and p values with adjustment according to root 1.2.

	Maximum invasive BP	Maximum non-invasive BP	Minimum invasive BP	Minimum non-invasive BP
Mean (Pa)	18234	16435	10126	10602
R value	0.901522		0.790786	
p value	<0.0001		<0.00001	

TABLE 2-6. Maximum and minimum invasive and non-invasive BP measurements, r and p values after adjustment by a root of 1.2.

2.3.5.2 Using 'raw' Pulsecor cuff Data

Although this produced a reasonable approximation of invasive pressure, I felt that manipulating the raw data rather than the data automatically processed by the Pulsecor machine may allow for more accuracy. Particularly, the area around the dicrotic notch was overly smoothed by the machine's inbuilt amalgamation and it is from this area that the backward expansion wave is produced.

In the Pulsecor Matlab array the unprocessed suprasystolic data was located as a Matlab file "SuprasystolicFiltered" (Figure 2-36). This was also available as an amalgamated file, "SuprasystolicBeatsOverlaid" (Figure 2-37).

Encouragingly, the dicrotic notch was more evident in these traces. The first step was to convert the traces to Pascals. This was done by using the given systolic and diastolic pressures with the amalgamated CentralPressureAverage and calculating the ratio between that and the systolic and diastolic mean of SuprasystolicBeatsOverlaid (FIGURE 2-38). When more than one Pulsecor reading was taken, they could be amalgamated to produce even longer stretches of data for integer processing (Figure 2-39).

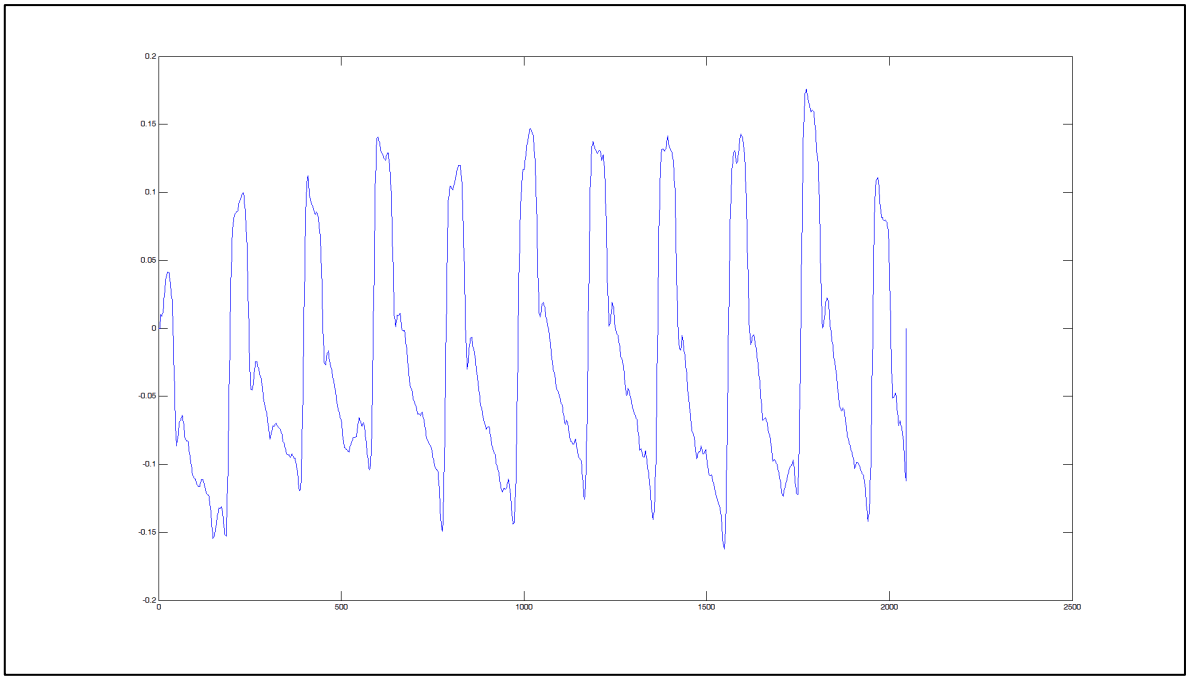

FIGURE 2-36. “Suprasystolicfiltered” from Pulsecor Matlab cell array.

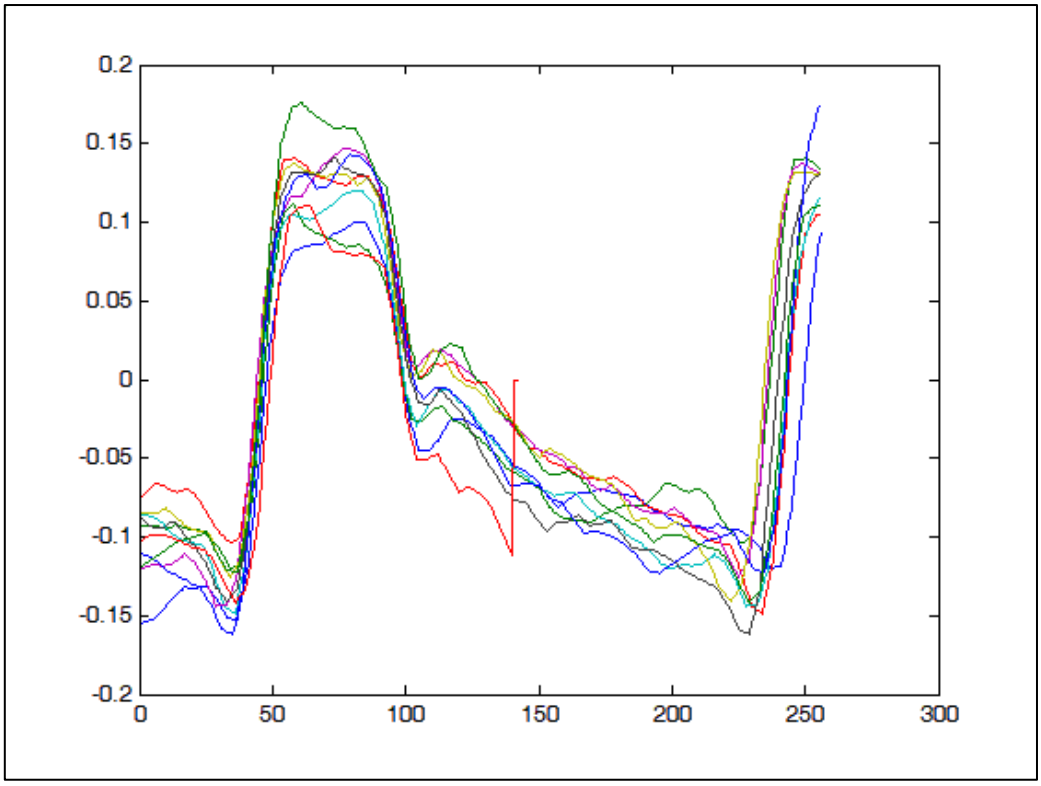

FIGURE 2-37. Suprasystolicbeatsoverlaid from Pulsecor Matlab cell array,

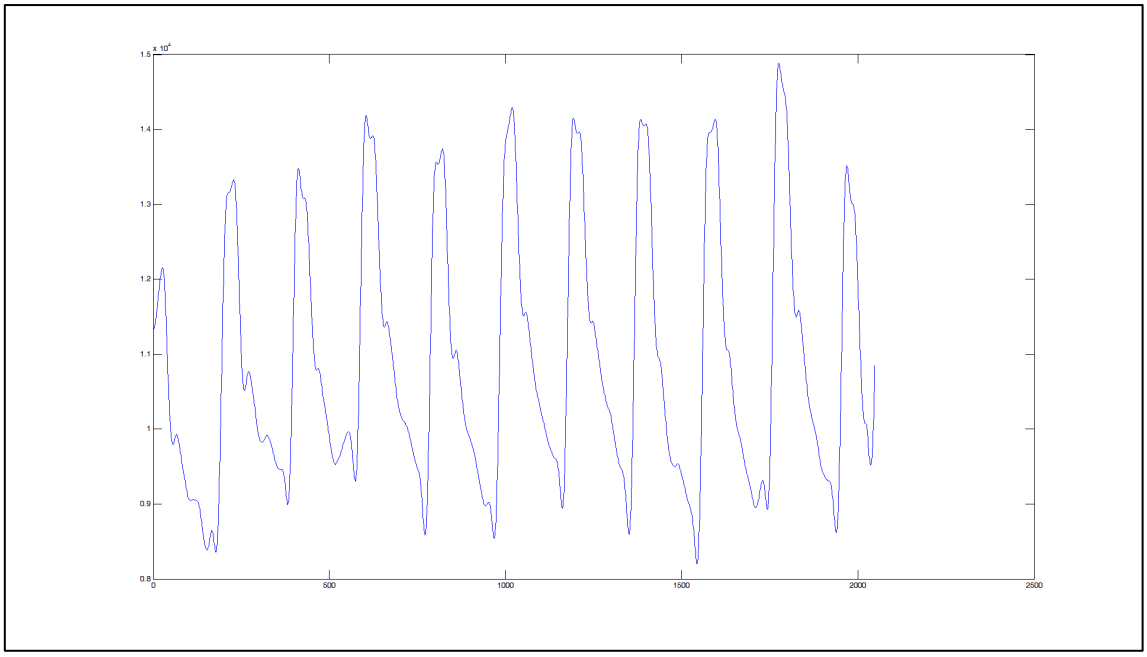

Figure 2-38. Pressure from Suprasystolicfiltered in Pascals.

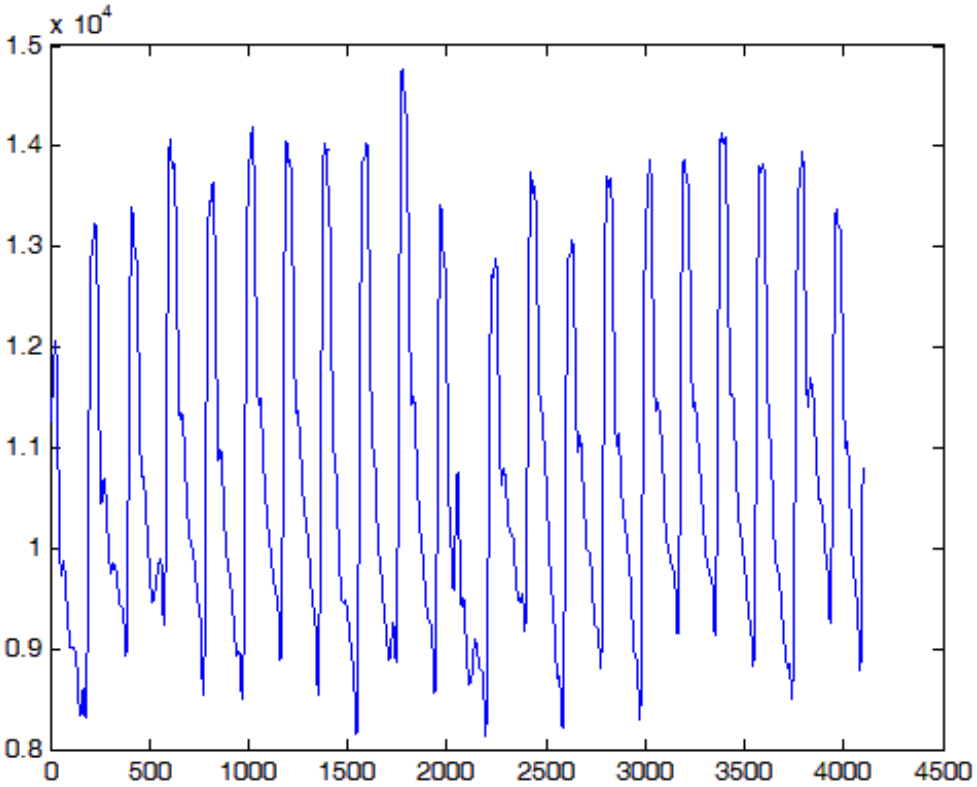

FIGURE 2-39. Amalgamated Pulsecor signals from two separate recordings. Data displayed in Pascals.

2.3.5.3 Ensembling of Raw Pulsecor Data

The Pulsecor machine provided an ensemble-averaged pressure file as SuprasystolicBeatsOverlaid. However, at times, the ensembling was inaccurate. Therefore, I set out to construct an automated ensembling programme using the differentials of pressure. At first, I concentrated on the second differential of pressure but I found greater accuracy with the first. My custom-built Matlab programme's parameters for differential assessment could be altered during its processing to allow greater accuracy as demonstrated in Figure 2-40 and Figure 2-41.

This was a useful software addition, particularly when the Pulsecor's own ensembling was less accurate (FIGURE 2-42). A further addition to the programme allowed individual beat selection was also enabled in case of irregular heart rhythms or inaccuracies mid-way through the recording.

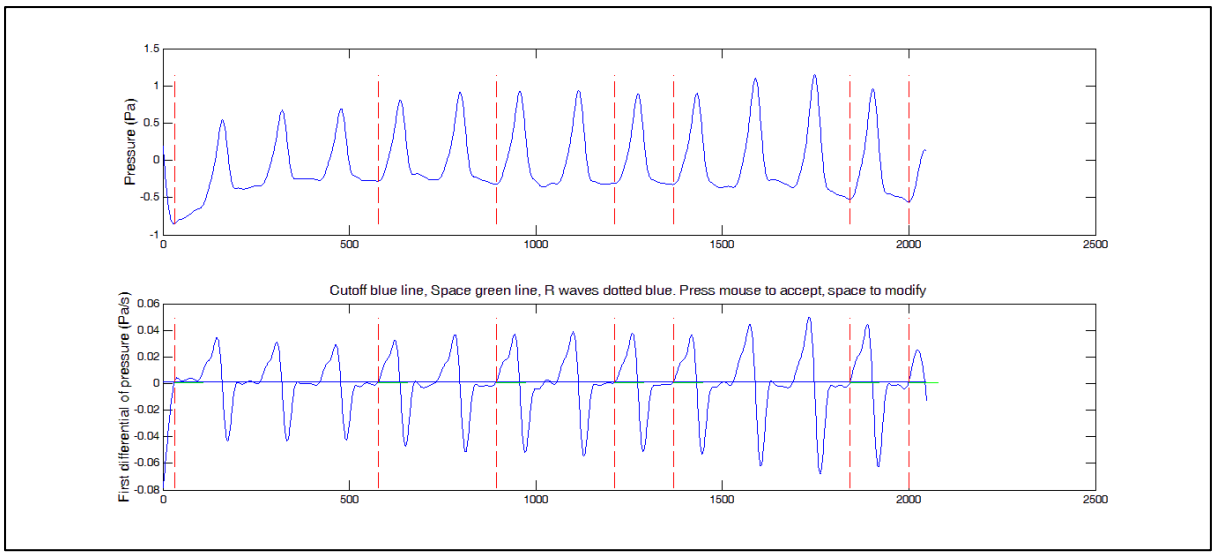

FIGURE 2-40. Pressure and its first differential with poor differential recognition

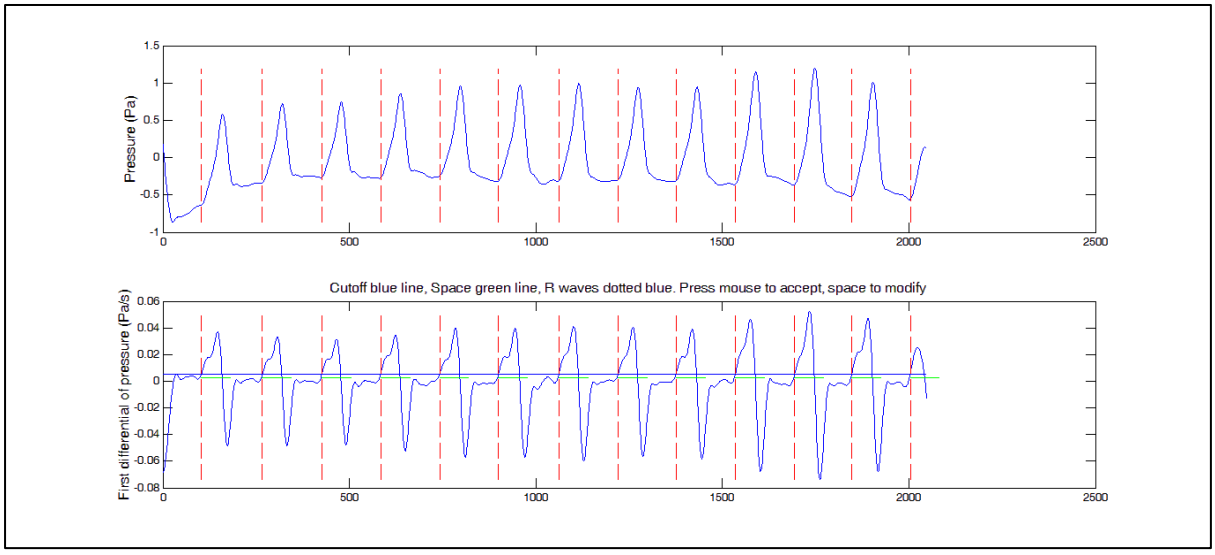

FIGURE 2-41. Pressure and its first differential with altered differential settings and good recognition

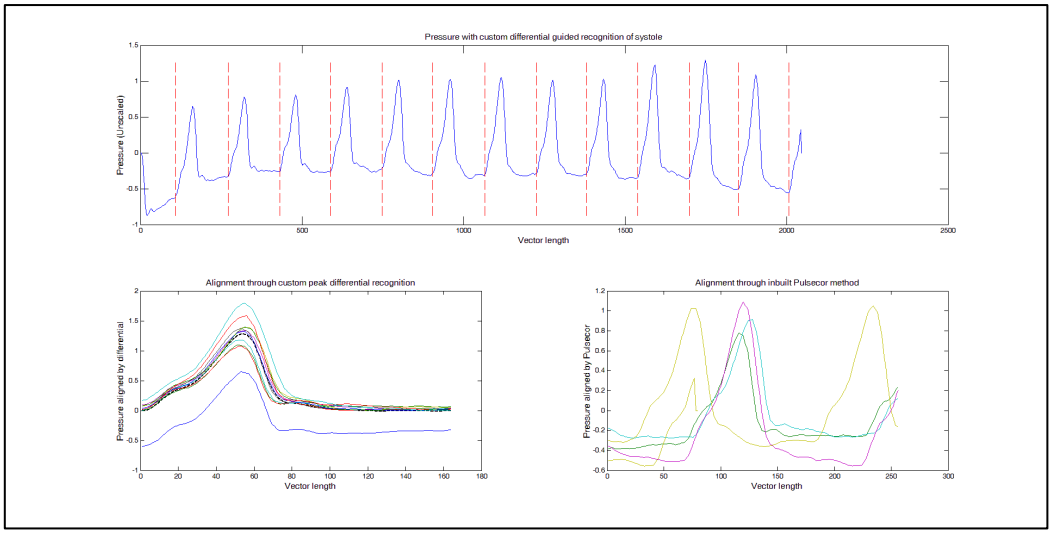

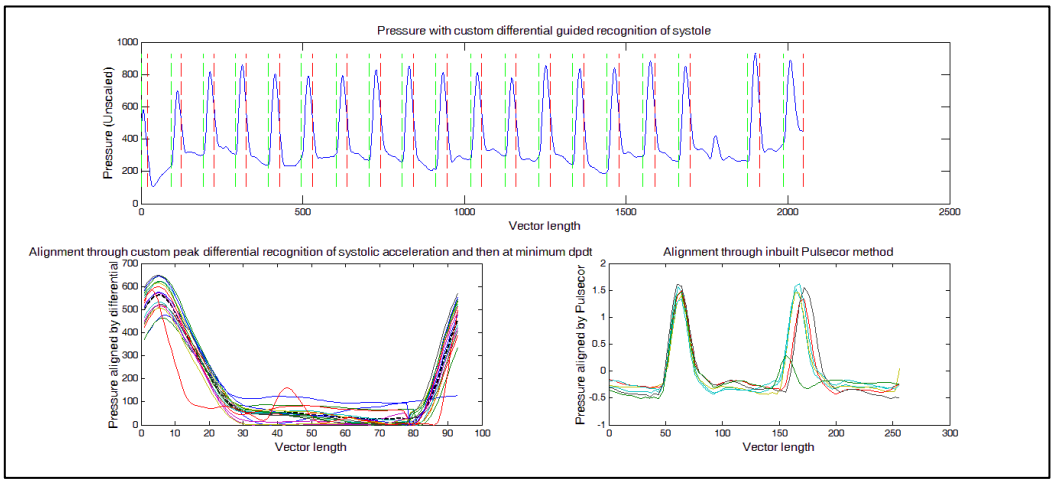

Figure 2-42**.** Pressure from Pulsecor divided by both custom-made and inbuilt software at rest (top diagram) and during exercise (lower diagram)

The upper panel demonstrates pressure divided up by cardiac cycle recognised by the peak of the first differential (upper panel) from the above bespoke Matlab programme. The lower left panel shows the resultant ensembled pressure (pre-scaling) from this programme and the lower right panel Pulsecor's own attempt at alignment. As can be seen, in this case the Pulsecor software failed to appropriately align the pressure waveforms resulting in an inaccurate ensemble-average. This is particularly exacerbated with a tachycardic patient.

2.3.5.4 Comparison of Invasive and Non-invasive Pressure Data

A similar process as above was applied to compare simultaneously acquired non-invasive and invasively pressure signals using this 'raw' Pulsecor data. The data was processed in a total of 48 simultaneous measurements in 30 patients undergoing coronary angiography with invasive data obtained either via the catheter tip or from a pressure wire.

Initial work demonstrated the pressure traces to be more comparable when using the raw Pulsecor data. There remained a slight underestimation and a conversion factor was again applied in an attempt to modify the pressure traces appropriately. As a reflection of the improved signal with the raw Pulsecor data, the conversion factor was much lower than required with the amalgamated signals (1.03163 for systole and 1.02976 for diastole). An example of these traces, along with the modified traces is shown in Figure 2-43.

Using this modification approach, a good correlation was seen with the absolute values of systolic (invasive 18526Pa, non-invasive 19806Pa, $r = 0.85$, $p < 0.001$) and diastolic (invasive 9837Pa, non-invasive 11161Pa). A reasonable correlation was seen with the other sections of pressure curve analysis as demonstrated in Table 2-7 and Figure 2-44.

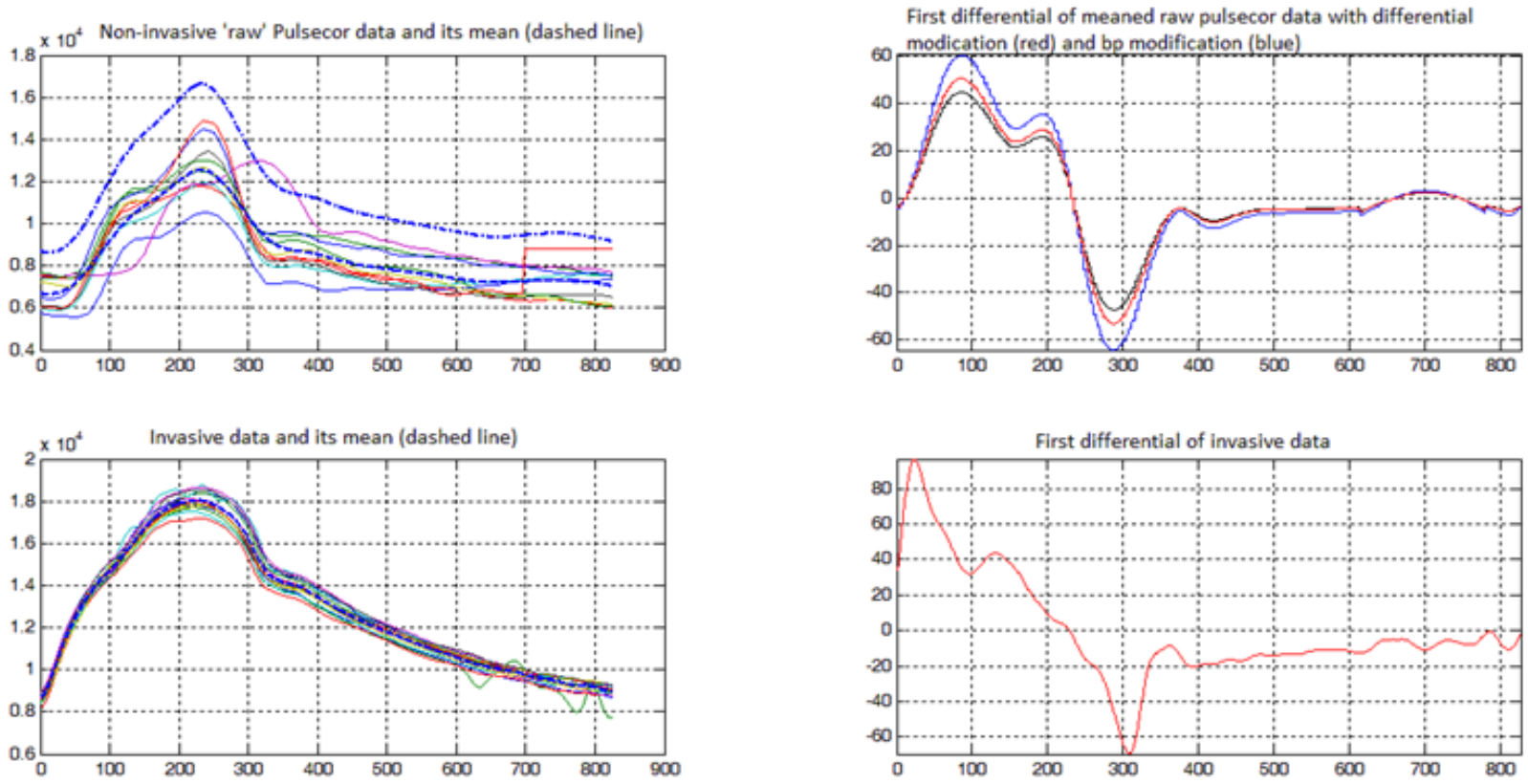

FIGURE 2-43. Invasive and non-invasive (from 'raw', power-modified Pulsecor data) pressure and its first differential.

Pressure (left) and differential of pressure (right) traces. Upper panels demonstrating non-invasive traces derived from the raw Pulsecor data and its differential with a power modification either of the original pressure trace (blue) or after differentiation (red). Lower panels demonstrate invasive data and its first differential.

	1	1	2	2	3	3	4	4	5	5
Mean	19375	9550	-82	-79	21	8	8533	8427	-5171	-5922
Correlation		0.570		0.6678		0.2607		0.800		0.7680
P value		<0.01		<0.01		0.07		<0.01		<0.01

TABLE 2-7. Different sections of the pressure curves for simultaneously acquired invasive (left) and non-invasive (right) data.

The non-invasive pressure curve is modified by a root of 1.03163 in systole and 1.02976 in diastole.

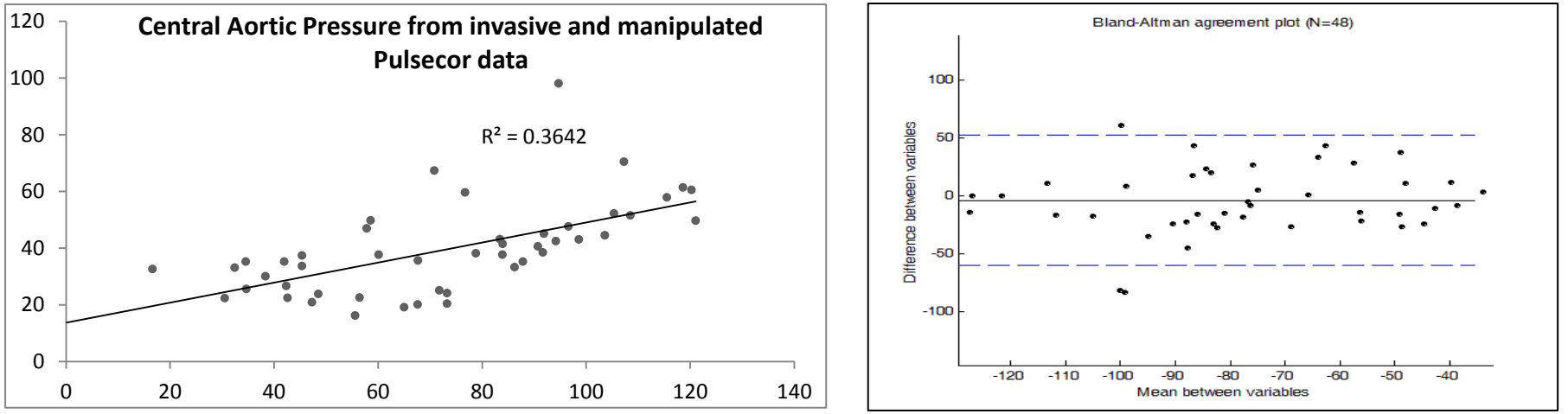

FIGURE 2-44. Correlation scatter graph and Bland-Altman agreement between the minimum dpdt of invasive versus non-invasively derived pressure.

The non-invasive pressure is produced from raw Pulsecor data and modified as above. Data is displayed as positive values.

2.3.5.5 Further Pulsecor Work

Whilst this work with Pulsecor enabled an even higher accuracy for pressure calculation, the data from which it was derived was ultimately a measure of more peripheral pressure. Additionally, the mathematical manipulation required increased the chance of error magnification. Therefore, in order to attempt to estimate wave-intensity with ultimate accuracy, a measure of central pressure was required that did not require mathematical amplification. Also, as has been demonstrated above, using the Pulsecor-ensembled CentralPressureAverage resulted in inaccuracies, often due to its mis-selection of beats which was particularly apparent in arrhythmias, including atrial fibrillation or sinus arrhythmia. Therefore, manual selection and alignment of the raw central-estimation of pressure would hopefully negate all these issues

The unprocessed Pulsecor file was stored in the Pulsecor array as AOChannel0. The data from this channel was unscaled and suffered from a trending baseline providing a pressure trace as demonstrated in Figure 2-45. This pressure trace was detrended using a fast Fourier transform (Figure 2-46)

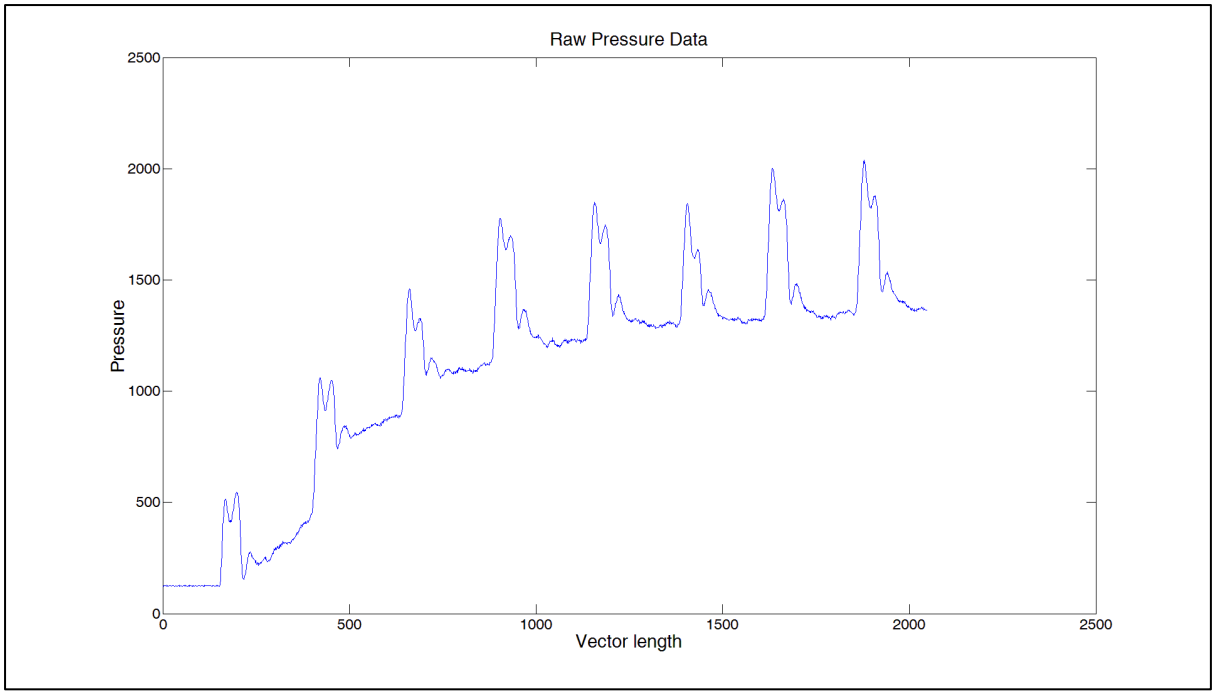

FIGURE 2-45. Untrended raw pressure data extracted from Pulsecor.AOChannel0.

The pressure is unscaled and trends upwards.

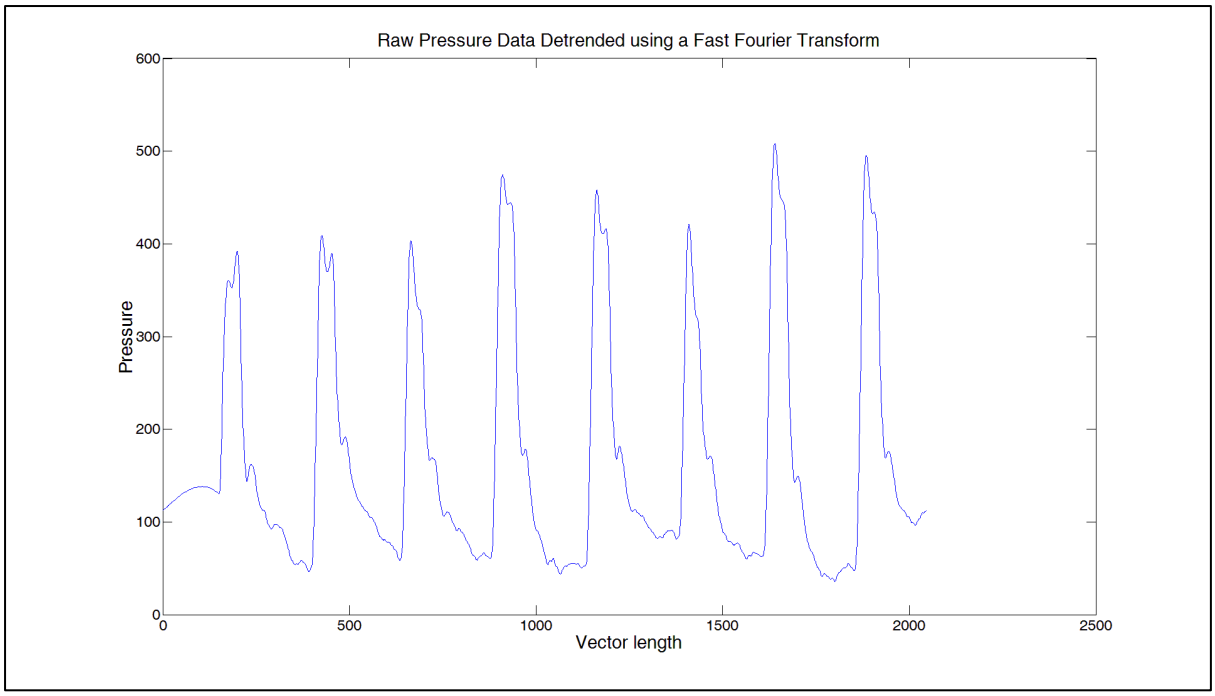

FIGURE 2-46. Raw data detrended using a fast Fourier transform.

It remains unscaled.

As can be seen, there is now a much better preservation of the dicrotic notch which had become obliterated in non-selected alignment such as that inherent to the Pulsecor device. Therefore, I sought to align the Pulsecor data not according to the foot-to-foot method but according to the minimum dpdt which would therefore preserve the integrity of the diastolic portion more successfully (Figure 2-47).

Once processed in this fashion the mean unscaled trace was scaled according the systolic and diastolic calculated central aortic pressures provided by the Pulsecor machine using the following formula:

$$\text{Central 'Bespoke' Pressure} = (d-c) * (x- a) / (b – a) + c$$

d = Systolic central aortic pressure, c = Diastolic central aortic pressure, b = Maximum value of unscaled raw data, a = Minimum valve of unscaled raw data, x = Vector of Raw unscaled data

EQUATION 2-2. SCALING OF CENTRAL PRESSURE ACCORDING TO THE PULSECOR-PROVIDED SYSTOLIC AND DIASTOLIC PRESSURES

2.3.5.5.1 Correlation with Invasive Pressure

Once again, using this new technique, the non-invasive data was correlated with the invasive data. There was a slight underestimated of systolic pressure non-invasively (18226 vs 16648 Pa) but with a good correlation ($r = 0.84$, $p < 0.001$); diastolic pressure was also estimated appropriately (9813 invasively vs 10508 Pa non-invasively, $r = 0.89$, $p < 0.001$) (Table 2-8, FIGURE 2-48). The cross correlation coefficient of the two waveforms was an average of 0.9723..

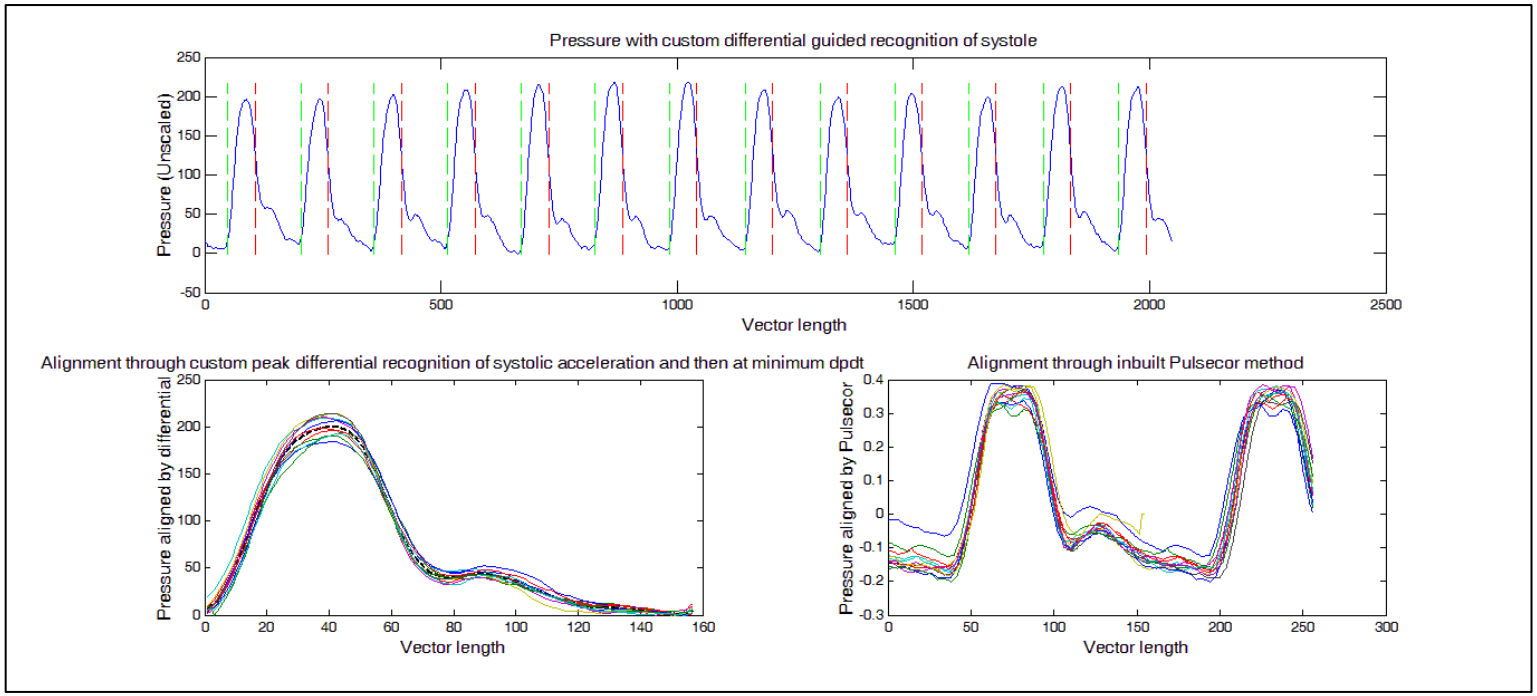

FIGURE 2-47. Pressure alignment using custom and inherent Pulsecor software.

The upper panel shows the raw pressure traces and each cardiac cycle is divided firstly according to a foot-to-foot method using peak dpdt (green dashed line). After initial ensembling they are further modified to align by minimum dpdt (red dashed line). This two-step process was essential to prevent 'jumps' at the point of minimum dpdt alignment due to the fact that alternate beats were being spliced together to create the individual pressure cycle. The summation is demonstrated in the lower left panel and compared to Pulsecor's inbuilt alignment of the raw (unprocessed) peripheral data.

	1	1	2	2	3	3	4	4	5	5
mean	111	60.2	-72	-40	23.9	-4.75	8040	5879	-4348	-4622
correlation		0.27		0.60		-0.066		0.68		0.63
P values		<0.01		<0.01		0.7		<0.01		<0.01

TABLE 2-8. Correlation between invasive and non-invasive pressure using ADCChannel0

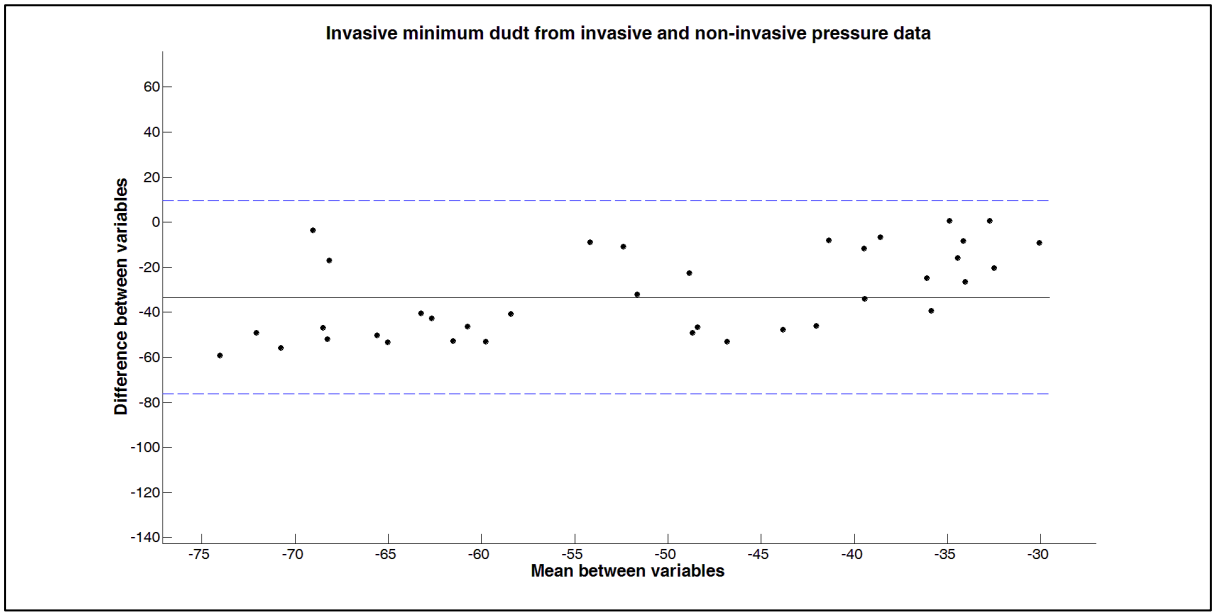

Figure 2-48. Bland-Altman plot of invasive versus non-invasive coronary pressure data with non-invasive data detrended and manipulated from raw-data using a fast Fourier transform and scaling.

2.3.6 CONCLUSIONS

I have demonstrated that whilst it is impossible to directly measure coronary pressure waveforms, a good approximation can be achieved from suprasystolic pressure recordings using the Pulsecor device. The device itself contains an inbuilt amalgamation programme but this results in inaccuracies, particularly in the diastolic portion of the waveform. Mathematical manipulation can be used to improve this but with the inherent risk of amplification of any errors.

Therefore, an alternative is to access the raw Pulsecor data which has numerous theoretical advantages. Using a detrending protocol involving a fast Fourier transformation, along with scaling according the Pulsecor's own estimation of central pressure, an accurate central aortic pressure waveform can be obtained that needs no mathematical amplification. Alignment is key and to preserve the diastolic portion of this waveform I have devised a programme to recognise and align according to the minimum dpdt.

Finally, I have also shown that not only is pressure a significant part of the wave intensity calculation, that central pressure can be accurately assumed to represent coronary pressure providing there are no coronary lesions. In summary, I now have an accurate, non-invasive estimation of the coronary pressure waveform.

2.4 VARIABLE 3: NON-INVASIVE CALCULATION OF WAVESPEED

2.4.1 INTRODUCTION

Necessary for the derivation of wave-intensity analysis is the calculation of wavespeed. The pulse wave velocity within vessels has been of interest for some time as it is thought to reflect arterial stiffness and later life cardiovascular risk(Blacher et al., 1999, Muiesan et al., 2010, Coutinho et al., 2011). The standard approach to measuring wavespeed is in a 'foot-to-foot' fashion, by recording pressure traces at two points in the vessel of interest and calculating the time taken for a rise in pressure to be transmitted from proximal to distal site. Wavespeed is then the distance between points of measurement divided by this time. This can be achieved either through simultaneous measurements or through individual measurements gated to the ECG.

Attempts to calculate foot-to-foot wavespeed in coronary arteries is impossible because the arteries are too short to provide measurable and reliable pressure changes from two separate sites. Alternative techniques that use single point estimations of wavespeed, such as P-U loop analysis (a technique that has been validated in vitro(Khir and Parker, 2002), in dogs(Khir and Parker, 2005) and in humans(Khir et al., 2001) are also not possible in the coronary artery because influences on pressure occur from either end of the artery. However, an invasive single-point measurement of coronary wavespeed (c) has been proposed by Davies *et al.(Davies et al., 2006b)* that avoids these issues. The formula for this is:

$$c = 1/\rho \sqrt{(\sum dP^2 / \sum dU^2)}$$

where ρ is the density of blood, P is pressure and U is velocity measured at the same point.

EQUATION 2-3. SINGLE POINT WAVESPEED CALCULATION

This method has been validated against aortic wavespeed calculated by the foot-to-foot method and both coronary and aortic wavespeed calculated through this method has been shown to increase with age(SIMONSON and NAKAGAWA, 1960, Rogers et al., 2001, Aguado-Sierra et al., 2006). However, this method has come under some criticism as adenosine (which influences the microcirculation but not epicardial vessels) causes effects on single-point wavespeed which are thought to be inconsistent with wavespeed behaviour. However, with no gold-standard for wavespeed calculation, the single-point measurement is thought to provide a good estimate with low variation.

Recently, a new method has been proposed to measure wavespeed by assessing vessel size changes (in a method similar to tonometry of proximal vessels) and flow velocity and as such can produce aortic wave-intensity through the use of cMR(Biglino et al., 2012b). This has been applied to disease states in the assessment of hypoplastic left heart therapy in children showing aortic reconstruction to create a more unfavourable ventricular-vascular coupling and reduced aortic distensibility. However, echocardiography is not discriminatory enough to provide this information on vessel size expansion.

Whilst echocardiography can accurately estimate the rate of coronary blood flow(Rigo et al., 2010, Hozumi et al., 1998a, Hozumi et al., 1998b) it is not as effective at estimating

these minute changes in vessel size. Likewise, a foot-to-foot estimation of wave speed is not possible in the coronary arteries because two distinct measurably-distant points cannot be discerned using non-invasive measures. Therefore, the single-point equation is required to estimate wave speed using non-invasive measures of flow and pressure.

2.4.2 METHOD

2.4.2.1 Demographics

In total, 26 patients (11 male) with unobstructed coronary arteries were recruited during diagnostic angiography. Patients were selected either because they were relatively low risk for coronary disease or were having a workup angiogram for aortic valve surgery (normal aortic valve =16). Patients were only included in the study if there were no coronary lesions seen at angiography as this is known to affect the single-point wavespeed calculation(Kolyva et al., 2008).

2.4.2.2 Invasive and non-invasive data acquisition.

Simultaneous invasive measurements of pressure and flow were recorded as described in section 2.5.2.2. Wavespeed was calculated according to the single point equation as previously described(Davies et al., 2011, Davies et al., 2006a, Davies et al., 2006b).

Immediately following angiography, non-invasive measures of pressure and flow were recorded as described in section 2.5.2.3.

2.4.3 RESULTS

2.4.3.1 Methods of calculating non-invasive wavespeed

2.4.3.1.1 Integer versus mean calculation of wavespeed

Because of the multiplicative nature of wave-intensity analysis, coronary wavespeed is an important value to calculate accurately. The single-point equation when used invasively requires an integer number of cardiac cycles (Davies et al., 2006b). However, prior to the ability to manipulate the raw Pulsecor data, the only measurement initially available was a mean vector and so data could only be calculated across a single mean cardiac cycle.

Therefore, initially I set out to ascertain the importance of an integer-based calculation compared to a single averaged cardiac cycle on the same invasive measurements.

In the 26 patients with unobstructed coronary arteries, invasive single point wavespeed was calculated using across both an integer number of cardiac cycles and then after the same cycles had been averaged to form a single cardiac-cycle. A correlation was seen in both left main stem measurements (n=21, average = 15.23 vs 17.00m/s, r= 0.171, $p<0.001$) and the left anterior descending artery (n=26, average = 18.31 vs 17.4, r=0.630, $p<0.001$) (Figure 2-49 and Figure 2-50).

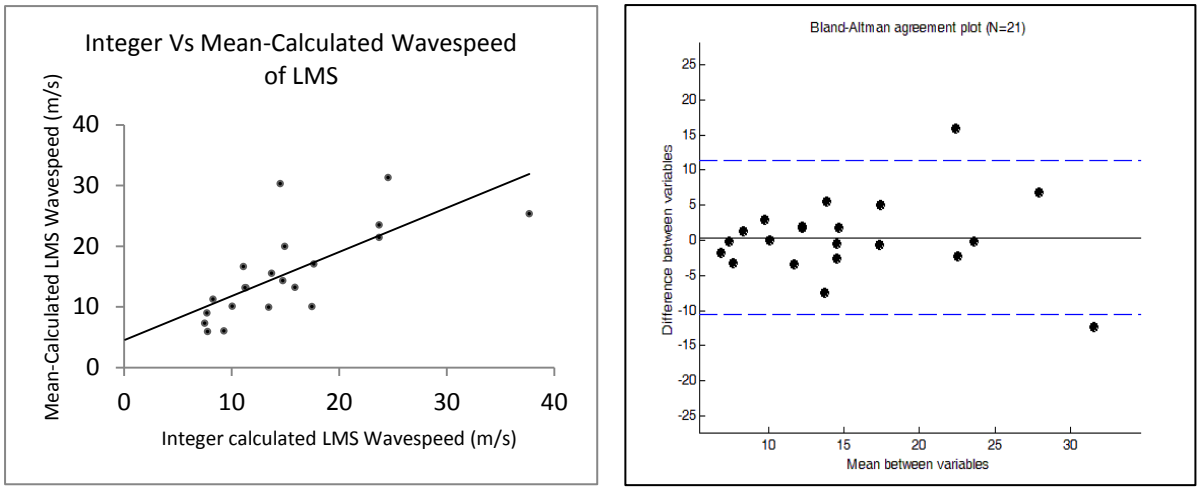

FIGURE 2-49. Scatter and Bland-Altman plot of integer versus mean-calculation of wavespeed of left main stem.

There are differences between the values obtained but there remains a reasonable correlation.

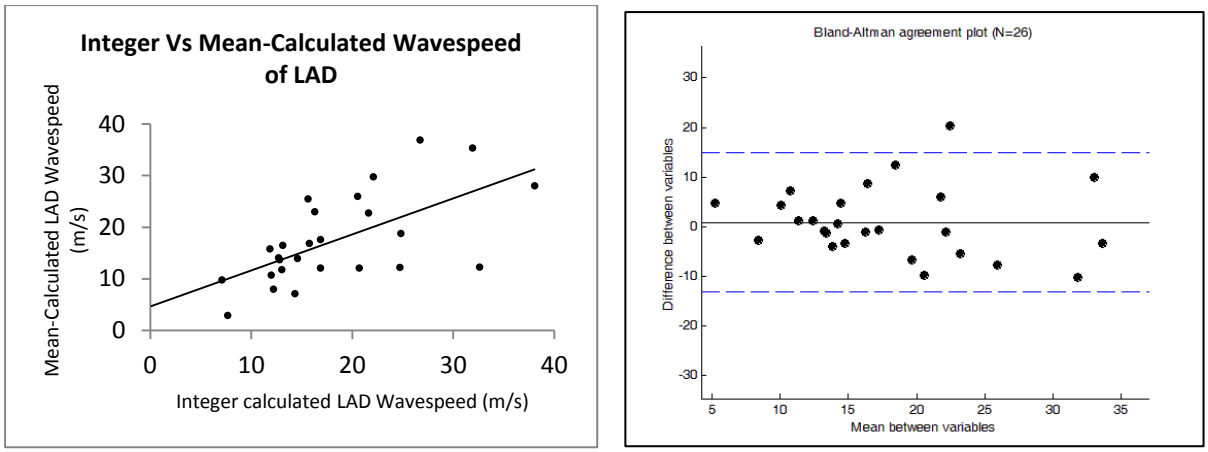

FIGURE 2-50. Scatter and Bland-Altman plot of integer versus mean-calculation of wavespeed of left anterior descending artery.

Again, there are differences in the values obtained with a reasonable resultant correlation.

2.4.3.2 Possible approaches to calculating wavespeed non-invasively

It was therefore apparently possible to construct wavespeed with reasonable accuracy from non-invasively generated vectors of mean flow and pressure over a single cardiac cycle. However, the optimum technique would obviously mimic the invasive method most closely and as several integer values of flow were obtained, I next used this integer technique for flow, paired against repeated mean pressure traces.

In order to use this method, stability of flow was essential so that pressure could be assumed to be equally stable and thus the mean trace could be used against each flow trace. Because flow traces were often not consecutively recorded, when they are spliced together to create a long period of flow as is necessary for integer-wavespeed assessment, there may be large spikes in the differentials where two parts join together. These areas will obviously create false weight to the denominator of the single-point wavespeed calculation (Figure 2-51). Options for removing this were manual splicing out of these sections (Figure 2-52) or smoothing of the flow traces using a Savitzky-Golay filter (Figure 2-53)(Savitzky and Golay, 1964). Additionally, as the Pulsecor was already ensemble averaged, some smoothing had already occurred through this method meaning smoothing of the flow signal may also be appropriate.

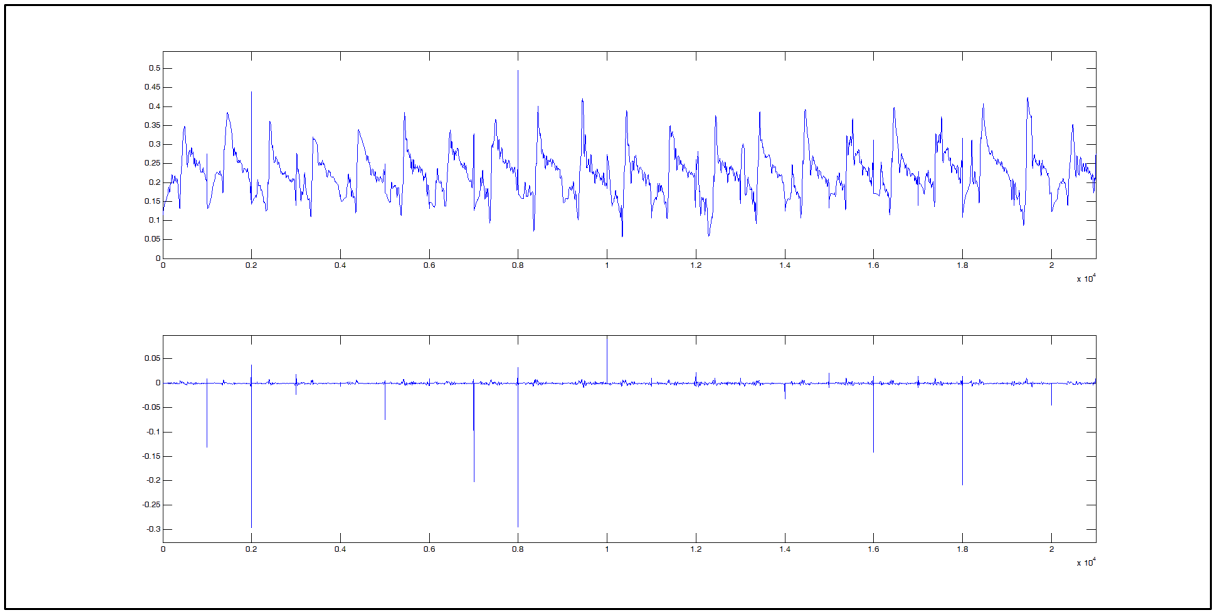

FIGURE 2-51. Amalgamated flow trace and its first differential without smoothing or splicing

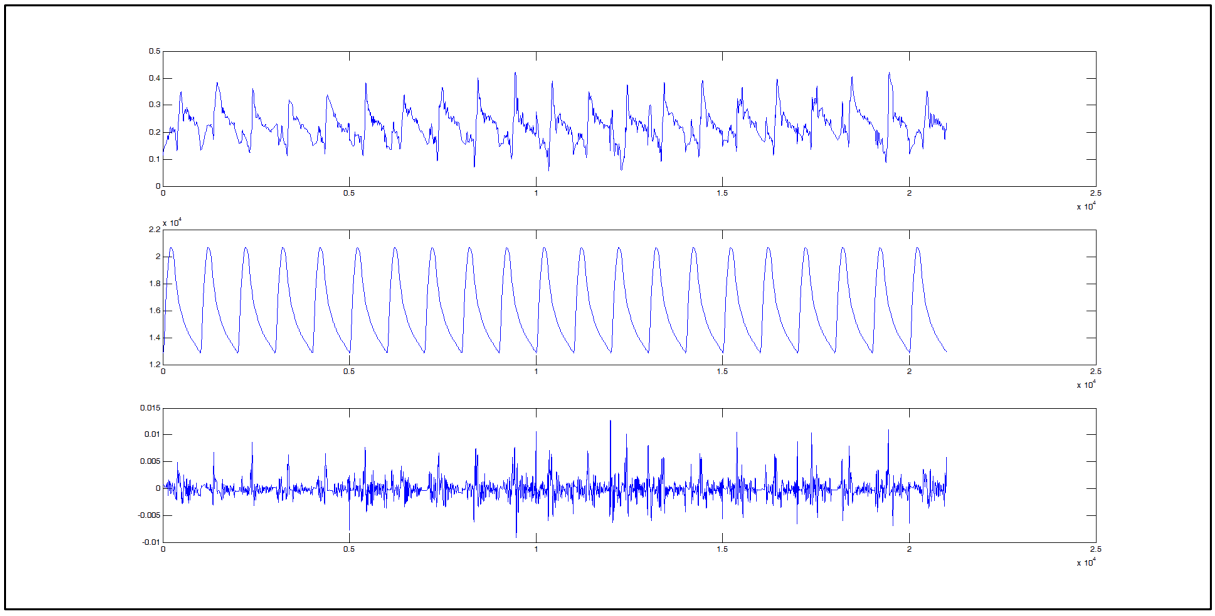

FIGURE 2-52. Flow trace (top panel) and its first differential (bottom panel) with pressure (middle panel) after splicing out of obvious jumps created by amalgamating flow traces.

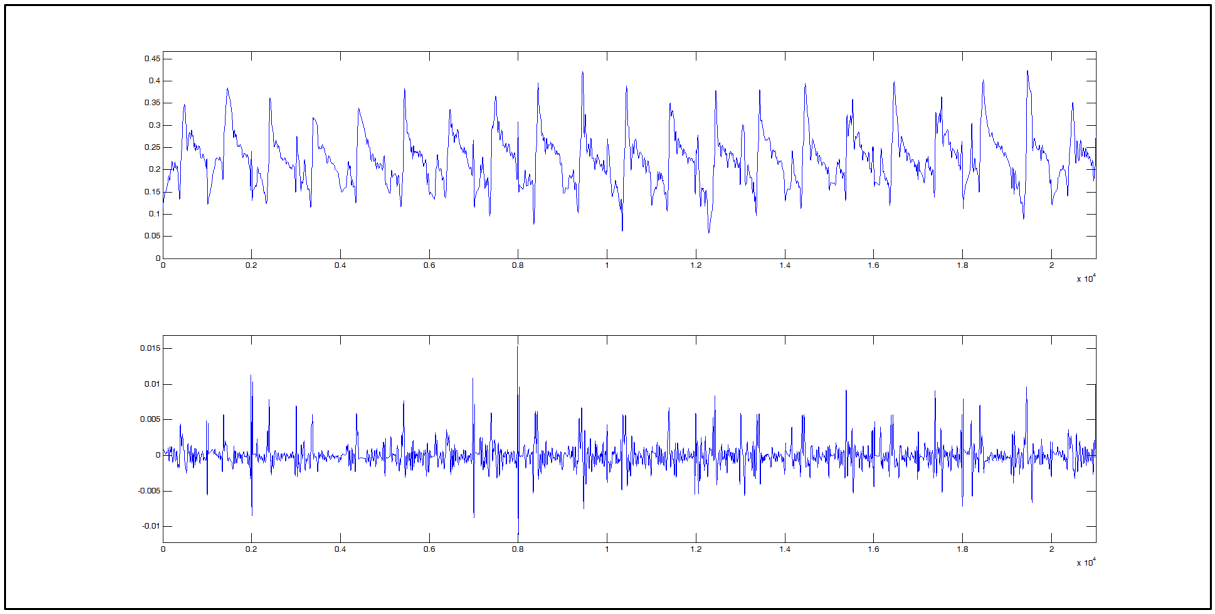

FIGURE 2-53. Flow trace (top panel) and its first differential (bottom panel) after the flow trace is smoothed using a Savitzky-Golay filter.

To test the best method of wavespeed construction, several approaches were attempted using Matlab with its inbuilt Savitzky-Golay filter or a custom built splicing programme:

1) Wavespeed construction from mean flow
2) Wavespeed construction from integer measurements with no smoothing and no splicing
3) Wavespeed construction from integer measurements with smoothed flow, non-smoothed Pulsecor and no splicing
4) Wavespeed construction from integer measurements with unsmoothed but 'spliced' flow and non-smoothed Pulsecor.

All methods were correlated against invasive measurements obtained through single-point Combowire assessment.

Mean invasive LAD wavespeed was 18.2±8.4m/s. Using mean flow and mean pressure (#1) resulted in an underestimation of wavespeed (10.4 m/s) with poor correlation (r=-0.29, p=0.14). Wavespeed constructed from unsmoothed un-spliced flow (#2) also underestimated wavespeed (13.1 m/s) albeit with a better correlation (r=0.575, p=0.002). Wavespeed with selective splicing (#3) also resulted in an underestimation (13.6 m/s) with a reasonable correlation (r=0.5271, p=0.006). The best approximation was with (#4) smoothed flow traces processed with integer summation (mean wavespeed = 18.0±5.4, r=0.62, p=0.001) (Figure 2-54).

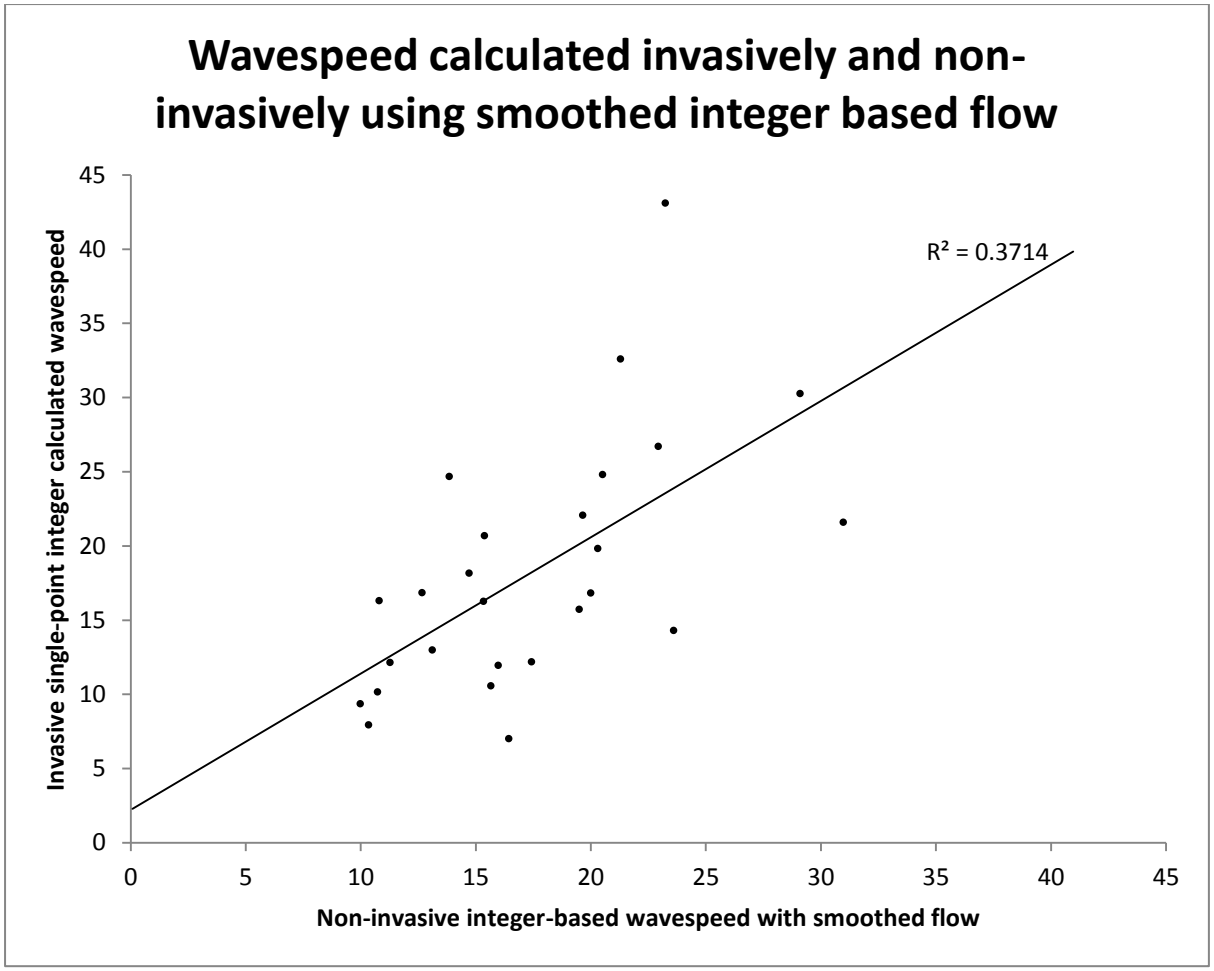

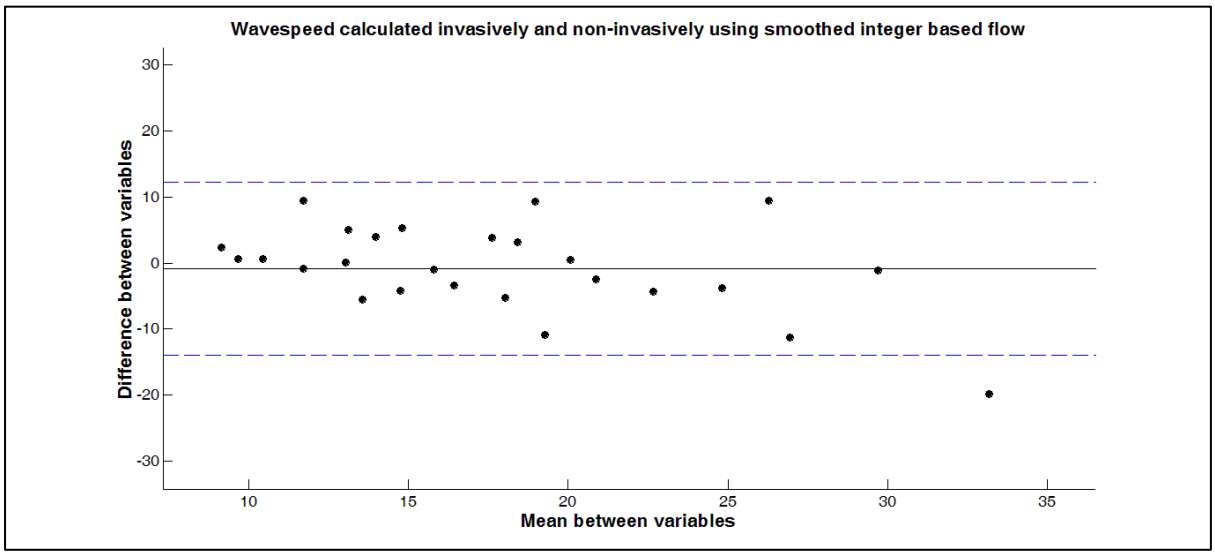

FIGURE 2-54. Scatter and Bland-Altman plots between invasive single-point generated wavespeed and non-invasively measured integer-calculated wavespeed with flow smoothed using a Savitzky-Golay filter.

2.4.3.3 Use of Unprocessed Pulsecor

Although these methods gave a reasonable approximation of wavespeed, it was ultimately felt that as an averaged approach to wavespeed calculation produced only an approximation of the integer-based equivalent, extraction of the unprocessed Pulsecor data would allow a more accurate calculation. Therefore, when this became possible attention was turned towards using this data, as described in section 2.3.5.5.

2.4.3.4 Calculation of Wavespeed Using Integer Pressure and Flow Signal

After the extraction of the Pulsecor data, the single-point wavespeed could be calculated using a completely integer-based approach. The maximum number of integer cardiac cycles used depended on the maximum number of flow or pressure files available. If more flow cycles were available then the optimum flow signals were manually selected (Figure 2-55).

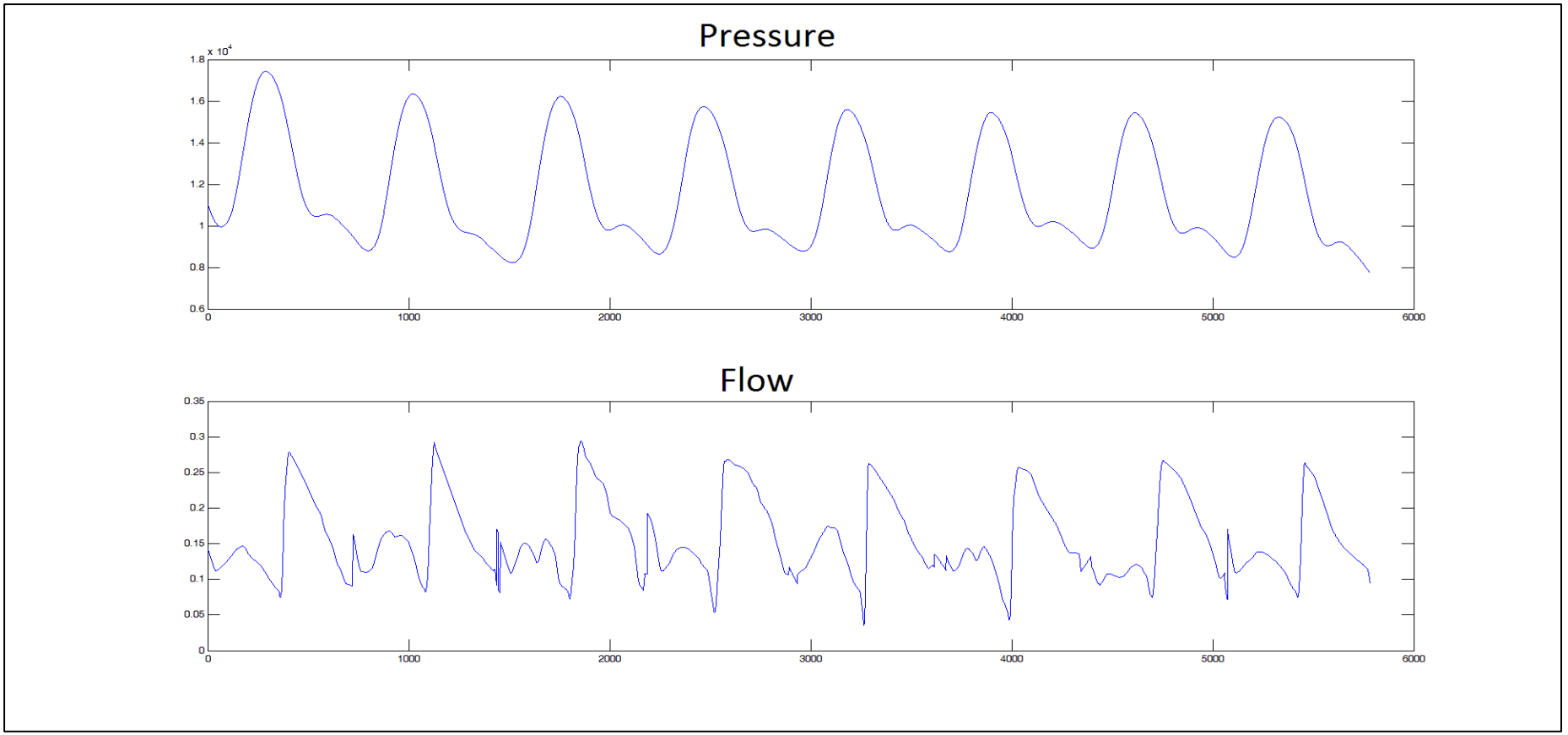

FIGURE 2-55. Pressure and flow used for integer based wavespeed analysis.

Pressure is derived from the raw detrended processed Pulsecor data and the optimum flow signals are manually selected and spliced together to form the most accurate flow signal.

2.4.3.4.1 Automated splicing of data

Finally, a custom built Matlab routine was constructed to remove the extreme differential points created by the splicing together of separate flow files. This was designed to recognise and remove any points greater than 4 times the standard deviation of the first differential of flow (Figure 2-56).

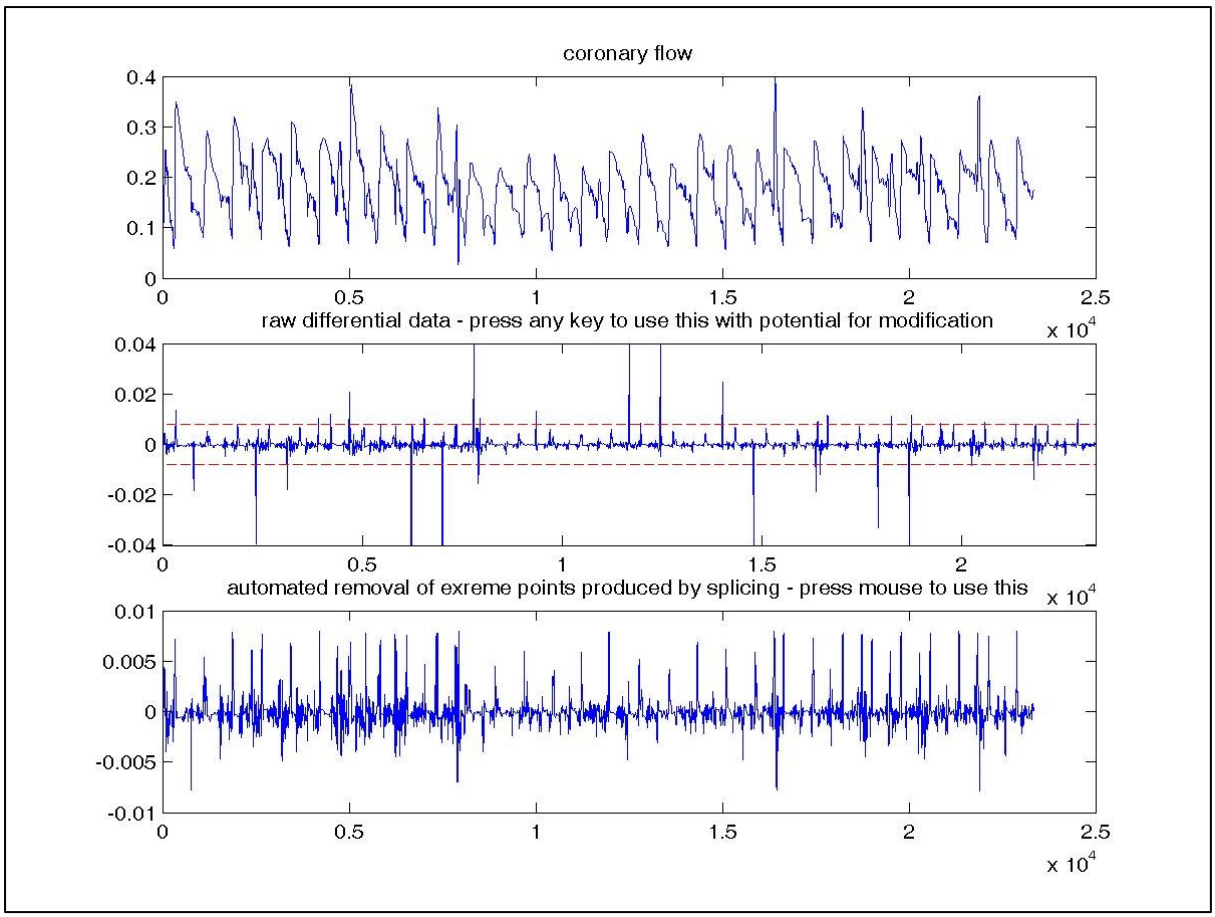

FIGURE 2-56. Automatic splicing of flow based on standard deviation of the first differential

Flow in the top panel, raw first differential in middle panel with 4-times the standard differential marked in dashed red line, first differential with points outside this 4xSD cut-off removed using an automated algorithm.

2.4.4 FINAL RESULTS

Analysis was performed in the same 26 patients. Mean invasive LAD wavespeed was 17.55±8.05m/s and mean non-invasive LAD wavespeed 18.8±7.04m/s with an r value of 0.69 ($p<0.001$). A Bland-Altman graph is displayed in Figure 2-57. This was the final approach used for non-invasive wavespeed calculation.

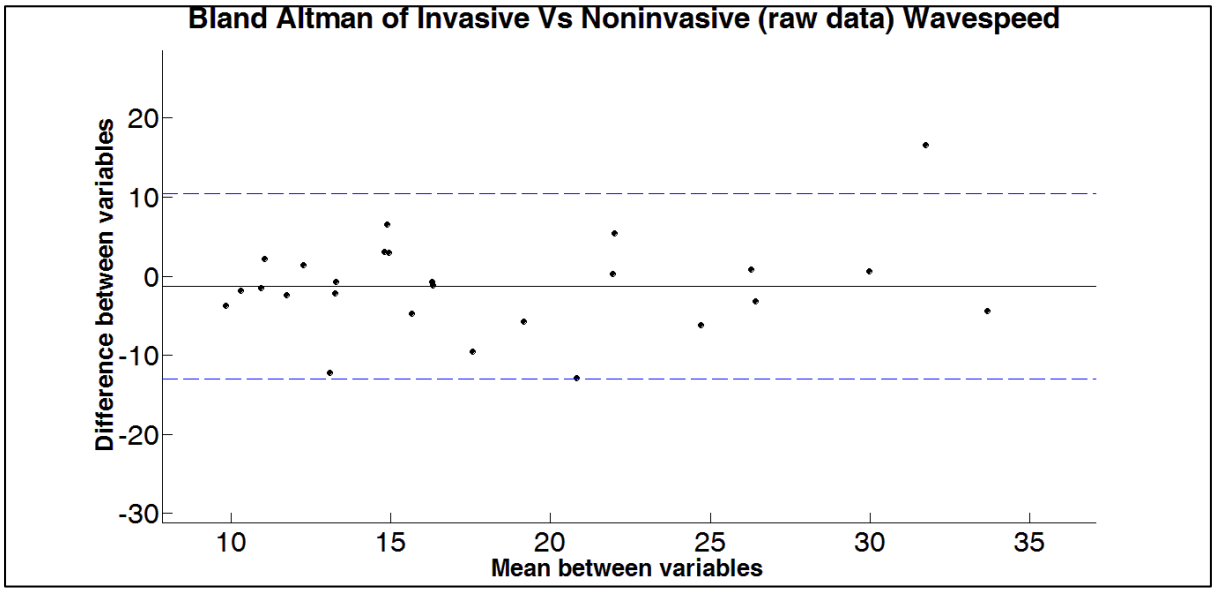

FIGURE 2-57. Bland-Altman plot of integer-based lad wavespeed derived invasively and non-invasively.

The non-invasive pressure data is extracted from the raw Pulsecor data and the optimum flow signals are selected when there are more flow cycles than pressure cycles.

2.4.4.1 Wavespeed and age

As arteries age, their elasticity declines. As a consequence, coronary artery wavespeed increases with age and this has been demonstrated invasively(Davies et al., 2006b). A correlation was seen using the above non-invasive method to calculate LAD wavespeed and age in patients with unobstructed coronary arteries (n=16, r=0.601, p=0.01 – Figure 2-58).

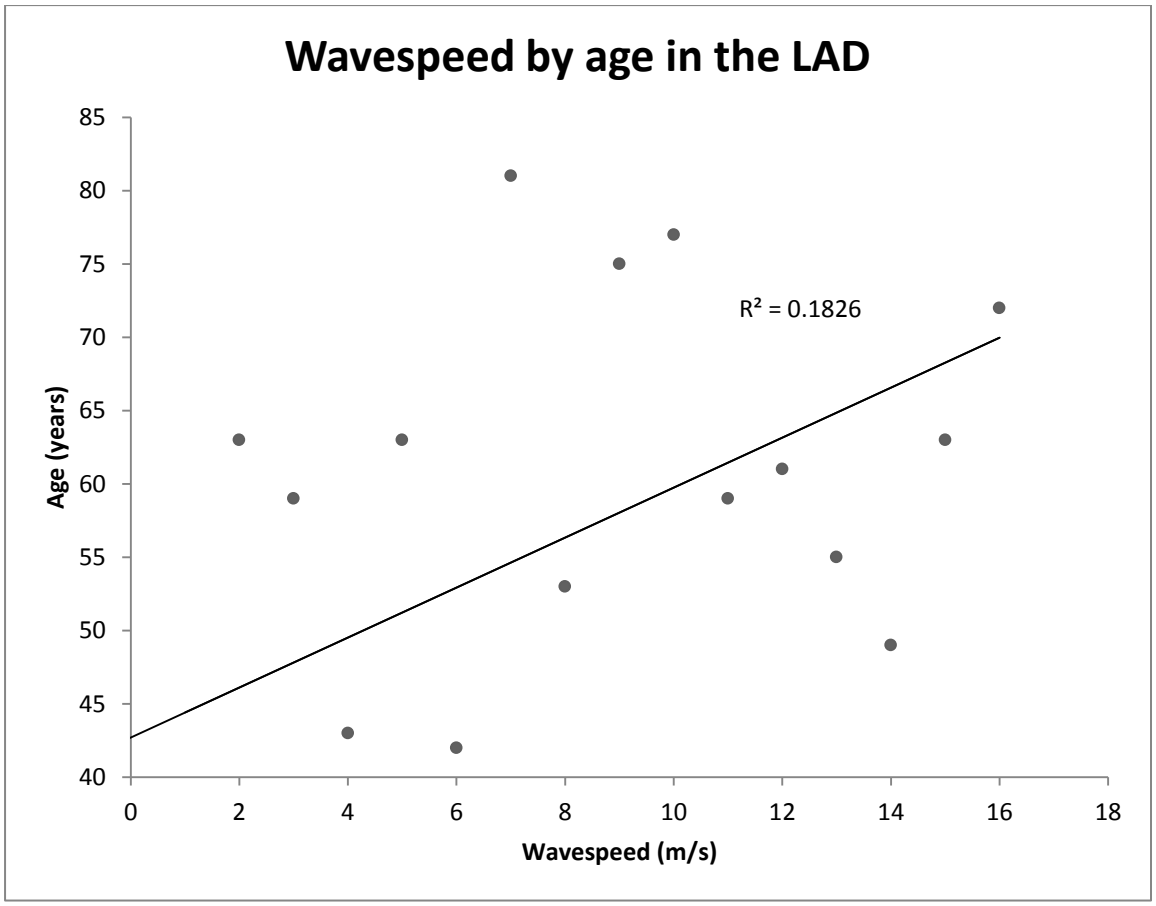

FIGURE 2-58. Non-invasively calculated coronary wavespeed according to age in 16 patients with unobstructed coronary arteries.

There is an increase in coronary wavespeed with age calculated through this method.

2.4.5 CONCLUSIONS

Wavespeed is an essential variable in the calculation of wave intensity analysis. Previous invasive work has shown it is possible to use a single-point equation in its calculation thus avoiding the foot-to-foot method which would be inappropriate for the small coronary arteries. Using a single-point calculation I have shown that it is possible to successfully apply this equation to non-invasively acquired coronary pressure and flow and that these equate to invasively acquired measures.

I have also delved into the most appropriate mathematical approach to performing this calculation. Key to the invasive data is the application of the formula across an integer number of cardiac cycles and I have shown that whilst it is possible to do this with an averaged single flow and pressure recording it is more accurate to maintain the integer approach. Therefore, it is essential to work with the unprocessed Pulsecor data to allow integer based calculations to be performed.

Finally I have gone on to apply this calculation to confirm that wavespeed increases with age in the coronary tree. This fact is already known but its confirmation further validates this non-invasive approach to measuring coronary wavespeed.

2.5 NON-INVASIVE CALCULATION OF THE BACKWARD EXPANSION WAVE

2.5.1 INTRODUCTION

I have shown that it is possible to accurately calculate coronary flow, pressure and wavespeed using non-invasive methods. Therefore, it should now be possible to perform wave intensity analysis and in particular generate the backward expansion wave.

2.5.1.1 Wave-Intensity Analysis: Mathematical Theory

Wave intensity attempts to explain phasic flow in terms of a series of wavefronts that underlie the changes in pressure and flow in arteries(Parker, 2009). Unlike traditional approaches to wave analysis using the Fourier decomposition, wave intensity analysis uses the time domain to quantify these wavefronts and can determine the relative importance of contributing factors.

When arteries are regarded as closed fluid-filled tubes, forces can act on them from either end with either a compressive or decompressive ('expansive') effect. Compressive forces acting from the proximal end have the same effect as decompressive forces from the distal end to accelerate fluid. Likewise, decompressive proximal forces or compressive distal forces act to cause deceleration (Figure 2-59).

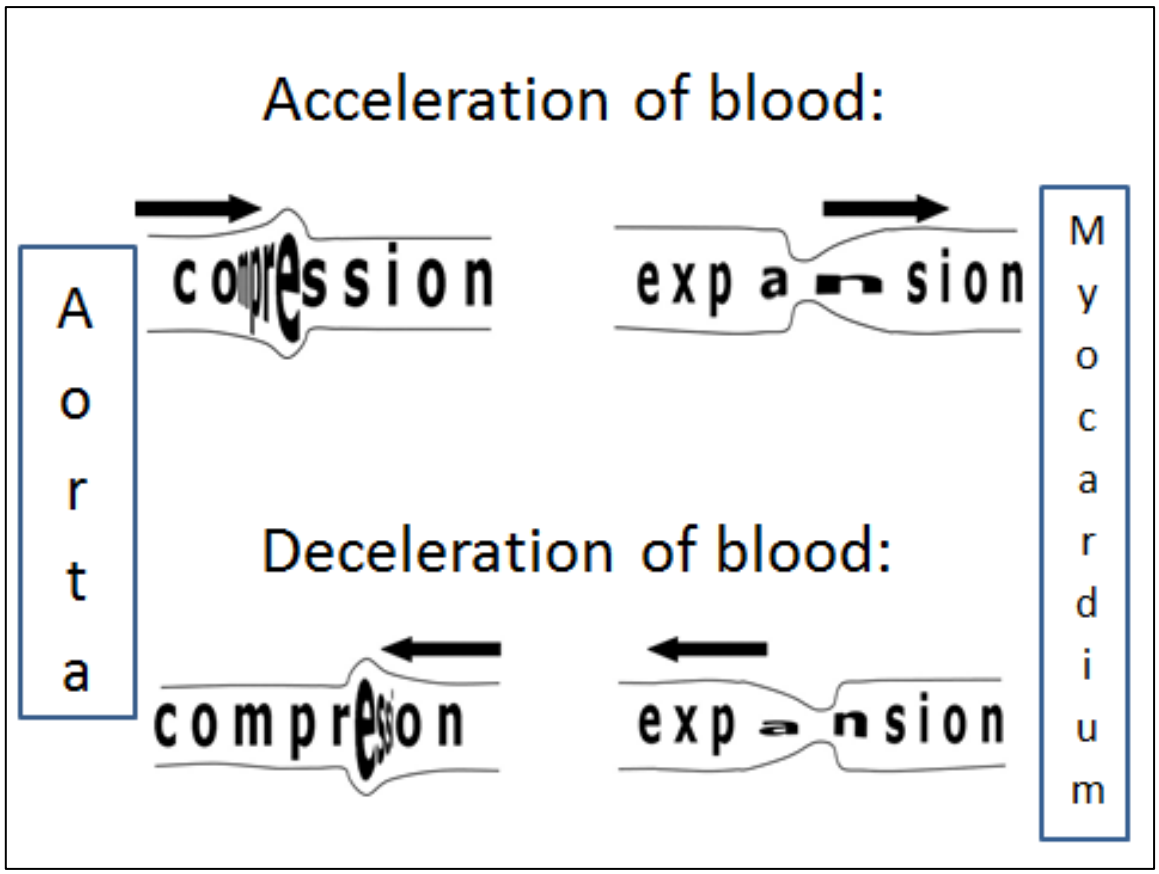

FIGURE 2-59. The effect of proximal (aortic) and distal (myocardium) originating compressive and expansive (decompressive) forces on blood flow (Davies et al., 2006a)

Wave intensity has the units of Watts per meters squared and is therefore the flux of energy per unit area carried by the wave as it propagates. The simplest wave-intensity measure is the product of change in velocity and change in pressure during the same interval (dPdU). This formula can be used to calculate net wave intensity measured at a single point quite easily using simultaneously measured pressure and flow.

However, in the coronary circulation problems arise because both proximally and distally originating forces may arrive simultaneously. Therefore, to distinguish forward and backward waves (i.e. non 'net' waves) from a single-point measurement requires additional mathematical steps.

Firstly, the water hammer equations are recognised and demonstrate the pressure and velocity relationship in any wavefront:

$$dP+ = \rho c dU+$$

$$dP- = \rho c dU-$$

where dP+ is the change in pressure from the proximal end and dP- is the change in pressure from the distal end.

EQUATION 2-4. WATERHAMMER EQUATIONS FOR PRESSURE AND VELOCITY IN ANY WAVEFRONT

Through use of these water-hammer equations and additivity the proximal and distal pressure changes can be separate out further to:

$$dP+ = \tfrac{1}{2} (dP + \rho c dU)$$

$$dP- = \tfrac{1}{2} (dP - \rho c dU)$$

or equivalently:

$$dU+ = \tfrac{1}{2} (dU + dP / \rho c)$$

$$dU- = \tfrac{1}{2} (dU - dP / \rho c)$$

EQUATION 2-5. PRESSURE AND VELOCITY CHANGES SEPARATED INTO PROXIMAL AND DISTAL ORIGINS

where a positive value in dP+ indicates an accelerating wave and a negative value a decelerating wave. Conversely, positive dP- values indicate a decelerating wave and

negative values an accelerating wave(Davies et al., 2011, Davies et al., 2006a, Parker, 2009).

Therefore, forward and backward wave intensity (WI) can be created from these respective products:

$$WI+ = + 1 / 4 \rho c (dP + \rho c dU)^2$$

$$WI- = - 1 / 4 \rho c (dP - \rho c dU)^2$$

EQUATION 2-6. WAVE INTENSITY SEPARATED INTO PROXIMAL AND DISTAL ORIGINS

In order to remove the potential bias of sampling frequency variation, the product of first time derivatives can be used(Davies et al., 2006a):

$$WI+ = 1 / 4\rho c (dP/dt + \rho c dU/dt)^2$$

$$WI- = - 1 / 4\rho c (dP/dt - \rho c dU/dt)^2$$

and finally:

$$WInet = WI+ + WI- = (dP/dt) * (dU/dt)$$

EQUATION 2-7. WAVE INTENSITY SEPARATED INTO PROXIMAL AND DISTAL ORIGINS FROM FIRST DIFFERENTIALS

2.5.2 METHODS

2.5.2.1 Patient recruitment

This validatory work was performed in seventeen patients (mean age 60 ± 12, 11 male). They were recruited from patients scheduled for coronary angiography in whom coronary artery disease was considered a relatively low probability. Exclusion criteria included previous coronary intervention, valvular pathology and regional wall motion abnormalities. The study was approved by a regional Ethics committee and all subjects gave written informed consent.

2.5.2.2 Invasive measurements

Formal diagnostic angiography was performed through a trans-femoral or trans-radial approach. Measurements were obtained if there was no angiographic evidence of coronary lesions as deemed by two experienced operators. The left coronary system was engaged with a Judkins guide catheter and intra-arterial heparin was administered. A 0.014-in-diameter sensor-tipped intracoronary wire (Combowire, Volcano Corp – Figure 2-60) was then passed into the mid-left anterior descending artery.

Analog output feeds were taken from the pressure-velocity console and ECG over a period of one minute of stable recording on a Combomap console. Data was exported and analysed offline with a custom software package designed with Matlab (Mathworks, Natick, MA) as has been previously been described by our group(Davies et al., 2011, Davies et al., 2006a).

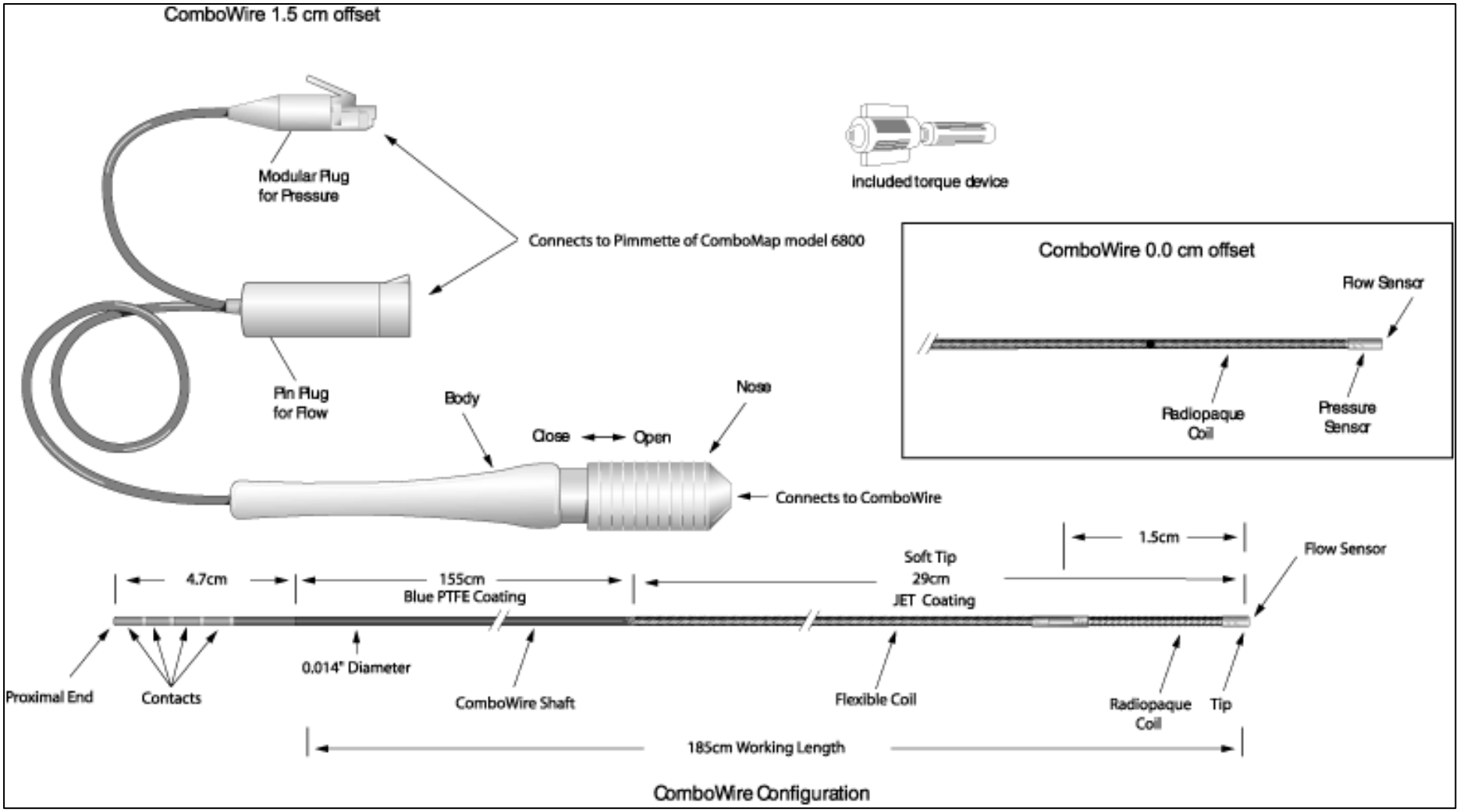

FIGURE 2-60. Schematic depiction of a Combowire (Volcano Corp).

2.5.2.3 Non-invasive

To ensure reproducibility and comparability, data was acquired in the same view in all patients in the mid-LAD. If possible, proximal LAD / LMS and distal LAD readings were taken as well. Multiple coronary flow signals were recorded from the same region (usually >20) and exported as jpg or bitmap files and processed as described in 2.2.2.5.

Central aortic pressure was measured using a suprasystolic brachial pressure sensor (Pulsecor, Auckland, New Zealand). Data was exported off-line and processed as described in 2.3.5. A minimum of 2 Pulsecor readings were obtained and readings were discarded if their fidelity was rated as anything less than 'good' according to the device.

2.5.2.3.1 Baseline echocardiography

Baseline echocardiographic readings were taken according to standard principles. LV mass was calculated according to the formula:

$$\text{LV mass} = 0.8 * (1.04 * (\text{LVEDD} + \text{PWDD} + \text{IVSD})^3 - \text{LVEDD}^3) + 0.6$$

EQUATION 2-8. LV MASS CALCULATED AT ECHOCARDIOGRAPHY

LVEDD = Left Ventricular End Diastolic Dimension, PWDD = Posterior wall thickness in diastole, IVSD = intraventricular septal thickness in diastole.

2.5.2.4 Minimisation of Influencing Factors

2.5.2.4.1 Physical Factors

To minimize the effects of physical exertion, all subjects rested in bed for 1 hour before angiography. Subjects who smoked were not excluded from the study but asked to refrain from smoking for 24 hours. Similarly, subjects were required to refrain from

coffee and alcohol for at least 12 hours before study. Subjects were also not studied within 9 hours of eating.

2.5.2.4.2 Psychological Factors

To minimize psychological stress, all subjects had careful explanation of the procedure during the consent phase and ample opportunity for further clarification and reassurance.

2.5.2.4.3 Pharmacological Factors

All oral and sublingual nitrates were stopped 24 hours before the procedure.

2.5.2.5 Statistics

STATA 11 (StatCorp LP) was used for analyses. Data is expressed as mean ± standard deviation. Correlation was assessed with the Pearson correlation coefficient. Student's t test was used to demonstrate the presence or absence of significant differences between groups. A value of $P<0.05$ was taken as statistically significant.

2.5.3 RESULTS

2.5.3.1 Patient demographics

Baseline demographics are shown in Table 2-9. Mean age was 60 years and more men were recruited than woman (65 vs 35%) as would be anticipated from a routine angiographic service. Baseline echocardiographic data is displayed in Table 2-10.

2.5.3.2 Backward expansion wave production

2.5.3.2.1 Alignment

One issue with the calculation of non-invasive wave intensity analysis is the absence of an integrated blood pressure and coronary flow measurement device. Therefore, the individual waveforms need to be aligned to each other accurately in order to obtain the wave-intensity profile. The Pulsecor machine does not have an ECG trace therefore true ECG-gating is not an option so alternatives were sought.

2.5.3.2.2 Invasive differential alignment

The first step towards achieving this was to assess the time delay between peak pressure and flow velocity differentials using a custom built Matlab programme (Figure 2-61).

Using this programme in this group of patients, the time between peak flow and peak pressure differentials that generate the backward expansion wave was 27±9ms. This value was used in the non-invasive programme where flow differential was aligned to 27ms after the pressure differential.

Age		60 ± 12
male (%)		11 (65)
hypertensive (%)		6 (35)
DM (%)		1 (6)
current smoker (%)		1 (6)
Meds	beta blocker (%)	3 (18)
	ace/arb	4 (24)
	ca channel	2 (12)
	bendroflumethiazide	2 (12)
	alpha blocker	1 (6)
	aspirin	9 (53)

TABLE 2-9. Baseline demographics.

Echo	LVEDd	4.4 ± 0.7
	LVEDs	2.9 ± 0.6
	IVSd	1.06 ± 0.23
	PWd	1.05 ± 0.22
	IVSs	1.6 ± 0.43
	PWs	1.7 ± 0.43
Mitral inflow	E	65.5 ± 16
	A	68.5 ± 17
Septal	e'	8.2 ± 2.3
	a'	9.6 ± 2.3
	s'	8.4 ± 2.7
Lateral	e'	10.6 ± 4.3
	a'	8.1 ± 4.4
	s'	9.0 ± 3.6
LV mass		165 ± 49

TABLE 2-10. Routine echocardiographic data

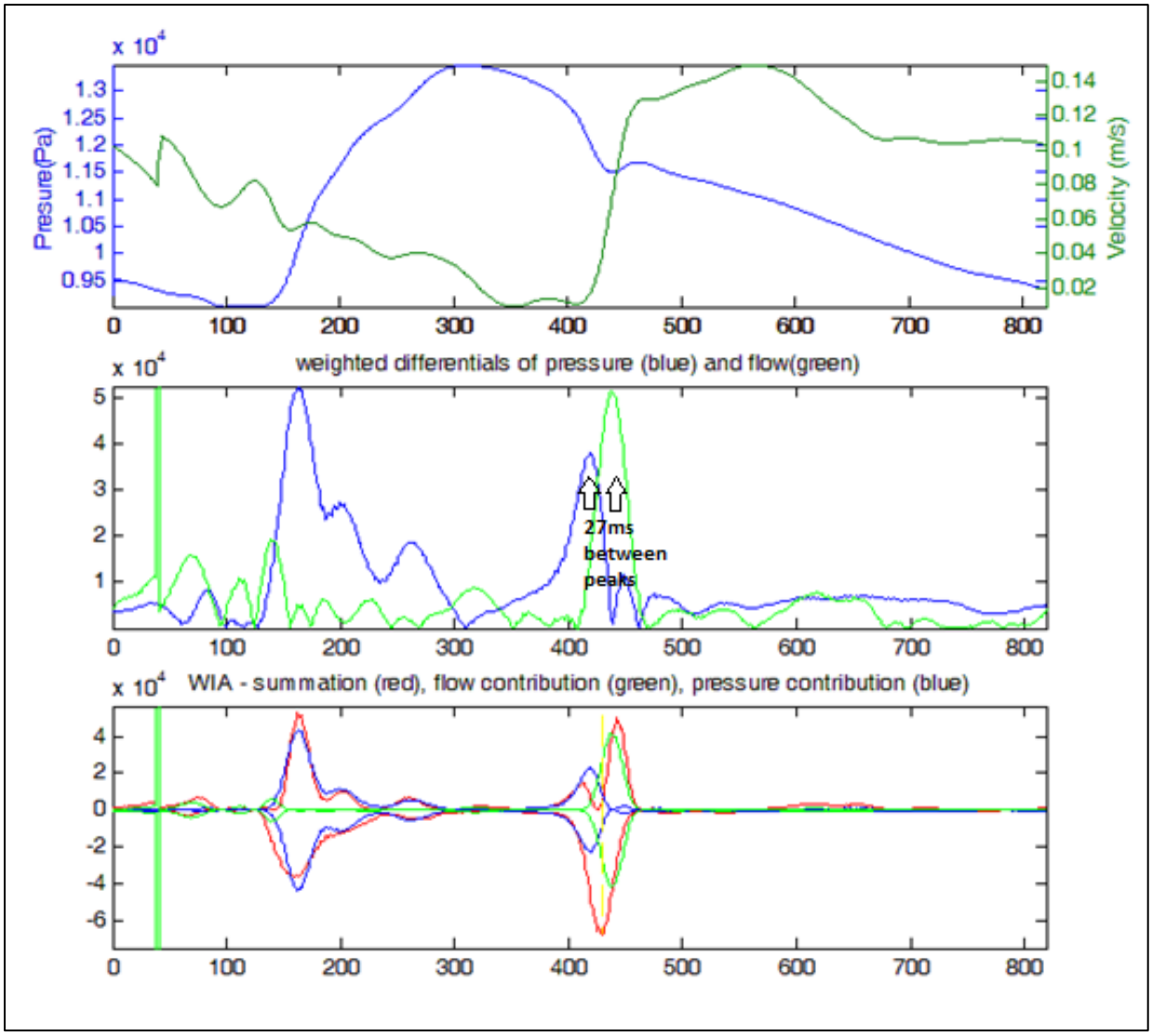

FIGURE 2-61. Wave intensity and the respective weighting from pressure and flow.

Matlab software was constructed to assess the relationship of weighted (according to the principles of wave-intensity analysis) pressure and flow and the resultant wave-intensity. Top panel showed pressure and flow, middle panel weighted differentials of pressure and flow (all as positive values) and bottom panel their timing in relation to the backwards expansion wave.

2.5.3.2.3 Alignment with coronary flow

With the option to process raw Pulsecor data, location of the dicrotic notch could be more accurately established. Therefore in an attempt to improve accuracy alignment of the onset of coronary flow with the dicrotic notch was performed. Additionally, through analysis of the invasive data, the location of coronary flow in relation to the dicrotic notch was noted to actually occur 20ms before closure of the aortic valve and the onset of the dicrotic notch (Figure 2-62). Therefore alignment at 20ms before the dicrotic notch was also attempted in the latter stages of analysis. However, the majority of the work performed was through differential alignment due to the higher discovered accuracy.

2.5.3.3 Non-invasive Backward Expansion Wave Construction

Over the course of this work, three approaches to non-invasive wave-intensity construction were applied. They are of increasing complexity largely reflecting the increasing ability to work with the Pulsecor data. Initially, the processed Pulsecor-assembled, mathematically-amplified pressure data was applied (2.3.5.1). Then the 'SupraSystolicFiltered' data was used (i.e. the raw tracings from the suprasystolic pressure sensor) with operator-ensembled pressure waveforms (2.3.5.2). Finally, it became possible to work with the raw manually-processed manually-aligned 'AOChannel0' data (2.3.5.5)

When does coronary flow start

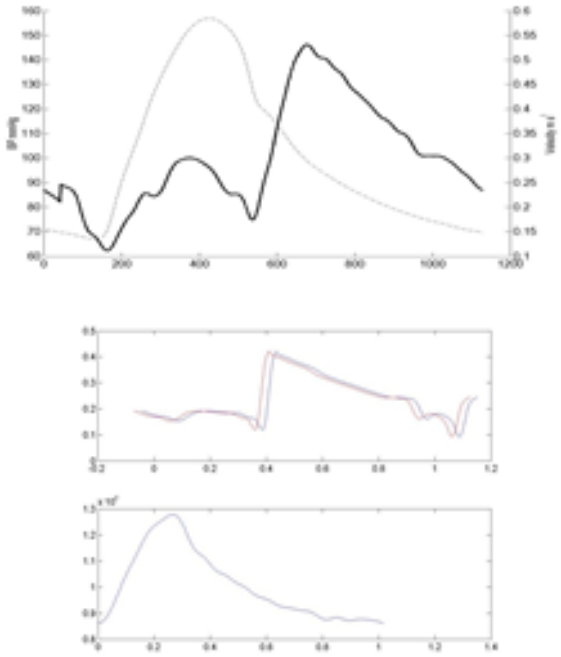

patient	time (ms)	patient	time(ms)
1	20	16	21
2	13	17	29
3	17	18	24
4	29	19	20
5	12	20	13
6	27	21	16
7	25	22	23
8	27	23	10
9	19	24	13
10	23	25	22
11	8	26	11
12	18	27	13
13	13	28	32
14	39	29	22
15	31	average	20.34

FIGURE 2-62. The onset of coronary flow in relation to the dicrotic notch

By assessing the timing of the onset of coronary flow in 29 invasive cases, the onset was noted to be 20.34ms before the dicrotic notch.

2.5.3.3.1 Processed Pulsecor Data

Pre-ensembled pressure measurements were obtained from the Pulsecor machine and modified according to the above mathematical factors (see 2.3.5.1). Peak backward expansion wave intensity was similar for both invasive and non-invasive groups (mean invasive 146632 ± 840709 $Wm^{-2}s^{-2}$ vs 149446 ± 93184 $Wm^{-2}s^{-2}$). There was a good correlation between the values ($r=0.72$, $p < 0.001$) (Figure 2-63)

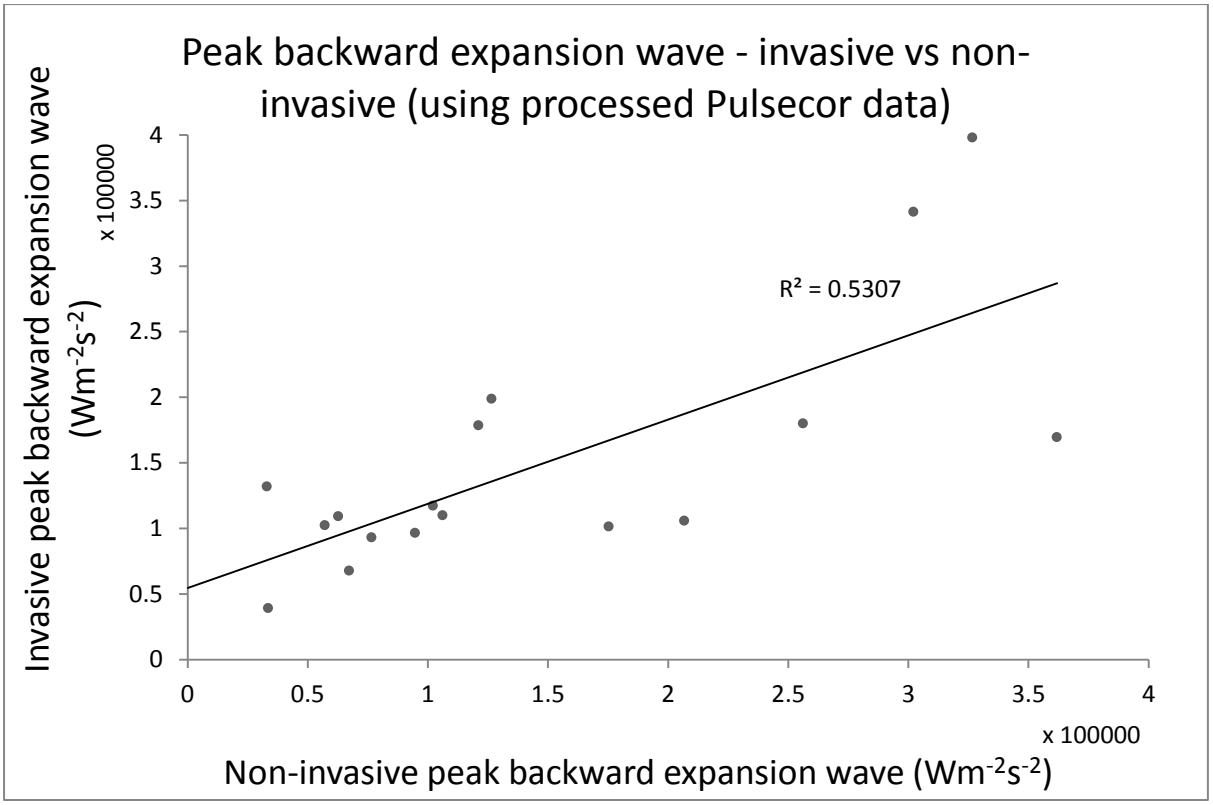

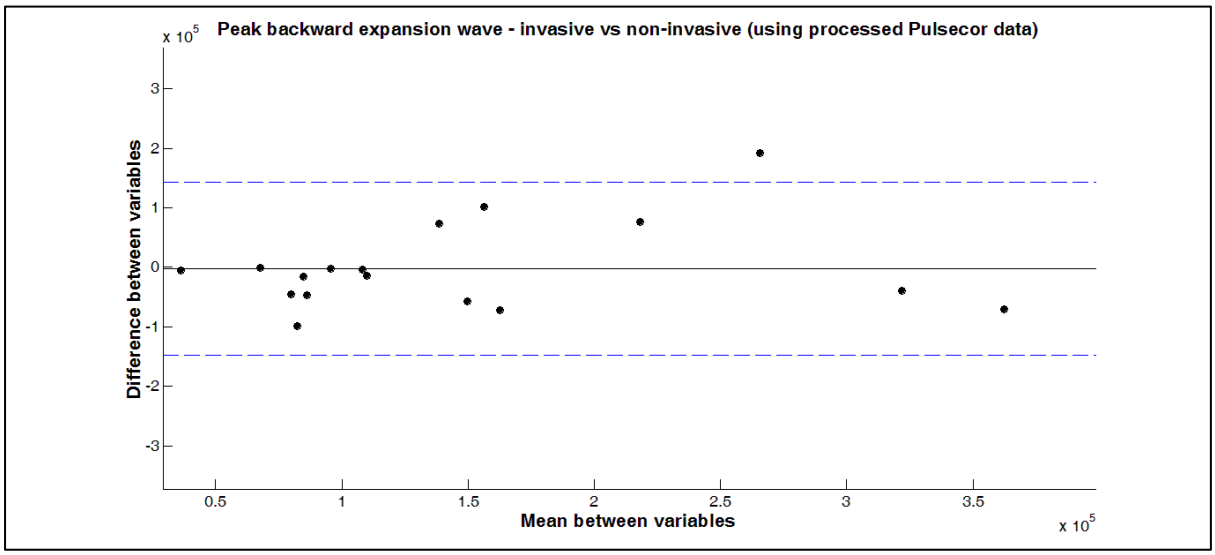

FIGURE 2-63. Scatter graph and Bland-Altman plot of non-invasive versus invasive peak backward wave-intensity using the technique described in 2.3.5.1.

Wave intensity is calculated using ensemble-averaged coronary flow and mathematically-processed Pulsecor. Data displayed as positive values

2.5.3.3.2 Further Work: Use of Raw Pulsecor Data

Once it became possible to work with the raw Pulsecor data, this was used in an effort to further improve the accuracy of the backward expansion wave. Through the process of data extraction, scaling and ensembling, a more accurate pressure measurement was processable (section 2.3.5.2).

Using this approach, the most accurate reconstruction of the backward expansion wave was possible. In the same 17 patients with normal coronary arteries, the mean peak backward expansion wave was -146632 ± 840709 $Wm^{-2}s^{-2}$ invasively and noninvasively -123872 ± 76153 $Wm^{-2}s^{-2}$ without pressure modification and 139122 ± 86586 $Wm^{-2}s^{-2}$ with pressure modification. Without pressure modification the correlation was good with an r value of 0.819 ($p<0.001$) and 0.820 ($p<0.001$) with pressure modification (Figure 2-64). Cumulative backward expansion wave was also calculated using the trapezoidal function on Matlab. Mean cumulative backward wave intensity was -5914262 ± 4990053 $Wm^{-2}s^{-1}$ invasively compared to -5460544 ± 4037460 $Wm^{-2}s^{-1}$ non-invasively (with pressure modification) ($r = 0.70$, $p = 0.01$) and 4863810 ± 3569202 $Wm^{-2}s^{-1}$ (without pressure modification ($r=0.70$, $p = 0.01$) (Figure 2-64).

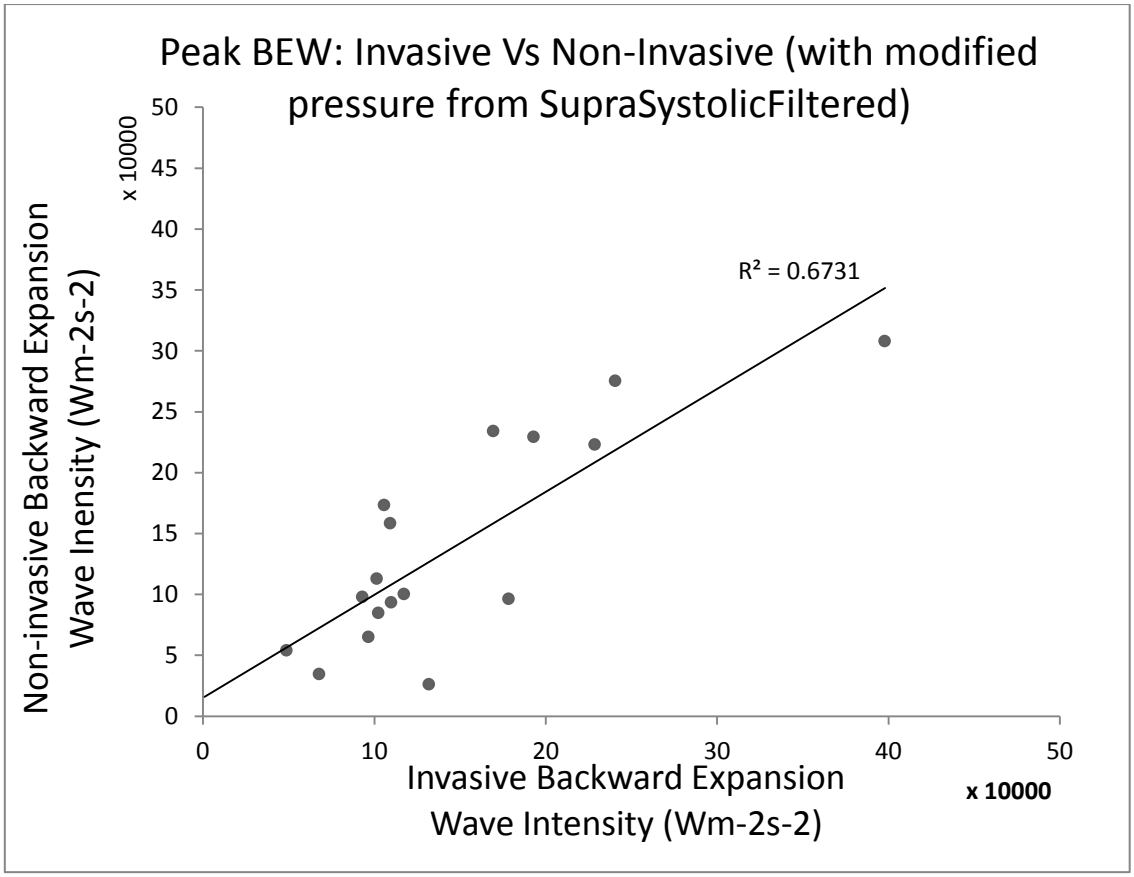

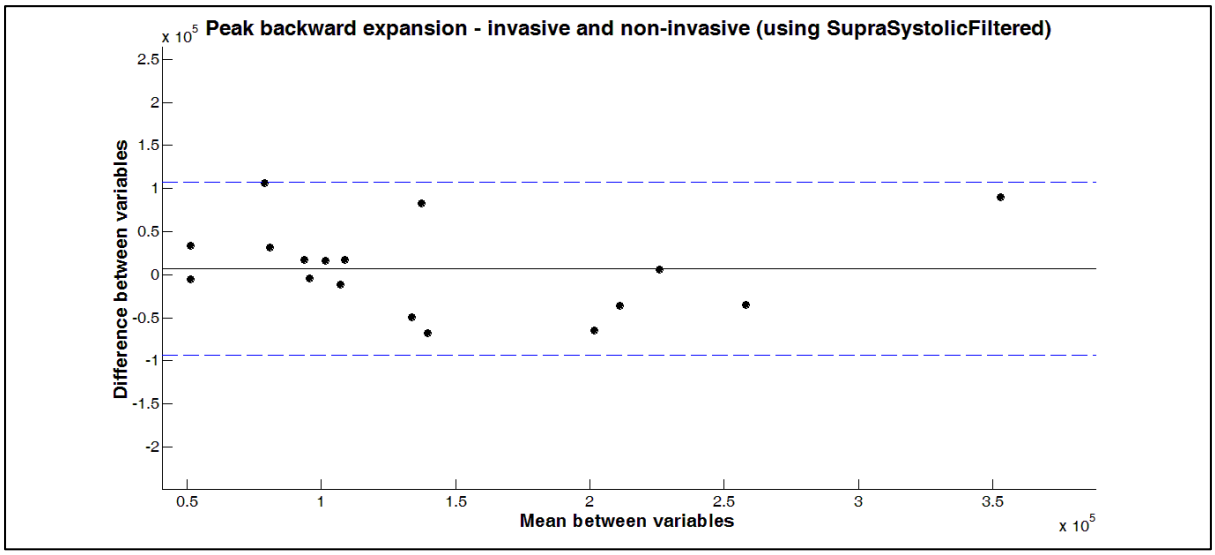

FIGURE 2-64. Scatter plot and Bland-Altman plot of invasive versus non-invasive peak backward wave intensity calculated according to 2.3.5.2..

Non-invasive wave intensity is calculated from manually ensemble Suprasystolicfiltered Pulsecor data and ensemble-averaged coronary flow. Data displayed as positive values.

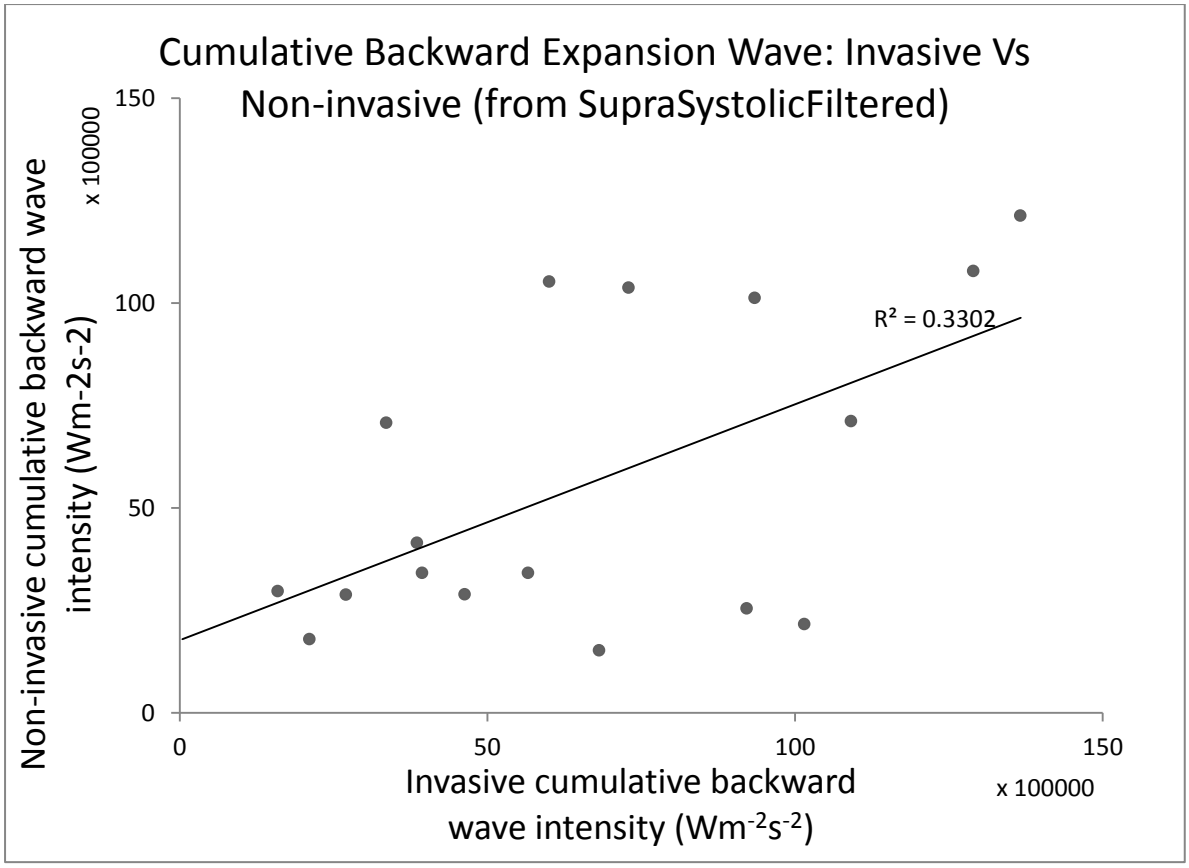

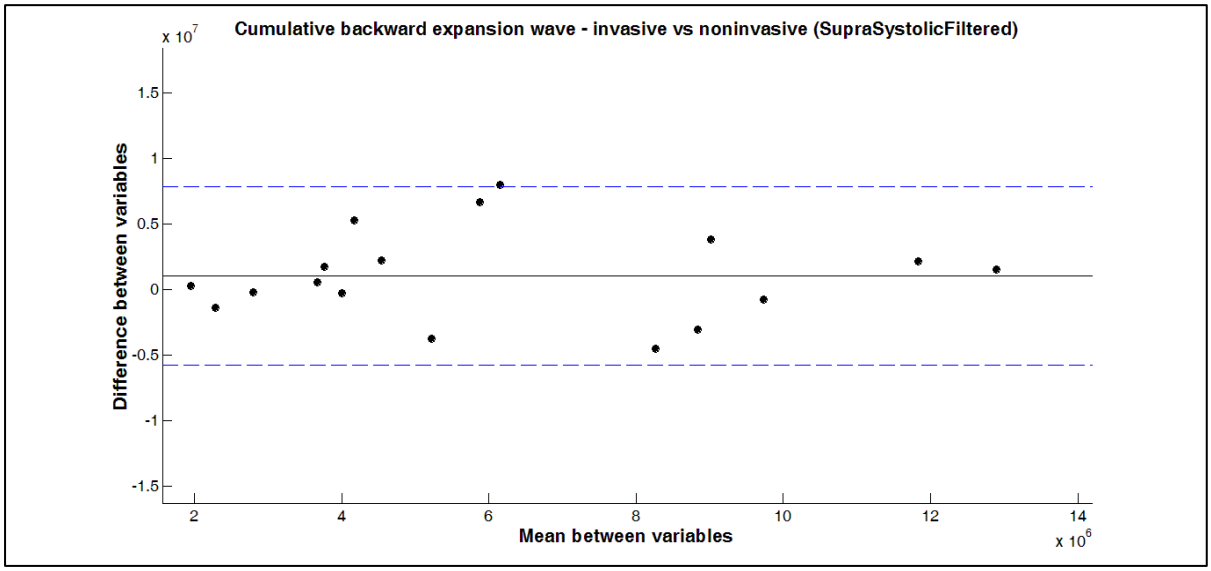

FIGURE 2-65. Scatter plot and Bland-Altman plot of invasive versus non-invasive cumulative backward wave intensity as described in 2.3.5.2.

Non-invasive wave intensity is calculated from ensembled Suprasystolicfiltered Pulsecor data and ensemble-averaged coronary flow. Data displayed as positive values.

2.5.3.3.3 Use of Raw Processed Pulsecor Data from ADCChannel0

Finally, once all the Pulsecor manipulations had been established (section 2.3.5.5), backward expansion wave was recalculated in the same 17 patients as demonstrated in Figure 2-66 . Mean peak backward expansion wave were very similar (-147551 ± 86739 $Wm^{-2}s^{-2}$ invasively vs. -144318.9 ± 82477 $Wm^{-2}s^{-2}$ non-invasively) with a good correlation ($r = 0.833$, $p < 0.001$) (Figure 2-67).

Using this technique, cumulative wave intensity was also very accurate with a mean value of – 6710497 ± 3882876 $Wm^{-2}s^{-1}$ invasively compared to -6704235 ± 4417512 $Wm^{-2}s^{-1}$ non-invasively and a correlation r value of 0.66 ($p = 0.005$) (Figure 2-68).

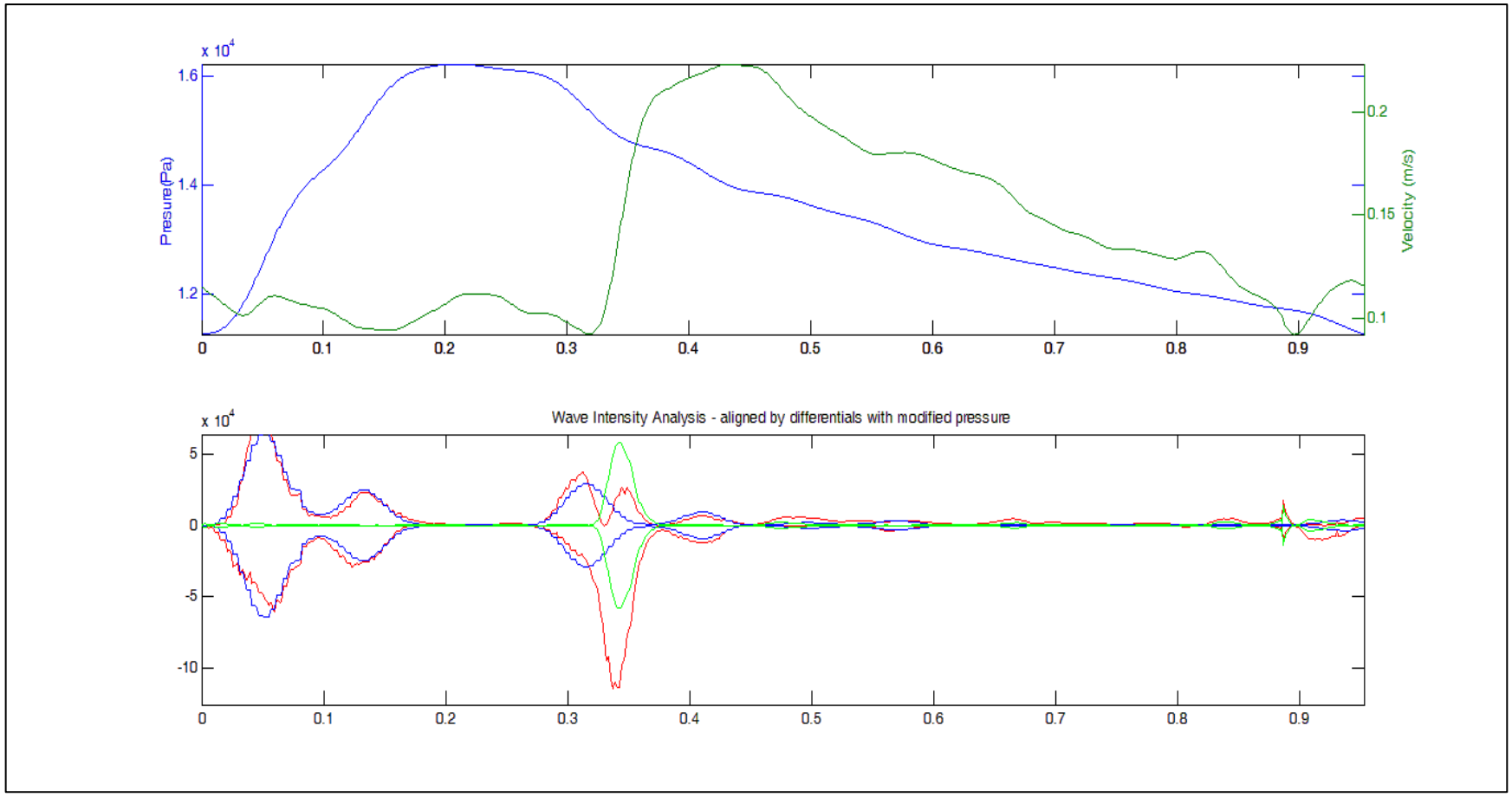

FIGURE 2-66. Non-invasively constructed coronary wave intensity.

Top panel showing pressure and flow measurements aligned by the peak of pressure and flow. Wave-intensity analysis (red) shown in the panel below with weighted pressure (blue) and flow (green) displayed.

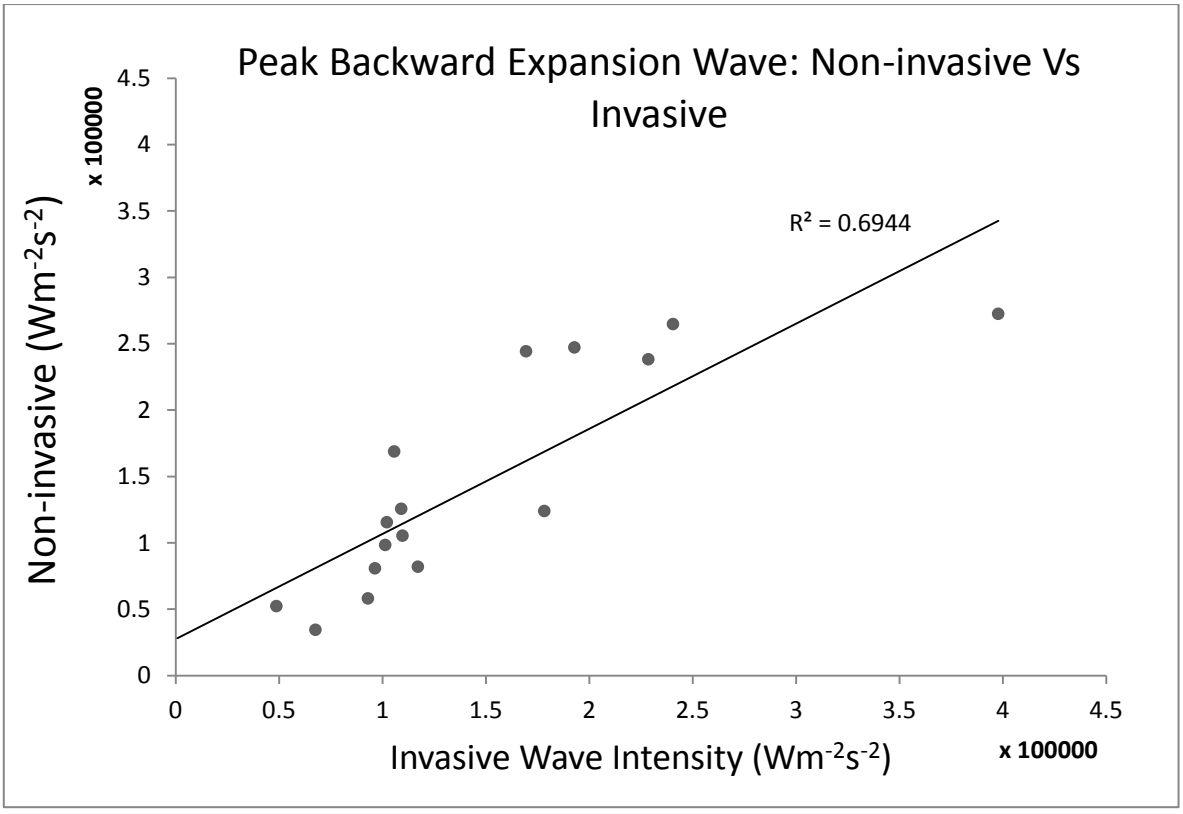

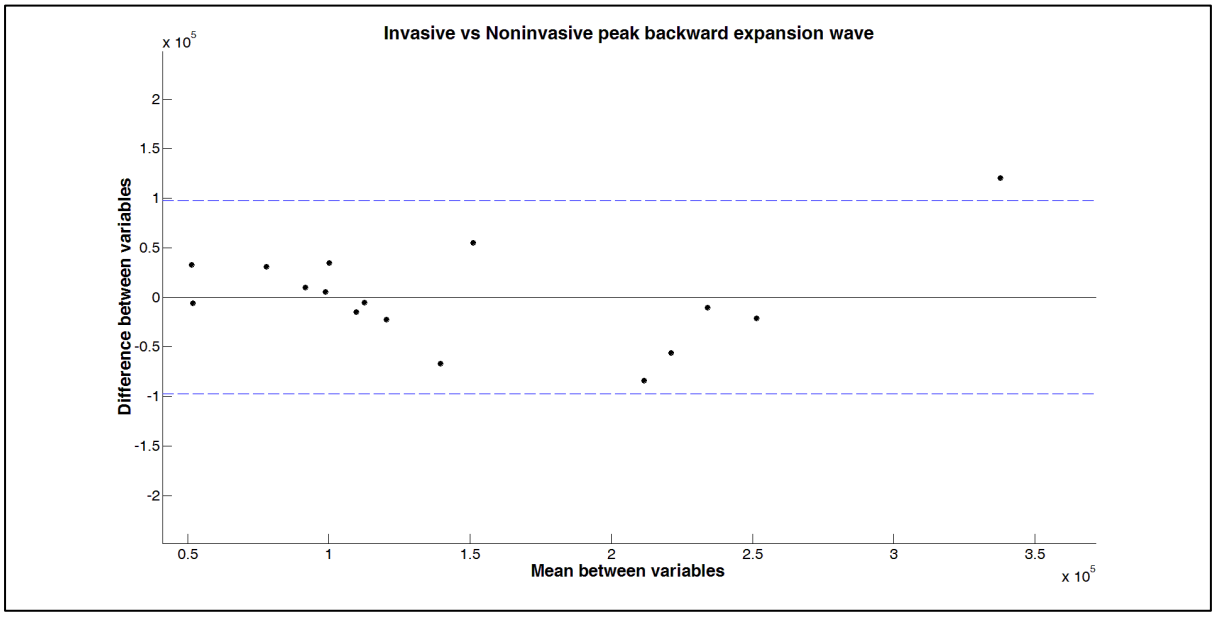

FIGURE 2-67. Correlation and Bland-Altman plot of invasive versus non-invasive peak backward expansion wave calculated according to section 2.3.5.5.

Non-invasive wave intensity is calculated using modified raw-Pulsecor data.

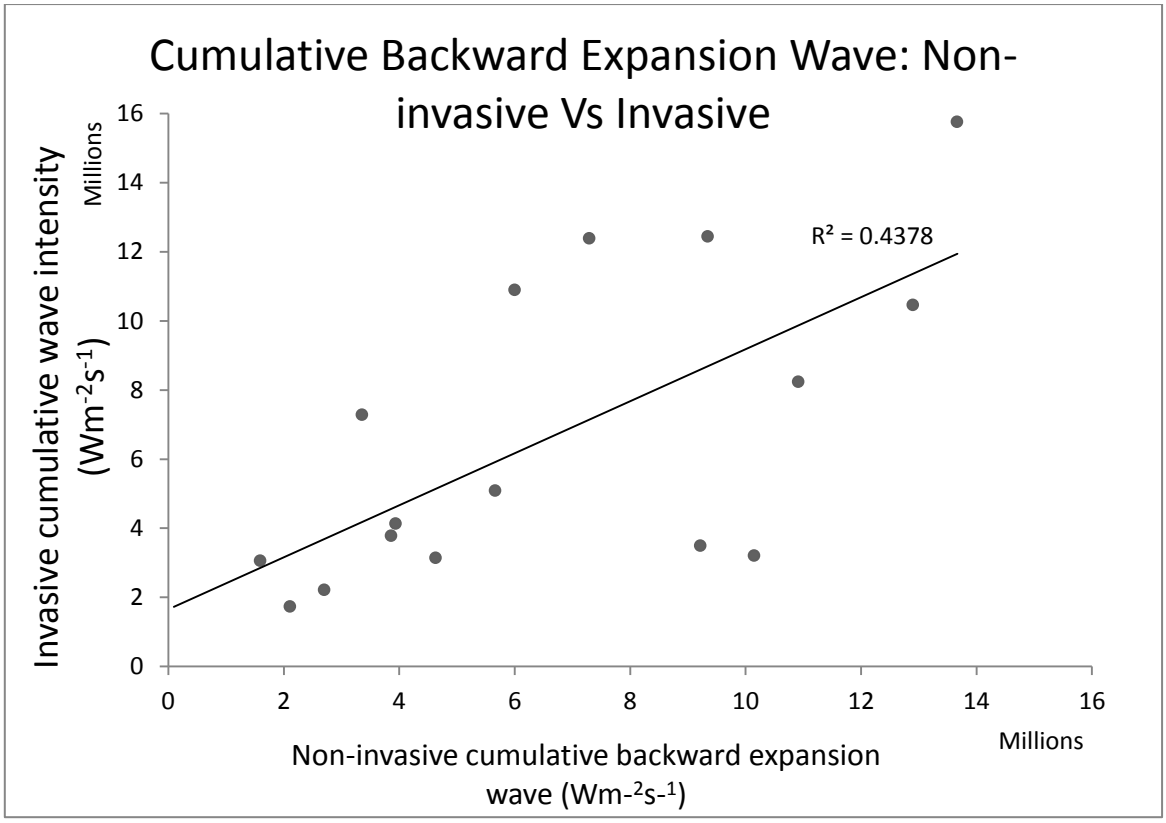

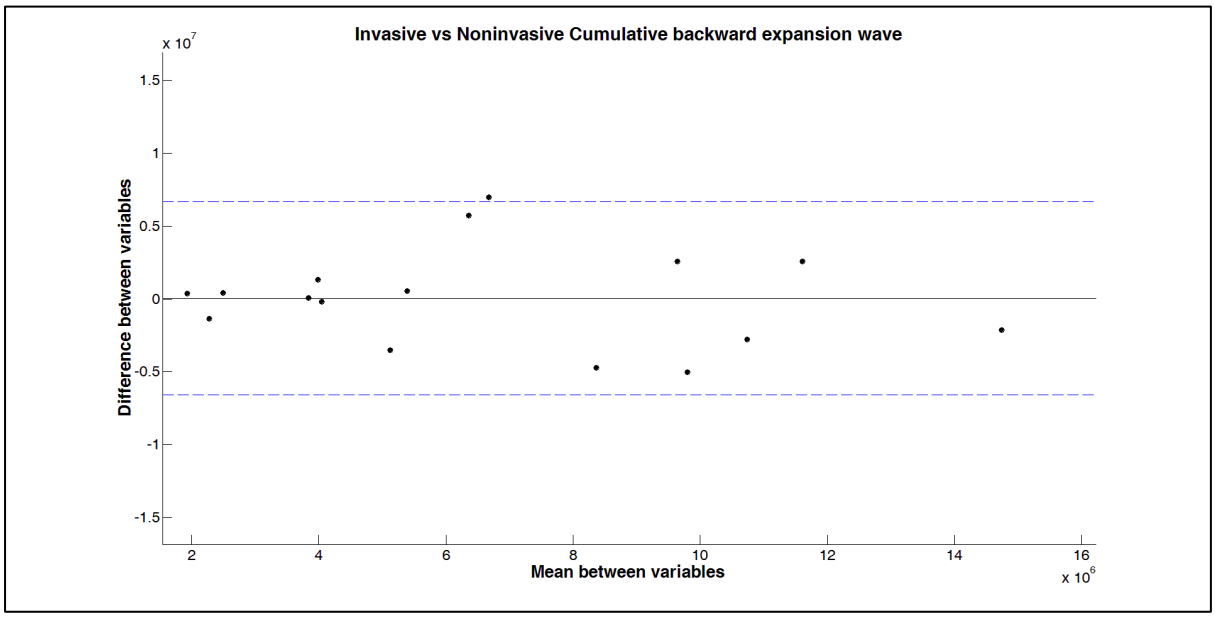

FIGURE 2-68. Correlation and Bland-Altman plot of invasive versus non-invasive cumulative backward expansion wave calculated according to section 2.3.5.5.

Non-invasive wave intensity is calculated using modified raw-Pulsecor data.

2.5.3.4 Alignment with coronary flow

After these initial modifications with alignment by differentials I used coronary flow alignment to the dicrotic notch as described in 2.5.3.2.3 to see if the accuracy could be enhanced. However, this alignment resulted in a wave-intensity pattern dominated by the flow signal with much less influence from the pressure signal (Figure 2-69). With coronary flow ensembled by r-wave guidance and mean coronary flow then aligned to the dicrotic notch, the peak backward expansion wave was underestimated (invasive -147551 vs non-invasive -59830 $Wm^{-2}s^{-2}$) with a correlation r value of 0.52 ($p = 0.03$). When flow was ensemble according to the onset of diastolic coronary acceleration the mean values were more appropriated (non-invasive -122782 $Wm^{-2}s^{-2}$) but the accuracy was not as high as alignment by differentials ($r = 0.58$, $p = 0.02$). Therefore, alignment by flow to the dicrotic notch was felt to be less helpful than differential alignment and this latter method was continued.

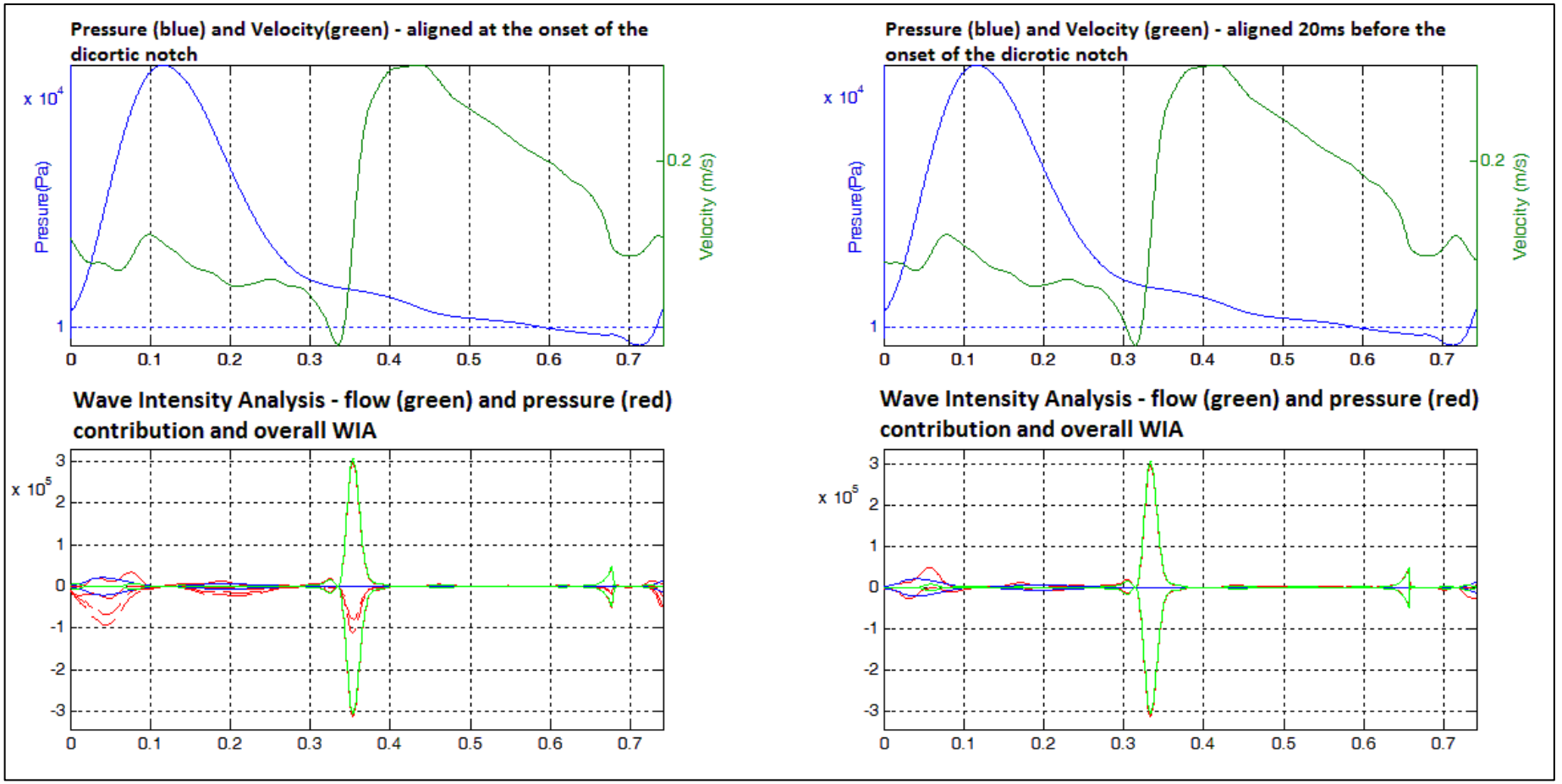

FIGURE 2-69. Wave intensity calculated according to alignment of flow with the dicrotic notch.

Alignment according to the dicrotic notch (with notch (left) and 20ms before(right)). Note the minimal effect exerted by pressure and the dominant effect of flow.

2.5.3.5 Addition of aortic valve disease patients

A further seven patients with a spectrum of aortic valve disease and unobstructed coronary arteries had same-day non-invasive and invasive wave-intensity analysis as described above. Again, a good correlation was seen between mean peak (invasive 154026 ± 68289 $Wm^{-2}s^{-2}$, non-invasive 139748 ± 108422 $Wm^{-2}s^{-2}$, r=0.77, p=0.04) and cumulative (invasive 8521726 ± 3896524, non-invasive 6449777 ± 3561035 $Wm^{-2}s^{-1}$) backward expansion wave according to 2.5.3.3.3 in these 7 patients.

When included with those patients with normal aortic valves, the correlation was strengthened with peak (invasive 150866 ± 78390 $Wm^{-2}s^{-2}$, non-invasive 140770 ± 87287 $Wm^{-2}s^{-2}$, r = 0.790, p<0.001)) (Figure 2-70) and cumulative (invasive 7181748 ± 3826425 $Wm^{-2}s^{-1}$, non-invasive 6481505 ± 4068804 $Wm^{-2}s^{-1}$, r=0.70, p < 0.001) (Figure 2-71).

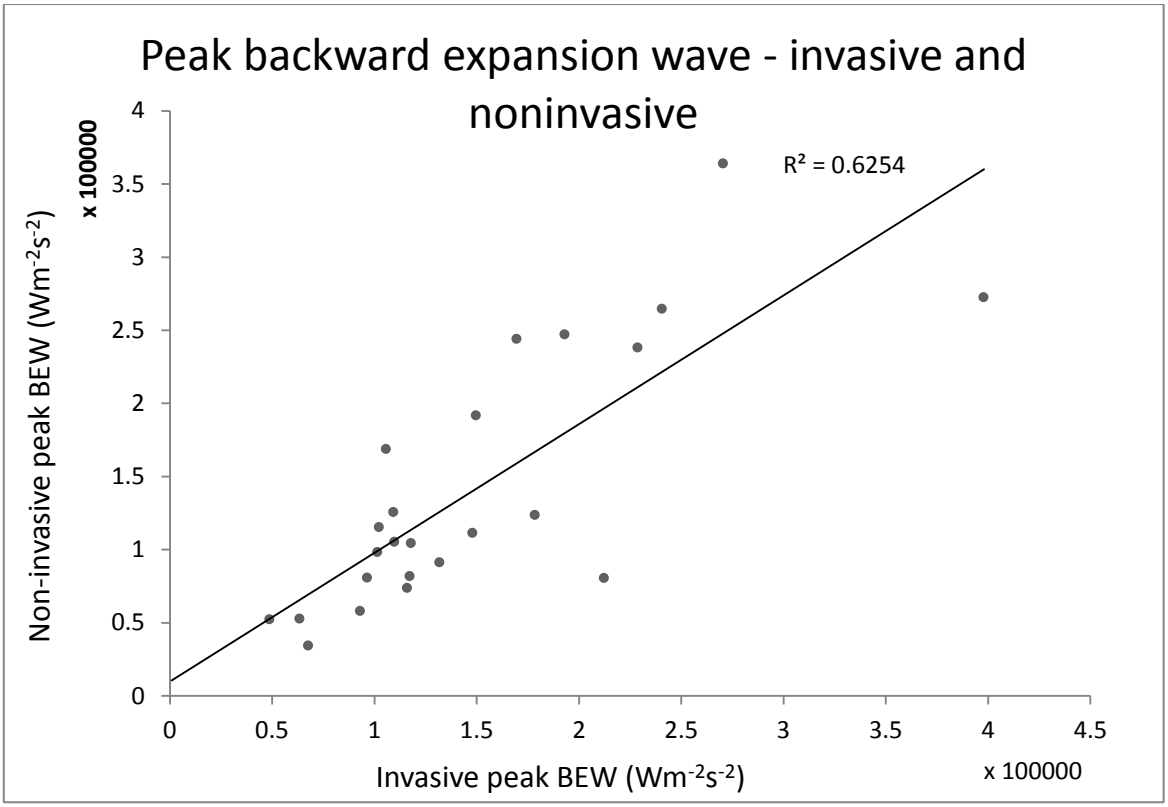

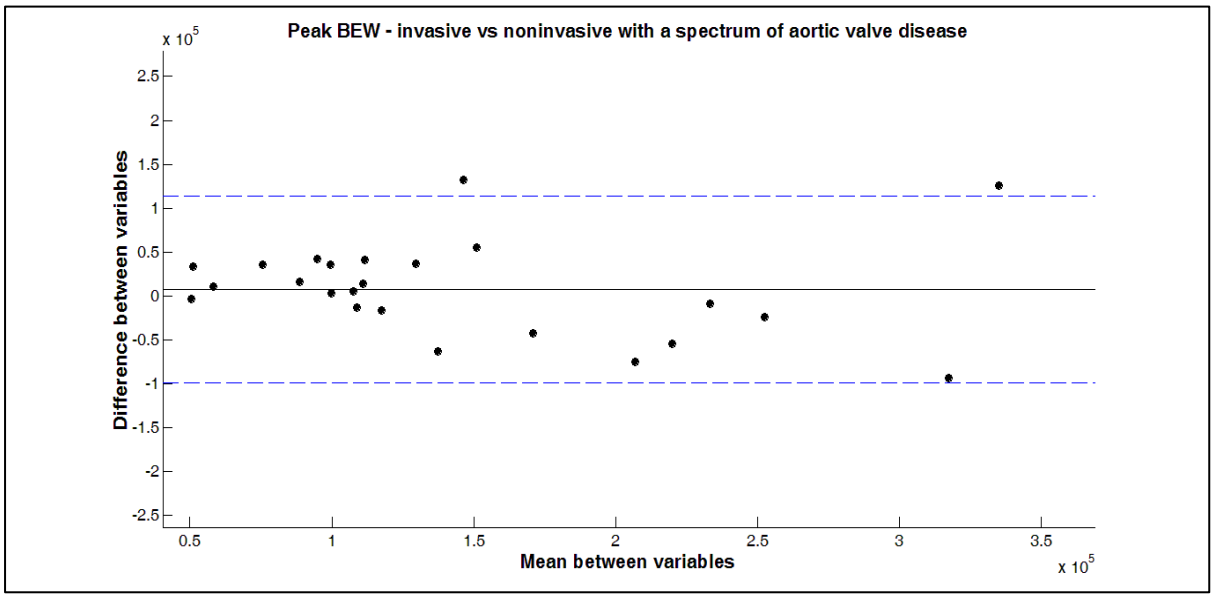

FIGURE 2-70. Scatter-graph and Bland-Altman analysis of peak backward wave-intensity measured invasively and non-invasively in patients with a spectrum of aortic valve disease.

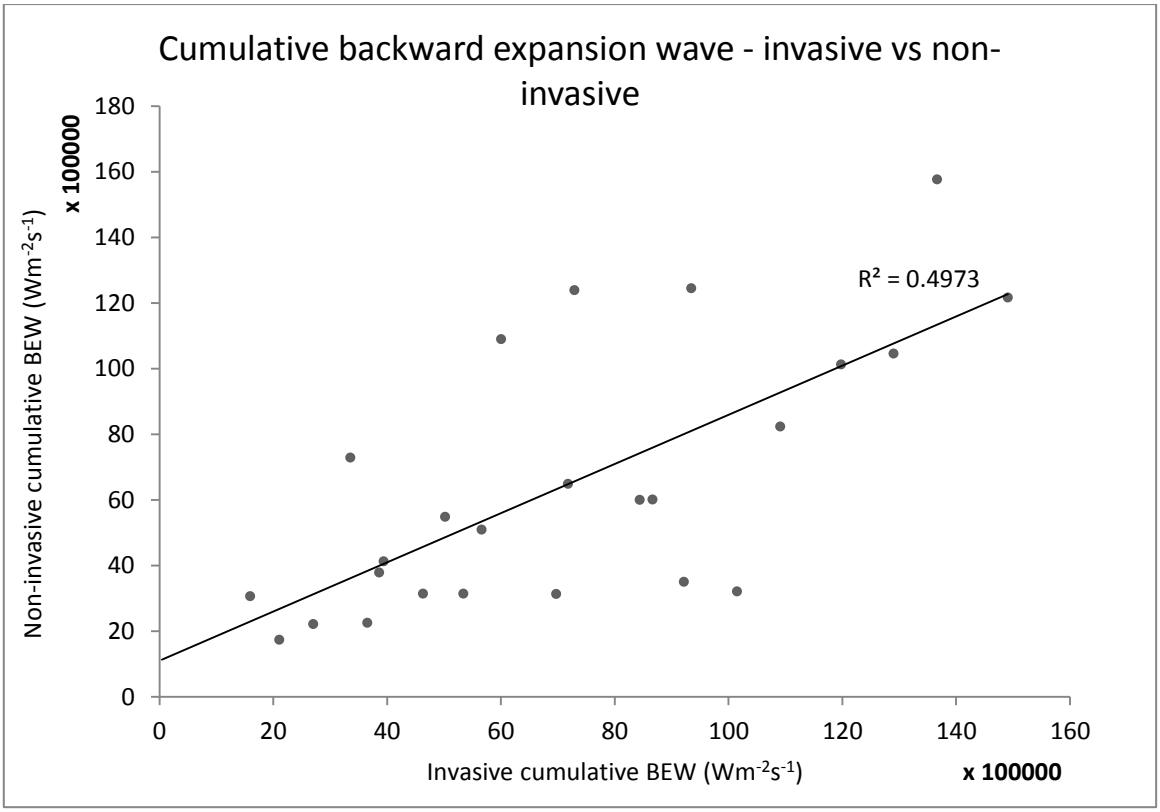

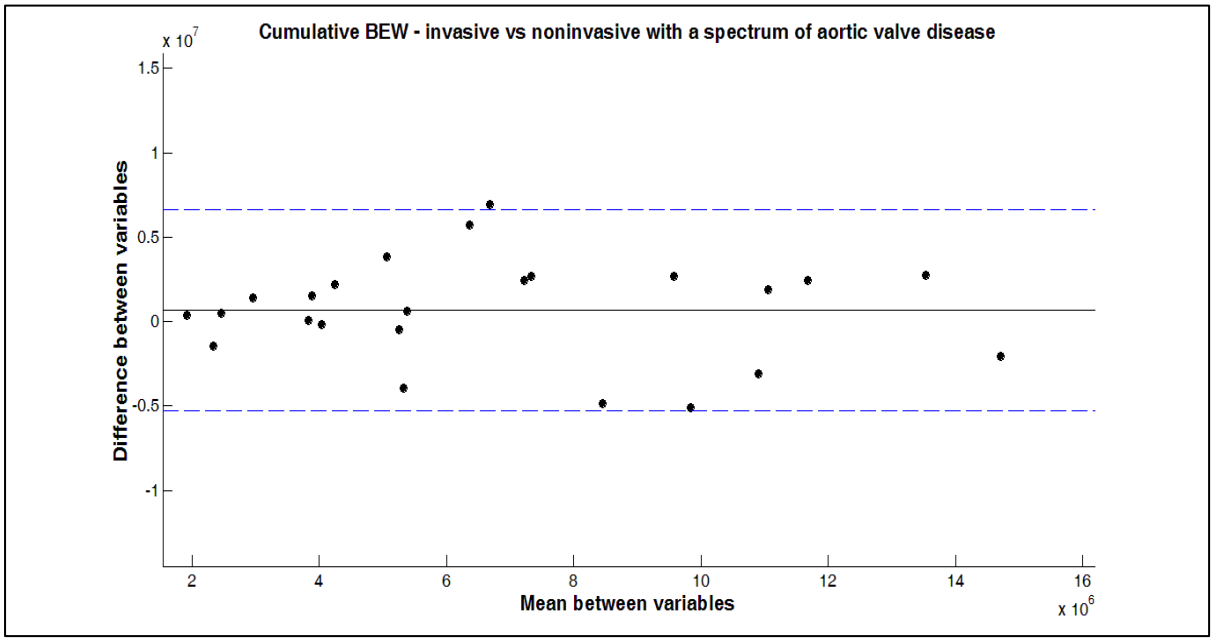

FIGURE 2-71. Scatter-graph and Bland-Altman analysis of cumulative backward wave-intensity invasively and non-invasively in patients with a spectrum of aortic valve disease.

2.6 EXERCISE INDUCED CHANGES IN NON-INVASIVELY MEASURED BACKWARD EXPANSION WAVE

2.6.1 INTRODUCTION

Previous work in subjects with normal structural hearts has shown a progressive increase in the backward expansion wave with increasing heart rate. This has been demonstrated in animal models using pacing (Sun et al., 2004) and in patients exercising during angiography(Lockie et al., 2012). This makes sense physiologically: at rest the haemoglobin concentration and oxygen extraction of coronary flow are already at 70-80% maximum capacity and therefore the resultant 5-fold increase in oxygen requirements of the myocardium during heavy exercise is largely served by an increase in coronary blood flow. Peak values of coronary blood flow in dynamic exercise are 3-5 times the resting level(Duncker and Bache, 2008) and this increase in flow must be driven by a larger energy wave.

In order to further validate my measures of non-invasive wave intensity I endeavoured to calculate the effect of exercise in patients with structural normal hearts with no evidence of coronary disease.

2.6.2 METHOD

2.6.2.1 Patients

9 patients (6 male) with no evidence of structural or coronary heart disease (demonstrated with transthoracic echocardiography and angiography) were invited to attend for assessment. Patients were also selected on the basis of good coronary flow windows. They were asked to withhold any rate-limiting pharmacological agents in the 48 hours prior to attendance and avoid alcohol, nicotine or nitrates in the preceding 24 hours.

2.6.2.2 Protocol

This employed the use of a dedicated exercise bike designed for exercise-echocardiography (Figure 2-72). The Pulsecor machine was applied to the left arm and operated by an assistant, ensuring there was no movement artefact during measurements. Coronary flow was interrogated continuously with increasing workload and heart rate aiming for a heart rate of 120bpm. A minimum of 3 recordings of the Pulsecor were taken: at rest, between 80-90 bpm and between 100-110bpm.

Post-data acquisition, the coronary flow images were digitalized as described. The heart rate was calculated using Matlab by an automated recognition of the Q waves on the ECG. Coronary flow was then grouped into discrete groups of 10bpm spreads of heart rate (from 50-60bpm to 100-110 bpm). They were then processed with the appropriate Pulsecor.

FIGURE 2-72. Ergoline exercise bike with simultaneously recorded Pulsecor.

The machine can be adjusted by work-rate independent of revolution speed allowing steady incremental increases in heart rate.

2.6.2.3 Statistics

Data was analysed using STATA version 11. ANOVA was performed with Sidak for correlation. A p value of <0.05 was deemed significant.

2.6.3 RESULTS

Although technically very challenging it did prove possible to achieve coronary flow data at graded-heart rates (Figure 2-73) with simultaneous Pulsecor measurements in these 9 patients.

2.6.3.1 Haemodynamic parameters

Baseline, mid-exercise and peak exercise haemodynamic parameters are demonstrated in Table 2-11. Coronary flow rose appropriately during exercise from 28.8 cm/s to 42.1 cm/s (p 0.06) (example - Figure 2-73) as did systolic pressure (124 to 141 mmHg, p=0.018). Diastolic pressure only modestly rose from 85 to 88mmHg (p=0.66).

Backward expansion wave was calculated as both a peak and cumulative value and a progressive increase was seen in both. Peak BEW was -100036 ± 65038.15 $Wm^{-2}s^{-2}$ at baseline and increased to -151531 ± 10275 $Wm^{-2}s^{-2}$ at moderate exercise and -204778.5 ± 68259 $Wm^{-2}s^{-2}$ at peak (p=0.02 vs rest). Cumulative BEW was 5393160 ± 3823324 $Wm^{-2}s^{-1}$ at rest and rose to 6779162 ± 2259721 $Wm^{-2}s^{-1}$ at moderate exercise and 14518790 ± 8939111 $Wm^{-2}s^{-2}$ at peak (p=0.03 vs rest) (Table 2-11, Figure 2-74).

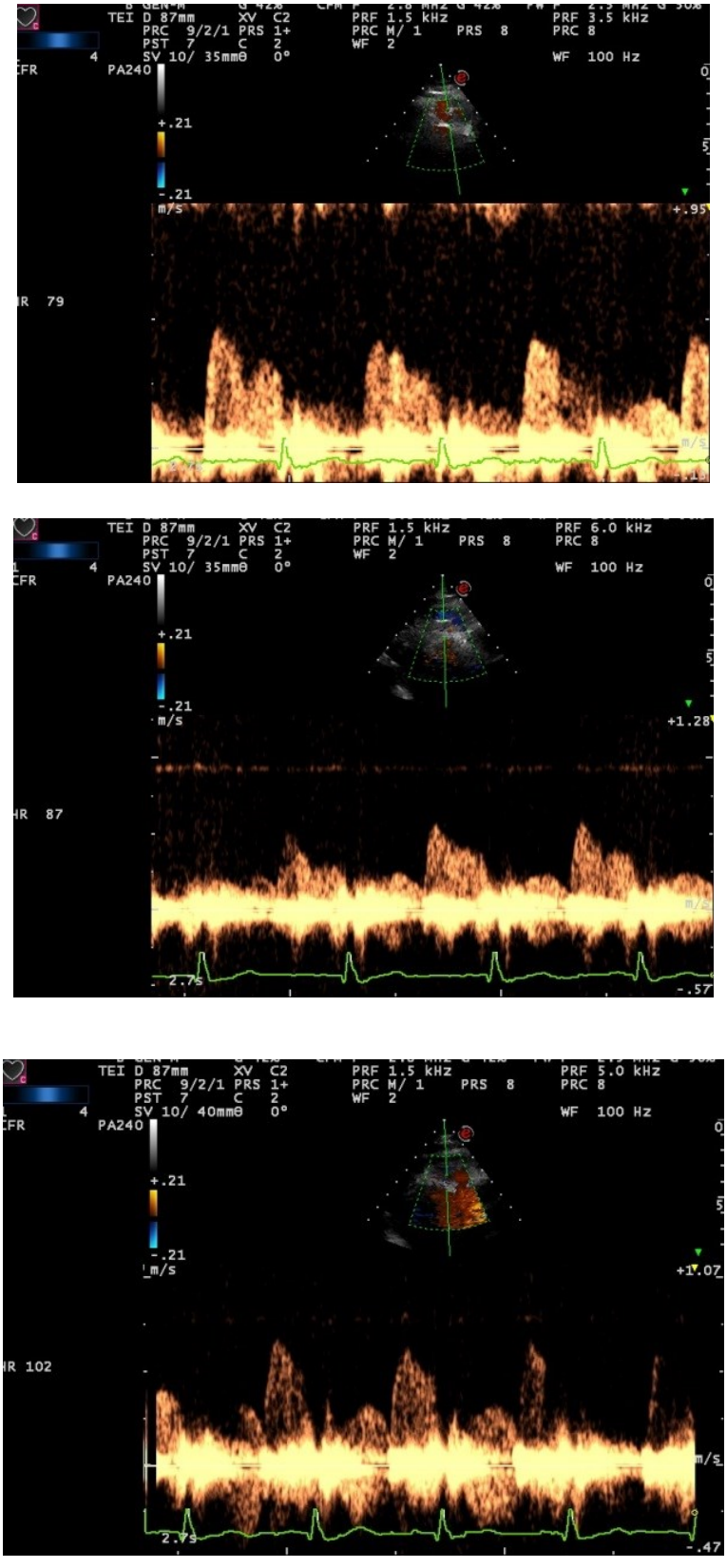

FIGURE 2-73. Coronary flow as measured by echocardiography with increasing heart rate with patient exercising on dedicated echo-exercise bike.

	Baseline	Mid-exercise	Peak-exercise
Heart Rate (bpm)	72.3 ± 9.8	85.8 ± 11.3	102.4 ± 9.7
Central systolic pressure (mmHg)	123.6 ± 16.5	130.2 ± 19.8	141.8 ± 25.3
Diastolic BP(mmHg)	85.12 ± 7.7	85.6	88.4
Peak velocity (cm/s)	28.8 ± 12.9	33.9 ± 14.3	42.1 ± 17.3
Mean velocity (cm/s)	18.5 ± 7.1	21.3 ± 8.0	25.5 ± 9.3
Peak backward expansion wave ($Wm^{-2}s^{-2}$)	10.0 ± 6.5 $x10^4$	15.1 ± 10.2 x 10^4	30.2 ± 20.4 x 10^4
Cumulative backward expansion wave ($Wm^{-2}s^{-1}$)	53.9 ± 38 x 10^5	83.4 ± 67.8 x 10^5	145.2 ± 89.4 x 10^5

TABLE 2-11. Baseline, mid-exercise and peak-exercise haemodynamic data for 9 patients with normal coronary arteries and structural normal hearts undergoing a graded exercise regimen.

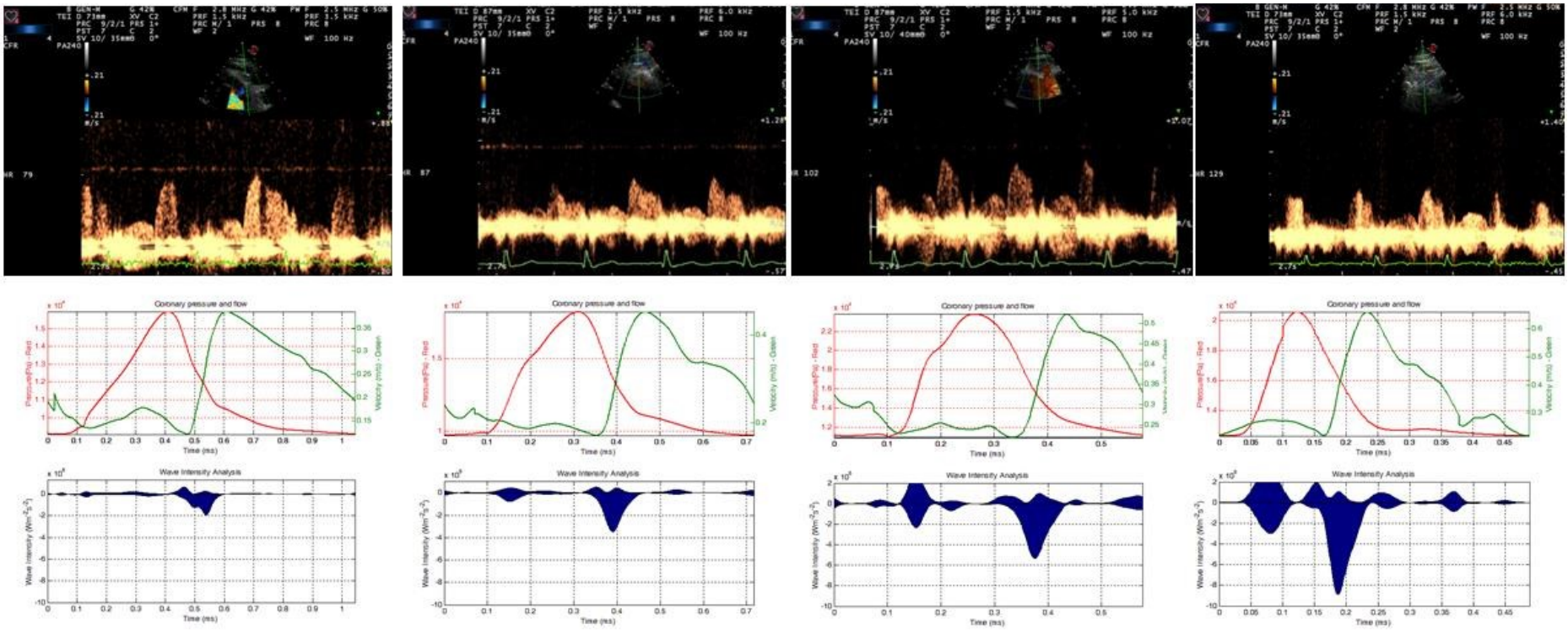

FIGURE 2-74. Coronary flow assessment and non-invasive wave-intensity analysis at increasing heart rates.

With exercise and a resultant increasing heart rate a progressive increase is seen in the in size of the cumulative and peak backward expansion wave. In turn this transmits a greater 'suction' from the myocardium to the proximal blood flow resulting in higher coronary flow rates per cardiac cycle. Although technically challenging, with a moderate level of experience, non-invasive coronary flow and the backward expansion wave can be measured at heart rates of 120bpm (far right panel).

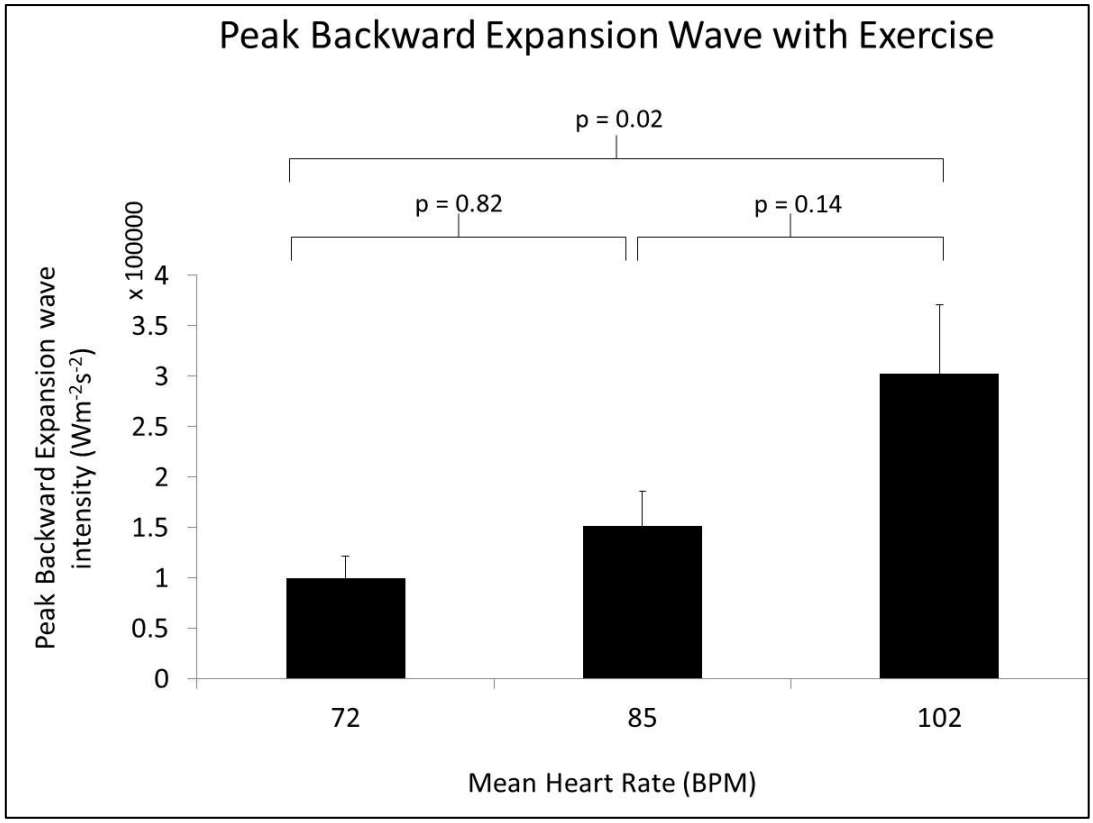

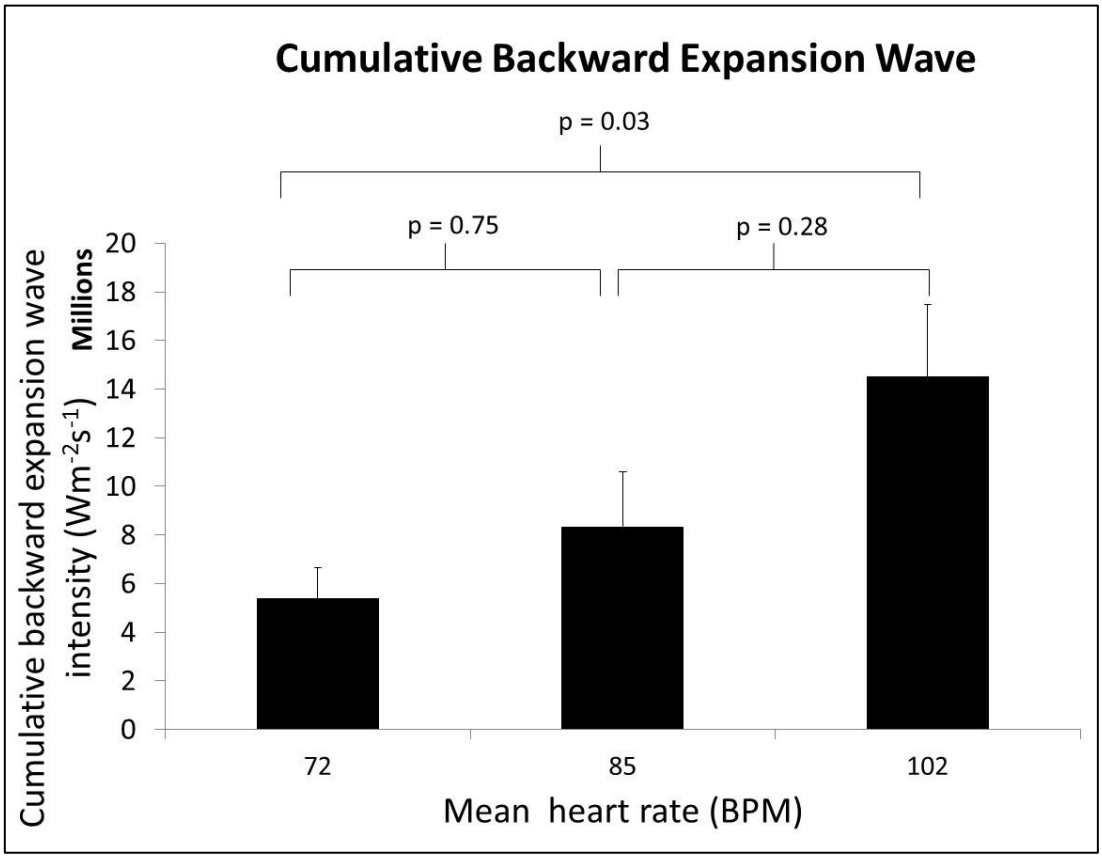

FIGURE 2-75. Peak and cumulative backward expansion wave during exercise.

There is a significant increase in both peak and cumulative backward expansion wave per heart beat accounting for the increase in flow generated during exercise. Data is displayed as mean with SEM bars.

2.6.4 CONCLUSIONS

In both human and animal models, the backward expansion wave has been shown to increase with increasing heart rate. By using an echo-exercise bike I have demonstrated that it is possible to perform exercise wave-intensity analysis and that the backward expansion wave responds as expected. This confirms experimental findings that have been performed invasively as well as further validates this method of wave-intensity assessment.

2.7 BACKWARD EXPANSION WAVE WITH LEFT VENTRICULAR MASS

Previous data has demonstrated a correlation between the percentage of backward expansion wave and LV thickness reflecting the inefficiency of increasing left ventricular hypertrophy. In 24 patients with normal coronary arteries and structurally normal hearts, left ventricular mass was calculated according to standard principles(Lang et al., 2005) and correlated with peak backward expansion wave. Whilst it did not reach significance (p=0.17), there was a similar trend between peak backward expansion wave with left ventricular mass (Figure 2-76).

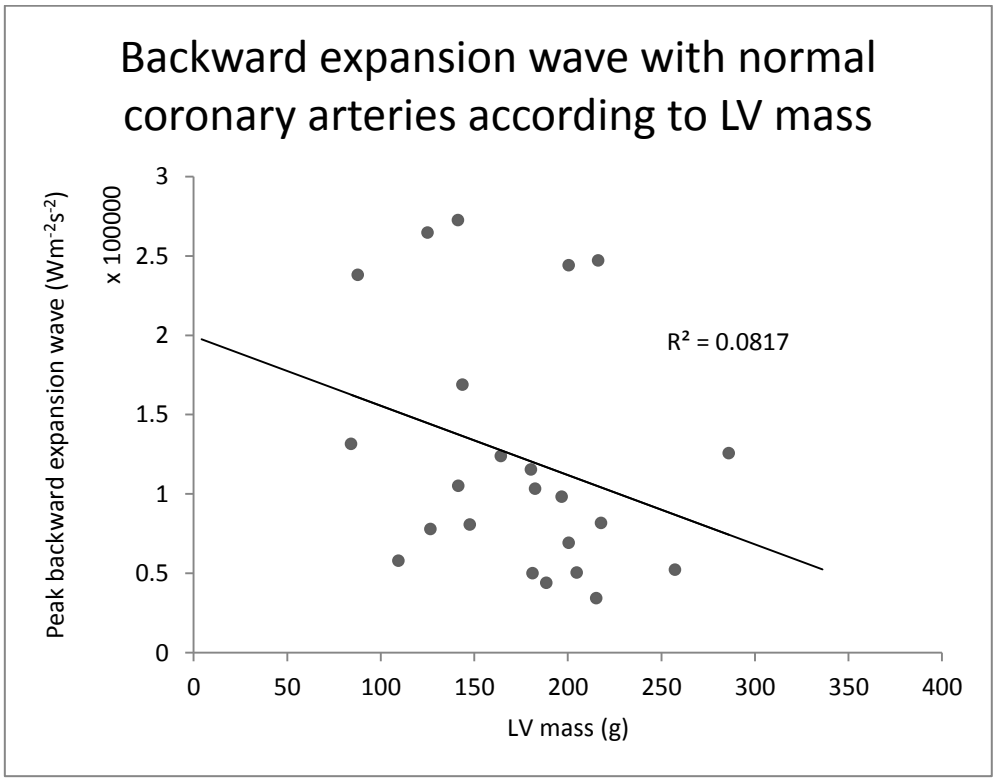

FIGURE 2-76. Peak backward expansion wave with left ventricular mass. There is a trend towards a smaller backward expansion wave with increasing lv mass.

2.8 REPRODUCIBILITY

Finally, to test reproducibility, 15 patients with unobstructed coronary arteries and structurally normal hearts, in whom non-invasive wave-intensity was measured were assessed twice. The protocol for the reassessment was:

1. Non-invasive assessment of coronary wave-intensity using inbuilt coronary flow pre-sets
2. Return to normal 'cardiology' pre-sets and full routine cardiac echocardiography
3. Return to coronary flow pre-sets and further non-invasive assessment of flow with repeat Pulsecor measurements

Coronary flow was not accurately obtained in 1 patient therefore they were excluded. In the remaining 14 a good reproducibility was obtained for both peak ($r=0.90$, $p<0.001$) and cumulative ($r=0.90$, $p<0.001$) backward expansion wave intensity (Figure 2-77).

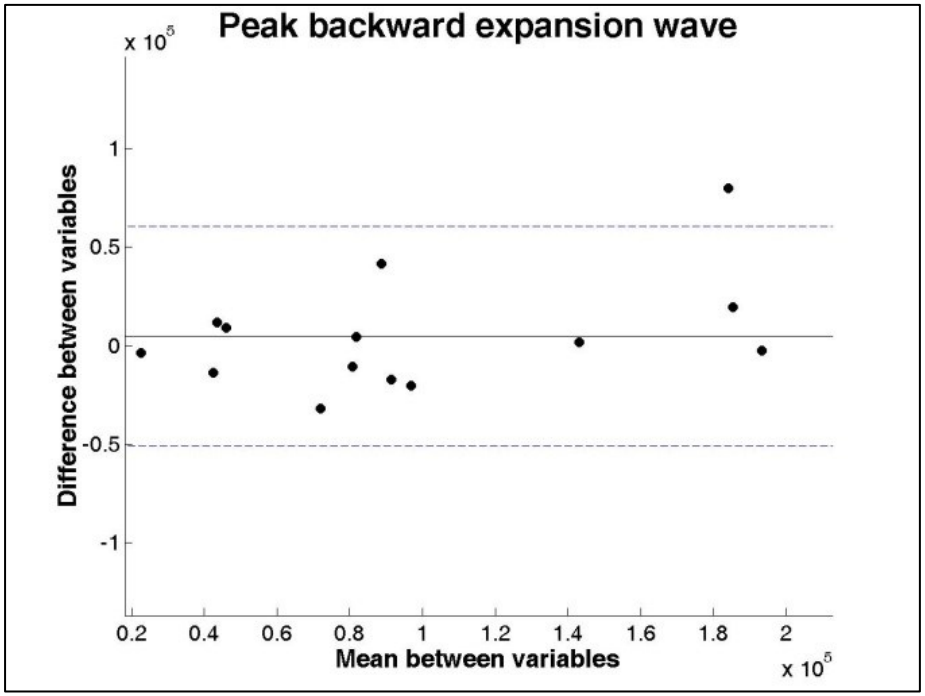

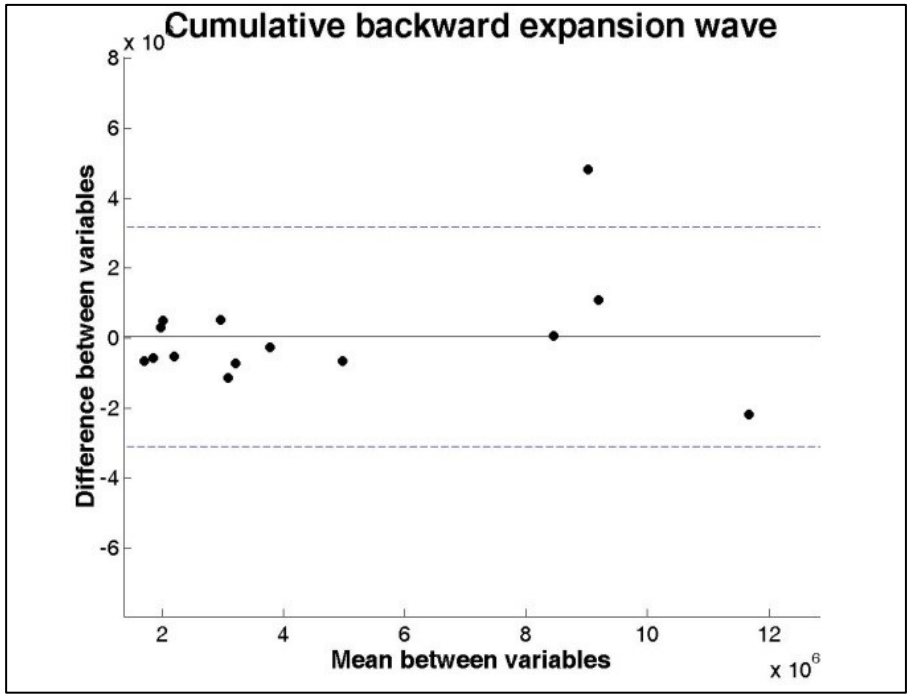

FIGURE 2-77. Peak and cumulative backward expansion wave reproducibility displayed as a Bland-Altman plot.

There is a good reproducibility with peak and cumulative non-invasively constructed backward expansion wave.

2.9 Construction of non-invasive wave intensity: Conclusions

Coronary wave-intensity analysis is a useful tool in the assessment of myocardial and coronary disease. It enables the quantification and qualification of the energy influencing the velocity of blood and as such provides information on the proximal (aortic) and distal (myocardial) influences of flow. The most usefully recognised wave within the cardiac cycle is the backward-travelling expansion wave which is responsible for generating coronary flow during diastole. Using non-invasive techniques, I have demonstrated that it is possible to construct a valid measure of this wave. I have also shown that it is reproducible and that it responds appropriately during aerobic exercise.

Direct visual assessment and pulse-wave measures of coronary flow have been possible with echocardiography for the last 2 decades. With improvements in probe- and processing-technology, the coronary flow signals obtained have been steadily improving. However, as alluded to above, by measuring flow alone, it is impossible to make an assumption regarding the direction the force generating flow originates from. Therefore, in order to make flow measures more useful clinically, a further variable is required. Previously, this has been the addition of a stressor agent to increase the inotropic and/or chronotropic cardiac state and thus allowing derivation of coronary flow reserve. However, by using coronary flow along with central pressure, coronary wave-intensity is able to give meaningful information regarding the myocardium without the need for stress.

The technique of coronary flow analysis is not without difficulties. It is important to use a machine which is geared towards coronary flow imaging. This is essential in order to visualise the acceleration of blood in early diastole and not just its peak. Additionally, unorthodox views are required to bring the LAD into the appropriate plane. Finally,

learning to adjust the settings of the machine beyond its pre-sets is also important. With a moderate level of experience coronary flow can be reliable obtained in approximately 80-90% of patients and validates well with simultaneous invasive measures.

Unlike coronary flow, less skill is required in the live acquisition of central pressure using the Pulsecor device. This is not always true during exercise where the presence of an assistant is vital to maintain arm stability during suprasystolic measurements. However, post-processing of this data to obtain a clean, reliable and useful sample is essential. This may mean removing inaccurate beats before re-ensembling as well as ensembling around a fixed point such as the peak negative dpdt in order to ensure that the diastolic portion is best preserved. I have demonstrated that the assumption that coronary pressure waveforms in non-obstructed arteries are the same as central aortic ones and that the pressure waveforms that can be obtained non-invasively, with appropriate post-processing after acquisition, are valid estimations of coronary pressure.

Calculation of wavespeed is necessary for wave-intensity analysis and this is performed using a single-point technique and I have shown the values obtained non-invasively in this fashion to correlate well with invasive measurements. I have demonstrated different ways of producing this value mathematically and have shown that integer based calculations, involving raw Pulsecor data is the most accurate.

Using these measurements I have gone on to calculate peak and cumulative measures of backward expansion wave in a group of patients with unobstructed coronary arteries with no significant cardiac structural abnormalities. A good correlation was found with similar invasive measurements. Additionally, previous invasive work has demonstrated that the backward expansion wave increases in animal models and humans with pacing

or exercise and a similar effect was seen in a group of 9 patients who underwent non-invasive wave-intensity assessment during static-bike exercise. This reinforces the validity of the measurements I obtained. Finally, I have gone on to show that non-invasive backward expansion wave construction is a reproducible technique.

Therefore, in summary, I have shown that it is possible to construct a coronary wave-intensity profile non-invasively. This technique obviously has applications in a variety of research and clinical settings, particularly in patients not scheduled for invasive assessments but in whom repeated measures of wave-intensity would be useful for guiding the need for, or effect of, therapy. This technique therefore forms a fundamental tool used throughout the rest of this thesis

3 CHAPTER 3: INVASIVE WAVE INTENSITY ANALYSIS IN SEVERE AORTIC STENOSIS AND THE ACUTE EFFECT OF AFTERLOAD REDUCTION

3.1 INTRODUCTION

3.1.1 INVASIVE WAVE INTENSITY ANALYSIS IN AORTIC STENOSIS

The initial step in the construction of the wave-intensity profile across the spectrum of aortic valve disease was the application of invasive wave-intensity analysis in patients with severe aortic stenosis. Invasive analysis can be employed here because these patients can conveniently undergo catheter based interrogation either as part of their work-up for aortic valve replacement or during their therapy with transcatheter aortic valve therapy. Therefore it was possible to follow conventional invasive assessment of their coronary wave-intensity profile as has previously been applied to normal subjects(Davies et al., 2006a).

3.1.2 TRANSCATHETER AORTIC VALVE IMPLANTATION (TAVI) AS AN EXPERIMENTAL MODEL

The introduction of the TAVI procedure allowed great versatility in the peri-procedural assessment of aortic stenosis before and after outflow tract obstruction relief. It has several advantages in this area, notably:

1. Absence of pericardotomy or the need for cardiopulmonary bypass thus preserving the underlying physiological status
2. The presence of invasive monitoring and the ability to easily interrogate the coronary arteries
3. The presence of a temporary pacing wire to provide a stressor of the myocardium

Therefore, intracoronary assessments during the TAVI procedure are not only possible but theoretically more physiologically appropriate than those that could be achieved during aortic valve replacement.

3.1.3 Pacing as a Stressor of Myocardium in Aortic Stenosis

Prior to the introduction of the TAVI procedure, the use of pacing to stress the myocardium has had a fairly limited application in the assessment of aortic stenosis. Previous work in dogs with LVH induced through aortic banding or coronary cusp plication has demonstrated abnormalities in subendocardial blood flow with right ventricular pacing compared to controls. There was a failure of the subendocardial blood flow to increase compared to the subepicardial layer in the same animal as well as both layers in control animals measured through radioactive microsphere assessment(Bache et al., 1981a, Alyono et al., 1986). This also corresponded to a deterioration in subendocardial fractional shortening(Nakano et al., 1989) and has also been shown to occur with dogs during exercise(Bache et al., 1981b).

Older studies have also employed pacing as a means to stress the heart in humans with aortic stenosis. Using an temporary pacing wire in the right atrium and incremental pacing rates angina has been demonstrated at higher heart rates, typically around 120-150 bpm(Fifer et al., 1986). Anecdotal reports in patients with more moderate aortic stenosis have documented the potential detrimental effects of ventricular pacing both clinically(Patel et al., 1977) and in terms of coronary flow reserve(Kawamoto et al., 2001) . However, largely the investigation of aortic stenosis has employed other investigative or experimental modalities and this is where the TAVI procedure allows for an expansion.

3.1.4 LEFT VENTRICULAR HYPERTROPHY IN AORTIC STENOSIS

Left ventricular hypertrophy involves the deposition of extracellular matrix and perivascular fibrosis(Schwartzkopff et al., 1992). This is a necessary step to preserve forward flow across an increasing outflow tract obstruction but is also detrimental to ventricular filling and ultimately coronary blood flow(Levy et al., 1990, Gaasch, 1979). It also means the work load and myocardial oxygen demand increases leading to a reduced coronary vascular reserve the details of which are outlined in chapter 1. This abnormal ventricular pathophysiology is the reason left ventricular hypertrophy is associated with a worse prognosis in patients without valvular heart disease but is essential in aortic stenosis to maintain an appropriate ejection fraction in the face of increase outflow tract obstruction.

Therefore, by assessing coronary physiology using wave intensity analysis during TAVI, it should be possible to ascertain the effect of aortic stenosis and the resultant left ventricular hypertrophy on the coronary circulation and the effect of aortic valve implantation (without an alteration in left ventricular hypertrophy) on this profile.

3.2 METHODS

Eleven patients (age, 80±9 years) scheduled for TAVI with fluoroscopically unobstructed coronary arteries participated in the study (Table 3-1). Transthoracic echocardiography was performed in all subjects (Table 3-2), and was repeated 5 to 7 days after TAVI (Table 3-3). In addition to Doppler parameters, 2 dimensional measurements were calculated offline on a McKeeson workstation. Exclusion criteria included any previous coronary intervention, significant regional wall motion abnormalities, cardiac dysrhythmias, or the use of nitrates in the preceding 24 hours. All subjects gave written informed consent in accordance with the protocol approved by the local ethics committee.

Female, n (%)	9 (82)
Age, y	80±9
Weight, kg	63±15
BMI, kg/m^2	24±3
Hypertension, n (%)	7 (64)
Diabetic, n	0
Medications, n (%)	
Statin	9 (82)
Antiplatelet	10 (90)
ACEI or A2	4 (36)
β-blocker	1 (9)
α-blocker	1 (9)
Calcium antagonist	3 (27)
Diuretic	7 (63)
Angina, n (%)	
Chest pain	2 (18)
Breathlessness	11 (100)
Presyncope/syncope	1 (9)

TABLE 3-1. Baseline demographics

LV mass, g	164±53
BSA LV mass, g	100±30
Peak gradient, mm Hg	81±24
Mean gradient, mm Hg	48±15
Area, cm^2	0.6±0.1
Echocardiographic parameters, mm	
LV EDD	40±10
LV ESD	30±13
LV PWD (d)	11±3
LV SD (d)	13±3
LV PWD (s)	15±3
LV SD (s)	16.5±3

TABLE 3-2. Baseline echo

	Before TAVI	After TAVI	*P*
Peak gradient, mm Hg	81±24	18±10	<0.001
Aortic valve			
Velocity time integral, cm	110±20	44±12	<0.001
Peak velocity, m/s	4.4±0.7	2.5±0.6	<0.001
Left ventricular outflow tract			
VTI	28±13	22±7	0.29
Peak velocity, m/s	0.8±0.3	1±0.2	0.2
Aortic regurgitation			
None	3	3	…
Mild	7	7	…
Moderate	1	1	…

TABLE 3-3. Echocardiographic parameters before and after TAVI.

3.2.1 STUDY PROTOCOL

Patients were intubated and ventilated, and a right ventricular pacing wire was positioned in the right ventricle via the right femoral vein. The left coronary artery was intubated with a Judkins left guide catheter; then, a sensor-tipped wire was passed into the proximal segment of the left main stem. Pressure and velocity recordings from aorta and coronary arteries were made with 0.014-in-diameter sensor-tipped wire (Combowire, Volcano Corp). Pressure and velocity were recorded for 1 minute at the intrinsic heart rate and then during pacing at 90 and 120 bpm. Afterward, TAVI was performed, an identical set of pressure- and flow-velocity measurements were made in

the coronary arteries again at the intrinsic rate and during pacing. Fluoroscopic images were used to ensure that the 2 measurement sets were made at identical locations.

3.2.2 Analysis of Hemodynamic Data

Analog output feeds were taken from the pressure-velocity console and ECG, fed into a National Instruments DAQ-Card AI-16E-4, and acquired at 1 kHz with Labview. Data were analysed offline with a custom software package designed with Matlab (Mathworks, Natick, MA). The blood pressure and Doppler velocity recordings were filtered with a Savitzky-Golay filter(Savitzky and Golay, 1964) and ensemble averaged with the ECG R wave for timing. Pressure and velocity-time integrals (VTIs) were calculated and VTI.min product calculated by multiplying VTI by heart rate. Values of VTI are corrected for body surface area and LV mass. All microcirculatory wave intensity values are reported as magnitudes (i.e., positive). The coronary physiological reserve was calculated as the difference (δ) in the peak intensity of the backward decompression (or suction) wave between resting and increased heart rate (90 and 120 bpm).

3.2.3 Percutaneous Aortic Valve Implantation

A 7F venous sheath was positioned in the femoral vein, and an 8F arterial sheath was positioned in the femoral artery. A temporary pacing wire was advanced via the femoral vein into the right ventricular apex to achieve a minimum pacing threshold of <1 V. With the use of an AL1 diagnostic catheter, an 0.035-in guidewire was used to cross the aortic valve via the femoral artery, and the stenotic valve was prepared using aortic

valvuloplasty with appropriate upsizing of the femoral arterial sheath. After valvuloplasty, the percutaneous valve was advanced through the stenotic aortic valve and deployed during a phase of rapid right ventricular pacing. In 10 cases, Edwards Sapien valves (Edwards Lifesciences) were used; in a single case, a Corevalve (Medtronic) was used. The mean valve diameter was 24.75 mm (range, 23–29 mm). Interprocedural aortography and transoesophageal echocardiography were performed to check the position of the valve immediately before, during, and after valve deployment.

3.2.4 Statistical Analysis

STATA 11 (StatCorp LP) was used for analyses. The sample size was chosen (following our pilot study) to detect a 1.0×105-W · m−2 · s−2 reduction in microcirculatory diastolic suction wave, assuming an SD of 0.4×105 W · m−2 · s−2 with an α of 0.05 at 90% power. Correlation was assessed with the Pearson correlation coefficient. Mixed linear models were used to account for the repeated measures in comparisons of changes in hemodynamic variables at differing heart rates (intrinsic and 90 and 120 bpm). A value of $P<0.05$ was taken as statistically significant.

3.3 RESULTS

3.3.1 EFFECTS OF AORTIC STENOSIS ON CORONARY HAEMODYNAMICS

The baseline and pacing hemodynamic variables are summarized in Table 3-4 and Table 3-5. The backward expansion wave increased with increasing severity of aortic stenosis (r=0.59, P=0.05; Figure 3-1). After TAVI, resting coronary systolic pressure (115±9 versus 106±11 mm Hg; P=0.38), peak coronary flow velocity (54±6 versus 44±6 cm · s−1; P=0.2), and intrinsic heart rate remained unchanged (73±4 versus 73±3 bpm; P=0.96). Coronary waves were similar before and after TAVI, except for the backward expansion wave, which fell significantly in magnitude (1.9±0.3 versus 1.1±0.1×10−5 W · m−2 · s−2; P=0.02).

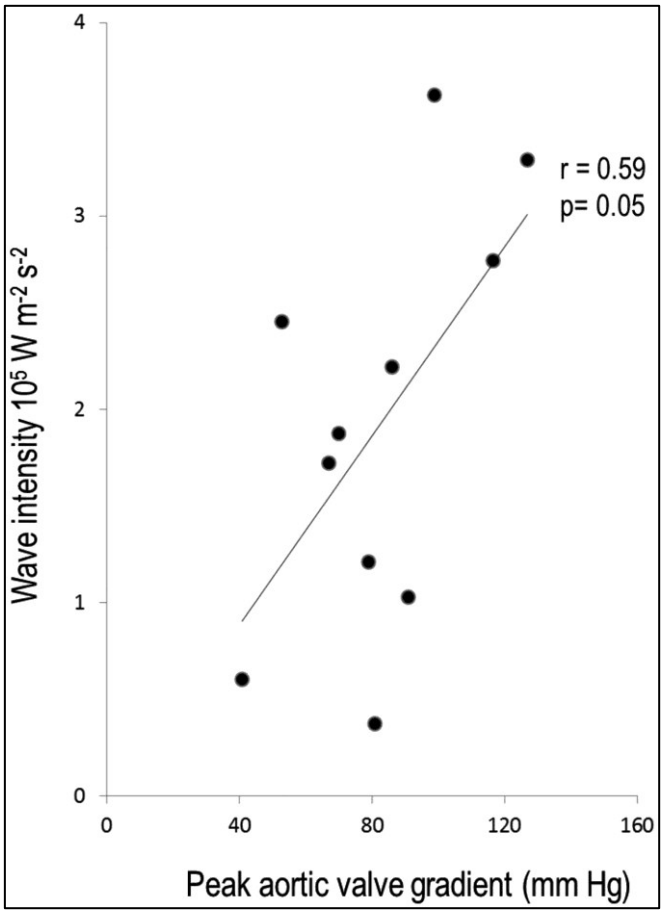

FIGURE 3-1. Increase in the BEW with increasing peak aortic gradient.

	Rest		90bpm		120bpm		
	Before	After	Before	After	Before	After	P
Flow Velocity							
Minimum	2±5	7±2	2±6	5±2	4±6	5±3	0.66
Maximum	54±6	44±6	58±4	45±4	60±7	52±5	0.67
Mean	27±3	26±4	29±3	25±2	29±5	28±2	0.23
VTI, cm							
VTI	49±12	21±4	19±4	17±2	18±5	16±2	0.037
VTI.min	3587±982	1561±300	1706±332	1494±216	2120±621	1937±273	0.006
Change from before to after TAVI		−27±11		−2.3±3		−1.5±4	
Pressure, mm Hg							
Minimum	54±5	53±6	56±4	56±7	56±4	58±7	0.15
Maximum	115±9	106±11	93±10	79±22	83±6	94±11	0.65
Mean	82±6	76±8	72±5	72±8	69±5	74±9	0.99
dP/dtmax	0.4±0.05	0.4±0.03	0.3±0.03	0.4±0.03	0.3±0.03	0.4±0.03	0.10
dP/dtmin	−0.4±0.05	−0.4±0.05	−0.3±0.03	−0.3±0.03	−0.2±0.03	−0.4±0.04	0.83
Pressure-time integral	63±6	58±7	44±3	43±5	37±3	39±4	0.026
Heart rate, bpm	73±4	73±3	90	90	120	120	

TABLE 3-4. Flow velocity and pressure with increasing heart rate before and after TAVI.

	Rest		90bpm		120bpm		
	Before	After	Before	After	Before	After	P
Peak wave intensity, $\times 10^5$ W · m^{-2} · s^{-2}							
Forward compression	1.7±0.4	2.7±0.6	1.4±0.4	1.8±0.3	1.0±0.3	1.9±0.3	0.58
Forward decompression	0.9±0.1	1.0±0.2	0.7±0.2	0.9±0.1	0.7±0.2	1.0±0.2	0.09
Early backward compression	1.8±0.6	1.2±0.3	1.5±0.5	1.1±0.1	1.4±0.4	1.5±0.2	0.15
Late backward compression	0.6±0.1	0.7±0.3	0.7±0.1	0.7±0.2	0.6±0.1	0.9±0.2	0.78
Backward expansion	1.9±0.3	1.1±0.1	1.4±0.3	1.0±0.5	1.1±0.2	1.4±0.2	0.001

TABLE 3-5. Peak wave intensity before and after TAVI with increasing heart rate.

3.3.2 Assessment of Physiological Coronary Reserve in Subjects With Severe Aortic Stenosis Before and After Percutaneous Aortic Valve Replacement

Physiological coronary reserve was assessed by pacing at 90 and 120 bpm (Table 3-5). The backward expansion wave fell with increasing heart rate before TAVI (β coefficient=−0.16×10−4 W · m−2 · s−2; P<0.001; Figure 4). After TAVI, this pattern was reversed, and the backward expansion wave was found to increase significantly (β coefficient=0.9×10−3 W · m−2 · s−2; P=0.014; Figure 4). Overall, comparing the changes before and after TAVI resulted in a significant beneficial increase in delta backward expansion wave with increasing heart rate (β coefficient=0.23×10−3 W · m−2 · s−2; P<0.001).

Before TAVI, the VTI was also found to decrease significantly with increasing heart rate (intrinsic rate, 49±12 cm versus 120 bpm 18±5 cm; ***P***<0.004). After TAVI, however, the VTI remained unchanged with increasing heart rate (intrinsic rate, 21±4 cm versus 120 bpm 16±2 cm; ***P***=0.06).

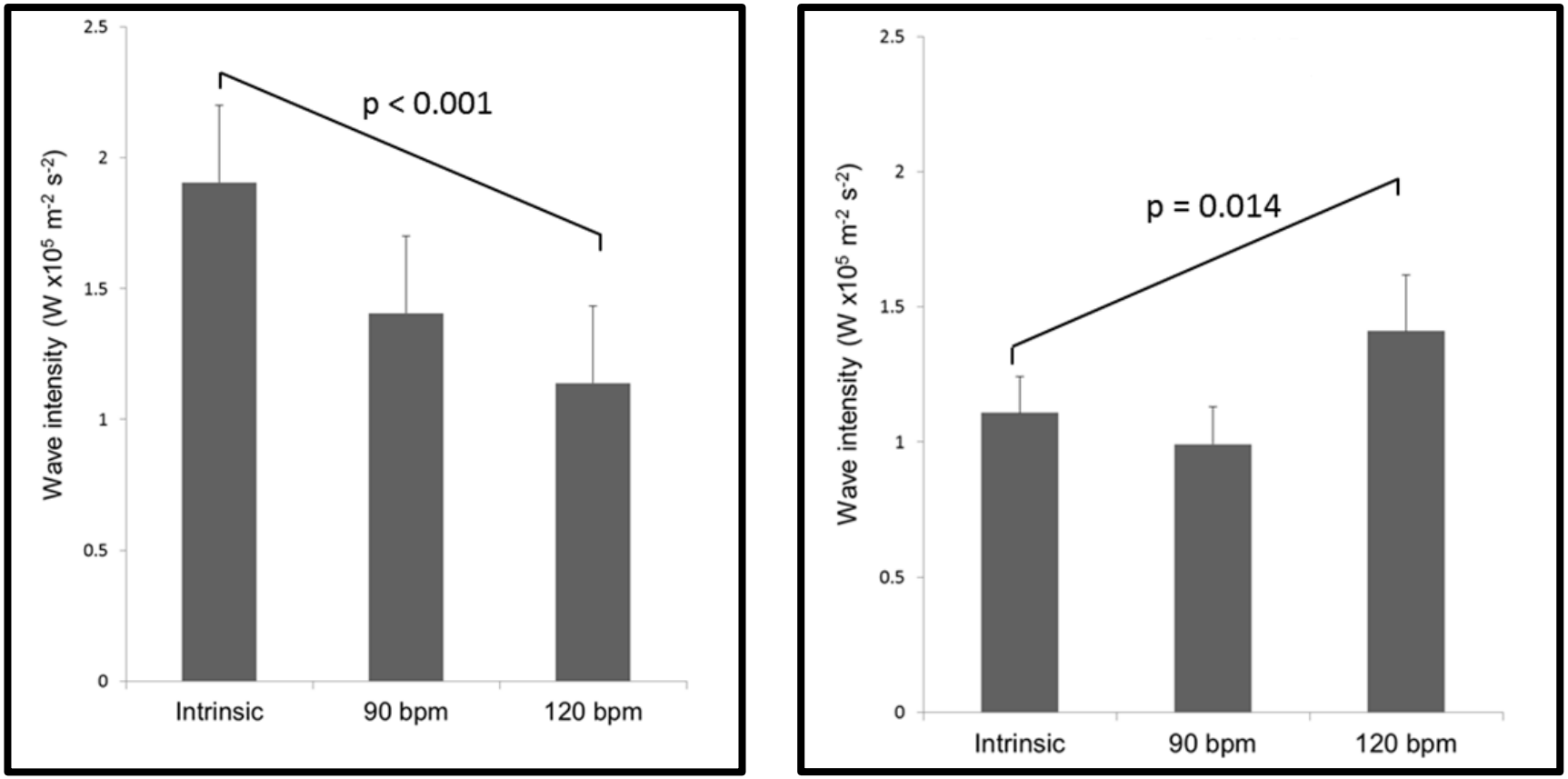

FIGURE 3-2. Improvement in physiological reserve in subjects with aortic stenosis after TAVI.

Physiological reserve was assessed by measuring the backward expansion wave at rest and then by pacing at 90 and 120 bpm. Before TAVI, the backward expansion wave decreased with increasing heart rate. After TAVI, the reverse was observed, and the backward expansion wave increased with increasing heart rate.

3.4 DISCUSSION

In aortic stenosis, the normal coronary physiological reserve is impaired. Instead of increasing when heart rate rises, the coronary diastolic suction wave decreases paradoxically. This phenomenon is reversed immediately after TAVI when this physiological reserve returns to a normal positive pattern.

3.4.1 ACCOUNTING FOR THE DETRIMENTAL HAEMODYNAMICS IN SEVERE AORTIC STENOSIS

Normal coronary perfusion is maintained by the balance (or coupling) between the pressure originating from the proximal (aortic) and distal (microcirculatory) ends of the coronary circulation. When the aortic valve is normal, these pressures are closely related during ejection because LV chamber pressure is a major determinant of both intra-myocardial stress and aortic pressure(Kassab et al., 2002). Any difference in the observed aortic and microcirculatory originating pressure waveforms observed early in systole is attributable to time delays in physiological processes for the period that the aortic valve remains shut (e.g., the isovolumic contraction phase at the onset of systole).

Because pressures at either end of the coronary artery are so closely matched during systole, net changes in coronary flow velocity during this period are normally minimal. In diastole, aortic valve closure decouples pressure in the aorta, and aortic pressure decays from end-systolic pressure in a quasi-exponential manner, whereas LV pressures and myocardial stress fall rapidly. As a result, the pressure gradient for coronary perfusion increases, resulting in an acceleration of coronary blood flow.

With increasing workload, this mechanism is exaggerated. The increased extremes of LV luminal pressure and intra-myocardial pressure create a larger coronary perfusion pressure gradient, resulting in increased coronary blood flow in early diastole.

The importance of ventricular pressure in the determination of coronary perfusion pressures by this coupled mechanism has previously been reported during pharmacological stress in dogs and, more recently, in humans by comparing the difference in coronary backward expansion wave subtended by either the LV or right ventricle(Sun et al., 2004).

3.4.2 TESTING PHYSIOLOGICAL RESERVE

Previous studies in animal models in the absence of aortic stenosis have demonstrated a marked increase in backward-originating waves with physiological stressors(Sun et al., 2000). In our human subjects, we expected to observe similar changes with pacing before TAVI at 90 and 120 bpm. Unexpectedly, rather than seeing an increase in backward expansion wave with physiological stress, we observed a marked fall, the opposite of what had been reported by Sun et al(Sun et al., 2000) when performing similar experiments in dogs in the absence of aortic stenosis.

We hypothesize that the fall in backward expansion wave with pacing was due to decoupling of the normal mechanisms essential for maintenance of normal coronary perfusion. To test this theory, we repeated identical pacing studies after TAVI. In these studies, we found that the microcirculatory originating suction wave no longer decreased but was found to increase by ≈50%, suggesting the restoration of mechanisms contributing to physiological reserve. This is likely to be a result of a

marked reduction in afterload (and consequent left shift on the Frank-Starling curve), a reduction in myocardial stress, and a recoupling of normal regulatory mechanisms for control of coronary perfusion (Figure 3-3).

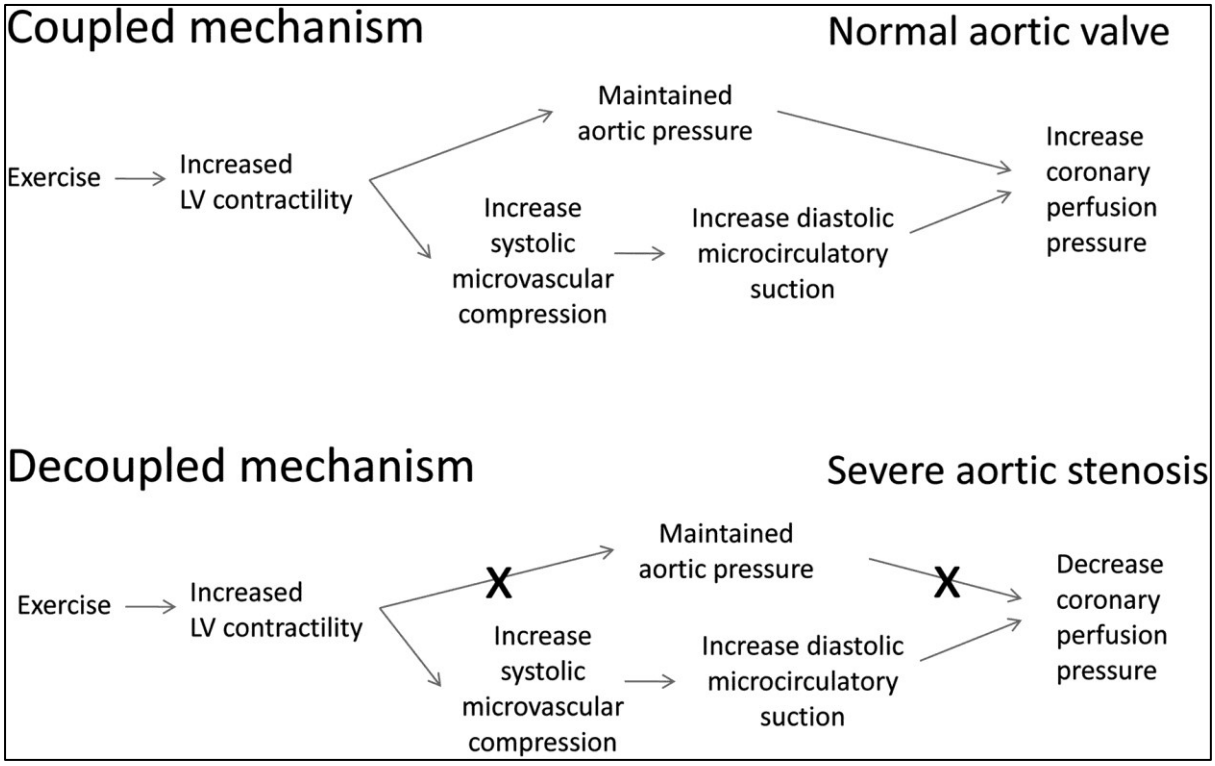

FIGURE 3-3. Decoupling of mechanisms of coronary perfusion in subjects with severe aortic stenosis.

In the coupled mechanism, rising left ventricular luminal pressure is transmitted across throughout the myocardium, compressing small perforating microcirculatory vessels. When the lv pressure exceeds the aortic pressure, the aortic valve opens, raising pressure at the proximal end of the coronary artery. During diastole, this process is reversed; left ventricular relaxation leads to closure of the aortic valve and decompression of the small microcirculatory vessels. This decompression generates a suction wave accelerating coronary blood flow, which is aided by maintenance of high perfusion pressures from the aorta, which falls more slowly. In the decoupled

mechanism in aortic stenosis, the delicate balance between lv pressure and aortic pressure is lost, and pressures originating at the microcirculatory end far exceed those from the aortic end.

3.4.3 Explaining Mechanisms of Angina

The decoupling of normal regulatory mechanisms of coronary blood flow in aortic stenosis that we observed may help explain why aortic stenosis patients with unobstructed arteries develop symptoms of angina. In such subjects, even the most modest increases in workload are unlikely to be met by an appropriate increase in coronary perfusion pressure, making them vulnerable to ischemia. This can be observed by considering the change in VTI before and after TAVI. The VTI, a measure of the quantity of blood being delivered to the myocardium over the course of the cardiac cycle, decreases with increasing heart rate before TAVI but remains unchanged after TAVI. We hypothesize that this reduction in VTI with increased heart rate before TAVI is due to an attenuation of coronary physiological reserve such that coronary blood flow velocity cannot be sufficiently increased to compensate for the increased heart rate (and most important, the reduction in length of the diastolic perfusion phase). This is most striking in the VTI.min product, in which a marked reduction can be seen between resting and increased heart rates. These findings are similar to the reduction in coronary vasodilator reserve observed by Rajappan et al(Rajappan et al., 2002) during pharmacological non-invasive PET assessment, although phasic changes in coronary blood flow were not measured. After TAVI, the physiological reserve is improved so that an increase in heart rate is accompanied by a relative increase in VTI (despite the shortening of the diastolic perfusion phase).

We know that in humans coronary flow reserve is reduced in aortic stenosis. Although this factor must in some way contribute to the potential for ischemia to develop, it is not clear that differences in the flow reserve account for angina symptoms(Gould and Carabello, 2003). Assessment of differential changes in waves occurring at different phases in the cardiac cycle in relation to symptoms may provide a better understanding of the relationship of coronary flow anginal symptoms. Although further studies are clearly required, it is interesting that a previous study reported that people with aortic stenosis and exertional symptoms showed smaller increases in coronary flow velocity in response to atrial pacing and dobutamine than those free of anginal symptoms(Petropoulakis et al., 1995).

3.4.4 Acute Reduction in Microcirculatory Suction Wave After Percutaneous Aortic Valve Replacement

After TAVI, the backward expansion wave was found to decrease at an intrinsic rate and the forward compression wave to increase. This decrease in the backward expansion wave is compatible, and indeed predictable, by the intra-myocardial muscle-pump model first described by Spaan et al(Spaan et al., 1981). In the intra-myocardial muscle-pump model, forward coronary blood flow is explained by the expansion in volume of the microcirculation (generating the suction wave) after release of compression during systole. Compression and recoil are interrelated in that larger compression leads to larger recoil. Under circumstances of high LV pressure and intramural stress, as observed in severe aortic stenosis, intramural vessels are highly compressed in systole, and recoil is commensurately increased to generate a large suction wave in early diastole.

3.5 STUDY LIMITATIONS

Each subject undergoing TAVI was sedated and ventilated during the entire course of the procedure. Because TAVI procedures last >90 minutes and can cause considerable variations in haemodynamics, it is routine for the anaesthetist to administer intravenous fluids and, in extreme circumstances, vasoactive drugs to maintain a stable blood pressure and to offset any fluid losses that occur during the procedure. This could affect hemodynamic measurements; however, any change would be small compared with the marked reduction in ventricular afterload after TAVI (pre-TAVI mean pressure gradient, 80±34 mm Hg). No significant difference in administration of vasoactive drugs was found between the 2 measurement phases. In addition, no change in pharmacological therapies was made during assessment of coronary physiological reserve, which took place over a period lasting only 3 minutes in each subject.

Because of the nature of the typical population selected for TAVI, we studied mainly symptomatic elderly women with severe aortic stenosis. Caution is therefore warranted in extrapolating these observations to other groups, such as men or younger patients undergoing conventional valve surgery, particularly because the latter group may have lesser degrees of myocardial fibrosis and lower levels of ventricular wall stress. Nevertheless, we believe that TAVI provides a more appropriate model to assess the immediate effects of relief of aortic stenosis on coronary physiology because it is less complicated by the effects associated with traditional open-chest valve surgery.

A high proportion of our subjects were labelled hypertensive on the basis of office measurements over the preceding years and had begun appropriate antihypertensive therapy. Consequently, high blood pressure contributed to additional afterload. However, high blood pressure is common in aortic stenosis, and given the prevalence of

hypertension in individuals >55 years of age, hypertension could be regarded as the norm rather than the exception. It is reasonable to assume that given the good blood pressure control achieved (systolic, 123±9 mm Hg; diastolic, 56±12 mm Hg), the vast majority of LV hypertrophy was due to the aortic stenosis as opposed to increased afterload from high blood pressure.

Blood pressure was found to be lower after TAVI. Although this finding seems surprising in view of the reduced ventricular load and could indicate an adverse effect of TAVI, a similar blood pressure response has been reported after open-chest aortic valve replacement(Bonow et al., 1988, Morita et al., 2003, Estafanous et al., 1978) which is thought to be due to modulation of baroreflexes rather than modulation of ventricular afterload per se.

We chose to use pacing rather than a pharmacological agent to increase heart rate. Although drug therapies may have more profound vasodilatory effects, these effects are not limited to the coronary circulation but have differential effects at different vascular beds and can cause large drops in blood pressure in patients with critical aortic stenosis. On the other hand, pacing is highly reproducible, is safe in patients with critical aortic stenosis, is an intrinsic part of the TAVI procedure, and is rapidly reversible on termination.

3.6 CONCLUSIONS

Severe aortic stenosis is detrimental to coronary haemodynamics. These effects are due to severe LV pressure loading and excessive ventricular wall stress. In subjects with severe aortic stenosis, coronary physiological reserve is severely impaired but improves immediately after TAVI. Quantifying these severe limitations in coronary physiological reserve may explain the angina symptoms and provide a tool for functional assessment of significance of aortic stenosis and the timing of valvular surgery.

4 RESTING NON-INVASIVE CORONARY WAVE INTENSITY IN SEVERE AORTIC STENOSIS, AFTER AORTIC VALVE INTERVENTION AND WITH THE REGRESSION OF LEFT VENTRICULAR HYPERTROPHY

4.1 INTRODUCTION

4.1.1 LEFT VENTRICULAR HYPERTROPHY

Previous large scale retrospective and prospective studies have demonstrated the unfavourable independent effect of left ventricular hypertrophy on prognosis. The Framington study showed that left ventricular mass measured by echocardiography was associated with cardiovascular events, cardiovascular deaths and death from all-cause independent of other cardiovascular risk factors(Levy et al., 1990, Haider et al., 1998, Levy et al., 1989). For every increment of 50g/meter height in LV mass the relative risk of cardiovascular disease was increased approximately 1.5-fold. Similarly, in 280 patients prospectively followed over 10 years, an echocardiographically-determined left ventricular mass of greater than 125g/m^2 was associated with an increased risk of cardiovascular death, events and all-cause mortality and this risk was stronger than that from blood pressure(Koren et al., 1991).

In the MAVI study, again echocardiographically-determined LV mass was a strong, continuous and independent predictor of cardiovascular morbidity in 1033 patients followed over 4 years(Verdecchia et al., 2001a). The same group demonstrated an independent link between LVH diagnosed through ECG or echocardiography and stroke or TIA in 2363 patients (Verdecchia et al., 2001b). The presence of left ventricular hypertrophy may also lead to the development of heart failure independent of other potential confounders(Drazner et al., 2004, Gardin et al., 2001). In patients who suffer an acute myocardial infarction, the presence of LVH conveys a poorer prognosis compared to those with normal LV geometry(Carluccio et al., 2000) and is an important contributor to the risk of sudden cardiac death in patients with coronary artery disease(Burke et al., 1996).

4.1.2 Left Ventricular Hypertrophy and Remodelling in Aortic Stenosis

Whilst left ventricular hypertrophy is a progressive adaption to pressure overload in severe aortic stenosis, the degree of hypertrophy appears variable(Dweck et al., 2012a) but its presence predicts the development of heart failure(Kupari et al., 2005). In a slightly converse but interesting animal experiments, chemical (Hill et al., 2000) or genetic(Esposito et al., 2002) abolition of a hypertrophic response in the face of pressure overload did not result in cardiac failure, at least in the short-term. Therefore it would appear that cardiac hypertrophy may not be necessary to maintain cardiac output in all patients and if it does appear, it carries a detrimental prognosis.

The presence of and degree of myocardial fibrosis in severe aortic stenosis as assessed by biopsy at the time of surgery is inversely correlated with the degree of left ventricular improvement after surgery(Azevedo et al., 2010) as well as functional status increase and mortality(Weidemann et al., 2009). Additionally, a good correlation is seen between the degree of myocardial fibrosis and left ventricular mass as assessed by MRI(Debl et al., 2006, Rudolph et al., 2009). Furthermore, the degree of hypertrophy seems to predict outcome following aortic valve replacement(Mehta et al., 2001, Orsinell et al., 1993) although it doesn't seem to influence outcome in the mid-term (28±9 months)(Gaudino et al., 2005).

Whilst the mortality benefit of an aortic valve replacement is relatively instantaneous in severe aortic stenosis there is some evidence that the risk of sudden death persists post-operatively albeit at a lower rate(McGiffin et al., 1993) implying that the negative effect of the residual left ventricular hypertrophy is not insubstantial and behaves similarly to non-valvular-driven LVH.

Following AVR, left ventricular hypertrophy regression occurs over a fairly long time course although the majority of the response occurs in the first year. Early work with echocardiography demonstrated a reduction in muscle mass by 20% over the first 6 months(Hildick-Smith and Shapiro, 2000) after aortic valve replacement, 31% over the first year(Waszyrowski et al., 1996) with a further 13% reduction 7 years later(Monrad et al., 1988). Similarly, using cine-angiography and endometrial biopsies the greatest reduction in muscle mass was seen in the first year but with further reductions over the following 5 years(Krayenbuehl et al., 1989). Using MRI, again there is a relative exponential decrease in LV mass following aortic valve replacement with a 15% reduction at 6 months(Biederman et al., 2011), a 30% reduction in LV mass at 1 year (Steadman et al., 2012, Rajappan et al., 2003) and further, albeit lesser reduction at four years(Biederman et al., 2011).

Transcatheter valve implantation also results in a similar pattern of left ventricular remodelling with an 18% reduction in LV mass as assessed by MRI at 6 months following TAVI(La Manna et al., 2013, Fairbairn et al., 2013). Additionally, in surgical patients with a patient-prosthesis mismatch at 10 years there is a reduction in the degree of LVH regression compared to patient's with well-matched prostheses(Kato et al., 2007).

The importance of left ventricular remodelling is thought to be favourable, at least in those non-aortic stenotic patients with hypertrophied ventricles as shown in several retrospective and epidemiological studies such as by ECG in the Framington (Levy et al., 1994) and HOPE cohort (Mathew et al., 2001), or by echocardiography in a prospective cohort of 304 patients(Yurenev et al., 1992) or the LIFE cohort(Devereux et al., 2004). However, this has not been supported in all studies(MacMahon et al., 1989, 1985). The

risk of atrial fibrillation is also reduced in patients who have a reduction in the left ventricular mass, independent of blood pressure lowering reduction or treatment modality(Okin et al., 2006). In vivo and vitro studies of rabbits treated with ACE-inhibition demonstrated the normalization of the electrophysiological abnormalities of ventricular hypertrophy with pharmacological regression of LVH(Rials et al., 1997).

4.1.3 Coronary Haemodynamics after Aortic Valve Replacement

Using a combination of echocardiography, MRI and PET scanning it has been possible to show an improvement in coronary microcirculatory function in conjunction with a regression in myocardial muscle mass following aortic valve replacement in 22 patients undergoing AVR (Rajappan et al., 2003). This study is in slight conflict with earlier work which demonstrated a failure of resting or hyperaemic myocardial blood flow to improve following aortic valve replacement as well as no correlation between myocardial blood flow reserve and myocardial hypertrophy or aortic valve gradient(Carpeggiani et al., 2008a). This latter study however performed its follow-up study 12 months after aortic valve replacement after a significant amount of LV regression had occurred and this may have impacted on the results.

Invasive coronary Doppler measurements of LAD flow velocity has been performed by another group pre-AVR and then repeated 1-1.5 years afterwards. There was a reduction in baseline diastolic mean velocity from 62 to 40cm/s but with an increase in CFR from 1.96 to 2.37. However, again, this study was not performed immediately after AVR and therefore there was some effect from left ventricular hypertrophy regression with a reduction in muscle mass from 354 to 223g(Nemes et al., 2002).

Similarly, non-invasive studies of CFR by transthoracic echocardiography showed an improvement in coronary flow reserve 6 months after aortic valve replacement (peak hyperaemic velocity 0.71 vs. 1.08cm/s) without a change in peak velocity of the distal LAD. Again, this study was performed at 6 months post AVR after a significant amount of left ventricular remodelling had occurred(Hildick-Smith and Shapiro, 2000). Interestingly this contradicts work using transoesophageal echo-generated coronary flow rates where resting mean systolic and diastolic flow was found to increase post-TAVI(Ben Dor et al., 2009). Obviously, the effect of anaesthesia and possibly inotropic support in this latter study plays a role which may account for some of this discrepancy.

Other work by Kenny *et al.* has shown difference in the coronary flow profile of patients – that of reversal of early systolic flow, a feature which returns to normal 1 week after replacement of the aortic valve(Kenny et al., 1994). This study also found a significant difference in the time taken from the onset of diastolic coronary acceleration to peak diastolic flow in severe aortic stenosis. However, no comment was made about the systolic function in these patients and poorer function may also have contributed to this latter finding.

Using intra-coronary assessments of blood flow, the beneficial effect of valvuloplasty has also been demonstrated on isoproterenol-induced hyperaemia with an additional reduction in myocardial lactate production noted in humans with severe aortic stenosis (Smucker et al., 1988).

4.1.4 Left Ventricular Hypertrophy Regression and Coronary Flow

Previous animal work has examined the relationship between coronary flow and left ventricular hypertrophy. In studies of renal-clipped rats, LV hypertrophy was associated with a tendency towards a reduced coronary flow reserve with a reversal after treatment of their hypertension(Wicker et al., 1983). Similar results have been found by a second group using aortic-banding and release to drive and reverse hypertrophy where flow reserve decreased with hypertrophy and normalised with its regression in rats(Sato et al., 1990) and guinea pigs(Kingsbury et al., 2002). Likewise, in spontaneously hypertensive rats coronary flow reserve generated by dipyridamole improved with losartan(Nunez et al., 1997) and lisinopril(Brilla et al., 1991a) induced LVH regression.

In dogs with aortic banding-induced LVH and aortoplasty-induced regression, coronary flow was measured with both adenosine and atrial-pacing as stressors. No significant difference was seen in the resting blood flow between controls, dogs with LVH and dogs with regressed LVH with an abnormal response to adenosine seen only in dogs with existing LVH. However, with atrial pacing, abnormalities persisted in coronary flow following aortoplasty which may reflect incomplete regression(Ishihara et al., 1992).

Taking this further, Ito *et al.* examined both short- and long-term aortic-banded rats exploring both their cardiac morphology as well as coronary reserve. In short-term banded animals, cardiac hypertrophy, medial hypertrophy and vascular fibrosis completely regressed and this was accompanied by a normalisation of coronary flow reserve. After long-term banding, medial hypertrophy regressed but the vascular fibrosis failed to improve and this was accompanied by a failure of coronary flow reserve to normalise. Therefore, it may be the fibrotic changes rather than the medial

hypertrophy that affect coronary flow reserve in hypertrophied hearts(Ito et al., 1993). Interesting in pre-operative severe aortic stenotic patients investigated by PET scanning there is a proportional relationship between total left ventricular myocardial blood flow and left ventricular mass; however, this relationship is lost during hyperaemia implying that the degree of coronary microcirculatory dysfunction is independent of the degree of myocyte hypertrophy(Rajappan et al., 2002), a phenomenon that has also been recognised in hypertrophic cardiomyopathy patients(Camici et al., 1991). It may be therefore that there are different morphological responses to aortic stenosis at a cellular level, perhaps related to the length of time for which the obstruction is present, which may determine the degree of myocardial dysfunction and recovery after intervention.

There has been some work in this field performed in humans. In 96 hypertensive patients, CFR measured non-invasively by transthoracic echocardiography improved with 6-months of treatment with losartan or ramipril in conjunction with an improvement in left ventricular mass(Xu et al., 2003) although an improvement in CFR is also seen following treatment with irbesartan independent of LV hypertrophy(Lethen et al., 2003a). A study of 122 patients with hypertension demonstrated the importance of optimal blood pressure control with patients not achieving adequate blood pressure control failing to achieve an improvement in CFR or LV mass reduction(Mizuno et al., 2012). In 15 hypertensive patients treated with enalapril, an 8% reduction in LV mass was associated with a 43% increase in coronary flow reserve(Motz and Strauer, 1996). It is possible that the pharmacological agents directly affect coronary haemodynamics and previous work has demonstrated candesartan to effect coronary flow reserve independent of LV mass regression(Tomas et al., 2006). However, comparisons

between verapamil and enalapril using PET scanning have demonstrated a direct effect of verapamil on CFR whereas enalapril had no effect(Parodi et al., 1997).

Work with PET scanning has not shown similar results. In 22 patients measured with PET pre-AVR and 1 year post-AVR an improvement in myocardial perfusion was demonstrated with a correlation between left ventricular mass regression and resting but not hyperaemic myocardial blood flow. Reduced extravascular compression and increased diastolic perfusion time were felt to be more important contributors to this favourable change and again suggest a degree of heterogeneity in the way myocardial hypertrophy impacts on coronary haemodynamics particularly in the hyperaemic state(Rajappan et al., 2003). A second smaller PET study demonstrated myocardial blood flow reserve to be depressed independently of myocardial hypertrophy and trans-valvular pressure gradient without any improvement at 12 months post-AVR - again this may reflect this heterogeneity, particularly as only 8 patients were included in the 12-month follow up (Carpeggiani et al., 2008a).

4.1.5 Left Ventricular Hypertrophy and Wave Intensity Analysis

Wave intensity analysis has been applied to patients with left ventricular hypertrophy in several situations. Firstly, in patients with normal valves and hypertension-driven LVH, and secondly in those with LVH and severe aortic stenosis.

4.1.5.1 Left Ventricular Hypertrophy with Normal Aortic Valves

Previous work by Davies *et al*. validating the principles of wave-intensity analysis in humans with normal coronary arteries has demonstrated the adverse effect of left ventricular hypertrophy on the backward expansion wave(Davies et al., 2006a). Whilst

the other 5 waves of the cardiac cycle were unconnected with the ventricular septal wall thickness, the backward expansion wave decreased with increasing thickness (r= -0.52, p<0.02). There was also a disruption in the ratio of the forward-travelling pushing wave to the backward-travelling expansion wave with a poorer transfer of energy between the two with LVH. This poor energy transfer may explain why patients with left ventricular hypertrophy have an impaired coronary flow reserve(Hamasaki et al., 2000) and in turn higher mortality(Levy et al., 1990, Schillaci et al., 2000).

4.1.5.2 Left Ventricular Hypertrophy in Aortic Stenosis

As described in detail in chapter 1, patients with aortic stenosis develop left ventricular hypertrophy in response to the gradient against which it pumps. However, in contrast to patients with hypertension-driven LVH the backward expansion wave is higher than normal individuals due to the increased force of diastolic myocardial-relaxation.

4.1.6 Hypothesized Changes in Wave-Intensity after Aortic Valve Intervention

After aortic valve intervention with regression of left ventricular hypertrophy further changes in the backward expansion wave may occur. Regression of LVH may improve energy transfer efficiency returning to a near-normal value (Figure 4-1). Therefore, to investigate this further, I set out to follow up a group of patients after aortic valve intervention using non-invasive measures of coronary wave-intensity.

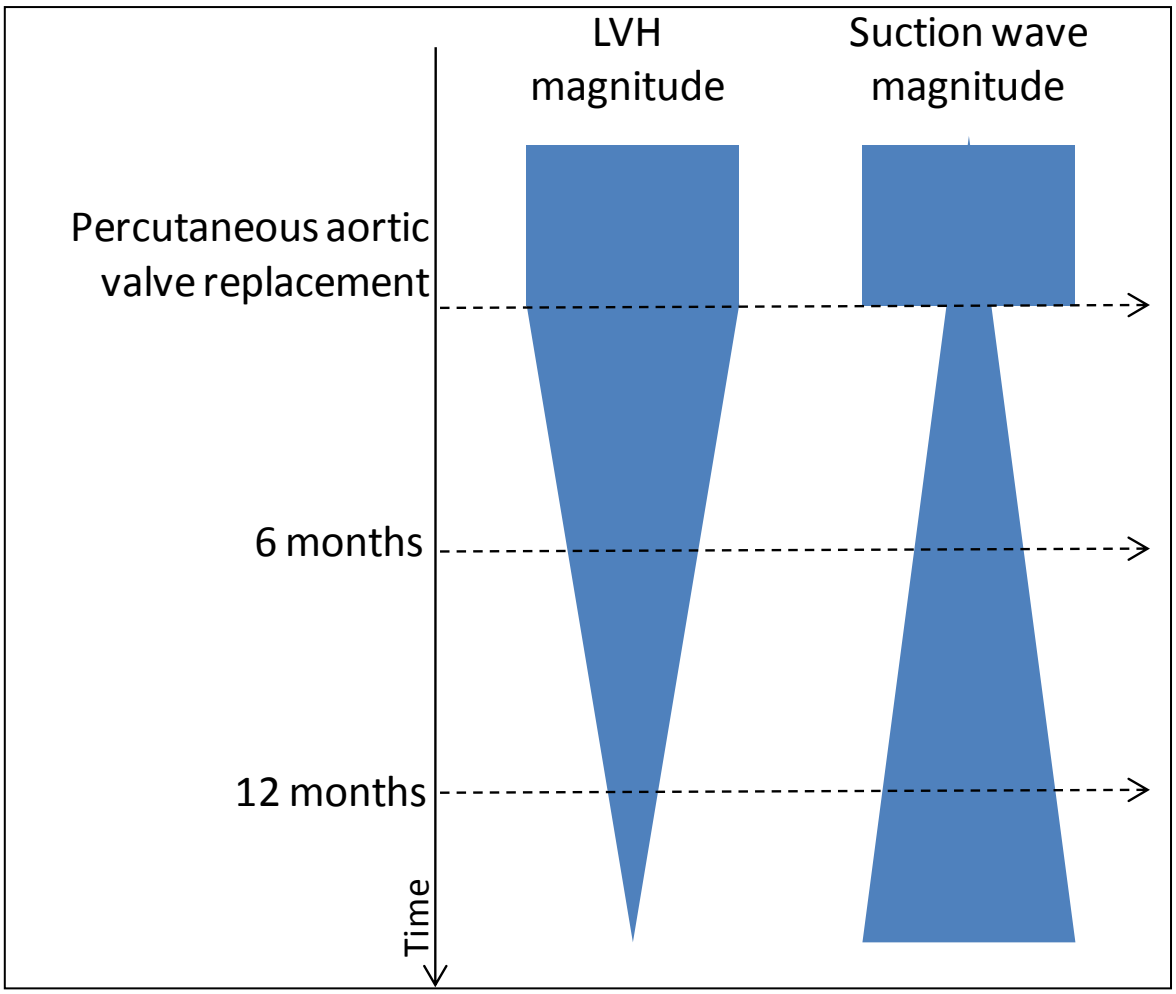

FIGURE 4-1. Anticipated changes in the backward expansion wave and left ventricular hypertrophy with time following aortic valve replacement.

As the left ventricle favourably remodels following valve replacement there is an increase in the backward expansion wave reflecting a more favourable energy transfer.

4.2 METHODS

Patients scheduled to undergo either aortic valve replacement or a transcatheter aortic valve implantation were recruited over a period of 18 months. Consent was obtained and local ethics approval was granted.

4.2.1 WAVE INTENSITY

Patients underwent non-invasive coronary wave-intensity analysis as described above. Briefly, patients were scanned in the left lateral position with a Pulsecor pressure cuff on the right arm. The left anterior descending artery was imaged from a modified parasternal long axis view and pulse-wave Doppler was applied. Simultaneously, 2 or more Pulsecor readings were sampled; readings were discarded if the fidelity was deemed less than 'good' according to the automated software. Data was processed an analysed offline.

For follow up purposes, TAVI patients in whom data was obtained invasively were also eligible for non-invasive follow-up at 6- and 12-months. The invasive data was gathered as described in chapter 3.2.1(Davies et al., 2011).

4.2.2 PROTOCOL

Initial non-invasive data was collected in the 24 hours prior to valve intervention. Patients then underwent transcatheter or surgical valve implantation according to clinical appropriateness. Non-invasive data was recollected on the day prior to discharge and then repeated at 6 months and one year in a subgroup of patients. LV mass was calculated according to the formula:

$$\text{LV MASS} = 0.8 * (1.04 * (\text{LVEDD} + \text{PWDD} + \text{IVSD})^3 - \text{LVEDD}^3) + 0.6$$

EQUATION 4-1. LV MASS CALCULATED FROM ECHOCARDIOGRAPHY

Aortic valve area, peak velocity and mean velocity was assessed using continuous and pulse wave assessment of the aortic valve and outflow tract and LVOT cross sectional measurements.

4.2.3 EXCLUSION CRITERIA

Patients were excluded if they had reduced left ventricular systolic function, more than mild co-existing valve disease and angiographically demonstrable coronary disease. For the follow-up, patients were further excluded if they developed a significant change in left ventricular function or the presence of more than mild paravalvular aortic regurgitation. Patients were also excluded if they had unfavourable echocardiographic windows at the initial assessment.

4.3 RESULTS

4.3.1 PRE-OPERATIVE INFORMATION

In total, 29 patients (14 male, mean age 76±8.9) were interrogated before and after aortic valve replacement / implantation. TAVI was performed in 7 patients and conventional aortic valve replacement in 22 patients. Baseline information is presented in Table 4-1. Haemodynamic information was obtained non-invasively in all aortic valve replacement patients and 4 TAVI patients. The remaining 3 TAVI patients had their peri-operative haemodynamics obtained invasively as previously described in section 3.2.1.

22 of these patients were followed up at 6 and 12 months with further non-invasive assessments. One patient was excluded during the follow up due to the presence of a moderate paravalvular leak. Of the remaining 21 patients, 20 (95%) had adequate data achievable at 6 months and 17 (81%) patients at 12 months.

Male (%)		14 (48)
Age		74.9 ± 9.6
Body surface area		1.86 ± 0.22
Medication		
	Calcium channel antagonist (%)	11 (38)
	Beta blocker (%)	12 (41)
	ACE-inhibitor (%)	7 (24)
	Angiotensin receptor blocker (%)	5 (17)
	Statin (%)	18 (62)
	Aspirin (%)	15 (51)
	Loop diuretic (%)	7 (24)
	Bendroflumethiazide (%)	3 (10)
Symptoms		
	Angina (%)	5 (17)
	Syncope (%)	2 (7)
	Dyspnoea (%)	21 (72)
Diabetic (%)		5 (17)

TABLE 4-1. Baseline pre-operative demographics of the 29 patients undergoing aortic valve intervention

4.3.2 PROCEDURAL DATA

Procedural data is presented in Table 4-2. 21 patients underwent surgery; of these 19 (90%) had a conventional tissue valve implanted, 1 (5%) a metallic valve and 1 (5%) a sutureless Percival valve. Eight patients underwent transcatheter valve implantation of which 5 (63%) patients received an Edwards valve and 3 (33%) a CoreValve. The approach was transapical in 5 (66%), subclavian in 1 (11%) and transfemoral in 2 (22%).

	Valve Type	**Approach**	**No**
TAVI	Edwards	Transapical	5
	CoreValve	Transfemoral	1
		Subclavian	2
Surgical	Tissue	Sternotomy	19
	Sutureless	Sternotomy	1
	Metallic	Sternotomy	1

TABLE 4-2. Procedural data for the 29 patients undergoing aortic valve intervention.

28% were transcatheter valves and 72% were implanted in a surgical fashion. The majority of valves were tissue (28/29). One valve was implanted with a 'sutureless' approach with conventional cardiopulmonary bypass.

4.3.3 ECHOCARDIOGRAPHIC MEASURES OF REMODELLING

Baseline, post-procedure and follow up data is presented in Table 4-3. There was a large decrease in LV mass from baseline (224g) to 6 months (153g, p<0.01) but with little further significant decrease in mass from 6 to 12 months (150g, p=0.7). Positive remodelling effects were also seen in left ventricular end diastolic dimensions which approached then reached significance at 6 (p=0.07) and 12 (p=0.04) months. Likewise, there was a decrease in systolic and posterior wall dimensions.

	Pre	6 months	p value	12 months	p value
LVEDD	4.5 ± 0.7	4.2 ± 0.6	0.07	4.0 ± 0.7	0.04
PWd	1.2 ± 0.2	1.0 ± 0.18	0.007	1.1 ± 0.2	0.005
IVSd	1.3 ± 0.2	1.1 ± 0.27	0.09	1.1 ± 0.2	0.005
LV mass	225 ± 58	156 ± 30	<0.001	139 ± 59	<0.001
LVEDS	2.9 ± 0.6	2.8 ± 0.6	0.99	2.9 ± 0.5	0.82
peak aortic velocity	4.5 ± 0.6	2.5 ± 0.4	<0.001	2.2 ± 0.6	<0.001

TABLE 4-3. Echocardiographic parameters pre and post aortic valve intervention and a 6 and 12 months.

LVEDD – left ventricular end dimension at end diastole. PWd – posterior wall thickness at end diastole. IVSd – intra-ventricular wall thickness at end diastole. LVEDS – left ventricular end dimension at end systole. P values are comparison against pre-procedure values.

4.3.4 Effect of aortic valve intervention on non-invasive coronary haemodynamic parameters

Non-invasive flow and pressure data is presented in Table 4-4. There was no significant change in coronary pressure pre- and post-procedure (systolic pre 15320, post 15185Pa (p=0.75); diastolic pre 8617 to 8695Pa (p=0.81)). There was a reduction in coronary flow peak (0.41m/s to 0.33m/s, p=0.0008) and mean (0.25m/s to 0.21m/s, p=0.006) velocity pre- and post-procedure but not minimum velocity (0.13m/s to 0.12m/s, p=0.03). Accompanying this was a dramatic reduction in the peak (-22.1 x 10^4 to -10.9 x 10^4 $Wm^{-2}s^{-2}$, $p < 0.0001$) and cumulative (-11.3 x 10^6 to 6.34 x 10^6 $Wm^{-2}s^{-1}$, $p<0.0001$) backward expansion wave intensity.

Data was also separated according to treatment strategy. There was no significant variation in the pre- or post-procedure measurements between the AVR and TAVI groups (Table 4-5).

	pre	post	p value
Peak velocity (m/s)	0.41±0.12	0.33±0.08	0.0008
Mean velocity (m/s)	0.25±0.06	0.21±0.06	0.04
Min velocity (m/s)	0.13±0.04	0.12±0.03	0.38
Systolic BP (Pa)	15204±2227	14931±1896	0.50
Mean BP (Pa)	10705±1551	10605±1456	0.76
Diastolic BP (Pa)	8772±1508	8767±1437	0.99
Peak backward expansion wave ($Wm^{-2}s^{-2} \times 10^4$)	-22.1 ± 8.03	-10.9 ± 6.78	<0.0001
Cumulative backward expansion wave ($Wm^{-2}s^{-1} \times 10^6$)	-11.3 ± 4.7	-6.34 ± 3.74	<0.0001

TABLE 4-4. Coronary flow and pressure pre- and post-aortic valve intervention.

There is a fall in velocity measures following aortic valve replacement or intervention. However, systolic, diastolic and mean pressure measures are unchanged. Peak and cumulative backward expansion wave values fall post procedure.

Peak Backward Expansion Wave					
	No of patients	Pre	p	Post	p
AVR	22	-22×10^{-4}	0.23	-11×10^{-4}	0.73
TAVI	7	-18×10^{-4}		-9.7×10^{-4}	
Cumulative Backward Expansion Wave					
	No of patients	Pre	p	Post	p
AVR	22	-1.0×10^{-7}	0.051	-6.1×10^{-6}	0.26453
TAVI	7	-1.1×10^{-7}		-6.2×10^{-6}	

TABLE 4-5. Backward expansion wave changes according to treatment modality.

There is no significant difference in the magnitude of the backward expansion wave or their changes pre- and post-procedure between conventional aortic valve replacement or transcatheter valve therapy.

4.3.5 SEPARATING OUT THE EFFECT OF LVH AND OUTFLOW TRACT OBSTRUCTION

In order to separate out the two components acting on backward expansion wave intensity, namely that of left ventricular hypertrophy and outflow tract obstruction, the post-procedure wave intensity value was subtracted from the pre-procedure value. Assuming that the post-procedure value is a measure of the impact of left ventricular hypertrophy on wave-intensity with a negligible effect from the aortic valve, this subtraction value should represent the isolated effect exerted by the aortic valve obstruction on wave intensity and should correlate more closely with aortic valve stenotic measures. The mean difference between pre- and post-cumulative backward expansion wave was $-4.7 \times 10^6 \pm 4.3 \times 10^6$ $Wm^{-2}s^{-1}$ compared with $-11 \times 10^6 \pm 5.5 \times 10^6$ $Wm^{-2}s^{-1}$ pre-procedurally; mean peak aortic velocity was $4.51 ms^{-1}$. By controlling for this post-procedure value the correlation between wave intensity and aortic stenosis improved from an r value of -0.29 using pre-procedure only ($p=0.14$) to -0.41 ($p=0.04$) using pre-procedure but accounting for the impact of left ventricular hypertrophy (Figure 4-2).

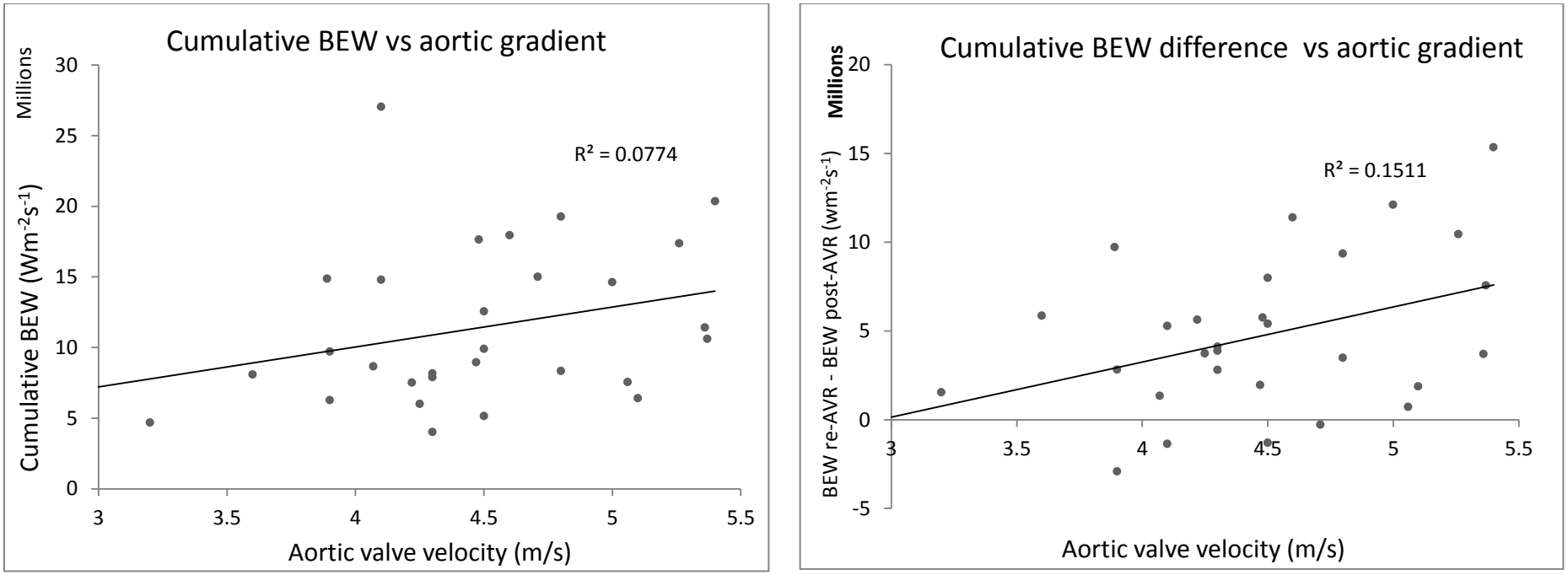

FIGURE 4-2. Improvement in correlation between aortic valve gradient and non-invasively calculated cumulative backward expansion wave when LVH is controlled

By subtracting the post-procedure backward expansion wave value (i.e. the value related to the degree of left ventricular hypertrophy only) the correlation improves between aortic valve gradient and wave intensity. This shows the negative but variable effect of left ventricular hypertrophy is evident even in severe aortic stenosis.

4.3.6 CORONARY HAEMODYNAMICS WITH LEFT VENTRICULAR HYPERTROPHY REGRESSION

Coronary haemodynamics are presented in Table 4-6. Immediately after aortic valve replacement there was a decrease in coronary flow rates but with no change in pressure parameters. Peak coronary flow fell from 43±14 cm/s to 33±9 cm/s ($p<0.01$) whereas systolic BP did not change significantly (15485 ± 2567 Pascals pre, 15115 ± 2988 Pascals post, $p=0.75$). At 6 months there was no change in coronary flow rate (35±10 cm/s, $p=0.58$) but with an increase in pressure (systolic post 15115 ± 2988 Pascals, 6 months 16545 ± 2286 Pascals, $p=0.02$). At 12 months, pressure measures were unchanged but there was a further slight decrease in coronary flow rate (peak velocity fell from 35 ± 10 to 29 ± 10 cm/s, $p=0.01$).

With regression of left ventricular hypertrophy there was an increase in the peak backward expansion wave. Immediately post-procedure the peak BEW was -107631 ± 65493 $Wm^{-2}s^{-2}$ and this increased to -215938 ± 126233 $Wm^{-2}s^{-2}$ at 6 months post-procedure ($p=0.003$) and in fact had returned to values similar to that pre-operatively ($p=0.91$). At 12 months, the value remained elevated at -155141 ± 87116 $Wm^{-2}s^{-2}$ ($p = 0.05$) (Figure 4-3).

	pre	post	p	6 months	p	12 months	p: 6 vs 12 months	p: post vs 12 months
peak velocity	43 ± 14	33 ± 9	<0.01	35 ± 10	0.58	29 ± 10	0.01	0.03
mean velocity	25 ± 6	21 ± 4	0.01	22 ± 6	0.32	19 ± 6	0.01	0.01
min velocity	13 ± 3	12 ± 3	0.68	13 ± 4	0.72	11 ± 4	0.01	0.09
systolic BP (Pa)	15485 ± 2567	15115 ± 2988	0.75	16545 ± 2286	0.02	17255 ± 2142	0.49	0.11
mean BP (Pa)	10809 ± 1807	10574 ± 2110	0.91	11559 ± 1761	0.07	12130 ± 1704	0.19	0.05
diastolic BP (Pa)	8663 ± 1739	8559 ± 1844	0.81	9352 ± 1511	0.05	9955 ± 1495	0.17	0.03
heart rate	70 ± 10	75 ± 10	0.01	69 ± 12	0.03	66 ± 12	0.39	0.005

TABLE 4-6. Coronary haemodynamics before and after aortic valve intervention and with regression of left ventricular hypertrophy.

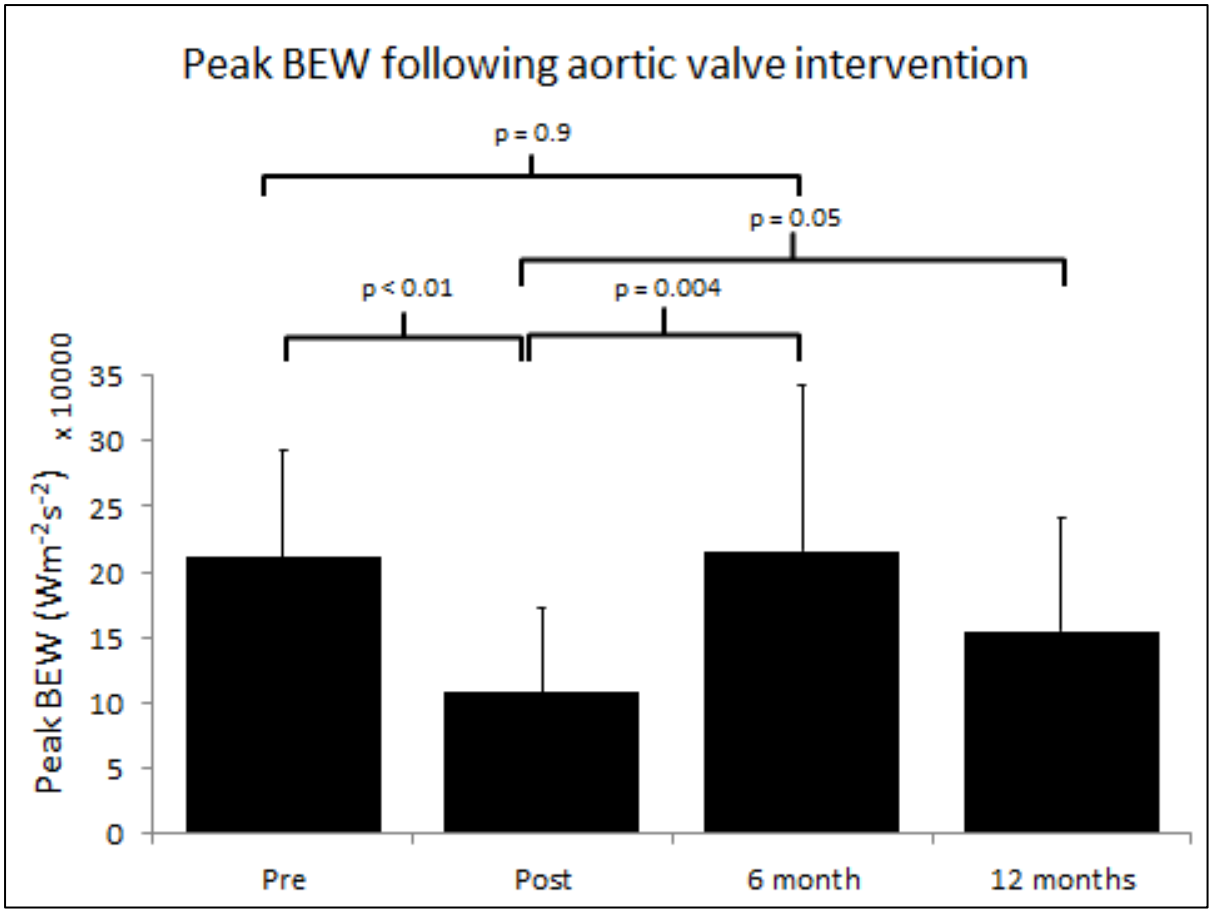

FIGURE 4-3. Change in the peak backward expansion wave over the year following aortic valve intervention.

There is an instant reduction in the magnitude of the BEW following aortic valve replacement or implantation. Over the next 6 months this value increases to a value equivalent to that seen pre-procedurally. At 12 months there is a slight reduction in this value but it remains greater than the immediate pre-intervention values.

4.4 DISCUSSION

Using the technique of non-invasive wave-intensity analysis I have successfully demonstrated that following aortic valve replacement or implantation there is a) an immediate reduction in the magnitude of the backward expansion wave and b) the backward expansion wave then increases with the regression of left ventricular hypertrophy in parallel to the decline in LV mass.

Previous work exploring the temporal effect of aortic valve replacement on coronary haemodynamics has been slightly hampered by the inability to perform multiple measurements on the same patients either because it requires administration of a stressor or measurements to be obtained invasively. For example, previous work has demonstrated an improvement in coronary flow reserve 6 months after aortic valve replacement compared to pre-operative measurements but interpretation is slightly damped by the significant amount of left ventricular remodelling that must have occurred in that time period (Hildick-Smith and Shapiro, 2000, Rajappan et al., 2003, Nemes et al., 2002). Therefore, the application of non-invasive, (stressor-free) wave-intensity analysis is highly desirable in investigating these patients as it allows sampling of coronary haemodynamics at various time points following aortic valve replacement. Additionally, it allows a measure of myocardial efficiency in the resting state thus removing any potential bias exerted by hyperdynamism where there may also be an alteration in the systolic : diastolic time ratio.

4.4.1 IMMEDIATE EFFECTS OF AFTERLOAD REDUCTION

The effects demonstrated in this study using non-invasive wave-intensity mirror that seen using peri-procedural invasive data acquisition in the TAVI population (Chapter 3). The key difference in these patients is that measurements are performed at rest in the absence of anaesthesia or inotropic agents and therefore more accurately reflect the resting physiological state. They therefore validate the information that has been obtained invasively. The values obtained were also of a similar magnitude ($19x10^4$ invasive vs $22x10^4$ $Wm^{-2}s^{-2}$ non-invasive pre-procedure, $11x10^4$ invasive vs $10.9x10^4$ non-invasive post-procedure) reinforcing the integrity of this non-invasive technique.

Pre-operatively, the peak and cumulative backward expansion wave was larger than that seen in individuals without valvular disease(Davies et al., 2006a) due to the increase force required to successfully oxygenate the harder working and increased volume of myocardial tissue. The backward expansion wave is a measurable representation of this increased force and occurs at the onset of diastole with myocardial relaxation. It is caused by the elastic recoil of the myocardial microvasculature generated from the potential energy imparted from systolic contraction.

A fall in this value is seen immediately post-operatively with an almost-50% reduction in the magnitude of the backward expansion wave after either TAVI or AVR with no differences between the two treatment modalities. Whilst there is no change in the coronary pressure, there is an accompanying fall in coronary flow velocity reflecting the reduction in force being applied to accelerate blood through the coronary artery. This in turn also reflects the greatly reduced systolic force (and its resultant diastolic myocardial elastic recoil) now required to eject blood through the aortic valve orifice.

4.4.2 SEPARATING OUT THE CONTRIBUTORS TO WAVE-INTENSITY

The negative effect of left ventricular hypertrophy on prognosis in patients without aortic stenosis is well known. This has also been seen pathophysiologically as a reduction in coronary flow reserve implying a disruption of normal coronary flow patterns and a relative ischaemia in the face of stress (Julius et al., 1997, Eberli et al., 1991, Marcus et al., 1982). Wave-intensity analysis, as a measure of energy transfer efficiency is also known to be impaired in left ventricular hypertrophy(Davies et al., 2006a).

Aortic stenosis often involves substantial left ventricular hypertrophy which could be anticipated to impair coronary energy transfer in this fashion. However, there is also an opposite positive force exerted on the coronary circulation by the increased diastolic relaxation indirectly generated from the stenotic aortic valve. Therefore, a dichotomy exists at a wave-intensity level in aortic stenosis between the presence of an increased energy force being applied to blood at a less 'efficient' level. This is reflected in measurements of wave-intensity that are obtained following a successful aortic valve implantation or replacement where a reduction in the magnitude of the backward expansion wave immediately occurs, to a level much lower than that seen in normal individuals.

In an attempt to separate these component features of wave intensity and to determine the true effect of the outflow tract obstruction on the backward expansion wave, I subtracted the post-procedure value from that measured pre-procedure. Theoretically, the post-procedure value reflects only the presence of left ventricular hypertrophy as the aortic valve gradient has been normalised. This isolated aortic-valve contribution to backward expansion wave correlated much more strongly with conventional

echocardiographic measures of aortic stenosis such as aortic valve peak velocity (r=-0.29, p=0.12 compared to r=-0.41, p=0.02).

This demonstrates the fact that even though the backward expansion wave magnitude is dominated in severe aortic stenosis by the outflow tract obstruction, the effect of left ventricular hypertrophy is both variable and significant. It may be, therefore, that aortic stenosis in the absence of left ventricular hypertrophy is a 'safer' state than with it and therefore, this may provide an option for further risk stratification, particularly in asymptomatic patients.

4.4.3 LEFT VENTRICULAR HYPERTROPHY REGRESSION FOLLOWING AORTIC VALVE INTERVENTION AND ITS EFFECT ON WAVE INTENSITY

The regression of left ventricular hypertrophy is a dynamic process maximal in the first 6 months after aortic valve intervention but also continuing measurably to one year and beyond. Both animal and human studies of coronary flow reserve have shown the beneficial effect of hypertrophy regression on this measure. However, there have been some slightly contradictory reports (Carpeggiani et al., 2008a) in addition to evidence that left ventricular hypertrophy may fail to completely regress in animal models at a histological level(Ito et al., 1993). However, using wave-intensity analysis after aortic valve intervention I have been able to measure a non-pharmacologically driven regression of LVH and in this setting, an increase in backward expansion wave occurs with the reduction of left ventricular mass reflecting a progressive increase in coronary efficiency (Figure 4-4).

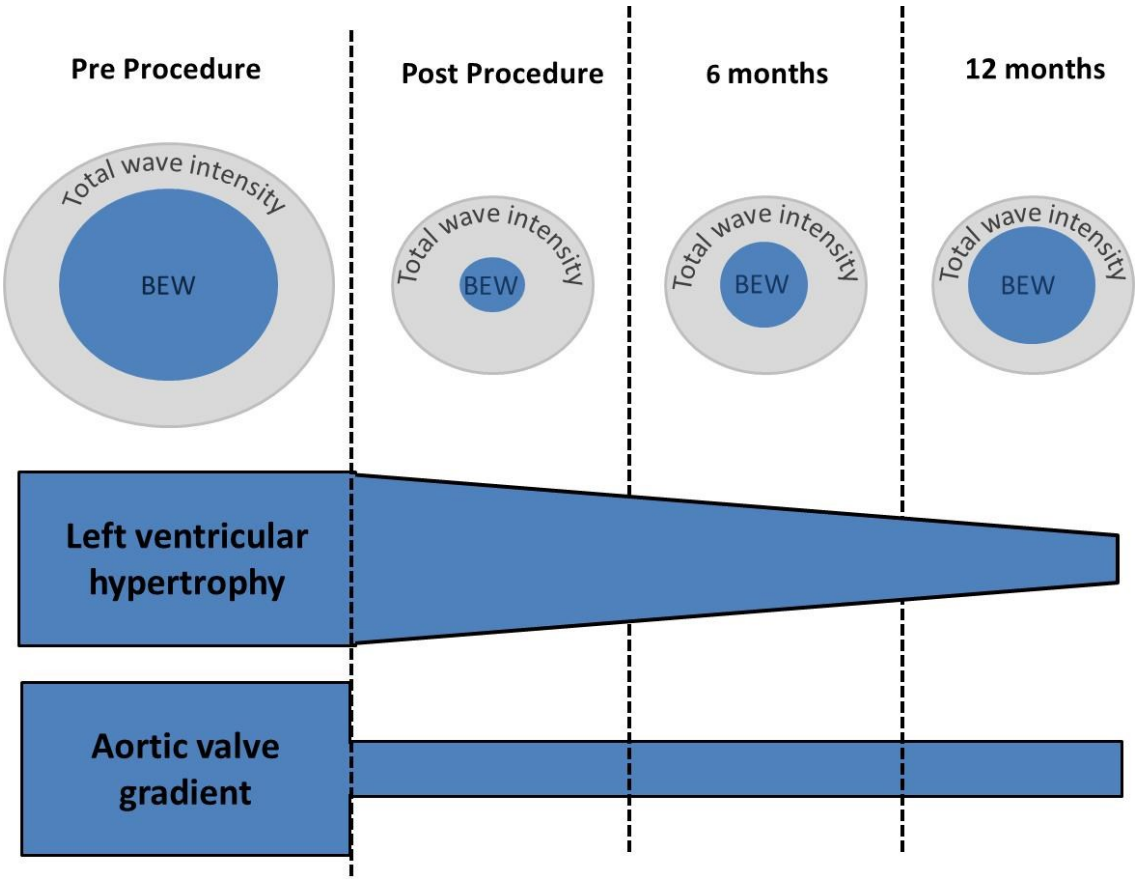

FIGURE 4-4**.** Schematic representation of the change in LVH and aortic valve gradient and their effect on wave intensity.

Immediately following aortic valve intervention the aortic valve gradient rapidly falls. This results in a reduction in the overall energy expenditure per cardiac cycle as well as a reduction in the backward expansion wave driving coronary flow. However, the presence of the now-dominant left ventricular hypertrophy results in a relative inefficiency with the a low percentage backward expansion wave. Over time there is a progressive reduction in the degree of left ventricular hypertrophy whilst the aortic valve gradient remains low and static. There is therefore no change in the overall energy expenditure per cardiac cycle. However, cardiac function becomes more efficient with a greater percentage backward expansion wave.

This data correlates with previous coronary flow reserve data in left ventricular hypertrophy and its regression (Wicker et al., 1983, Sato et al., 1990, Kingsbury et al., 2002, Kingsbury et al., 2000, Nunez et al., 1997, Brilla et al., 1991a, Ishihara et al., 1992, Ito et al., 1993, Xu et al., 2003, Lethen et al., 2003a, Mizuno et al., 2012, Motz and Strauer, 1996, Tomas et al., 2006, Parodi et al., 1997). Wave intensity can be regarded as a measure of the transferable energy from myocardium to blood flow and therefore reflects its efficiency. One can further hypothesize that a more efficient myocardium would be able to respond better to inotropic stimuli as in coronary flow reserve assessment. Therefore, as LVH improves, the myocardium becomes more energy efficient and this would recognisable as an improvement in coronary flow reserve.

Interestingly, there has been some conflicting data in animal and human models regarding coronary flow reserve changes with LVH regression. For example, with atrial pacing, abnormalities persist in dog models of LVH which the authors thought may represent incomplete hypertrophy regression(Ishihara et al., 1992). Additionally, the length of time and degree of remodelling that results may play a role as demonstrated in rat models where long-term aortic banding induced irreversible histological and physiological changes compared with medium-term banding(Ito et al., 1993). PET scanning has also alluded to the idea that the degree of left ventricular hypertrophy is not necessarily directly equivalent to the degree of microvascular dysfunction(Rajappan et al., 2003, Rajappan et al., 2002, Carpeggiani et al., 2008a, Camici et al., 1991). These factors most likely reinforce the fact that the fairly simplistic measure of LV mass does not precisely reflect the degree myocardial and of coronary dysfunction.

Human modelling of hypertension-driven LVH and its regression are harder to control independently as the addition of pharmacological agents may cause significant

confounding independent of LVH regression(Lethen et al., 2003a, Parodi et al., 1997) although there is a clear reduction in LV mass alongside an improvement in CFR in these studies(Xu et al., 2003, Mizuno et al., 2012, Tomas et al., 2006, Motz and Strauer, 1996).

4.4.4 ENERGY TRANSFER INEFFICIENCY WITH MYOCARDIAL HYPERTROPHY: HYPERTENSION VERSUS AORTIC STENOSIS

We know from previous work that myocardial hypertrophy in the absence of valvular disease impacts negatively on wave intensity. However, there are distinct differences between the patterns of fibrosis in humans depending on aetiology – whilst both hypertension and aortic stenosis result in myocytic hypertrophy and perimyocytic fibrosis, additional changes are seen with hypertension where intra-myocardial arteriole wall-thickening and perivascular fibrosis are also present. This may reflect the fact that hypertension-driven changes involve the coronary arteries as opposed to their relative sparing in aortic stenosis.

It was therefore previously unclear if the hypertrophy seen in severe aortic stenosis would have a similar negative impact on energy transfer as had been seen with hypertension-driven hypertrophy given the absence of these latter findings(Davies et al., 2006a). However, after aortic valve implantation or replacement when the dominant effect of wave intensity is that of hypertrophy, a reduced backward expansion wave is seen compared to that in normal individuals implying that despite subtle differences at a histological levels, the effect on coronary energy transfer is the same.

4.5 LIMITATIONS

Due to the technical challenge of measuring non-invasive wave intensity, particularly with the learning curve required and adoption of correct echo machine, not all patients could be followed up accurately. However, the patients in whom data was not gathered either at 6 or 12 months did not differ from those included at these time points in any way and so it is unlikely that this resulted in a significant bias.

Additionally, there was a change in echo machine used for the follow-up from a Phillips ie33 to an Esaote MyLabTwice. However, this would not change the absolute measurements obtained, simply enhance their accuracy. Patients were initially only included in the study if adequate echocardiographic views could be obtained. Therefore, if accurate images were obtained on the ie33, an even easier ascertainment of coronary flow was usually possible with the MyLabTwice.

There is also the possibility of other factors influencing coronary wave-intensity following aortic valve intervention such as pharmacological agents. Four patients had an alteration in cardiac-acting drugs (addition of beta-blockade x2, increase in amlodipine x1 and increase in ACE-inhibitor x1). However, whilst this may have acted on the regression of left ventricular hypertrophy it seems unlikely that the majority of these drugs (perhaps with the exception of the ACE-inhibitor) would alter the myocardium's suction force. Therefore, whilst these agents may improve the rate of LVH regression, this would only aid in appropriately demonstrating the relationship between LVH regression and favourable coronary wave-intensity.

4.6 Conclusion

Non-invasive wave intensity analysis is a viable and useful tool to assess the effects of aortic stenosis and its treatment. The initial reduction in outflow tract gradient is seen immediately following either transcatheter aortic valve implantation or conventional aortic valve replacement as a large fall in the cumulative and peak backward expansion wave. This reflects the decreased force required to eject blood in the post-procedural state.

After aortic valve replacement, the dominant effect modulating the backward expansion wave is the presence of myocardial hypertrophy. This results in a reduction in the magnitude of this wave compared to normal individuals. However, with regression of left ventricular hypertrophy, this value increases reflecting an improvement in the efficiency of the myocardium over time.

5 AORTIC STENOSIS PROGRESSION AND WAVE INTENSITY ANALYSIS CHANGES

5.1 INTRODUCTION

5.1.1 ESTABLISHED METHODS FOR ASSESSING AORTIC STENOSIS SEVERITY

5.1.1.1 Echocardiography

The primary haemodynamic parameters recommended by the European Association of Echocardiography for the assessment of aortic stenosis are jet velocity, mean transaortic gradient and valve area by continuity. Jet velocity is estimated using continuous wave Doppler ideally with a dedicated 'blind' probe. It has shown a good correlation with outcome in aortic stenosis even when the disease is less than severe(Rosenhek et al., 2004) or the patient asymptomatic(Otto et al., 1997) and can be useful if monitored serially(Rosenhek et al., 2001).

The transaortic pressure gradient is easily calculated using the Bernoulli equation. This is based on the concept that the pressure gradient across the valve is composed of the convective acceleration plus flow acceleration plus viscous friction. However, in severe aortic stenosis this can be conveniently shortened to:

$$\Delta P = 4V^2$$

EQUATION 5-1. CALCULATION OF THE PRESSURE GRADIENT ACROSS THE AORTIC VALVE USING PRESSURE (P) AND VELOCITY (V) INTHE MODIFIED BERNOULLI EQUATION – APPROPRIATE FOR HIGH VELOCITIES.

The peak gradient is therefore directly correlated with the measured peak velocity. If the peak velocity is lower than 3.5m/s however, the velocity proximal (Vp) to the obstruction should be incorporated as well as:

$$\Delta P = 4(V^2 - Vp^2)$$

EQUATION 5-2. CALCULATION OF THE PRESSURE GRADIENT USING THE BERNOULLI EQUATION AND INCORPORATING THE LVOT (VP) VELOCITY – APPROPRIATE FOR AORTIC VALVE LOWER VELOCITIES

The mean gradient is calculated by averaging the instantaneous gradients over the ejection period and therefore is produced conveniently through inbuilt software on all modern echo machines by tracing round the velocity envelope.

Doppler velocity and pressure gradients are dependent on flow rate. Valve area is largely independent of flow rate however and therefore can be useful in making the diagnosis of aortic stenosis independent of flow. Aortic valve area is particularly useful in patients with poor left ventricular function where flow rates are low and can be used to guide the need for surgery in these patients(Connolly et al., 2000, O'Sullivan et al., 2013, Pereira et al., 2002). It is based on the concept that stroke volume (SV) is conserved on both sides of the valve and that SV can be calculated as area multiplied by VTI. Therefore:

$$\text{AVA} = \text{LVOT CROSS SECTIONAL AREA} \times \text{LVOT VTI} / \text{AORTIC VALVE VTI}$$

EQUATION 5-3. CALCULATION OF THE AORTIC VALVE AREA (AVA) USING THE PRINCIPLE OF CONSERVATION OF STROKE VOLUME

The LVOT cross sectional area is calculated from the assumption that the LVOT is circular and therefore is $\pi \times \text{radius}^2$.

An alternative approach particularly in patients with a poor ejection fraction, is to calculate the dimensionless index, which is the ratio of LVOT to transaortic gradient(Hachicha et al., 2007). In order to further stratify these patients, stress echocardiography also has a role in ascertaining the contribution of the aortic valve to the failing ventricle(Blais et al., 2006).

In clinical practice it is unusual for many other modalities to play a role in the quantification of aortic stenosis. Nevertheless there are roles for other techniques as documented below.

5.1.1.2 Cardiac Catheterisation

Historically, measuring invasive pressure changes before and after the aortic valve was a useful way to quantify aortic stenosis. However, discrepancies were noted between echocardiographic flow-derived measures of severity when compared to pressure with invasive measures often underestimating the pressure changes compared to flow-derived Bernoulli-calculated non-invasive measures. It became apparent this was because of 'pressure recovery' – a phenomenon where pressure increases the further it is measured from the valve due to the reconversion of turbulent-flow-generated kinetic energy to potential energy downstream. This has been demonstrated experimentally(Niederberger et al., 1996, Baumgartner et al., 1993, Levine et al., 1989) and clinically(Schöbel et al., 1999). Despite formulae to correct for pressure recovery(Baumgartner et al., 1999) or energy loss(Garcia et al., 2000) this technique is rarely used in the routine assessment of aortic stenosis particularly with the knowledge that there is a modest degree of micro-embolisation when the valve is crossed (Omran et al., 2003).

5.1.1.3 Computerised Tomography

CT can be used to quantify aortic valve area and a good correlation has been seen with echocardiographically derived valve area(Feuchtner et al., 2006, Feuchtner et al., 2007, Bouvier et al., 2006). However, CT probably has a stronger role in qualifying aortic valve morphology at present(Chun et al., 2008, Sebastia et al., 2003).

5.1.1.4 Cardiac MRI

Cardiac MRI is useful for evaluating myocardial structure and function and may also have the ability to quantify aortic stenosis. Mapping of anterograde flow was first demonstrated to be possible using MRI scanning 20 years ago across both the mitral and aortic valve(Kilner et al., 1993) and by using the simplified Bernoulli equation the resultant mean and peak systolic gradients correlated well with cardiac catheterisation (and in fact was more accurate(John et al., 2003, Kupfahl et al., 2004)), transthoracic(Eichenberger et al., 1993) and transoesophageal Doppler(Reant et al., 2006), and indicator dilution(Sondergaard et al., 1993). Planimetry can be used to calculate aortic valve area and this has been validated experimentally(Strohm et al., 2001) and clinically(Debl et al., 2005) and improved on with more modern techniques(Schlosser et al., 2007). By mapping VTIs and aortic valve area, the continuity equation can also be employed through MRI scanning(Caruthers et al., 2003).

MRI scanning may also play a more complimentary role in severe aortic stenosis due to its ability to assess function and scarring. For example, it is possible to predict aerobic exercise capacity in severe aortic stenosis by assessing myocardial blood flow and myocardial perfusion reserve(Steadman et al., 2012). Prognostically, the presence of late-gadolinium enhancement on MRI scanning, a correlate of the degree of myocardial fibrosis, was able to predict the left ventricular functional improvement (mean ejection fraction in this study 53%) and all-cause mortality after aortic valve replacement in severe aortic stenosis(Azevedo et al., 2010).

5.1.1.5 Positron Emission Tomography

PET scanning has largely been confined to a research tool in the assessment of aortic stenosis. However, in severe aortic stenosis a reduction in myocardial blood flow

reserve has been demonstrated, with a relative independence from myocardial hypertrophy(Carpeggiani et al., 2008a, Rajappan et al., 2002). It has also proven useful in recognising the degree of inflammation and calcification in the aortic valve of these patients (Dweck et al., 2012b).

5.1.1.6 Valvuloarterial impedance (Zva)

As has already been mentioned, it is well accepted that the occurrence of LV dysfunction, symptoms and adverse outcomes does not always correlate with the classical markers of haemodynamic severity as measured by echocardiography. Some investigators have suggested that this is because these measures only take into account the pressure placed on the left ventricle by the stenotic valve and fail to take into account the additional burden presented by the arterial system which increases with age and shows significant variability(Mattace-Raso et al., 2006). Reduced arterial compliance, caused by increasing arterial stiffness, contributes to increased LV afterload and myocardial oxygen demand and diminished coronary flow during diastole(O'Rourke et al., 2002). Therefore, these investigators sought to integrate this into the assessment of LV burden in aortic stenosis.

Initial work in this field was with pigs where two sources of afterload were created by banding at both the supravalvular level and then at the distal aorta. With this distal afterload in place, there was a fall in peak-to-peak pressure gradients across the valve but an increase in the peak systolic LV wall stress as measured by echocardiography(Kadem et al., 2005). Elaboration of this concept required an accurate approximation of systemic arterial compliance (SAC) which can be achieved in a practical fashion using the systolic arterial pressure (SAP) to Stroke Volume index (SVi) ratio(Sunagawa et al., 1983, Chemla et al., 2003):

$$SAC = SAP / SVI$$

EQUATION 5-4. CALCULATION OF SYSTOLIC ARTERIAL COMPLIANCE (SAC) FROM SYSTOLIC ARTERIAL PRESSURE (SAP) AND SYSTOLIC VOLUME INDEX (SVI)

Stroke Volume index is calculated by relating stroke volume (SV) to the size of an individual using their Body Surface Area (BSA):

$$SVI = SV / BSA$$

EQUATION 5-5. CALCULATION OF STROKE VOLUME INDEX (SVI) FROM STROKE VOLUME (SV) AND BODY SURFACE AREA (BSA).

In turn, stroke volume can be calculated from echocardiography using the LVOT area and the LVOT Velocity Time Integral (VTI) so that:

$$SV = \text{LVOT AREA} \times \text{LVOT VTI} = \pi (\text{LVOT DIAMETER} / 2)^2 \times \text{LVOT VTI}$$

EQUATION 5-6. CALCULATION OF STROKE VOLUEME FROMM LVOT AREA AND VELOCITY TIME INTEGRAL

Finally, this needs to have the aortic valve mean pressure load (MG) integrated into it to produce the valvulo-arterial impedance (Zva):

$$ZVA = (SAP + MG) / SVI$$

EQUATION 5-7. CONSTRUCTION OF THE VALVULO-ARTERIAL IMPEDENCE

Initial work using this concept in 208 patients with moderate and severe aortic stenosis demonstrated that Zva was independently associated with LV dysfunction(Briand et al., 2005). Retrospective analysis of the 1591 patients in the SEAS (Simvastatin Ezetimibe in Aortic Stenosis) study demonstrated that LV global afterload (Zva) impacts unfavourably on LV myocardial function in asymptomatic patients with aortic stenosis.

Using speckle tracking, Zva was also found to be an independent marker of myocardial dysfunction in asymptomatic aortic stenosis(Lancellotti et al., 2010b). However, a further study showed that Zva was not helpful in distinguishing true and pseudo-severe aortic stenosis in low-flow low-gradient cases (although this study also reinforced the link between Zva and low ejection fraction and reduced contractile reserve as assessed by dobutamine stress echocardiography)(Levy et al., 2011).

Zva is also associated with outcome. Of 163 patients with moderate and severe aortic stenosis followed over a mean of 20 months, a higher Zva was associated with an increased risk of events (operation, symptoms or death)(Lancellotti et al., 2010a). Additionally, a retrospective analysis of 544 patients with at least moderate aortic stenosis also showed the four-year event rate to be significantly higher in those with a high Zva(Hachicha et al., 2009). Using ROC curves in the former study, a Zva value of 4.9 mmHg / ml / m^2 was identified as the best cut-off value associated with events. The latter study showed a Zva of greater than 4.5 mmHg / ml / m^2 increased the mortality risk by 2.76-fold.

5.1.2 CORONARY HAEMODYNAMICS IN LOW-FLOW LOW-GRADIENT AORTIC STENOSIS

In order to distinguish true- from pseudo-aortic stenosis in patients with low-flow low-gradient aortic stenosis dobutamine stress-echocardiography has been used to demonstrate those patients with contractile reserve from those without(Monin et al., 2001, Schwammenthal et al., 2001). Other methods to distinguish these patients using projected effective orifice area at a normal transvalvular flow rate has been shown to correlate reasonably with patient sub classification(Blais et al., 2006). Alternatively, the degree of calcification is also a predictor of the severity of aortic stenosis and this can be

useful in this situation(Cueff et al., 2011). PET scanning is a useful tool for demonstrating coronary vasodilator reserve(Rajappan et al., 2002) and has been used to distinguish patients with low-flow low-gradient aortic stenotic patients(Burwash et al., 2008).

5.1.3 Wave Intensity Analysis in Aortic Stenosis

Up until now it has not been possible to gather wave-intensity data on patients with more moderate degrees of aortic stenosis. This is because they are largely asymptomatic and therefore have no need to undergo invasive coronary assessments necessary for coronary pressure and flow assessment. However, certain predications can be made regarding mild and moderate aortic stenosis based on previous wave intensity work.

Again, there is a balance between the detrimental effect of myocardial hypertrophy and the increased intra-myocardial force generated by driving blood against a stenotic aortic valve. The former results in a reduction in the backward expansion wave responsible for transferring energy to drive coronary flow(Davies et al., 2006a) whilst the latter results in a progressive increase in this force due to the transmission of greater systolic compression to diastolic relaxation and resultant coronary suction(Davies et al., 2011).

Of these two opposing pathophysiological efforts, it is likely that the latter will dominate although its effect will be attenuated by the former. For example, it has already been shown that in patients pre-TAVI with severe aortic stenosis, the backward expansion wave is much greater than in control patients and that once the aortic stenosis and

stenotic forces are relieved, there is a large decline in these values (see chapter 4). Therefore, overall there is likely to be a linear or quasi-linear relationship between backward peak and cumulative wave intensity and conventional echocardiographic measures of aortic stenosis in patients with normal left ventricular function.

To further elaborate on wave-intensity in lesser degrees of aortic stenosis it is now possible to apply non-invasive wave-intensity analysis to these patients using the methods described above.

5.2 METHODS

25 patients (11 female, mean age 72 ± 13) with varying degrees of aortic stenosis and preserved left ventricular function were recruited for non-invasive wave intensity assessments. Patients were either asymptomatic or had undergone a coronary angiogram showing no coronary lesions. Other exclusion criteria were concomitant moderate or severe aortic insufficiency or mitral valve disease or left ventricular ejection fraction <50%.

Patients were identified either at the time of angiography or through a manual search of a hospital database. They were invited to attend and asked to abstain for nicotine, caffeine or nitrate therapy (if applicable) for 24 hours beforehand.

5.2.1 WAVE INTENSITY ANALYSIS

Wave-intensity was measured either invasively at the time of angiography (n=3) or using non-invasive assessment with transthoracic echocardiography and Pulsecor assessment (n=21). Briefly, the invasive assessment involved intubation of the left main stem with a Judkins guide catheter followed by administration of intra-arterial heparin. The Combowire (Volcano Corp - Figure 2-60) was then advanced into the mid-LAD and a continuous recording of 1 minute was taken once a stable signal had been achieved. Data was recorded onto a Combomap console and wave-intensity analysis performed offline using custom built Matlab (Mathworks, Natick, MA) software.

Non-invasive assessment was performed using an Esaote MyLabTwice (Esaote, Genoa, Italy) and a Pulsecor Cardioscope II (Pulsecor, Auckland, New Zealand). Coronary flow was imaged using a modified parasternal long axis view with inbuilt coronary flow

probe parameters activated. A minimum of 20 coronary flow signals were recorded and exported as a bmp file. A minimum of 2 Pulsecor readings (incorporating 6-10 beats per recording) were taken simultaneously (of fidelity 'good' or above) and exported as a Matlab file. Wave intensity was calculated using custom built Matlab (Mathworks, Natick, MA) software.

5.2.2 AORTIC VALVE STENOSIS SEVERITY

All patients also had conventional echocardiographic measures of aortic stenosis with the use of the modified Bernoulli equation, standard continuity equation for valve area and mean gradient calculated from flow VTI.

5.2.3 LV MASS

LV mass was calculated according to the standard echocardiographic formula:

$$\text{LV mass} = 0.8 \times (1.04 \times (\text{LVEDD} + \text{PWDD} + \text{IVSD})^3 - \text{LVEDD}^3) + 0.6$$

LVEDD = Left Ventricular End Diastolic Dimension, PWDD = Posterior wall thickness in diastole, IVSD = intraventricular septal thickness in diastole.

5.2.4 GLOBAL LV HEMODYNAMIC LOAD

As a measure of global LV load, the valvuloarterial impedance was calculated according to previously described methods(Hachicha et al., 2009):

$$Zva = (SAP + MG) / SVI$$

where SAP is the systolic arterial pressure and MG is the mean transvalvular pressure gradient.

Advantageously, I used the Pulsecor-derived measure of central systolic arterial pressure for SAP rather than peripheral systolic pressure which seemed more appropriate for measuring the global LV haemodynamic load.

5.2.5 STATISTICS

Continuous data were expressed as mean ± SD. Correlation was ascertained using a Pearson's correlation coefficient. $p<0.05$ is taken as significant. Student's unpaired t test was used for comparisons between groups.

5.3 RESULTS

5.3.1 DEMOGRAPHICS

Baseline demographics are displayed in Table 5-1. 15 patients (60%) were treated for hypertension but overall the BP control was good (systolic mean 125 ± 18mmHg). All patients were asymptomatic.

Age	72 ± 13
Male (%)	15 (56)
Diabetes	3
Hypertension	15
Smoker	2
Weight, kg	79 ± 21
Height, m	171 ± 10
BSA , m^2	1.1 ± 0.3
Systolic central BP, mmHg	125 ± 18

TABLE 5-1. Baseline demographic data

5.3.2 ECHOCARDIOGRAPHIC DATA

Echocardiographic data is displayed in Table 5-2. There was a wide spectrum of aortic valve disease from mild to severe. The minimum aortic gradient was 23mmHg (2.41m/s) and maximum 117 (5.43m/s). Mean gradient ranged from 13 to 77mmHg (mean 33mmHg). LV mass varied appropriately (mean 186±62.5) given the spectrum of aortic valve disease as did LV dimensions (LVEDd range: 3.4-5.9).

	Mean	Standard Deviation	Minimum	Maximum
LVEDd	4.61	0.68	3.40	5.91
LVEDs	3.01	0.60	2.00	4.10
IVSd	1.13	0.22	0.70	1.60
PWd	1.04	0.24	0.50	1.60
LV mass (kg)	186	62.5	84.1	321
Peak gradient	59	32	23	117
Mean gradient	33	20	13	75
Peak velocity	3.7	1.04	2.41	5.43
AVA	0.97	0.37	1.60	0.40

TABLE 5-2. Echocardiographic data

5.3.3 WAVE INTENSITY ANALYSIS

Wave-intensity arranged according to AVmax is shown in Table 5-3 and by Zva in Table 5-4. Across both spectrums of classification there is an increase in peak and cumulative backward expansion wave magnitude although this is most obvious when the cumulative backward expansion wave is classified by Zva.

When lowest and highest magnitudes of division were compared, when classified by AVmax, the difference was not significant (AVmax 2-3m/s BEW = -118944 $Wm^{-2}s^{-2}$ vs AVmax 5-6m/s BEW = -264696 $Wm^{-2}s^{-2}$, p =0.051) whereas this reached significant when divided by Zva (2-4 $mmHgml^{-1}m^{-2}$ BEW = -141789 $Wm^{-2}s^{-2}$ vs 8-10 $mmHgml^{-1}m^{-2}$ BEW = -370553 $Wm^{-2}s^{-2}$, p=0.02), (Figure 5-1).

Correlation scatter graphs were constructed for aortic valve area, mean gradient, AVmax and Zva against peak and cumulative wave intensity. Data for cumulative wave intensity is shown in Figure 5-2. The correlation coefficient steadily increased with the highest r value associated with valvulo-arterial impedance (Zva): AVA r=0.41 (p=0.04), Mean gradient r = -0.51 (p=0.01), AVmax r=-0.5 (p=0.01), Zva r = -0.66 (p<0.001) (Figure 5-2).

AVmax	n	AVA	Peak BEW	Cumulative BEW
2-3	8	1.3	$11.9 \pm 5.4 \times 10^4$	$64.8 \pm 31.7 \times 10^5$
3-4	7	1.1	$18.4 \pm 9.17 \times 10^4$	$88.1 \pm 40.6 \times 10^5$
4-5	4	0.9	$14.7 \pm 4.77 \times 10^4$	$65.6 \pm 16.8 \times 10^5$
5-6	6	0.7	$30.0 \pm 23.1 \times 10^4$	$155.8 \pm 77.0 \times 10^5$

TABLE 5-3. Wave intensity arranged according to AVmax categories.

There is a steady appropriate increase in peak and cumulative backward expansion wave with progressive aortic valve gradient.

Zva (mmHg ml^{-1} m^{-2})	n	Peak BEW ($Wm^{-2}s^{-2}$)	Cumulative BEW ($Wm^{-2}s^{-1}$)	AVA (cm^2)	AVmax (ms^{-1})	Mean gradient (mmHg)
2-4	9	-14.1×10^4	-71.6×10^5	1.2	3.4	26
4-6	7	-13.9×10^4	-76.5×10^5	1.0	3.6	31
6-8	5	-18.0×10^4	-82.8×10^5	0.95	3.6	32
8-10	4	-37.1×10^4	-180.0×10^5	0.74	4.0	42

TABLE 5-4. Wave intensity arranged according to Zva categories.

Again, there is a steady appropriate increase in peak and cumulative backward expansion wave. The Zva categories broadly match the valve area and gradients.

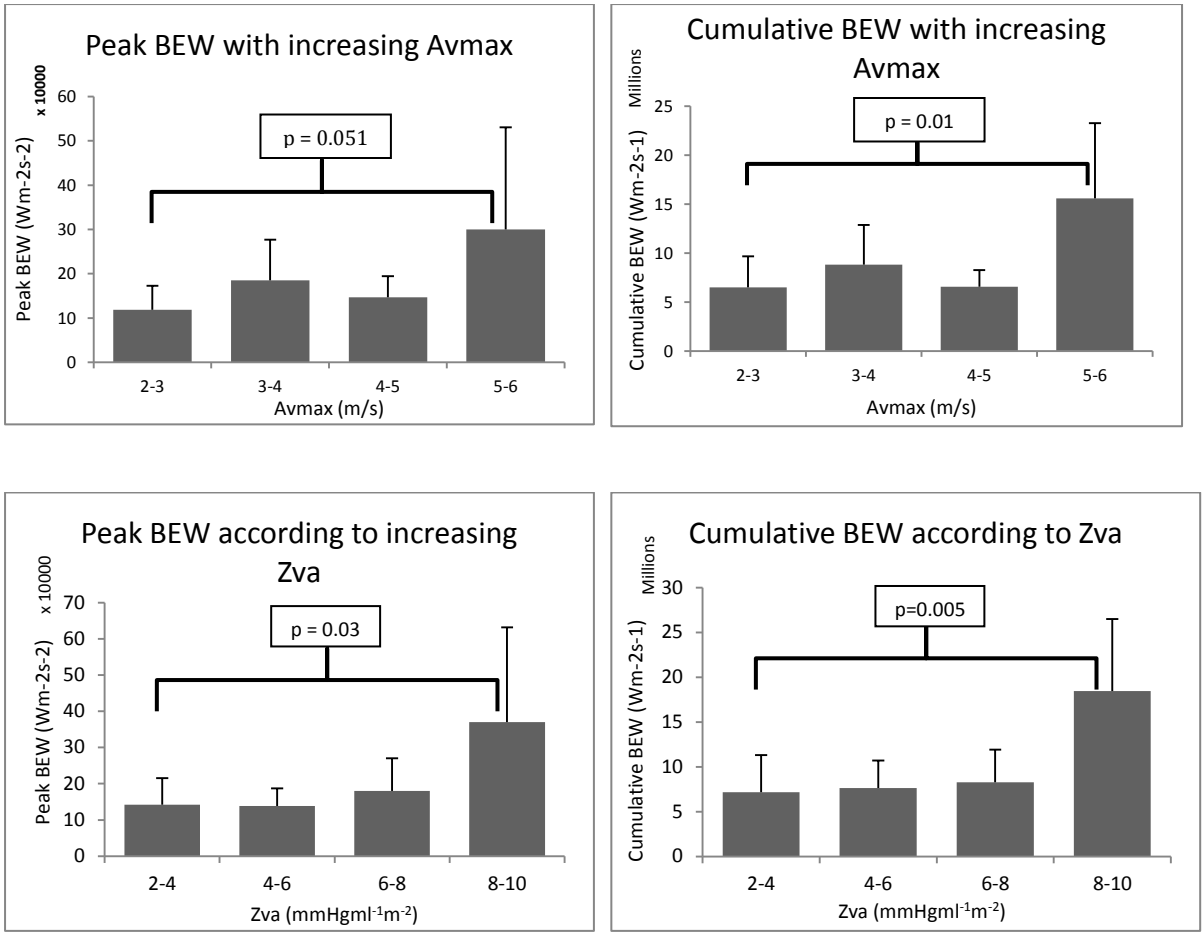

FIGURE 5-1. Peak and cumulative backward expansion waves according to AVmax and Zva.

Wave intensity values are displayed as positive with error bars reflecting SEM. Using both peak and cumulative measures of BEW there is an increase in BEW with AVmax although this is only significant with cumulative measures. When Zva was used both cumulative and peak BEW were significant with a more impressive p value than seen with AVmax.

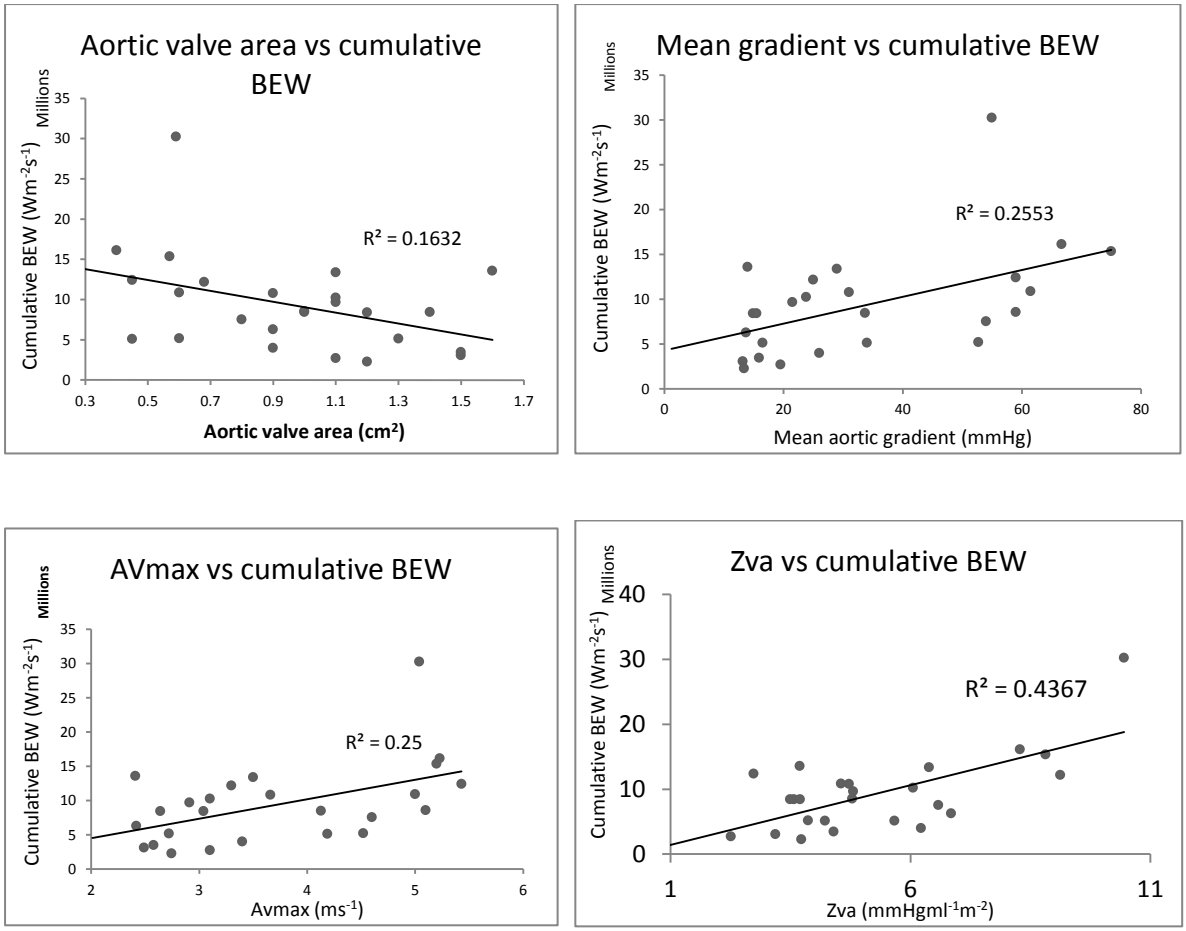

FIGURE 5-2. Cumulative backward expansion wave with aortic valve area, mean aortic gradient, AVmax and Zva

Again, there was an appropriate correlation with both AVmax and Zva and the backward expansion wave. However, the most accurate correlation was seen with the valvulo-arterial impedance particularly with the cumulative BEW.

5.4 DISCUSSION

Using non-invasive wave-intensity I have demonstrated that it is possible to assess coronary energy transfer across a spectrum of aortic valve disease. Using this technique, I have shown that the increasing valve gradient and resultant increase in systolic contraction and corresponding diastolic relaxation is indeed the dominant effect on coronary wave intensity. As aortic valve disease progresses, the peak and cumulative backward expansion wave increases in response to the increased intra-ventricular forces. This is therefore both a new measure of the severity of aortic stenosis as well as a physiological validation of our concepts of wave-intensity in aortic stenosis.

5.4.1 AORTIC STENOSIS VARIABILITY

The process of aortic stenosis progression is a dynamic one and shows a great deal of chronological and pathological variability between patients. Additionally, as has been highlighted by various MRI studies, the response of the left ventricle to the increased pressure load in terms of myocardial hypertrophy and underlying fibrosis is also highly variable as the disease progresses(Debl et al., 2006, Rudolph et al., 2009, Dweck et al., 2012a); post-operatively the amount of fibrosis is linked with LV recovery and outcome(Azevedo et al., 2010). Therefore, whilst conventional echocardiographic measures of aortic stenosis are practical and easily applicable within clinical practice, they remain slightly crude in providing information about the entirety of cardiac function within aortic stenosis.

For example, risk stratification and outcome following aortic valve surgery in moderate or severe aortic stenosis can be predicted more accurately when additional assessments

of LV function are included with strain or exercise echocardiography (Ng et al., 2011, Maréchaux et al., 2010, Poulsen et al., 2007). Additionally, BNP correlates better with outcome over the usual echocardiographic measures of aortic stenosis(Gerber et al., 2003, Bergler-Klein et al., 2004, Weber et al., 2006). These studies reinforce the fact that it is the impaction of the pressure gradient on the left ventricle (rather than the pressure gradient itself) and the response of the left ventricle to this burden that drives prognosis and outcome.

Therefore, it is not a surprise therefore that wave-intensity analysis, a measure that incorporates ventricular function as well as the direct haemodynamic effects of a stenotic aortic valve does not have a perfectly linear relationship with simple measures of aortic valve stenosis. Moreover, wave-intensity should provide a more accurate measurement of the impact of aortic stenosis and correlates with other measures of aortic stenotic burden would provide a useful direction for future work.

5.4.2 Fibrosis Versus Hypertrophy

One thing that is unclear is the differing effects and deposition patterns of myocardial fibrosis and hypertrophy in aortic stenosis. Although imaging studies using MRI have shown the two entities are closely linked there is obviously some inherent variability between the presence and absence of fibrosis in patients with LVH. Histological studies seem to suggest that the change from hypertrophy to fibrosis is involved in the transition to heart failure in aortic stenosis(Hein et al., 2003) and indeed, if mid-wall fibrosis as well as LVH is noted on MRI, patients with severe aortic stenosis tend to have a poorer outcome (Azevedo et al., 2010). Basic transthoracic echocardiography can only document hypertrophy and left ventricular function and can provide little information on the degree of fibrosis although we assume the former to be a surrogate for the latter.

Therefore, it is not certain whether wave-intensity is negatively impact upon by the presence of fibrosis in these aortic stenotic patients or whether it is a mechanical effect exerted by the hypertrophy although it is perhaps most likely a combination of the two. This may also introduce a degree of variability into the wave-intensity values if LVH alone is measured in aortic stenosis; ultimately however, this tool may prove useful in the long-term in separating these components perhaps when used in conjunction with MRI scanning.

Additionally, as has been commented on in detail in previous chapters, in aortic stenosis the second influence on the backward expansion wave is the presence of myocardial hypertrophy which exerts an effect counter to that of the stenotic valve. This may explain why, particularly in the mild- and moderate-aortic stenotic range where the two opposing forces may be of similar magnitude, there is not a perfectly linear relationship between conventional measures of aortic stenosis and wave-intensity.

5.4.3 ACCOUNTING FOR VASCULAR LOAD

Previous work has demonstrated the importance of accounting for the pressure effect beyond the valve in risk stratification in aortic stenosis(Briand et al., 2005, Lancellotti et al., 2010a, Lancellotti et al., 2010b, Hachicha et al., 2009). Given that this impedance value is believed to be a more accurate measurement of the pressure effect on the left ventricle, assessing valvulo-arterial impedance should provide a more accurate correlation with wave-intensity analysis and this is indeed the case. This is therefore a validation of the valvulo-arterial impedance concept where a higher Zva results in greater energy exchange at a myocardial level through an increased systolic force translating to an increased diastolic relaxation.

5.5 Conclusion

I have successfully demonstrated the application of non-invasive wave-intensity to a group of patients with no invasive sampling option and have gone on to show that the backward expansion wave increases with increasing severity of aortic stenosis. I have also confirmed the relative crudity of simple echocardiographic measures of severity which provide information about the valve but not about the effect it is having on the underlying myocardium. Finally I have demonstrated that the valvulo-arterial impedance calculation provides a more accurate measure of energy exchange at the myocardial level.

The use of non-invasive wave-intensity analysis may therefore form an alternate option in the assessment of aortic valve disease. Future work may direct itself at correlating other measures of myocardial function with wave-intensity in these patients through use of non-invasive coronary flow reserve or speckle-tracking. It will also be interesting to recognise differences in the wave-intensity profile based on the variability of fibrosis and hypertrophy documented at MRI.

6 CHAPTER 6: CONCLUSIONS AND FUTURE DIRECTIONS

6.1 SUMMARY OF MAIN FINDINGS

6.1.1 MYOCARDIAL ISCHAEMIA IN AORTIC STENOSIS

Myocardial ischaemia is a detrimental problem in aortic stenosis. Its cause is largely linked with the two dominant pathological features in aortic stenosis: the stenotic aortic valve and the resultant but necessary left ventricular hypertrophy. At present, in the majority of cases we are reliant on relatively crude measures to assess and time intervention in aortic stenosis such as the presence of symptoms combined with echocardiographic-derived values of valve gradients and ejection fraction.

In up to 50% of patients with chest pain and aortic stenosis, unobstructed coronary arteries are noted at angiography(Gould and Carabello, 2003). However, using more sophisticated techniques it is possible to recognise abnormalities in the coronary physiology of these patients through use of lactic acid sampling, thallium scans and 24-hour Holter monitors, invasive coronary Doppler techniques, resting coronary flow rates, contrast and stress echocardiography and PET scanning.

Previous animal and human works has endeavoured to recognise the pathophysiological features that contribute to abnormal coronary physiology in aortic stenosis. The most important abnormalities appear to be exerted through extravascular compression effects, a shortened diastolic perfusion time, reduced capillary density, increased oxygen diffusion distances and low coronary sinus pressures. What is certainly most clear from all these studies is that the effect of aortic stenosis on the left ventricle is only indirectly assessed by quantifying the aortic valve using echo. There is a large variability in the way the left ventricle responds to the increased outflow tract obstruction and therefore what would be more useful in the assessment of aortic

stenosis would be an easily applicable measurement that can be used to quantify this global burden.

6.1.2 INVASIVE WAVE INTENSITY ANALYSIS IN SEVERE AORTIC STENOSIS

Wave intensity analysis may be such a measurement. This concept is based on fluid dynamics and is a temporal-based assessment of energy transfer that provides a measure of both magnitude and direction of energy acting on the coronary blood flow. It has been applied to normal coronary arteries and shown an inverse relationship with left ventricular hypertrophy reflecting the inefficiency of this state(Davies et al., 2006a).

With the expansion of the TAVI procedure to higher risk patients with severe aortic stenosis, it has become possible to conveniently measure wave-intensity peri-procedurally in these patients. I have shown that severe aortic stenosis results in an increase in the magnitude of the backward suction wave responsible for antegradely driving coronary flow and that this is likely a reflection of the increased force of contraction which is then transmitted as an increased force of relaxation due to the elastic properties of the left ventricle. More interestingly, this wave profile changes unfavourably pre-TAVI and returns to the physiological norm(Lockie et al., 2012, Sun et al., 2000) post-TAVI in response to pacing. This implies a discoordination and worsening efficiency of energy transfer in aortic stenotic patients with increasing heart rate and is likely to be involved in the generation of symptoms in these patients.

Wave-intensity analysis is a very useful tool in this setting to provide key information about these aortic stenotic patients. However, until now its main disadvantage is that it requires invasive measurements of coronary flow and pressure albeit from a single

sensor tipped wire. The ability to perform coronary wave-intensity non-invasively would therefore be highly desirable in order to perform multiple measurements in the same individual.

6.1.3 NON-INVASIVE CORONARY WAVE INTENSITY

It has been possible to measure coronary flow using transthoracic echocardiography for over 20 years. However, as hardware technology improved, the quality of the signal obtained is now higher than ever and allows for accurate discrimination of the period of diastolic acceleration necessary for the construction of non-invasive wave-intensity. Additionally, much work in the field of invasive coronary pressure (particularly that involving Fractional Flow Reserve) has demonstrated that the central aortic pressure is a good reflection of the pressure in the coronary arteries providing there is an absence of obstructions. There are now several ways to estimate central aortic, and therefore indirectly coronary, pressure non-invasively.

Using these two techniques simultaneously has allowed the development of non-invasive coronary wave-intensity analysis. In this thesis I have gone on to validate this technique in 17 patients with unobstructed coronary arteries. In a further 9 patients I have shown this technique produces an appropriate response during exercise as seen with invasive measurements and a trend towards the appropriate response with increasing left ventricular mass. Finally I have demonstrated the technique to be easily reproducible.

6.1.4 APPLICATION OF NON-INVASIVE WAVE INTENSITY IN PATIENTS WITH AORTIC STENOSIS

As the gradient across the aortic valve increases, there is a progressive increase in the force required to eject blood across this valve. This is accompanied by an increase in the trans-capillary compression during systole and the potentially stored elastic energy in the myocardium from this compression is transferred to a kinetic force as the capillaries re-expand resulting in coronary acceleration. Although reports are slightly conflicting, the majority of data supports the notion that coronary flow rates increase with increasing aortic stenosis and this is certainly demonstrated here.

Using a spectrum of aortic valve disease patients I have shown that this theory does indeed hold true when assessed with non-invasive wave-intensity analysis where there is a reasonable correlation between the aortic valve gradient and the peak and the cumulative backward expansion wave. Additionally, previous work by other groups has also highlighted the importance of incorporating the arterial stiffness burden that acts in tandem with the aortic valve gradient to impact on the left ventricle(Briand et al., 2005). Therefore, we would anticipate that the Zva (the valvuloarterial impedance) which is a measure of the global force acting on the left ventricle would more accurately correlate with coronary energy transfer than simple echocardiographic measures of aortic stenotic severity and this is indeed found to be the case.

Therefore it appears that the backward expansion wave responds as anticipated with increasing severity of aortic stenosis. Additionally, I have also shown that the backward expansion wave decreases in magnitude appropriately after TAVI or conventional AVR as has been seen invasively. This confirms this phenomenon and also shows that it is not just confined to patients undergoing the TAVI procedure but also to AVR patients,

nor is it a result of the inotropic or adrenergic influences apparent peri-procedurally during TAVI.

Interestingly, the reduction in backward expansion wave is to a level much less than normal and this is most likely an effect of the residual myocardial hypertrophy which is known to add inefficiency to energy transfer. However, with the removal of the outflow tract obstruction, there is a regression of left ventricular hypertrophy over time and importantly, this translates to a progressive increase in the backward expansion wave to levels similar to that seen in normal individuals.

6.2 FURTHER HYPOTHESES – WHAT HAPPENS IN THE FAILING VENTRICLE?

Using these techniques, I have been able to give an idea of the 'life cycle' of wave-intensity with aortic stenosis. However, there is a final clinical scenario that I have not explored fully and may prove an important future direction of research – that is of aortic stenosis with the failing left ventricle. The hypothesis is that as the LV starts to fail from the continual afterload burden, its force of contraction and resultant relaxation would also decline, perhaps in a similarly linear fashion.

To that end, it is interesting to note some of the very early work on coronary flow in aortic stenosis using transoesophageal echocardiography noted that patients with severe aortic stenosis and angina, presyncope or syncope have higher than average coronary flow rates but flow rates in those with shortness of breath did not differ from controls. One possible implication from this study, which did not comment on LV systolic function in their patient group, is that when patient's hearts are failing (causing dyspnoea), coronary flow rates may fall(Omran et al., 2011).

I have performed non-invasive wave-intensity in some of these patients with failing LV secondary to aortic stenosis and not coronary disease or another cause. Initial pilot work suggests that there appears to be two patterns of coronary flow in these patients: 1) patients in whom peak coronary flow rate is maintained but the rate of acceleration is reduced and 2) patients in whom peak coronary flow is reduced (Figure 6-1). This former pattern has been recognised in the literature but linked crudely with severity rather than severity plus LV impairment in early studies(Kenny et al., 1994).

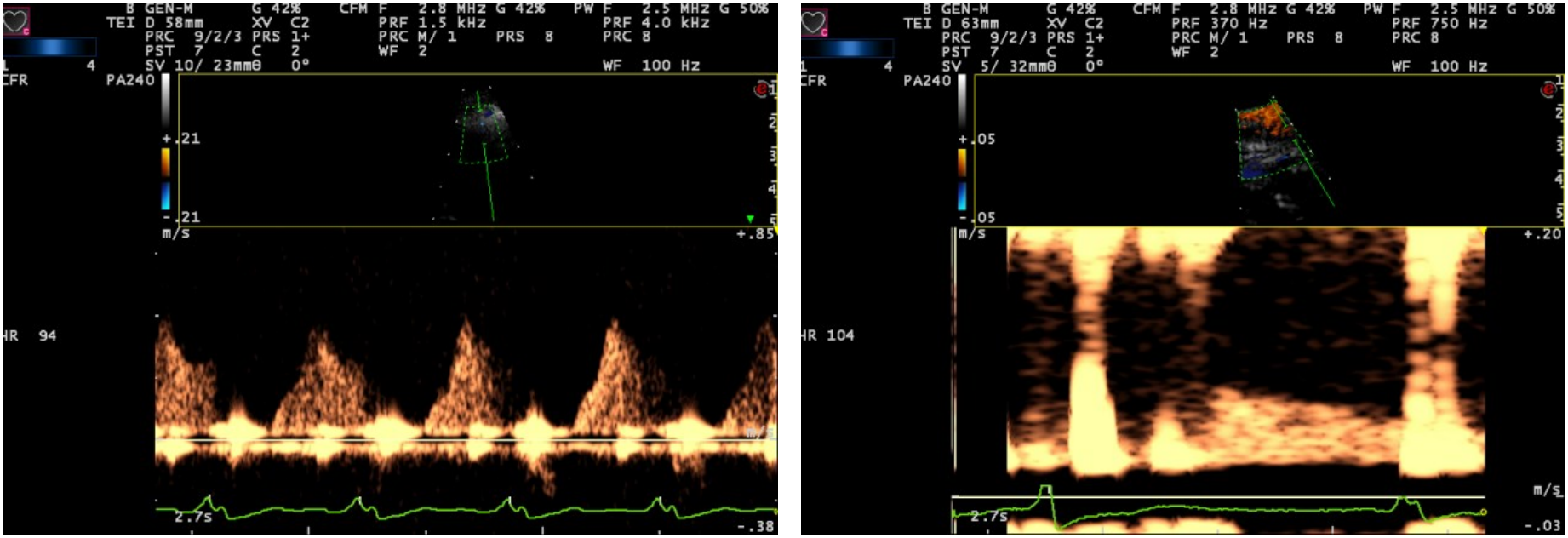

FIGURE 6-1. Flow patterns in severe aortic stenosis with severe LV impairment.

Note the different scales in these two examples. The left hand panel demonstrates the first example where peak coronary flow rates are preserved but acceleration reduced compared to the right hand panel where coronary flow rates are reduced.

Both of these patients had greatly reduced peak backward expansion wave (-45661 and -31688 $Wm^{-2}s^{-2}$) but very different cumulative expansion waves ($-43x10^5$ versus $-18x10^5$ $Wm^{-2}s^{-1}$). This can be seen graphically in Figure 6-2.

Therefore, it would appear that despite a severely impaired LV, the patient with the preserved peak coronary flow rate still has the ability to generate a significant energy transfer compared to the low coronary flow rate patient. One could hypothesize further that wave-intensity may in fact be able to distinguish patients with severe aortic stenosis and severe LV impairment who would do well following aortic valve replacement by assessing the ratio of peak-to-cumulative backward expansion wave magnitude. This is demonstrated pictorially in Figure 6-3.

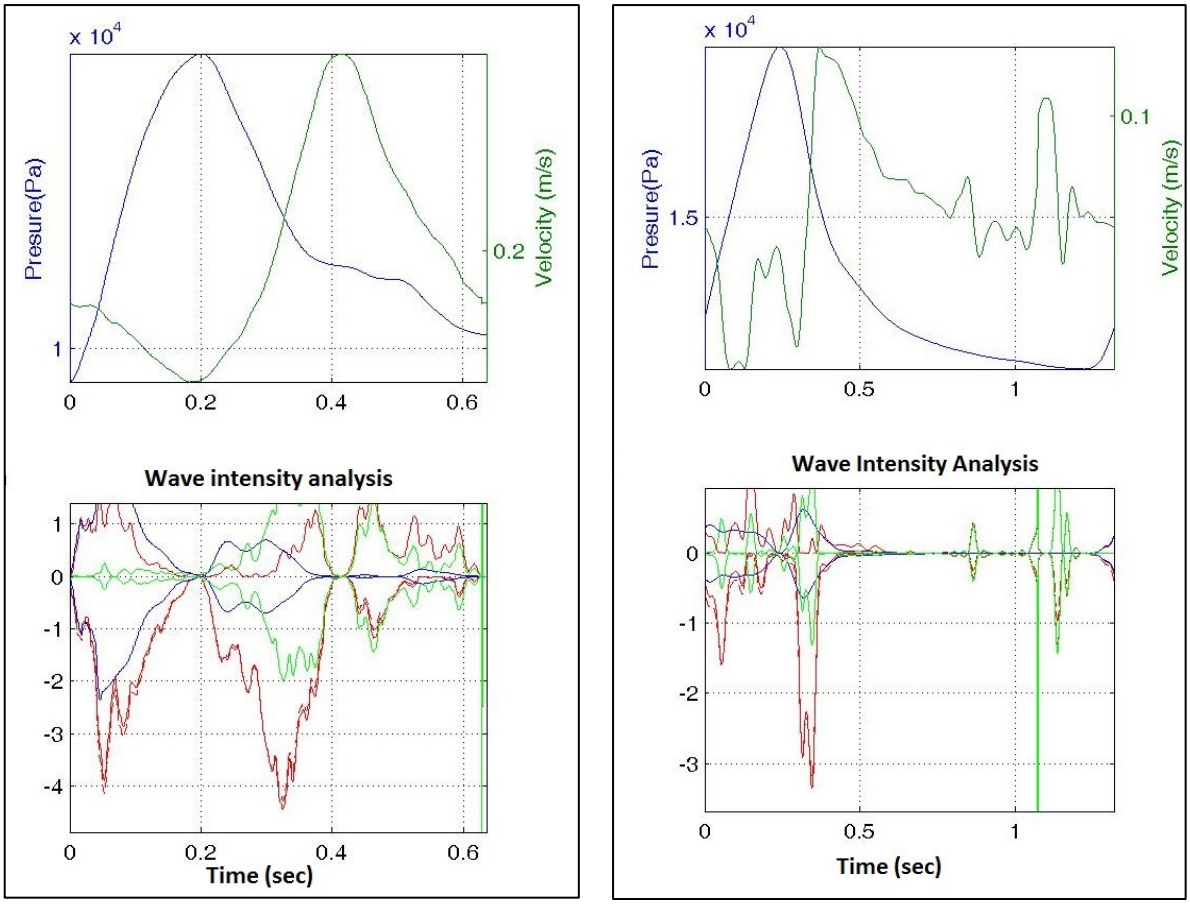

FIGURE 6-2. Coronary wave intensity analysis in severe aortic stenosis with severe left ventricular impairment.

The upper panels demonstrate coronary flow (blue) and pressure (green) and the lower panels overall wave-intensity (red), and the influence of flow (green) and pressure (blue). Note the backward expansion waves are similar in peak but there is a much larger area under the curve in the left hand panel where coronary flow rates are preserved with a slower acceleration rate.

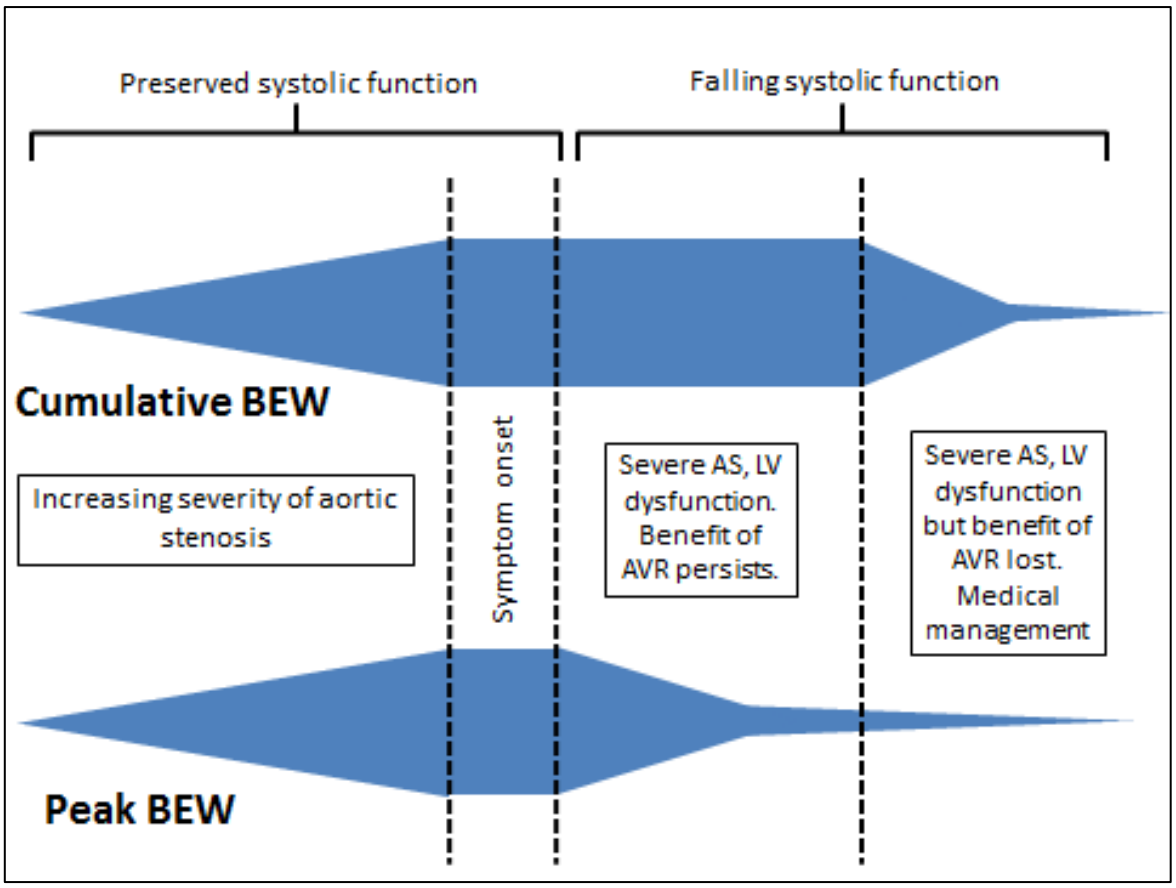

FIGURE 6-3. Figurative representation of the changes occurring with the peak and cumulative BEW as severe aortic stenosis progresses to left ventricular dysfunction.

With the onset of LV dysfunction there is initially a decline in the peak backward expansion wave. The cumulative backward expansion wave is preserved. As time progresses further, the cumulative backward expansion wave also declines reflecting a loss of the ability of the left ventricle to recover following at aortic valve intervention. At this point aortic valve replacement or TAVI will provide no benefit and medical therapy is the appropriate management strategy.

6.3 THE BACKWARD EXPANSION WAVE IN AORTIC STENOSIS

Through the use of non-invasive techniques, it is therefore now possible to construct the complete life-cycle of the backward expansion wave in aortic stenosis (Figure 6-4).

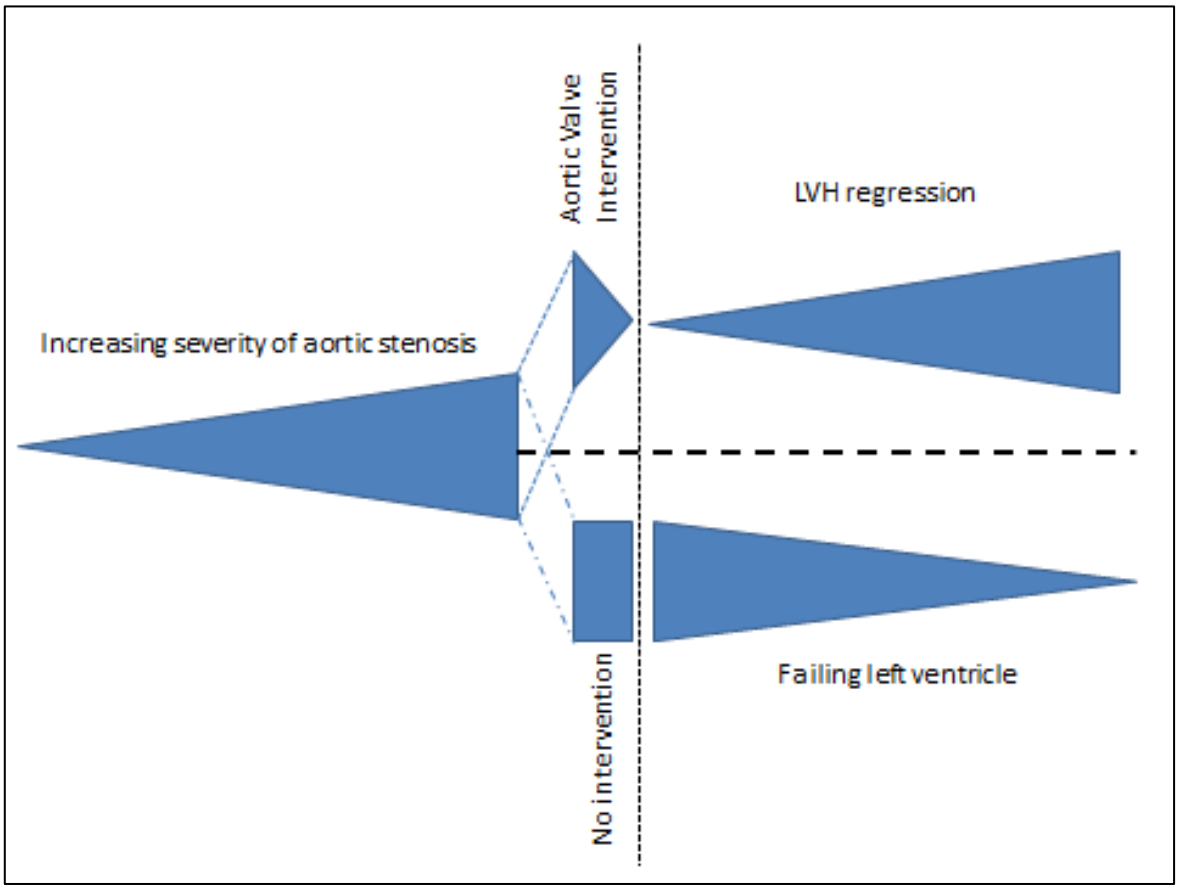

FIGURE 6-4. Suggested graphical representation of the backward expansion wave throughout the development and treatment of aortic stenosis.

There is a progressive increase in its value until it reaches a point when the LV is detrimentally ischaemic. At this point aortic valve intervention (TAVI or AVR) will result in a large decrease in its size followed by a steady increase with the regression of LVH. Alternatively, if no intervention occurs the left ventricle starts to fail and the backward expansion wave falls slowly and presumably irreversibly (see FIGURE 6-3)

6.4 MYOCARDIAL FIBROSIS VERSUS HYPERTROPHY

One other unanswered but interesting area of potential exploration is the distinction between myocardial fibrosis and hypertrophy. Whilst the two pathologies are present in aortic stenosis there appears to be a degree of variability and it may be that they respond differently following aortic valve intervention. One can imagine the hypertrophy can regress fully but fibrosis may be irreversible. This may create some variability in the response of the backward expansion wave following aortic valve replacement and may even account for some of the differences in the two patients above with coexisting severe left ventricular dysfunction. It also may explain why the relationship between worsening aortic stenosis and wave intensity is not entirely linear.

Therefore, a future direction of study would be in linking MRI data and outcome with wave-intensity analysis and discerning the effect of late-gadolinium enhancement changes from non-fibrotic hypertrophy and resultant wave intensity recovery following intervention. Additionally, discerning the differing effects of fibrosis and hypertrophy on wave-intensity expression would also be insightful.

6.5 WAVE INTENSITY ANALYSIS – CLINICAL APPLICATION

The potential for the use of wave-intensity analysis in the assessment of aortic stenosis is multi-faceted. Firstly, it obviously can provide a non-invasive assessment of left ventricular burden. The key theme throughout this thesis is that whilst simple echocardiographic measures of aortic stenosis severity are helpful in risk-quantification on a crude level, the left ventricle is influenced by many other factors as well (such as arterial impedance) and its response to this is also variable (varying degrees of

hypertrophy and/or fibrosis). Therefore, an assessment of the effect of aortic stenosis on the left ventricle is highly desirable in these patients and that is what wave intensity provides.

Additionally, I have demonstrated the use of non-invasive wave intensity analysis during exercise in patients with normal hearts and the effect of pacing on wave intensity analysis in patients with severe aortic stenosis. The next step could be to use non-invasive exercise wave-intensity measures as an assessment of myocardial reserve to aid in the appropriate timing of intervention particularly in asymptomatic patients or patients with moderate aortic stenosis. In patients with a fall in the backward expansion wave with exercise a move towards intervention would be appropriate; if the backward expansion wave is preserved or increased a more conservative strategy could be adopted.

Finally, it may also have a role in the assessment of low-flow low-gradient aortic stenosis where the left ventricle is failing and the flow is low. In these patients, it can be hard to discern whether the low flow rates through the valve are appropriate for the ventricular function or whether there is significant impaction from a severely stenotic but underestimated aortic valve. By assessing the ratio of cumulative-to-peak backward expansion wave intensity, it may be possible to recognise an energy reserve in the form of a preserved cumulative backward expansion wave and thus a high ratio. This is an area that obviously needs further exploration.

6.6 CONCLUSIONS

Aortic stenosis is a dynamic and variable disease state. The key feature of this condition is not the degree of back-pressure exerted by the aortic valve but how the left ventricle responds and adapts to this afterload. Wave-intensity analysis provides both an invasive and non-invasive way to assess the left ventricular load in these patients and therefore has the potential to provide a more accurate risk stratification and outcome prediction in these patients.

Non-invasive wave intensity has the advantage that unlike MRI it is relatively inexpensive and unlike stress testing it requires no inotropic action. Its disadvantage is in a relative high degree of technical skill to achieve accurate coronary-flow measurements. It is also not yet clear as to what effect coronary lesions would have on the wave-intensity profile and therefore it may not have a role in all patients or in those who have undergone previous bypass surgery.

However, I believe this thesis has greatly advanced our understanding at a technical level of the behaviour of the backward expansion wave and at a clinical level it may have a role in the assessment of individual patient risk in a variety of settings. Further work is encouraged in this field to elucidate the varying effects of valvular, arterial and hypertrophy on wave-intensity in these complex patients coupled with other modalities such as MRI and exercise echocardiography.

1985. Five-year findings of the Hypertension Detection and Follow-up Program. Prevention and reversal of left ventricular hypertrophy with antihypertensive drug therapy. Hypertension Detection and Follow-up Program Cooperative Group. *Hypertension,* 7**,** 105-12.

AGUADO-SIERRA, J., PARKER, K. H., DAVIES, J. E., FRANCIS, D., HUGHES, A. D. & MAYET, J. 2006. Arterial pulse wave velocity in coronary arteries. *Conf Proc IEEE Eng Med Biol Soc,* 1**,** 867-70.

AKAT, K., BORGGREFE, M. & KADEN, J. J. 2008. Aortic valve calcification - basic science to clinical practice. *Heart,* 95**,** 616-623.

ALYONO, D., ANDERSON, R. W., PARRISH, D. G., DAI, X. Z. & BACHE, R. J. 1986. Alterations of myocardial blood flow associated with experimental canine left ventricular hypertrophy secondary to valvular aortic stenosis. *Circulation Research,* 58**,** 47-57.

ANTONY, I., NITENBERG, A., FOULT, J. M. & APTECAR, E. 1993. Coronary vasodilator reserve in untreated and treated hypertensive patients with and without left ventricular hypertrophy. *Journal of the American College of Cardiology,* 22**,** 514-520.

ANVERSA, P., RICCI, R. & OLIVETTI, G. 1986. Coronary capillaries during normal and pathological growth. *Canadian Journal of Cardiology,* 2**,** 104-113.

ARONOW, W. S., AHN, C., SHIRANI, J. & KRONZON, I. 1999. Comparison of frequency of new coronary events in older subjects with and without valvular aortic sclerosis. *The American Journal of Cardiology,* 83**,** 599-600.

AZEVEDO, C. F., NIGRI, M., HIGUCHI, M. L., POMERANTZEFF, P. M., SPINA, G. S., SAMPAIO, R. O., TARASOUTCHI, F., GRINBERG, M. & ROCHITTE, C. E. 2010. Prognostic significance of myocardial fibrosis quantification by histopathology and magnetic resonance imaging in patients with severe aortic valve disease. *J Am Coll Cardiol,* 56**,** 278-87.

BACHE, R. J., VROBEL, T. R., ARENTZEN, C. E. & RING, W. S. 1981a. Effect of maximal coronary vasodilation on transmural myocardial perfusion during tachycardia in dogs with left ventricular hypertrophy. *Circulation Research,* 49**,** 742-750.

BACHE, R. J., VROBEL, T. R., RING, W. S., EMERY, R. W. & ANDERSEN, R. W. 1981b. Regional myocardial blood flow during exercise in dogs with chronic left ventricular hypertrophy. *Circulation Research,* 48**,** 76-87.

BAUMGARTNER, H., SCHIMA, H., TULZER, G. & KUHN, P. 1993. Effect of stenosis geometry on the Doppler-catheter gradient relation in vitro: a manifestation of pressure recovery. *J Am Coll Cardiol,* 21**,** 1018-25.

BAUMGARTNER, H., STEFENELLI, T., NIEDERBERGER, J., SCHIMA, H. & MAURER, G. 1999. "Overestimation" of catheter gradients by Doppler ultrasound in patients with aortic stenosis: a predictable manifestation of pressure recovery. *J Am Coll Cardiol,* 33**,** 1655-61.

BEN DOR, I., GOLDSTEIN, S. A., WAKSMAN, R., SATLER, L. F., LI, Y., SYED, A. I., MALUENDA, G., COLLINS, S. D., SUDDATH, W. O., TORGUSON, R., XUE, Z., KANESHIGE, K., OKUBAGZI, P., WANG, Z., KENT, K. M. & PICHARD, A. D. 2009. Effects of Percutaneous Aortic Valve Replacement on Coronary Blood Flow Assessed With Transesophageal Doppler Echocardiography in Patients With Severe Aortic Stenosis. *The American Journal of Cardiology,* 104**,** 850-855.

BERGLER-KLEIN, J., KLAAR, U., HEGER, M., ROSENHEK, R., MUNDIGLER, G., GABRIEL, H., BINDER, T., PACHER, R., MAURER, G. & BAUMGARTNER, H. 2004. Natriuretic Peptides Predict Symptom-Free Survival and Postoperative Outcome in Severe Aortic Stenosis. *Circulation,* 109**,** 2302-2308.

BIEDERMAN, R., MAGOVERN, J., GRANT, S., WILLIAMS, R., YAMROZIK, J., VIDO, D., RATHI, V., RAYARAO, G., CARUPPANNAN, K. & DOYLE, M. 2011. LV reverse remodeling imparted by

aortic valve replacement for severe aortic stenosis; is it durable? A cardiovascular MRI study sponsored by the American Heart Association. *Journal of Cardiothoracic Surgery,* 6**,** 53.

BIGLINO, G., SCHIEVANO, S., STEEDEN, J. A., NTSINJANA, H., BAKER, C., KHAMBADKONE, S., DE LEVAL, M. R., HSIA, T. Y., TAYLOR, A. M. & GIARDINI, A. 2012a. Reduced ascending aorta distensibility relates to adverse ventricular mechanics in patients with hypoplastic left heart syndrome: noninvasive study using wave intensity analysis. *J Thorac Cardiovasc Surg,* 144**,** 1307-13; discussion 1313-4.

BIGLINO, G., STEEDEN, J. A., BAKER, C., SCHIEVANO, S., TAYLOR, A. M., PARKER, K. H. & MUTHURANGU, V. 2012b. A non-invasive clinical application of wave intensity analysis based on ultrahigh temporal resolution phase-contrast cardiovascular magnetic resonance. *J Cardiovasc Magn Reson,* 14**,** 57.

BISHOP, S. P., POWELL, P. C., HASEBE, N., SHEN, Y. T., PATRICK, T. A., HITTINGER, L. & VATNER, S. F. 1996. Coronary Vascular Morphology in Pressure-overload Left Ventricular Hypertrophy. *Journal of Molecular and Cellular Cardiology,* 28**,** 141-154.

BLACHER, J., ASMAR, R., DJANE, S., LONDON, G. M. & SAFAR, M. E. 1999. Aortic Pulse Wave Velocity as a Marker of Cardiovascular Risk in Hypertensive Patients. *Hypertension,* 33**,** 1111-1117.

BLAIS, C., BURWASH, I. G., MUNDIGLER, G., DUMESNIL, J. G., LOHO, N., RADER, F., BAUMGARTNER, H., BEANLANDS, R. S., CHAYER, B., KADEM, L., GARCIA, D., DURAND, L.-G. & PIBAROT, P. 2006. Projected Valve Area at Normal Flow Rate Improves the Assessment of Stenosis Severity in Patients With Low-Flow, Low-Gradient Aortic Stenosis: The Multicenter TOPAS (Truly or Pseudo-Severe Aortic Stenosis) Study. *Circulation,* 113**,** 711-721.

BLEASDALE, R. A., MUMFORD, C. E., CAMPBELL, R. I., FRASER, A. G., JONES, C. J. & FRENNEAUX, M. P. 2003. Wave intensity analysis from the common carotid artery: a new noninvasive index of cerebral vasomotor tone. *Heart Vessels,* 18**,** 202-6.

BONOW, R. O., CARABELLO, B. A., CHATTERJEE, K., DE LEON, A. C., JR., FAXON, D. P., FREED, M. D., GAASCH, W. H., LYTLE, B. W., NISHIMURA, R. A., O'GARA, P. T., O'ROURKE, R. A., OTTO, C. M., SHAH, P. M. & SHANEWISE, J. S. 2008. 2008 Focused Update Incorporated Into the ACC/AHA 2006 Guidelines for the Management of Patients With Valvular Heart Disease: A Report of the American College of Cardiology/American Heart Association Task Force on Practice Guidelines (Writing Committee to Revise the 1998 Guidelines for the Management of Patients With Valvular Heart Disease): Endorsed by the Society of Cardiovascular Anesthesiologists, Society for Cardiovascular Angiography and Interventions, and Society of Thoracic Surgeons. *Circulation,* 118**,** e523-e661.

BONOW, R. O., DODD, J. T., MARON, B. J., O'GARA, P. T., WHITE, G. G., MCINTOSH, C. L., CLARK, R. E. & EPSTEIN, S. E. 1988. Long-term serial changes in left ventricular function and reversal of ventricular dilatation after valve replacement for chronic aortic regurgitation. *Circulation,* 78**,** 1108-1120.

BOUVIER, E., LOGEART, D., SABLAYROLLES, J.-L., FEIGNOUX, J., SCHEUBLÉ, C., TOUCHE, T., THABUT, G. & COHEN-SOLAL, A. 2006. Diagnosis of aortic valvular stenosis by multislice cardiac computed tomography. *European Heart Journal,* 27**,** 3033-3038.

BREISCH, E. A., WHITE, F. C., NIMMO, L. E. & BLOOR, C. M. 1986. Cardiac vasculature and flow during pressure-overload hypertrophy. *American Journal of Physiology - Heart and Circulatory Physiology,* 251**,** H1031-H1037.

BRIAND, M., DUMESNIL, J. G., KADEM, L., TONGUE, A. G., RIEU, R., GARCIA, D. & PIBAROT, P. 2005. Reduced Systemic Arterial Compliance Impacts Significantly on Left Ventricular Afterload and Function in Aortic Stenosis: Implications for Diagnosis and Treatment. *Journal of the American College of Cardiology,* 46**,** 291-298.

BRILLA, C. G., JANICKI, J. S. & WEBER, K. T. 1991a. Cardioreparative effects of lisinopril in rats with genetic hypertension and left ventricular hypertrophy. *Circulation,* 83**,** 1771-9.

BRILLA, C. G., JANICKI, J. S. & WEBER, K. T. 1991b. Impaired diastolic function and coronary reserve in genetic hypertension. Role of interstitial fibrosis and medial thickening of intramyocardial coronary arteries. *Circulation Research,* 69**,** 107-115.

BRUSH, J. E., CANNON, R. O., SCHENKE, W. H., BONOW, R. O., LEON, M. B., MARON, B. J. & EPSTEIN, S. E. 1988. Angina Due to Coronary Microvascular Disease in Hypertensive Patients without Left Ventricular Hypertrophy. *New England Journal of Medicine,* 319**,** 1302-1307.

BURKE, A. P., FARB, A., LIANG, Y. H., SMIALEK, J. & VIRMANI, R. 1996. Effect of hypertension and cardiac hypertrophy on coronary artery morphology in sudden cardiac death. *Circulation,* 94**,** 3138-45.

BURWASH, I. G., LORTIE, M., PIBAROT, P., DE KEMP, R. A., GRAF, S., MUNDIGLER, G., KHORSAND, A., BLAIS, C., BAUMGARTNER, H., DUMESNIL, J. G., HACHICHA, Z., DASILVA, J. & BEANLANDS, R. S. B. 2008. Myocardial blood flow in patients with low-flow, low-gradient aortic stenosis: differences between true and pseudo-severe aortic stenosis. Results from the multicentre TOPAS (Truly or Pseudo-Severe Aortic Stenosis) study. *Heart,* 94**,** 1627-1633.

CAIATI, C., MONTALDO, C., ZEDDA, N., MONTISCI, R., RUSCAZIO, M., LAI, G., CADEDDU, M., MELONI, L. & ILICETO, S. 1999. Validation of a new noninvasive method (contrast-enhanced transthoracic second harmonic echo Doppler) for the evaluation of coronary flow reserve: Comparison with intracoronary Doppler flow wire. *Journal of the American College of Cardiology,* 34**,** 1193-1200.

CAMICI, P., CHIRIATTI, G., LORENZONI, R., BELLINA, R. C., GISTRI, R., ITALIANI, G., PARODI, O., SALVADORI, P. A., NISTA, N., PAPI, L. & L'ABBATE, A. 1991. Coronary vasodilation is impaired in both hypertrophied and nonhypertrophied myocardium of patients with hypertrophic cardiomyopathy: A study with nitrogen-13 ammonia and positron emission tomography. *Journal of the American College of Cardiology,* 17**,** 879-886.

CARLUCCIO, E., TOMMASI, S., BENTIVOGLIO, M., BUCCOLIERI, M., FILIPPUCCI, L., PROSCIUTTI, L. & COREA, L. 2000. Prognostic value of left ventricular hypertrophy and geometry in patients with a first, uncomplicated myocardial infarction. *Int J Cardiol,* 74**,** 177-83.

CARPEGGIANI, C., NEGLIA, D., PARADOSSI, U., PRATALI, L., GLAUBER, M. & L'ABBATE, A. 2008a. Coronary flow reserve in severe aortic valve stenosis: a positron emission tomography study. *J Cardiovasc Med (Hagerstown),* 9**,** 893-8.

CARPEGGIANI, C., NEGLIA, D., PARADOSSI, U., PRATALI, L., GLAUBER, M. & L'ABBATE, A. 2008b. Coronary flow reserve in severe aortic valve stenosis: a positron emission tomography study. *Journal of Cardiovascular Medicine,* 9.

CARUTHERS, S. D., LIN, S. J., BROWN, P., WATKINS, M. P., WILLIAMS, T. A., LEHR, K. A. & WICKLINE, S. A. 2003. Practical Value of Cardiac Magnetic Resonance Imaging for Clinical Quantification of Aortic Valve Stenosis: Comparison With Echocardiography. *Circulation,* 108**,** 2236-2243.

CHAN, K. L., TEO, K., DUMESNIL, J. G., NI, A., TAM, J. & FOR THE, A. I. 2010. Effect of Lipid Lowering With Rosuvastatin on Progression of Aortic Stenosis. *Circulation,* 121**,** 306-314.

CHANDRA, H. R., GOLDSTEIN, J. A., CHOUDHARY, N., O'NEILL, C. S., GEORGE, P. B., GANGASANI, S. R., CRONIN, L., MARCOVITZ, P. A., HAUSER, A. M. & O'NEILL, W. W. 2004. Adverse outcome in aortic sclerosis is associated with coronary artery disease and inflammation. *Journal of the American College of Cardiology,* 43**,** 169-175.

CHEMLA, D., ANTONY, I., LECARPENTIER, Y. & NITENBERG, A. 2003. Contribution of systemic vascular resistance and total arterial compliance to effective arterial elastance in humans. *Am J Physiol Heart Circ Physiol,* 285**,** H614-20.

CHUA, D. & KALB, K. 2006. Statins and Progression of Calcified Aortic Stenosis. *The Annals of Pharmacotherapy,* 40**,** 2195-2199.

CHUN, E. J., CHOI, S. I., LIM, C., PARK, K. H., CHANG, H. J., CHOI, D. J., KIM, D. H., LEE, W. & PARK, J. H. 2008. Aortic stenosis: evaluation with multidetector CT angiography and MR imaging. *Korean J Radiol,* 9**,** 439-48.

CONNOLLY, H. M., OH, J. K., SCHAFF, H. V., ROGER, V. L., OSBORN, S. L., HODGE, D. O. & TAJIK, A. J. 2000. Severe Aortic Stenosis With Low Transvalvular Gradient and Severe Left Ventricular Dysfunction: Result of Aortic Valve Replacement in 52 Patients. *Circulation,* 101**,** 1940-1946.

CORTIGIANI, L., RIGO, F., GHERARDI, S., BOVENZI, F., MOLINARO, S., PICANO, E. & SICARI, R. 2012. Coronary flow reserve during dipyridamole stress echocardiography predicts mortality. *JACC Cardiovasc Imaging,* 5**,** 1079-85.

COUTINHO, T., TURNER, S. T. & KULLO, I. J. 2011. Aortic Pulse Wave Velocity Is Associated With Measures of Subclinical Target Organ Damage. *JACC: Cardiovascular Imaging,* 4**,** 754-761.

COWELL, S. J., NEWBY, D. E., PRESCOTT, R. J., BLOOMFIELD, P., REID, J., NORTHRIDGE, D. B. & BOON, N. A. 2005. A Randomized Trial of Intensive Lipid-Lowering Therapy in Calcific Aortic Stenosis. *New England Journal of Medicine,* 352**,** 2389-2397.

CRABOS, M., COSTE, P., PACCALIN, M., TARIOSSE, L., DARET, D., BESSE, P. & BONORON-ADÈLE, S. 1997. Reduced Basal NO-mediated Dilation and Decreased Endothelial NO-synthase Expression in Coronary Vessels of Spontaneously Hypertensive Rats. *Journal of Molecular and Cellular Cardiology,* 29**,** 55-65.

CUEFF, C., SERFATY, J.-M., CIMADEVILLA, C., LAISSY, J.-P., HIMBERT, D., TUBACH, F., DUVAL, X., IUNG, B., ENRIQUEZ-SARANO, M., VAHANIAN, A. & MESSIKA-ZEITOUN, D. 2011. Measurement of aortic valve calcification using multislice computed tomography: correlation with haemodynamic severity of aortic stenosis and clinical implication for patients with low ejection fraction. *Heart,* 97**,** 721-726.

DAIMON, M., WATANABE, H., YAMAGISHI, H., MURO, T., AKIOKA, K., HIRATA, K., TAKEUCHI, K. & YOSHIKAWA, J. 2001. Physiologic assessment of coronary artery stenosis by coronary flow reserve measurements with transthoracic doppler echocardiography: comparison with exercise thallium-201 single-photon emission computed tomography. *Journal of the American College of Cardiology,* 37**,** 1310-1315.

DAVIES, J. E., SEN, S., BROYD, C., HADJILOIZOU, N., BAKSI, J., FRANCIS, D. P., FOALE, R. A., PARKER, K. H., HUGHES, A. D., CHUKWUEMEKA, A., CASULA, R., MALIK, I. S., MIKHAIL, G. W. & MAYET, J. 2011. Arterial Pulse Wave Dynamics After Percutaneous Aortic Valve Replacement / Clinical Perspective. *Circulation,* 124**,** 1565-1572.

DAVIES, J. E., WHINNETT, Z. I., FRANCIS, D. P., MANISTY, C. H., AGUADO-SIERRA, J., WILLSON, K., FOALE, R. A., MALIK, I. S., HUGHES, A. D., PARKER, K. H. & MAYET, J. 2006a. Evidence of a Dominant Backward-Propagating "Suction" Wave Responsible for Diastolic Coronary Filling in Humans, Attenuated in Left Ventricular Hypertrophy. *Circulation,* 113**,** 1768-1778.

DAVIES, J. E., WHINNETT, Z. I., FRANCIS, D. P., WILLSON, K., FOALE, R. A., MALIK, I. S., HUGHES, A. D., PARKER, K. H. & MAYET, J. 2006b. Use of simultaneous pressure and velocity measurements to estimate arterial wave speed at a single site in humans. *American Journal of Physiology - Heart and Circulatory Physiology,* 290**,** H878-H885.

DEBL, K., DJAVIDANI, B., BUCHNER, S., LIPKE, C., NITZ, W., FEUERBACH, S., RIEGGER, G. & LUCHNER, A. 2006. Delayed hyperenhancement in magnetic resonance imaging of left ventricular hypertrophy caused by aortic stenosis and hypertrophic cardiomyopathy: visualisation of focal fibrosis. *Heart,* 92**,** 1447-51.

DEBL, K., DJAVIDANI, B., SEITZ, J., NITZ, W., SCHMID, F. X., MUDERS, F., BUCHNER, S., FEUERBACH, S., RIEGGER, G. & LUCHNER, A. 2005. Planimetry of aortic valve area in aortic stenosis by magnetic resonance imaging. *Invest Radiol,* 40**,** 631-6.

DEVEREUX, R. B., WACHTELL, K., GERDTS, E. & ET AL. 2004. PRognostic significance of left ventricular mass change during treatment of hypertension. *JAMA,* 292**,** 2350-2356.

DRAZNER, M. H., RAME, J. E., MARINO, E. K., GOTTDIENER, J. S., KITZMAN, D. W., GARDIN, J. M., MANOLIO, T. A., DRIES, D. L. & SISCOVICK, D. S. 2004. Increased left ventricular mass is a risk factor for the development of a depressed left ventricular ejection fraction within five years: the Cardiovascular Health Study. *J Am Coll Cardiol,* 43**,** 2207-15.

DUNCKER, D. J. & BACHE, R. J. 2008. Regulation of Coronary Blood Flow During Exercise. *Physiological Reviews,* 88**,** 1009-1086.

DWECK, M., JOSHI, S., MURIGU, T., GULATI, A., ALPENDURADA, F., JABBOUR, A., MACEIRA, A., ROUSSIN, I., NORTHRIDGE, D., KILNER, P., COOK, S., BOON, N., PEPPER, J., MOHIADDIN, R., NEWBY, D., PENNELL, D. & PRASAD, S. 2012a. Left ventricular remodeling and hypertrophy in patients with aortic stenosis: insights from cardiovascular magnetic resonance. *Journal of Cardiovascular Magnetic Resonance,* 14**,** 50.

DWECK, M. R., JONES, C., JOSHI, N. V., FLETCHER, A. M., RICHARDSON, H., WHITE, A., MARSDEN, M., PESSOTTO, R., CLARK, J. C., WALLACE, W. A., SALTER, D. M., MCKILLOP, G., VAN BEEK, E. J., BOON, N. A., RUDD, J. H. & NEWBY, D. E. 2012b. Assessment of valvular calcification and inflammation by positron emission tomography in patients with aortic stenosis. *Circulation,* 125**,** 76-86.

EBERLI, RITTER, M., SCHWITTER, J., BORTONE, A., SCHNEIDER, J., HESS, O. M. & KRAYENBUEHL, H. P. 1991. Coronary reserve in patients with aortic valve disease before and after successful aortic valve replacement. *European Heart Journal,* 12**,** 127-138.

ECKER, T., GOBEL, C., HULLIN, R., RETTIG, R., SEITZ, G. & HOFMANN, F. 1989. Decreased cardiac concentration of cGMP kinase in hypertensive animals. An index for cardiac vascularization? *Circulation Research,* 65**,** 1361-1369.

EICHENBERGER, A. C., JENNI, R. & VON SCHULTHESS, G. K. 1993. Aortic valve pressure gradients in patients with aortic valve stenosis: quantification with velocity-encoded cine MR imaging. *AJR Am J Roentgenol,* 160**,** 971-7.

ESPOSITO, G., RAPACCIUOLO, A., NAGA PRASAD, S. V., TAKAOKA, H., THOMAS, S. A., KOCH, W. J. & ROCKMAN, H. A. 2002. Genetic Alterations That Inhibit In Vivo Pressure-Overload Hypertrophy Prevent Cardiac Dysfunction Despite Increased Wall Stress. *Circulation,* 105**,** 85-92.

ESTAFANOUS, F. G., TARAZI, R. C., BUCKLEY, S. & TAYLOR, P. C. 1978. Arterial hypertension in immediate postoperative period after valve replacement. *British Heart Journal,* 40**,** 718-724.

FAIRBAIRN, T. A., STEADMAN, C. D., MATHER, A. N., MOTWANI, M., BLACKMAN, D. J., PLEIN, S., MCCANN, G. P. & GREENWOOD, J. P. 2013. Assessment of valve haemodynamics, reverse ventricular remodelling and myocardial fibrosis following transcatheter aortic valve implantation compared to surgical aortic valve replacement: a cardiovascular magnetic resonance study. *Heart,* 99**,** 1185-91.

FALLEN, E. L., ELLIOTT, W. C. & GORLIN, R. I. C. H. 1967. Mechanisms of Angina in Aortic Stenosis. *Circulation,* 36**,** 480-488.

FEUCHTNER, G. M., DICHTL, W., FRIEDRICH, G. J., FRICK, M., ALBER, H., SCHACHNER, T., BONATTI, J., MALLOUHI, A., FREDE, T., PACHINGER, O., ZUR NEDDEN, D. & MULLER, S. 2006. Multislice computed tomography for detection of patients with aortic valve stenosis and quantification of severity. *J Am Coll Cardiol,* 47**,** 1410-7.

FEUCHTNER, G. M., MULLER, S., BONATTI, J., SCHACHNER, T., VELIK-SALCHNER, C., PACHINGER, O. & DICHTL, W. 2007. Sixty-four slice CT evaluation of aortic stenosis using planimetry of the aortic valve area. *AJR Am J Roentgenol,* 189**,** 197-203.

FIFER, M. A., BOURDILLON, P. D. & LORELL, B. H. 1986. Altered left ventricular diastolic properties during pacing-induced angina in patients with aortic stenosis. *Circulation,* 74**,** 675-83.

FLEWITT, J. A., HOBSON, T. N., WANG, J., JOHNSTON, C. R., SHRIVE, N. G., BELENKIE, I., PARKER, K. H. & TYBERG, J. V. 2007. Wave intensity analysis of left ventricular filling: application of windkessel theory. *American Journal of Physiology - Heart and Circulatory Physiology,* 292**,** H2817-H2823.

FUSEJIMA, K. 1987. Noninvasive measurement of coronary artery blood flow using combined two-dimensional and Doppler echocardiography. *Journal of the American College of Cardiology,* 10**,** 1024-1031.

GAASCH, W. H. 1979. Left ventricular radius to wall thickness ratio. *The American Journal of Cardiology,* 43**,** 1189-1194.

GALIUTO, L., LOTRIONTE, M., CREA, F., ANSELMI, A., BIONDI-ZOCCAI, G. G. L., DE GIORGIO, F., BALDI, A., BALDI, F., POSSATI, G., GAUDINO, M., VETROVEC, G. W. & ABBATE, A. 2006. Impaired coronary and myocardial flow in severe aortic stenosis is associated with increased apoptosis: a transthoracic Doppler and myocardial contrast echocardiography study. *Heart,* 92**,** 208-212.

GALIUTO, L., SESTITO, A., BARCHETTA, S., SGUEGLIA, G. A., INFUSINO, F., LA ROSA, C., LANZA, G. & CREA, F. 2007. Noninvasive Evaluation of Flow Reserve in the Left Anterior Descending Coronary Artery in Patients With Cardiac Syndrome X. *The American Journal of Cardiology,* 99**,** 1378-1383.

GARCIA, D., CAMICI, P. G., DURAND, L. G., RAJAPPAN, K., GAILLARD, E., RIMOLDI, O. E. & PIBAROT, P. 2009. Impairment of coronary flow reserve in aortic stenosis. *Journal of Applied Physiology,* 106**,** 113-121.

GARCIA, D., PIBAROT, P., DUMESNIL, J. G., SAKR, F. & DURAND, L.-G. 2000. Assessment of Aortic Valve Stenosis Severity: A New Index Based on the Energy Loss Concept. *Circulation,* 101**,** 765-771.

GARDIN, J. M., MCCLELLAND, R., KITZMAN, D., LIMA, J. A., BOMMER, W., KLOPFENSTEIN, H. S., WONG, N. D., SMITH, V. E. & GOTTDIENER, J. 2001. M-mode echocardiographic predictors of six- to seven-year incidence of coronary heart disease, stroke, congestive heart failure, and mortality in an elderly cohort (the Cardiovascular Health Study). *Am J Cardiol,* 87**,** 1051-7.

GAUDINO, M., ALESSANDRINI, F., GLIECA, F., LUCIANI, N., CELLINI, C., PRAGLIOLA, C., MORELLI, M., CANOSA, C., NASSO, G. & POSSATI, G. 2005. Survival after aortic valve replacement for aortic stenosis: does left ventricular mass regression have a clinical correlate? *European Heart Journal,* 26**,** 51-57.

GERBER, I. L., STEWART, R. A., LEGGET, M. E., WEST, T. M., FRENCH, R. L., SUTTON, T. M., YANDLE, T. G., FRENCH, J. K., RICHARDS, A. M. & WHITE, H. D. 2003. Increased plasma natriuretic peptide levels reflect symptom onset in aortic stenosis. *Circulation,* 107**,** 1884-90.

GOULD, K. L. & CARABELLO, B. A. 2003. Why Angina in Aortic Stenosis With Normal Coronary Arteriograms? *Circulation,* 107**,** 3121-3123.

GRADMAN, A. H. & ALFAYOUMI, F. 2003. From Left Ventricular Hypertrophy to Congestive Heart Failure: Management of Hypertensive Heart Disease. *Progress in Cardiovascular Diseases,* 48**,** 326-341.

GRIGGS, D. M., CHEN, C. C. & TCHOKOEV, V. V. 1973. Subendocardial anaerobic metabolism in experimental aortic stenosis. *American Journal of Physiology -- Legacy Content,* 224**,** 607-612.

GROSSMAN, W., JONES, D. & MCLAURIN, L. P. 1975. Wall stress and patterns of hypertrophy in the human left ventricle. *The Journal of Clinical Investigation,* 56**,** 56-64.

HACHICHA, Z., DUMESNIL, J. G., BOGATY, P. & PIBAROT, P. 2007. Paradoxical Low-Flow, Low-Gradient Severe Aortic Stenosis Despite Preserved Ejection Fraction Is Associated With Higher Afterload and Reduced Survival. *Circulation,* 115**,** 2856-2864.

HACHICHA, Z., DUMESNIL, J. G. & PIBAROT, P. 2009. Usefulness of the valvuloarterial impedance to predict adverse outcome in asymptomatic aortic stenosis. *J Am Coll Cardiol,* 54**,** 1003-11.

HADJILOIZOU, N., DAVIES, J. E., MALIK, I. S., AGUADO-SIERRA, J., WILLSON, K., FOALE, R. A., PARKER, K. H., HUGHES, A. D., FRANCIS, D. P. & MAYET, J. 2008. Differences in cardiac microcirculatory wave patterns between the proximal left mainstem and proximal right coronary artery. *American Journal of Physiology - Heart and Circulatory Physiology,* 295**,** H1198-H1205.

HAIDER, A. W., LARSON, M. G., BENJAMIN, E. J. & LEVY, D. 1998. Increased left ventricular mass and hypertrophy are associated with increased risk for sudden death. *J Am Coll Cardiol,* 32**,** 1454-9.

HAMASAKI, S., AL SUWAIDI, J., HIGANO, S. T., MIYAUCHI, K., HOLMES, D. R., JR. & LERMAN, A. 2000. Attenuated coronary flow reserve and vascular remodeling in patients with hypertension and left ventricular hypertrophy. *J Am Coll Cardiol,* 35**,** 1654-60.

HEIN, S., ARNON, E., KOSTIN, S., SCHONBURG, M., ELSASSER, A., POLYAKOVA, V., BAUER, E. P., KLOVEKORN, W. P. & SCHAPER, J. 2003. Progression from compensated hypertrophy to failure in the pressure-overloaded human heart: structural deterioration and compensatory mechanisms. *Circulation,* 107**,** 984-91.

HILDICK-SMITH, D. J. R. & SHAPIRO, L. M. 2000. Coronary flow reserve improves after aortic valve replacement for aortic stenosis: an adenosine transthoracic echocardiography study. *Journal of the American College of Cardiology,* 36**,** 1889-1896.

HILL, J. A., KARIMI, M., KUTSCHKE, W., DAVISSON, R. L., ZIMMERMAN, K., WANG, Z., KERBER, R. E. & WEISS, R. M. 2000. Cardiac Hypertrophy Is Not a Required Compensatory Response to Short-Term Pressure Overload. *Circulation,* 101**,** 2863-2869.

HOLLANDER, E. H., WANG, J. J., DOBSON, G. M., PARKER, K. H. & TYBERG, J. V. 2001. Negative wave reflections in pulmonary arteries. *Am J Physiol Heart Circ Physiol,* 281**,** H895-902.

HORSTKOTTE, D. & LOOGEN, F. 1988. The natural history of aortic valve stenosis. *European Heart Journal,* 9**,** 57-64.

HOZUMI, T., YOSHIDA, K., AKASAKA, T., ASAMI, Y., OGATA, Y., TAKAGI, T., KAJI, S., KAWAMOTO, T., UEDA, Y. & MORIOKA, S. 1998a. Noninvasive assessment of coronary flow velocity and coronary flow velocity reserve in the left anterior descending coronary artery by Doppler echocardiography: Comparison with invasive technique. *Journal of the American College of Cardiology,* 32**,** 1251-1259.

HOZUMI, T., YOSHIDA, K., OGATA, Y., AKASAKA, T., ASAMI, Y., TAKAGI, T. & MORIOKA, S. 1998b. Noninvasive Assessment of Significant Left Anterior Descending Coronary Artery Stenosis by Coronary Flow Velocity Reserve With Transthoracic Color Doppler Echocardiography. *Circulation,* 97**,** 1557-1562.

HUTCHISON, S. J., SHEN, A., SOLDO, S., HLA, A., KAWANISHI, D. T. & CHANDRARATNA, P. A. 1996. Transesophageal assessment of coronary flow velocity reserve during â€œregularâ€ and â€œhighâ€-dose dipyridamole stress testing. *The American Journal of Cardiology,* 77**,** 1164-1168.

ILICETO, S., MARANGELLI, V., MEMMOLA, C. & RIZZON, P. 1991. Transesophageal Doppler echocardiography evaluation of coronary blood flow velocity in baseline conditions and during dipyridamole-induced coronary vasodilation. *Circulation,* 83**,** 61-9.

ISAAZ, K., BRUNTZ, J. F., PARIS, D., ETHEVENOT, G. & ALIOT, E. 1994. Abnormal coronary flow velocity pattern in patients with left ventricular hypertrophy, angina pectoris, and normal coronary arteries: A transesophageal Doppler echocardiographic study. *American Heart Journal,* 128**,** 500-510.

ISHIHARA, K., ZILE, M. R., NAGATSU, M., NAKANO, K., TOMITA, M., KANAZAWA, S., CLAMP, L., DEFREYTE, G. & CARABELLO, B. A. 1992. Coronary blood flow after the regression of pressure-overload left ventricular hypertrophy. *Circulation Research,* 71**,** 1472-81.

ITO, N., ISOYAMA, S., TAKAHASHI, T. & TAKISHIMA, T. 1993. Coronary Dilator Reserve and Morphological Changes After Relief of Pressure-overload in Rats. *Journal of Molecular and Cellular Cardiology,* 25**,** 3-14.

JOHN, A. S., DILL, T., BRANDT, R. R., RAU, M., RICKEN, W., BACHMANN, G. & HAMM, C. W. 2003. Magnetic resonance to assess the aortic valve area in aortic stenosisHow does it compare to current diagnostic standards? *Journal of the American College of Cardiology,* 42**,** 519-526.

JULIUS, B. K., SPILLMANN, M., VASSALLI, G., VILLARI, B., EBERLI, F. R. & HESS, O. M. 1997. Angina Pectoris in Patients With Aortic Stenosis and Normal Coronary Arteries: Mechanisms and Pathophysiological Concepts. *Circulation,* 95**,** 892-898.

JUST, H., FREY, M. & ZEHENDER, M. 1996. Calcium antagonist drugs in hypertensive patients with angina pectoris. *European Heart Journal,* 17**,** 20-24.

KADEM, L., DUMESNIL, J. G., RIEU, R., DURAND, L. G., GARCIA, D. & PIBAROT, P. 2005. Impact of systemic hypertension on the assessment of aortic stenosis. *Heart,* 91**,** 354-361.

KALKMAN, E. A. J., BILGIN, Y. M., HAREN, P. V., SUYLEN, R. J. V., SAXENA, P. R. & SCHOEMAKER, R. G. 1996. Determinants of coronary reserve in rats subjected to coronary artery ligation or aortic banding. *Cardiovascular Research,* 32**,** 1088-1095.

KANG, D. H., PARK, S. J., RIM, J. H., YUN, S. C., KIM, D. H., SONG, J. M., CHOO, S. J., PARK, S. W., SONG, J. K., LEE, J. W. & PARK, P. W. 2010. Early Surgery Versus Conventional Treatment in Asymptomatic Very Severe Aortic Stenosis. *Circulation,* 121**,** 1502-1509.

KASSAB, G. S., GREGERSEN, H., NIELSEN, S. L., LU, X., TANKO, L. B. & FALK, E. 2002. Remodelling of the left anterior descending artery in a porcine model of supravalvular aortic stenosis. *Journal of Hypertension,* 20.

KATO, Y., SUEHIRO, S., SHIBATA, T., SASAKI, Y. & HIRAI, H. 2007. Impact of Valve Prosthesis-Patient Mismatch on Long-Term Survival and Left Ventricular Mass Regression After Aortic Valve Replacement for Aortic Stenosis. *Journal of Cardiac Surgery,* 22**,** 314-319.

KAUFMANN, P. A. & CAMICI, P. G. 2005. Myocardial Blood Flow Measurement by PET: Technical Aspects and Clinical Applications. *Journal of Nuclear Medicine,* 46**,** 75-88.

KAWAMOTO, R., IMAMURA, T., KAWABATA, K., DATE, H., ISHIKAWA, T., MAENO, M., NAGOSHI, T., FUJIURA, Y., MATSUYAMA, A., MATSUO, T., KOIWAYA, Y. & ETO, T. 2001. Microvascular angina in a patient with aortic stenosis. *Jpn Circ J,* 65**,** 839-41.

KELLY, T. A., ROTHBART, R. M., COOPER, C. M., KAISER, D. L., SMUCKER, M. L. & GIBSON, R. S. 1988. Comparison of outcome of asymptomatic to symptomatic patients older than 20 years of age with valvular aortic stenosis. *The American Journal of Cardiology,* 61**,** 123-130.

KENNEDY, K. D., NISHIMURA, R. A., HOLMES, D. R., JR. & BAILEY, K. R. 1991. Natural history of moderate aortic stenosis. *Journal of the American College of Cardiology,* 17**,** 313-319.

KENNY, A., WISBEY, C. R. & SHAPIRO, L. M. 1994. Profiles of coronary blood flow velocity in patients with aortic stenosis and the effect of valve replacement: a transthoracic echocardiographic study. *Br Heart J,* 71**,** 57-62.

KHIR, A. W., HENEIN, M. Y., KOH, T., DAS, S. K., PARKER, K. H. & GIBSON, D. G. 2001. Arterial waves in humans during peripheral vascular surgery. *Clin Sci (Lond),* 101**,** 749-57.

KHIR, A. W. & PARKER, K. H. 2002. Measurements of wave speed and reflected waves in elastic tubes and bifurcations. *J Biomech,* 35**,** 775-83.

KHIR, A. W. & PARKER, K. H. 2005. Wave intensity in the ascending aorta: effects of arterial occlusion. *Journal of biomechanics,* 38**,** 647-655.

KILNER, P. J., MANZARA, C. C., MOHIADDIN, R. H., PENNELL, D. J., SUTTON, M. G., FIRMIN, D. N., UNDERWOOD, S. R. & LONGMORE, D. B. 1993. Magnetic resonance jet velocity mapping in mitral and aortic valve stenosis. *Circulation,* 87**,** 1239-48.

KINGSBURY, M., MAHNKE, A., TURNER, M. & SHERIDAN, D. 2002. Recovery of coronary function and morphology during regression of left ventricular hypertrophy. *Cardiovascular Research,* 55**,** 83-96.

KINGSBURY, M. P., TURNER, M. A., FLORES, N. A., BOVILL, E. & SHERIDAN, D. J. 2000. Endogenous and Exogenous Coronary Vasodilatation are Attenuated in Cardiac Hypertrophy: a Morphological Defect? *Journal of Molecular and Cellular Cardiology,* 32**,** 527-538.

KITAI, T., HONDA, S., OKADA, Y., TANI, T., KIM, K., KAJI, S., EHARA, N., KINOSHITA, M., KOBORI, A., YAMAMURO, A., KITA, T. & FURUKAWA, Y. 2011. Clinical outcomes in non-surgically managed patients with very severe versus severe aortic stenosis. *Heart*.

KOLYVA, C., SPAAN, J. A., PIEK, J. J. & SIEBES, M. 2008. Windkesselness of coronary arteries hampers assessment of human coronary wave speed by single-point technique. *Am J Physiol Heart Circ Physiol,* 295**,** H482-90.

KOREN, M. J., DEVEREUX, R. B., CASALE, P. N., SAVAGE, D. D. & LARAGH, J. H. 1991. Relation of left ventricular mass and geometry to morbidity and mortality in uncomplicated essential hypertension. *Ann Intern Med,* 114**,** 345-52.

KOYANAGI, S., EASTHAM, C. L., HARRISON, D. G. & MARCUS, M. L. 1982. Increased size of myocardial infarction in dogs with chronic hypertension and left ventricular hypertrophy. *Circulation Research,* 50**,** 55-62.

KRAYENBUEHL, H. P., HESS, O. M., MONRAD, E. S., SCHNEIDER, J., MALL, G. & TURINA, M. 1989. Left ventricular myocardial structure in aortic valve disease before, intermediate, and late after aortic valve replacement. *Circulation,* 79**,** 744-55.

KUME, T., AKASAKA, T., KAWAMOTO, T., WATANABE, N., YOSHITANI, H., AKIYAMA, M., KOYAMA, Y., NEISHI, Y., WADA, N. & YOSHIDA, K. 2004. [Mechanisms of impaired coronary flow reserve in patients with aortic stenosis: transthoracic Doppler echocardiographic study]. *J Cardiol,* 43**,** 173-8.

KUPARI, M., TURTO, H. & LOMMI, J. 2005. Left ventricular hypertrophy in aortic valve stenosis: preventive or promotive of systolic dysfunction and heart failure? *European Heart Journal,* 26**,** 1790-1796.

KUPARI, M., VIRTANEN, K. S., TURTO, H., VIITASALO, M., MÄNTTÄRI, M., LINDROOS, M., KOSKELA, E., LEINONEN, H., POHJOLA-SINTONEN, S. & HEIKKILÄ, J. 1992. Exclusion of coronary artery disease by exercise thallium-201 tomography in patients with aortic valve stenosis. *The American Journal of Cardiology,* 70**,** 635-640.

KUPFAHL, C., HONOLD, M., MEINHARDT, G., VOGELSBERG, H., WAGNER, A., MAHRHOLDT, H. & SECHTEM, U. 2004. Evaluation of aortic stenosis by cardiovascular magnetic resonance imaging: comparison with established routine clinical techniques. *Heart,* 90**,** 893-901.

LA MANNA, A., SANFILIPPO, A., CAPODANNO, D., SALEMI, A., CADONI, A., CASCONE, I., POLIZZI, G., FIGUERA, M., PITTALA, R., PRIVITERA, C. & TAMBURINO, C. 2013. Left ventricular reverse remodeling after transcatheter aortic valve implantation: a cardiovascular magnetic resonance study. *Journal of Cardiovascular Magnetic Resonance,* 15**,** 39.

LANCELLOTTI, P., DONAL, E., MAGNE, J., MOONEN, M., O'CONNOR, K., DAUBERT, J.-C. & PIERARD, L. A. 2010a. Risk stratification in asymptomatic moderate to severe aortic stenosis: the importance of the valvular, arterial and ventricular interplay. *Heart,* 96**,** 1364-1371.

LANCELLOTTI, P., DONAL, E., MAGNE, J., O'CONNOR, K., MOONEN, M. L., COSYNS, B. & PIERARD, L. A. 2010b. Impact of global left ventricular afterload on left ventricular function in asymptomatic severe aortic stenosis: a two-dimensional speckle-tracking study. *European Journal of Echocardiography,* 11**,** 537-543.

LANG, R. M., BIERIG, M., DEVEREUX, R. B., FLACHSKAMPF, F. A., FOSTER, E., PELLIKKA, P. A., PICARD, M. H., ROMAN, M. J., SEWARD, J., SHANEWISE, J. S., SOLOMON, S. D., SPENCER, K. T., ST JOHN SUTTON, M. & STEWART, W. J. 2005. Recommendations for Chamber Quantification: A Report from the American Society of Echocardiography's Guidelines and Standards Committee and the Chamber Quantification Writing Group, Developed in Conjunction with the European Association of Echocardiography, a Branch of the European Society of Cardiology. *Journal of the American Society of Echocardiography : official publication of the American Society of Echocardiography,* 18**,** 1440-1463.

LEON, M. B., SMITH, C. R., MACK, M., MILLER, D. C., MOSES, J. W., SVENSSON, L. G., TUZCU, E. M., WEBB, J. G., FONTANA, G. P., MAKKAR, R. R., BROWN, D. L., BLOCK, P. C., GUYTON, R. A., PICHARD, A. D., BAVARIA, J. E., HERRMANN, H. C., DOUGLAS, P. S., PETERSEN, J. L., AKIN, J. J., ANDERSON, W. N., WANG, D. & POCOCK, S. 2010. Transcatheter Aortic-Valve Implantation for Aortic Stenosis in Patients Who Cannot Undergo Surgery. *New England Journal of Medicine,* 363**,** 1597-1607.

LETHEN, H., TRIES, H. P., KERSTING, S. & LAMBERTZ, H. 2003a. Validation of noninvasive assessment of coronary flow velocity reserve in the right coronary artery. *European Heart Journal,* 24**,** 1567-1575.

LETHEN, H., TRIES, H. P., KERSTING, S. & LAMBERTZ, H. 2003b. Validation of noninvasive assessment of coronary flow velocity reserve in the right coronary artery: A comparison of transthoracic

echocardiographic results with intracoronary Doppler flow wire measurements. *European Heart Journal,* 24**,** 1567-1575.

LEVINE, R. A., JIMOH, A., CAPE, E. G., MCMILLAN, S., YOGANATHAN, A. P. & WEYMAN, A. E. 1989. Pressure recovery distal to a stenosis: Potential cause of gradient "verestimation" by Doppler echocardiography. *Journal of the American College of Cardiology,* 13**,** 706-715.

LEVY, D., ANDERSON, K. M., SAVAGE, D. D., BALKUS, S. A., KANNEL, W. B. & CASTELLI, W. P. 1987. Risk of ventricular arrhythmias in left ventricular hypertrophy: The Framingham Heart Study. *The American Journal of Cardiology,* 60**,** 560-565.

LEVY, D., GARRISON, R. J., SAVAGE, D. D., KANNEL, W. B. & CASTELLI, W. P. 1989. Left ventricular mass and incidence of coronary heart disease in an elderly cohort. The Framingham Heart Study. *Ann Intern Med,* 110**,** 101-7.

LEVY, D., GARRISON, R. J., SAVAGE, D. D., KANNEL, W. B. & CASTELLI, W. P. 1990. Prognostic Implications of Echocardiographically Determined Left Ventricular Mass in the Framingham Heart Study. *New England Journal of Medicine,* 322**,** 1561-1566.

LEVY, D., SALOMON, M., D'AGOSTINO, R. B., BELANGER, A. J. & KANNEL, W. B. 1994. Prognostic implications of baseline electrocardiographic features and their serial changes in subjects with left ventricular hypertrophy. *Circulation,* 90**,** 1786-93.

LEVY, F., LUC MONIN, J., RUSINARU, D., PETIT-EISENMANN, H., LELGUEN, C., CHAUVEL, C., ADAMS, C., METZ, D., LELEU, F., GUERET, P. & TRIBOUILLOY, C. 2011. Valvuloarterial impedance does not improve risk stratification in low-ejection fraction, low-gradient aortic stenosis: results from a multicentre study. *European Journal of Echocardiography,* 12**,** 358-363.

LI, Y. & GUO, L. 2013. Clinical value of carotid wave intensity analysis for differentiating nonobstructive hypertrophic cardiomyopathy from left ventricular hypertrophy secondary to systemic hypertension. *J Clin Ultrasound,* 41**,** 151-7.

LIN, A. C. W., LOWE, A., SIDHU, K., HARRISON, W., RUYGROK, P. & STEWART, R. 2012. Evaluation of a novel sphygmomanometer, which estimates central aortic blood pressure from analysis of brachial artery suprasystolic pressure waves. *Journal of Hypertension,* 30**,** 1743-1750 10.1097/HJH.0b013e3283567b94.

LINDROOS, M., KUPARI, M., HEIKKILA, J. & TILVIS, R. 1993. Prevalence of aortic valve abnormalities in the elderly: An echocardiographic study of a random population sample. *Journal of the American College of Cardiology,* 21**,** 1220-1225.

LOCKIE, T. P., ROLANDI, M. C., GUILCHER, A., PERERA, D., DE SILVA, K., WILLIAMS, R., ASRRESS, K. N., PATEL, K., PLEIN, S., CHOWIENCZYK, P., SIEBES, M., REDWOOD, S. R. & MARBER, M. S. 2012. Synergistic adaptations to exercise in the systemic and coronary circulations that underlie the warm-up angina phenomenon. *Circulation,* 126**,** 2565-74.

LOWE, A., HARRISON, W., EL-AKLOUK, E., RUYGROK, P. & AL-JUMAILY, A. M. 2009. Non-invasive model-based estimation of aortic pulse pressure using suprasystolic brachial pressure waveforms. *Journal of Biomechanics,* 42**,** 2111-2115.

LU, P. J., YANG, C. F., WU, M. Y., HUNG, C. H., CHAN, M. Y. & HSU, T. C. 2012. Wave intensity analysis of para-aortic counterpulsation. *Am J Physiol Heart Circ Physiol,* 302**,** H1481-91.

MACMAHON, S., COLLINS, G., RAUTAHARJU, P., CUTLER, J., NEATON, J., PRINEAS, R., CROW, R. & STAMLER, J. 1989. Electrocardiographic left ventricular hypertrophy and effects of antihypertensive drug therapy in hypertensive participants in the Multiple Risk Factor Intervention Trial. *Am J Cardiol,* 63**,** 202-10.

MANISTY, C. H., ZAMBANINI, A., PARKER, K. H., DAVIES, J. E., FRANCIS, D. P., MAYET, J., MCG THOM, S. A., HUGHES, A. D. & INVESTIGATORS, O. B. O. T. A.-S. C. O. T. 2009. Differences in the Magnitude of Wave Reflection Account for Differential Effects of Amlodipine- Versus Atenolol-Based Regimens on Central Blood Pressure: An Anglo-Scandinavian Cardiac Outcome Trial Substudy. *Hypertension,* 54**,** 724-730.

MARCUS, M. L., DOTY, D. B., HIRATZKA, L. F., WRIGHT, C. B. & EASTHAM, C. L. 1982. Decreased Coronary Reserve - A Mechanism for Angina Pectoris in Patients with Aortic Stenosis and Normal Coronary Arteries. *New England Journal of Medicine,* 307**,** 1362-1366.

MARECHAUX, S., ENNEZAT, P. V., LEJEMTAL, T. H., POLGE, A. S., DE GROOTE, P., NEVIERE, R., LE TOURNEAU, T. & DEKLUNDER, G. 2007. Left ventricular response to exercise in aortic stenosis: an exercise echocardiographic study. *Echocardiography,* 24**,** 955-959.

MARÉCHAUX, S., HACHICHA, Z., BELLOUIN, A., DUMESNIL, J. G., MEIMOUN, P., PASQUET, A., BERGERON, S., ARSENAULT, M., LE TOURNEAU, T., ENNEZAT, P. V. & PIBAROT, P. 2010. Usefulness of exercise-stress echocardiography for risk stratification of true asymptomatic patients with aortic valve stenosis. *European Heart Journal,* 31**,** 1390-1397.

MATHEW, J., SLEIGHT, P., LONN, E., JOHNSTONE, D., POGUE, J., YI, Q., BOSCH, J., SUSSEX, B., PROBSTFIELD, J., YUSUF, S. & INVESTIGATORS, F. T. H. O. P. E. 2001. Reduction of Cardiovascular Risk by Regression of Electrocardiographic Markers of Left Ventricular Hypertrophy by the Angiotensin-Converting Enzyme Inhibitor Ramipril. *Circulation,* 104**,** 1615-1621.

MATTACE-RASO, F. U. S., VAN DER CAMMEN, T. J. M., HOFMAN, A., VAN POPELE, N. M., BOS, M. L., SCHALEKAMP, M. A. D. H., ASMAR, R., RENEMAN, R. S., HOEKS, A. P. G., BRETELER, M. M. B. & WITTEMAN, J. C. M. 2006. Arterial Stiffness and Risk of Coronary Heart Disease and Stroke: The Rotterdam Study. *Circulation,* 113**,** 657-663.

MAZZONE, A., EPISTOLATO, M. C., DE CATERINA, R., STORTI, S., VITTORINI, S., SBRANA, S., GIANETTI, J., BEVILACQUA, S., GLAUBER, M., BIAGINI, A. & TANGANELLI, P. 2004. Neoangiogenesis, T-lymphocyte infiltration, and heat shock protein-60 are biological hallmarks of an immunomediated inflammatory process in end-stage calcified aortic valve stenosis. *Journal of the American College of Cardiology,* 43**,** 1670-1676.

MCAINSH, A. M., TURNER, M. A., O'HARE, D., NITHYTHYANANTHAN, R., JOHNSTON, D. G., O'GORMAN, D. J. & SHERIDAN, D. J. 1995. Cardiac hypertrophy impairs recovery from ischaemia because there is a reduced reactive hyperaemic response. *Cardiovascular Research,* 30**,** 113-121.

MCCANN, G. P., STEADMAN, C. D., RAY, S. G., NEWBY, D. E. & ON BEHALF OF THE BRITISH HEART VALVE, S. 2011. Managing the asymptomatic patient with severe aortic stenosis: randomised controlled trials of early surgery are overdue. *Heart,* 97**,** 1119-1121.

MCGIFFIN, D. C., O'BRIEN, M. F., GALBRAITH, A. J., MCLACHLAN, G. J., STAFFORD, E. G., GARDNER, M. A., POHLNER, P. G., EARLY, L. & KEAR, L. 1993. An analysis of risk factors for death and mode-specific death after aortic valve replacement with allograft, xenograft, and mechanical valves. *J Thorac Cardiovasc Surg,* 106**,** 895-911.

MCGOLDRICK, R. B., KINGSBURY, M., TURNER, M. A., SHERIDAN, D. J. & HUGHES, A. D. 2007. Left ventricular hypertrophy induced by aortic banding impairs relaxation of isolated coronary arteries. *Clinical Science,* 113**,** 473-478.

MEHTA, R. H., BRUCKMAN, D., DAS, S., TSAI, T., RUSSMAN, P., KARAVITE, D., MONAGHAN, H., SONNAD, S., SHEA, M. J., EAGLE, K. A. & DEEB, G. M. 2001. Implications of increased left ventricular mass index on in-hospital outcomes in patients undergoing aortic valve surgery. *J Thorac Cardiovasc Surg,* 122**,** 919-28.

MEIMOUN, P., GERMAIN, A. L., ELMKIES, F., BENALI, T., BOULANGER, J., ESPANEL, C., CLERC, J., ZEMIR, H., LUYCX-BORE, A. & TRIBOUILLOY, C. 2012. Factors associated with noninvasive coronary flow reserve in severe aortic stenosis. *J Am Soc Echocardiogr,* 25**,** 835-41.

MEIMOUN, P., MALAQUIN, D. E., BENALI, T., BOULANGER, J., ZEMIR, H., SAYAH, S., LUYCX-BORE, A., DOUTRELAN, L. & TRIBOUILLOY, C. 2009. Non-Invasive Coronary Flow Reserve After Successful Primary Angioplasty for Acute Anterior Myocardial Infarction Is an Independent Predictor of Left Ventricular Recovery and In-Hospital Cardiac Events. *Journal of the American Society of Echocardiography,* 22**,** 1071-1079.

MIHALJEVIC, T., PAUL, S., COHN, L. H. & WECHSLER, A. 2003. Pathophysiology of aortic valve disease. *Cardiac Surgery in the Adult.* New York McGraw-Hil

MIYAGAWA, S., MASAI, T., FUKUDA, H., YAMAUCHI, T., IWAKURA, K., ITOH, H. & SAWA, Y. 2009. Coronary Microcirculatory Dysfunction in Aortic Stenosis: Myocardial Contrast Echocardiography Study. *The Annals of Thoracic Surgery,* 87**,** 715-719.

MIZUNO, R., FUJIMOTO, S., SAITO, Y. & OKAMOTO, Y. 2012. Optimal Antihypertensive Level for Improvement of Coronary Microvascular Dysfunction: The Lower, the Better? *Hypertension,* 60**,** 326-332.

MONIN, J. L., MONCHI, M., GEST, V., DUVAL-MOULIN, A. M., DUBOIS-RANDE, J. L. & GUERET, P. 2001. Aortic stenosis with severe left ventricular dysfunction and low transvalvular pressure gradients: risk stratification by low-dose dobutamine echocardiography. *J Am Coll Cardiol,* 37**,** 2101-7.

MONRAD, E. S., HESS, O. M., MURAKAMI, T., NONOGI, H., CORIN, W. J. & KRAYENBUEHL, H. P. 1988. Time course of regression of left ventricular hypertrophy after aortic valve replacement. *Circulation,* 77**,** 1345-1355.

MORITA, S., OCHIAI, Y., TANOUE, Y., HISAHARA, M., MASUDA, M. & YASUI, H. 2003. Acute volume reduction with aortic valve replacement immediately improves ventricular mechanics in patients with aortic regurgitation. *The Journal of Thoracic and Cardiovascular Surgery,* 125**,** 283-289.

MOTZ, W. & STRAUER, B. E. 1996. Improvement of Coronary Flow Reserve After Long-term Therapy With Enalapril. *Hypertension,* 27**,** 1031-1038.

MOURA, L. M., RAMOS, S. F., ZAMORANO, J. L., BARROS, I. M., AZEVEDO, L. F., ROCHA-GONÇALVES, F. & RAJAMANNAN, N. M. 2007. Rosuvastatin Affecting Aortic Valve Endothelium to Slow the Progression of Aortic Stenosis. *Journal of the American College of Cardiology,* 49**,** 554-561.

MUELLER, T. M., MARCUS, M. L., KERBER, R. E., YOUNG, J. A., BARNES, R. W. & ABBOUD, F. M. 1978. Effect of renal hypertension and left ventricular hypertrophy on the coronary circulation in dogs. *Circulation Research,* 42**,** 543-549.

MUIESAN, M. L., SALVETTI, M., PAINI, A., MONTEDURO, C., ROSEI, C. A., AGGIUSTI, C., BELOTTI, E., BERTACCHINI, F., GALBASSINI, G., STASSALDI, D., CASTELLANO, M. & ROSEI, E. A. 2010. Pulse wave velocity and cardiovascular risk stratification in a general population: the Vobarno study. *J Hypertens,* 28**,** 1935-43.

NAKANO, K., CORIN, W. J., SPANN, J. F., JR., BIEDERMAN, R. W., DENSLOW, S. & CARABELLO, B. A. 1989. Abnormal subendocardial blood flow in pressure overload hypertrophy is associated with pacing-induced subendocardial dysfunction. *Circulation Research,* 65**,** 1555-1564.

NEMES, A., FORSTER, T., KOVACS, Z., THURY, A., UNGI, I. & CSANADY, M. 2002. The effect of aortic valve replacement on coronary flow reserve in patients with a normal coronary angiogram. *Herz,* 27**,** 780-4.

NG, A. C., DELGADO, V., BERTINI, M., ANTONI, M. L., VAN BOMMEL, R. J., VAN RIJNSOEVER, E. P., VAN DER KLEY, F., EWE, S. H., WITKOWSKI, T., AUGER, D., NUCIFORA, G., SCHUIJF, J. D., POLDERMANS, D., LEUNG, D. Y., SCHALIJ, M. J. & BAX, J. J. 2011. Alterations in multidirectional myocardial functions in patients with aortic stenosis and preserved ejection fraction: a two-dimensional speckle tracking analysis. *Eur Heart J,* 32**,** 1542-50.

NIEDERBERGER, J., SCHIMA, H., MAURER, G. & BAUMGARTNER, H. 1996. Importance of Pressure Recovery for the Assessment of Aortic Stenosis by Doppler Ultrasound: Role of Aortic Size, Aortic Valve Area, and Direction of the Stenotic Jet In Vitro. *Circulation,* 94**,** 1934-1940.

NUNEZ, E., HOSOYA, K., SUSIC, D. & FROHLICH, E. D. 1997. Enalapril and Losartan Reduced Cardiac Mass and Improved Coronary Hemodynamics in SHR. *Hypertension,* 29**,** 519-524.

O'GORMAN, D. J., THOMAS, P., TURNER, M. A. & SHERIDAN, D. J. 1992. Investigation of impaired coronary vasodilator reserve in the guinea pig heart with pressure induced hypertrophy. *European Heart Journal,* 13**,** 697-703.

O'ROURKE, M. F., STAESSEN, J. A., VLACHOPOULOS, C., DUPREZ, D. & PLANTE, G. E. 2002. Clinical applications of arterial stiffness; definitions and reference values. *Am J Hypertens,* 15**,** 426-44.

O'SULLIVAN, C. J., STORTECKY, S., HEG, D., PILGRIM, T., HOSEK, N., BUELLESFELD, L., KHATTAB, A. A., NIETLISPACH, F., MOSCHOVITIS, A., ZANCHIN, T., MEIER, B., WINDECKER, S. & WENAWESER, P. 2013. Clinical outcomes of patients with low-flow, low-gradient, severe aortic stenosis and either preserved or reduced ejection fraction undergoing transcatheter aortic valve implantation. *European Heart Journal*.

OKIN, P. M., WACHTELL, K., DEVEREUX, R. B., HARRIS, K. E., JERN, S., KJELDSEN, S. E., JULIUS, S., LINDHOLM, L. H., NIEMINEN, M. S., EDELMAN, J. M., HILLE, D. A. & DAHLOF, B. 2006. Regression of electrocardiographic left ventricular hypertrophy and decreased incidence of new-onset atrial fibrillation in patients with hypertension. *JAMA,* 296**,** 1242-8.

OMRAN, H., FEHSKE, W. & RABIHIEH, R. 2011. Relationship between symptoms and profile of coronary artery blood flow velocities in patients with aortic valve stenosis: a study using transoesophageal echocardiography. *Heart,* 75**,** 377-383.

OMRAN, H., SCHMIDT, H., HACKENBROCH, M., ILLIEN, S., BERNHARDT, P., DER RECKE, G., FIMMERS, R., FLACKE, S., LAYER, G., POHL, C., LÜDERITZ, B., SCHILD, H. & SOMMER, T. 2003. Silent and apparent cerebral embolism after retrograde catheterisation of the aortic valve in valvular stenosis: a prospective, randomised study. *The Lancet,* 361**,** 1241-1246.

OPHERK, D., MALL, G., ZEBE, H., SCHWARZ, F., WEIHE, E., MANTHEY, J. & KUBLER, W. 1984. Reduction of coronary reserve: a mechanism for angina pectoris in patients with arterial hypertension and normal coronary arteries. *Circulation,* 69**,** 1-7.

ORSINELL, D. A., AURIGEMMA, G. P., BATTISTA, S., KRENDEL, S. & GAASCH, W. H. 1993. Left ventricular hypertrophy and mortality after aortic valve replacement for aortic stenosisA high risk subgroup identified by preoperative ralation wall thickness. *Journal of the American College of Cardiology,* 22**,** 1679-1683.

OTTO, C. M., BURWASH, I. G., LEGGET, M. E., MUNT, B. I., FUJIOKA, M., HEALY, N. L., KRAFT, C. D., MIYAKE-HULL, C. Y. & SCHWAEGLER, R. G. 1997. Prospective Study of Asymptomatic Valvular Aortic Stenosis : Clinical, Echocardiographic, and Exercise Predictors of Outcome. *Circulation,* 95**,** 2262-2270.

OTTO, C. M., LIND, B. K., KITZMAN, D. W., GERSH, B. J. & SISCOVICK, D. S. 1999. Association of Aortic-Valve Sclerosis with Cardiovascular Mortality and Morbidity in the Elderly. *New England Journal of Medicine,* 341**,** 142-147.

PARKER, K. H. 2009. An introduction to wave intensity analysis. *Med Biol Eng Comput,* 47**,** 175-88.

PARODI, O., NEGLIA, D., PALOMBO, C., SAMBUCETI, G., GIORGETTI, A., MARABOTTI, C., GALLOPIN, M., SIMONETTI, I. & L'ABBATE, A. 1997. Comparative Effects of Enalapril and Verapamil on Myocardial Blood Flow in Systemic Hypertension. *Circulation,* 96**,** 864-873.

PATEL, A. K., YAP, V. U. & THOMSEN, J. H. 1977. ADverse effects of right ventricular pacing in a patient with aortic stenosis, hemodynamic documentation and management. *CHEST Journal,* 72**,** 103-105.

PAULUS, W. J., HEYNDRICKX, G. R., NELLENS, P. & ANDRIES, E. 1988. Impaired relaxation of the hypertrophied left ventricle in aortic stenosis: effects of aortic valvuloplasty and of postextrasystolic potentiation. *European Heart Journal,* 9**,** 25-30.

PAYNE, R. A. & WEBB, D. J. 2008. Peripheral Augmentation Index: Shouldering the Central Pressure Load. *Hypertension,* 51**,** 37-38.

PENNY, D. J., MYNARD, J. P. & SMOLICH, J. J. 2008. Aortic wave intensity analysis of ventricular-vascular interaction during incremental dobutamine infusion in adult sheep. *American Journal of Physiology - Heart and Circulatory Physiology,* 294**,** H481-H489.

PEREIRA, J. J., LAUER, M. S., BASHIR, M., AFRIDI, I., BLACKSTONE, E. H., STEWART, W. J., MCCARTHY, P. M., THOMAS, J. D. & ASHER, C. R. 2002. Survival after aortic valve replacement for severe

aortic stenosis with low transvalvular gradients and severe left ventricular dysfunction. *J Am Coll Cardiol,* 39**,** 1356-63.

PETROPOULAKIS, P. N., KYRIAKIDIS, M. K., TENTOLOURIS, C. A., KOUROUCLIS, C. V. & TOUTOUZAS, P. K. 1995. Changes in Phasic Coronary Blood Flow Velocity Profile in Relation to Changes in Hemodynamic Parameters During Stress in Patients With Aortic Valve Stenosis. *Circulation,* 92**,** 1437-1447.

PIJLS, N. H. J., VAN GELDER, B., VAN DER VOORT, P., PEELS, K., BRACKE, F. A. L. E., BONNIER, H. J. R. M. & EL GAMAL, M. I. H. 1995. Fractional Flow Reserve: A Useful Index to Evaluate the Influence of an Epicardial Coronary Stenosis on Myocardial Blood Flow. *Circulation,* 92**,** 3183-3193.

PIRAT, B., BOZBAS, H., SIMSEK, V., YILDIRIR, A., SADE, L. E., GURSOY, Y., ALTIN, C., ATAR, I. & MUDERRISOGLU, H. 2008. Impaired coronary flow reserve in patients with metabolic syndrome. *Atherosclerosis,* 201**,** 112-116.

PIZZUTO, F., VOCI, P., MARIANO, E., EMILIO PUDDU, P., SARDELLA, G. & NIGRI, A. 2001. Assessment of flow velocity reserve by transthoracic Doppler echocardiography and venous adenosine infusion before and after left anterior descending coronary artery stenting. *Journal of the American College of Cardiology,* 38**,** 155-162.

POULSEN, S. H., SOGAARD, P., NIELSEN-KUDSK, J. E. & EGEBLAD, H. 2007. Recovery of left ventricular systolic longitudinal strain after valve replacement in aortic stenosis and relation to natriuretic peptides. *J Am Soc Echocardiogr,* 20**,** 877-84.

PURCELL, H. J. & KALRA, P. R. 2011. *Cardiology volume 2.* Elsevier Mosby

RAFIQUE, A. M., BINER, S., RAY, I., FORRESTER, J. S., TOLSTRUP, K. & SIEGEL, R. J. 2009. Meta-Analysis of Prognostic Value of Stress Testing in Patients With Asymptomatic Severe Aortic Stenosis. *The American Journal of Cardiology,* 104**,** 972-977.

RAJAMANNAN, N. M., SUBRAMANIAM, M., SPRINGETT, M., SEBO, T. C., NIEKRASZ, M., MCCONNELL, J. P., SINGH, R. J., STONE, N. J., BONOW, R. O. & SPELSBERG, T. C. 2002. Atorvastatin Inhibits Hypercholesterolemia-Induced Cellular Proliferation and Bone Matrix Production in the Rabbit Aortic Valve. *Circulation,* 105**,** 2660-2665.

RAJANI, R., RIMINGTON, H. & CHAMBERS, J. B. 2010. Treadmill exercise in apparently asymptomatic patients with moderate or severe aortic stenosis: relationship between cardiac index and revealed symptoms. *Heart,* 96**,** 689-695.

RAJAPPAN, K., RIMOLDI, O. E., CAMICI, P. G., BELLENGER, N. G., PENNELL, D. J. & SHERIDAN, D. J. 2003. Functional Changes in Coronary Microcirculation After Valve Replacement in Patients With Aortic Stenosis. *Circulation,* 107**,** 3170-3175.

RAJAPPAN, K., RIMOLDI, O. E., DUTKA, D. P., ARIFF, B., PENNELL, D. J., SHERIDAN, D. J. & CAMICI, P. G. 2002. Mechanisms of Coronary Microcirculatory Dysfunction in Patients With Aortic Stenosis and Angiographically Normal Coronary Arteries. *Circulation,* 105**,** 470-476.

RAKUSAN, K., FLANAGAN, M. F., GEVA, T., SOUTHERN, J. & VAN PRAAGH, R. 1992. Morphometry of human coronary capillaries during normal growth and the effect of age in left ventricular pressure-overload hypertrophy. *Circulation,* 86**,** 38-46.

REANT, P., LEDERLIN, M., LAFITTE, S., SERRI, K., MONTAUDON, M., CORNELOUP, O., ROUDAUT, R. & LAURENT, F. 2006. Absolute assessment of aortic valve stenosis by planimetry using cardiovascular magnetic resonance imaging: comparison with transesophageal echocardiography, transthoracic echocardiography, and cardiac catheterisation. *Eur J Radiol,* 59**,** 276-83.

REDBERG, R. F., SOBOL, Y., CHOU, T. M., MALLOY, M., KUMAR, S., BOTVINICK, E. & KANE, J. 1995. Adenosine-Induced Coronary Vasodilatation During Transesophageal Doppler Echocardiography : Rapid and Safe Measurement of Coronary Flow Reserve Ratio Can Predict Significant Left Anterior Descending Coronary Stenosis. *Circulation,* 92**,** 190-196.

RIALS, S. J., WU, Y., XU, X., FILART, R. A., MARINCHAK, R. A. & KOWEY, P. R. 1997. Regression of left ventricular hypertrophy with captopril restores normal ventricular action potential duration,

dispersion of refractoriness, and vulnerability to inducible ventricular fibrillation. *Circulation,* 96**,** 1330-6.

RIGO, F. 2005. Coronary flow reserve in stress-echo lab. From pathophysiologic toy to diagnostic tool. *Cardiovascular Ultrasound,* 3**,** 8.

RIGO, F., CORTIGIANI, L., GHERARDI, S., SICARI, R., GALDERISI, M., BOVENZI, F. & PICANO, E. 2007. Coronary Microvascular Dysfunction and Prognosis in Hypertrophic Cardiomyopathy: a Doppler Echocardiography Study. *Circulation,* 116**,** 369-369.

RIGO, F., GHERARDI, S., GALDERISI, M., PRATALI, L., CORTIGIANI, L., SICARI, R. & PICANO, E. 2006. The prognostic impact of coronary flow-reserve assessed by Doppler echocardiography in non-ischaemic dilated cardiomyopathy. *European Heart Journal,* 27**,** 1319-1323.

RIGO, F., MURER, B., OSSENA, G. & FAVARETTO, E. 2008. Transthoracic echocardiographic imaging of coronary arteries: tips, traps, and pitfalls. *Cardiovascular Ultrasound,* 6**,** 7.

RIGO, F., TONA, F. R., CATI, A., GROLLA, E., DJORDJEVIC-DIKIC, A., SARAIS, C., MILORAD TESIC, T. & ILIECTO, S. 2010. Coronary flow velocity assessment on left anterior coronary artery as a marker of atherosclerosis: reliability and accuracy of transthoracic echocardiographic study compared to Doppler flow wire. *European Heart Journal,* 31**,** 254-254.

RODRIGUEZ-PORCEL, M., ZHU, X. Y., CHADE, A. R., AMORES-ARRIAGA, B., CAPLICE, N. M., RITMAN, E. L., LERMAN, A. & LERMAN, L. O. 2006. Functional and structural remodeling of the myocardial microvasculature in early experimental hypertension. *American Journal of Physiology - Heart and Circulatory Physiology,* 290**,** H978-H984.

ROGERS, W. J., HU, Y.-L., COAST, D., VIDO, D. A., KRAMER, C. M., PYERITZ, R. E. & REICHEK, N. 2001. Age-associated changes in regional aortic pulse wave velocity. *Journal of the American College of Cardiology,* 38**,** 1123-1129.

ROSENHEK, R., BINDER, T., PORENTA, G., LANG, I., CHRIST, G., SCHEMPER, M., MAURER, G. & BAUMGARTNER, H. 2001. Predictors of Outcome in Severe, Asymptomatic Aortic Stenosis. *New England Journal of Medicine,* 343**,** 611-617.

ROSENHEK, R., KLAAR, U., SCHEMPER, M., SCHOLTEN, C., HEGER, M., GABRIEL, H., BINDER, T., MAURER, G. & BAUMGARTNER, H. 2004. Mild and moderate aortic stenosis: Natural history and risk stratification by echocardiography. *European Heart Journal,* 25**,** 199-205.

ROSENHEK, R., ZILBERSZAC, R., SCHEMPER, M., CZERNY, M., MUNDIGLER, G., GRAF, S., BERGLER-KLEIN, J., GRIMM, M., GABRIEL, H. & MAURER, G. 2010. Natural History of Very Severe Aortic Stenosis. *Circulation,* 121**,** 151-156.

ROSS, J., JR. & BRAUNWALD, E. 1968. Aortic Stenosis. *Circulation,* 38**,** V-61.

ROSS, J. J., JR., MINTZ, G. S. & CHANDRASEKARAN, K. 1990. Transthoracic two-dimensional high frequency (7.5 MHz) ultrasonic visualization of the distal left anterior descending coronary artery. *Journal of the American College of Cardiology,* 15**,** 373-377.

RUDOLPH, A., ABDEL-ATY, H., BOHL, S., BOYE, P., ZAGROSEK, A., DIETZ, R. & SCHULZ-MENGER, J. 2009. Noninvasive detection of fibrosis applying contrast-enhanced cardiac magnetic resonance in different forms of left ventricular hypertrophy relation to remodeling. *J Am Coll Cardiol,* 53**,** 284-91.

RUSCAZIO, M., MONTISCI, R., COLONNA, P., CAIATI, C., CHEN, L., LAI, G., CADEDDU, M., PIRISI, R. & ILICETO, S. 2002. Detection of coronary restenosis aftercoronary angioplasty by contrast-enhanced transthoracic echocardiographic Doppler assessment of coronary flow velocity reserve. *Journal of the American College of Cardiology,* 40**,** 896-903.

SATO, F., ISOYAMA, S. & TAKISHIMA, T. 1990. Normalization of impaired coronary circulation in hypertrophied rat hearts. *Hypertension,* 16**,** 26-34.

SAVITZKY, A. & GOLAY, M. J. E. 1964. Smoothing and Differentiation of Data by Simplified Least Squares Procedures. *Analytical Chemistry,* 36**,** 1627-1639.

SCHELER, S., MOTZ, W. & STRAUER, B. E. 1992. Transient myocardial ischaemia in hypertensives: missing link with left ventricular hypertrophy. *European Heart Journal,* 13**,** 62-65.

SCHILLACI, G., VERDECCHIA, P., PORCELLATI, C., CUCCURULLO, O., COSCO, C. & PERTICONE, F. 2000. Continuous Relation Between Left Ventricular Mass and Cardiovascular Risk in Essential Hypertension. *Hypertension,* 35**,** 580-586.

SCHLOSSER, T., MALYAR, N., JOCHIMS, M., BREUCKMANN, F., HUNOLD, P., BRUDER, O., ERBEL, R. & BARKHAUSEN, J. 2007. Quantification of aortic valve stenosis in MRI-comparison of steady-state free precession and fast low-angle shot sequences. *Eur Radiol,* 17**,** 1284-90.

SCHÖBEL, W. A., VOELKER, W., HAASE, K. K. & KARSCH, K.-R. 1999. Extent, determinants and clinical importance of pressure recovery in patients with aortic valve stenosis. *European Heart Journal,* 20**,** 1355-1363.

SCHWAMMENTHAL, E., VERED, Z., MOSHKOWITZ, Y., RABINOWITZ, B., ZISKIND, Z., SMOLINSKI, A. K. & FEINBERG, M. S. 2001. Dobutamine echocardiography in patients with aortic stenosis and left ventricular dysfunction: predicting outcome as a function of management strategy. *Chest,* 119**,** 1766-77.

SCHWARTZKOPFF, B., FRENZEL, H., DIEKERHOFF, J., BETZ, P., FLASSHOVE, M., SCHULTE, H. D., MUNDHENKE, M., MOTZ, W. & STRAUER, B. E. 1992. Morphometric investigation of human myocardium in arterial hypertension and valvular aortic stenosis. *European Heart Journal,* 13**,** 17-23.

SEBASTIA, C., QUIROGA, S., BOYE, R., PEREZ-LAFUENTE, M., CASTELLA, E. & ALVAREZ-CASTELLS, A. 2003. Aortic stenosis: spectrum of diseases depicted at multisection CT. *Radiographics,* 23 Spec No**,** S79-91.

SEN, S., ESCANED, J., MALIK, I. S., MIKHAIL, G. W., FOALE, R. A., MILA, R., TARKIN, J., PETRACO, R., BROYD, C., JABBOUR, R., SETHI, A., BAKER, C. S., BELLAMY, M., AL-BUSTAMI, M., HACKETT, D., KHAN, M., LEFROY, D., PARKER, K. H., HUGHES, A. D., FRANCIS, D. P., DI MARIO, C., MAYET, J. & DAVIES, J. E. 2012. Development and Validation of a New Adenosine-Independent Index of Stenosis Severity From Coronary Wave–Intensity Analysis: Results of the ADVISE (ADenosine Vasodilator Independent Stenosis Evaluation) Study. *Journal of the American College of Cardiology,* 59**,** 1392-1402.

SILVA, K. D., GUILCHER, A., LOCKIE, T., MARBER, M., REDWOOD, S., PLEIN, S. & PERERA, D. 2012. CORONARY WAVE INTENSITY: A NOVEL INVASIVE TOOL FOR PREDICTING MYOCARDIAL VIABILITY FOLLOWING ACUTE CORONARY SYNDROMES. *Journal of the American College of Cardiology,* 59**,** E421-E421.

SIMONSON, E. & NAKAGAWA, K. 1960. Effect of Age on Pulse Wave Velocity and "Aortic Ejection Time" in Healthy Men and in Men with Coronary Artery Disease. *Circulation,* 22**,** 126-129.

SKALIDIS, E. I. & VARDAS, P. E. 2008. Coronary blood flow and flow reserve in aortic stenosis: effect of aortic valve therapy. *Hellenic J Cardiol,* 49**,** 379-381.

SMISETH, O. A., THOMPSON, C. R., LOHAVANICHBUTR, K., LING, H., ABEL, J. G., MIYAGISHIMA, R. T., LICHTENSTEIN, S. V. & BOWERING, J. 1999. The pulmonary venous systolic flow pulse—its origin and relationship to left atrial pressure. *Journal of the American College of Cardiology,* 34**,** 802-809.

SMUCKER, M. L., TEDESCO, C. L., MANNING, S. B., OWEN, R. M. & FELDMAN, M. D. 1988. Demonstration of an imbalance between coronary perfusion and excessive load as a mechanism of ischemia during stress in patients with aortic stenosis. *Circulation,* 78**,** 573-82.

SONDERGAARD, L., HILDEBRANDT, P., LINDVIG, K., THOMSEN, C., STAHLBERG, F., KASSIS, E. & HENRIKSEN, O. 1993. Valve area and cardiac output in aortic stenosis: quantification by magnetic resonance velocity mapping. *Am Heart J,* 126**,** 1156-64.

SPAAN, J. A., BREULS, N. P. & LAIRD, J. D. 1981. Diastolic-systolic coronary flow differences are caused by intramyocardial pump action in the anesthetized dog. *Circulation Research,* 49**,** 584-593.

STEADMAN, C. D., JEROSCH-HEROLD, M., GRUNDY, B., RAFELT, S., NG, L. L., SQUIRE, I. B., SAMANI, N. J. & MCCANN, G. P. 2012. Determinants and Functional Significance of Myocardial Perfusion Reserve in Severe Aortic Stenosis. *JACC: Cardiovascular Imaging,* 5**,** 182-189.

STODDARD, M. F., PRINCE, C. R. & MORRIS, G. T. 1995. Coronary flow reserve assessment by dobutamine transesophageal doppler echocardiography. *Journal of the American College of Cardiology,* 25**,** 325-332.

STROHM, O., SCHULZ-MENGER, J., HANLEIN, D., DIETZ, R. & FRIEDRICH, M. G. 2001. Magnetic resonance planimetry of the vena contracta as a new approach to assessment of stenotic heart valves: an in vitro study. *J Magn Reson Imaging,* 14**,** 31-4.

SUN, Y. H., ANDERSON, T. J., PARKER, K. H. & TYBERG, J. V. 2000. Wave-intensity analysis: a new approach to coronary hemodynamics. *Journal of Applied Physiology,* 89**,** 1636-1644.

SUN, Y. H., ANDERSON, T. J., PARKER, K. H. & TYBERG, J. V. 2004. Effects of left ventricular contractility and coronary vascular resistance on coronary dynamics. *American Journal of Physiology - Heart and Circulatory Physiology,* 286**,** H1590-H1595.

SUNAGAWA, K., MAUGHAN, W. L., BURKHOFF, D. & SAGAWA, K. 1983. Left ventricular interaction with arterial load studied in isolated canine ventricle. *Am J Physiol,* 245**,** H773-80.

TAAMS, M. A., GUSSENHOVEN, E. J., CORNEL, J. H., THE, S. H. K., ROELANDT, J. R. T. C., LANC+‰E, C. T. & BRAND, M. V. D. 1988. Detection of left coronary artery stenosis by transoesophageal echocardiography. *European Heart Journal,* 9**,** 1162-1166.

TOMANEK, R. J., WANGLER, R. D. & BAUER, C. A. 1985. Prevention of coronary vasodilator reserve decrement in spontaneously hypertensive rats. *Hypertension,* 7**,** 533-540.

TOMAS, J. P., MOYA, J. L., BARRIOS, V., CAMPUZANO, R., GUZMAN, G., MEGIAS, A., RUIZ-LERIA, S., CATALAN, P., MARFIL, T., TARANCON, B., MURIEL, A. & GARCIA-LLEDO, A. 2006. Effect of candesartan on coronary flow reserve in patients with systemic hypertension. *J Hypertens,* 24**,** 2109-14.

VAHANIAN, A., BAUMGARTNER, H., BAX, J., BUTCHART, E., DION, R., FILIPPATOS, G., FLACHSKAMPF, F., HALL, R., IUNG, B., KASPRZAK, J., NATAF, P., TORNOS, P., TORRACCA, L., WENINK, A., PRIORI, S. G., BLANC, J. J., BUDAJ, A., CAMM, J., DEAN, V., DECKERS, J., DICKSTEIN, K., LEKAKIS, J., MCGREGOR, K., METRA, M., MORAIS, J. O., OSTERSPEY, A., TAMARGO, J., ZAMORANO, J. L., ZAMORANO, J. L., ANGELINI, A., ANTUNES, M., FERNANDEZ, M. A. G., GOHLKE-BAERWOLF, C., HABIB, G., MCMURRAY, J., OTTO, C., PIERARD, L., POMAR, J. L., PRENDERGAST, B., ROSENHEK, R., UVA, M. S. & TAMARGO, J. 2007. Guidelines on the management of valvular heart disease. *European Heart Journal,* 28**,** 230-268.

VERDECCHIA, P., CARINI, G., CIRCO, A., DOVELLINI, E., GIOVANNINI, E., LOMBARDO, M., SOLINAS, P., GORINI, M. & MAGGIONI, A. P. 2001a. Left ventricular mass and cardiovascular morbidity in essential hypertension: the MAVI study. *J Am Coll Cardiol,* 38**,** 1829-35.

VERDECCHIA, P., PORCELLATI, C., REBOLDI, G., GATTOBIGIO, R., BORGIONI, C., PEARSON, T. A. & AMBROSIO, G. 2001b. Left ventricular hypertrophy as an independent predictor of acute cerebrovascular events in essential hypertension. *Circulation,* 104**,** 2039-44.

VILLA, E., TROISE, G., CIRILLO, M., BRUNELLI, F., TOMBA, M., MHAGNA, Z., TASCA, G. & QUAINI, E. 2006. Factors affecting left ventricular remodeling after valve replacement for aortic stenosis. An overview. *Cardiovascular Ultrasound,* 4**,** 25.

VILLARI, B., HESS, O. M., MEIER, C., PUCILLO, A., GAGLIONE, A., TURINA, M. & KRAYENBUEHL, H. P. 1992. Regression of coronary artery dimensions after successful aortic valve replacement. *Circulation,* 85**,** 972-978.

VINTEN-JOHANSEN, J. & WEISS, H. R. 1980. Oxygen consumption in subepicardial and subendocardial regions of the canine left ventricle. The effect of experimental acute valvular aortic stenosis. *Circulation Research,* 46**,** 139-145.

WASSERTHEURER, S., KROPF, J., WEBER, T., VAN DER GIET, M., BAULMANN, J., AMMER, M., HAMETNER, B., MAYER, C. C., EBER, B. & MAGOMETSCHNIGG, D. 2010. A new oscillometric method for pulse wave analysis: comparison with a common tonometric method. *J Hum Hypertens,* 24**,** 498-504.

WASZYROWSKI, T., KASPRZAK, J. D., KRZEMIŃSKA-PAKUŁA, M., DROŻ, J., DZIATKOWIAK, A. & ZASŁONKA, J. 1996. Regression of left ventricular dilatation and hypertrophy after aortic valve replacement. *International Journal of Cardiology,* 57**,** 217-225.

WEBER, M., HAUSEN, M., ARNOLD, R., NEF, H., MOELLMAN, H., BERKOWITSCH, A., ELSAESSER, A., BRANDT, R., MITROVIC, V. & HAMM, C. 2006. Prognostic value of N-terminal pro-B-type natriuretic peptide for conservatively and surgically treated patients with aortic valve stenosis. *Heart,* 92**,** 1639-44.

WEBER, T., WASSERTHEURER, S., RAMMER, M., MAURER, E., HAMETNER, B., MAYER, C. C., KROPF, J. & EBER, B. 2011. Validation of a Brachial Cuff-Based Method for Estimating Central Systolic Blood Pressure. *Hypertension,* 58**,** 825-832.

WEIDEMANN, F., HERRMANN, S., STÖRK, S., NIEMANN, M., FRANTZ, S., LANGE, V., BEER, M., GATTENLÖHNER, S., VOELKER, W., ERTL, G. & STROTMANN, J. M. 2009. Impact of Myocardial Fibrosis in Patients With Symptomatic Severe Aortic Stenosis. *Circulation,* 120**,** 577-584.

WEN, H., TANG, H., LI, H., KANG, Y., PENG, Y. & ZHOU, W. 2010. [Carotid arterial wave intensity in assessing the hemodynamic change in patients with chronic heart failure]. *Sheng Wu Yi Xue Gong Cheng Xue Za Zhi,* 27**,** 578-82.

WESTERHOF, B. E., GUELEN, I., STOK, W. J., LASANCE, H. A. J., ASCOOP, C. A. P. L., WESSELING, K. H., WESTERHOF, N., BOS, W. J. W., STERGIOPULOS, N. & SPAAN, J. A. E. 2008. Individualization of transfer function in estimation of central aortic pressure from the peripheral pulse is not required in patients at rest. *Journal of Applied Physiology,* 105**,** 1858-1863.

WICKER, P., TARAZI, R. C. & KOBAYASHI, K. 1983. Coronary blood flow during the development and regression of left ventricular hypertrophy in renovascular hypertensive rats. *The American Journal of Cardiology,* 51**,** 1744-1749.

XU, R., ZHANG, Y., ZHANG, M., GE, Z. M., LI, X. C. & ZHANG, W. 2003. [Relationship between regression of hypertensive left ventricular hypertrophy and improvement of coronary flow reserve]. *Zhonghua Yi Xue Za Zhi,* 83**,** 658-61.

YANG, D. K., CHOI, B. Y., LEE, Y. H., KIM, Y. G., CHO, M. C., HONG, S. E., KIM, D. H., HAJJAR, R. J. & PARK, W. J. 2007. Gene profiling during regression of pressure overload-induced cardiac hypertrophy. *Physiological Genomics,* 30**,** 1-7.

YETKIN, E. & WALTENBERGER, J. 2009. Molecular and cellular mechanisms of aortic stenosis. *International Journal of Cardiology,* 135**,** 4-13.

YURENEV, A. P., DYAKONOVA, H. G., NOVIKOV, I. D., VITOLS, A., PAHL, L., HAYNEMANN, G., WALLRABE, D., TSIFKOVA, R., ROMANOVSKA, L., NIDERLE, P. & ET AL. 1992. Management of essential hypertension in patients with different degrees of left ventricular hypertrophy. Multicenter trial. *Am J Hypertens,* 5**,** 182S-189S.

ZAMBANINI, A., CUNNINGHAM, S. L., PARKER, K. H., KHIR, A. W., THOM, G. & HUGHES, A. D. 2005. Wave-energy patterns in carotid, brachial, and radial arteries: a noninvasive approach using wave-intensity analysis. *American Journal of Physiology - Heart and Circulatory Physiology,* 289**,** H270-H276.

ZEHETGRUBER, M., MUNDIGLER, G., CHRIST, G., M+¶RTL, D., PROBST, P., BAUMGARTNER, H., MAURER, G. & SIOSTRZONEK, P. 1995. Estimation of coronary flow reserve by transesophageal coronary sinus Doppler measurements in patients with syndrome X and patients with significant left coronary artery disease. *Journal of the American College of Cardiology,* 25**,** 1039-1045.

ZHU, Y. H., ZHU, Y. Z., SPITZNAGEL, H., GOHLKE, P. & UNGER, T. 1996. Substrate metabolism, hormone interaction, and angiotensin-converting enzyme inhibitors in left ventricular hypertrophy. *Diabetes,* 45**,** S59-S65.